The Role of Mitochondrial Dynamics in Pancreatic β-Cell Function and the Development of Type 2 Diabetes

A dissertation

submitted by

Linsey Stiles

In partial fulfillment of the requirements

for the degree of

Doctor of Philosophy

in

Pharmacology and Experimental Therapeutics

TUFTS UNIVERSITY

Sackler School of Biomedical Sciences

November, 2011

ADVISER: Orian Shirihai MD., Ph.D.

Abstract

The prevalence of obesity and type 2 diabetes is increasing rapidly in all age groups. Therefore, a better understanding of the pathogenesis of these diseases is critical for the development of novel treatments and interventions. Mitochondria play an important role in the regulation of metabolism throughout the body. Specifically, they have a particularly critical role in pancreatic β-cells. Mitochondria work to integrate nutrient signals, such as glucose, and generate secretagogues for both the triggering and amplifying pathways of insulin secretion. We sought to further describe how β-cell mitochondria respond to physiological and toxic nutrient environments and, in turn, how they affect β-cell function in response to these nutrients. We first characterized mitochondrial dynamics in β-cells. Mitochondria go through continuous cycles of fusion and fission, yet a description of β-cell mitochondrial dynamics and how fusion and fission contribute to β-cell function had not previously been investigated. Despite their short size, β-cell mitochondria undergo continuous cycles of fusion and fission. A toxic, high-nutrient environment, termed glucolipotoxicity, leads to mitochondrial fragmentation *in vitro,* which is the result of inhibition of mitochondrial fusion. Maintaining mitochondrial morphology by inhibiting mitochondrial fission restored mitochondrial fusion capacity and prevented the cell death caused by glucolipotoxicity. To examine the role of β-cell mitochondrial fusion *in vivo*, we measured the expression of the mitochondrial fusion protein, Mfn2, in islets from animals fed a high-fat diet. We observed a decrease in Mfn2 expression in the islets of these animals as well as in other animal models of diabetes.

To determine the role of reduced fusion in diet-induced obesity and diabetes, we excised Mfn2 from insulin-producing cells. In the absence of Mfn2, β-cell mitochondria became fragmented, while other islet cell types retained normal mitochondrial morphology. βMfn2KO mice became obese and exhibited metabolic dysfunction, including impaired glucose tolerance that occurred before the development of obesity. These mice also displayed an increase in basal insulin secretion and uncoordinated glucose-stimulated insulin secretion. Basal hypersecretion of insulin is a hallmark of metabolic dysfunction; however, the mechanism behind increased insulin secretion is still unclear. Consequently, we investigated mechanisms that could contribute to hypersecretion in βMfn2KO islets. We found that these islets have increased basal and uncoupled oxygen consumption indicative of a harder working, less efficient electron transport chain. Similarly, both acute fuel challenges and chronic elevation of nutrients induced proton leak in β-cells. We found that the induction of leak in response to nutrients is regulated, in part, by reactive oxygen species (ROS) and the adenine nucleotide translocase (ANT). We hypothesize that ROS generation in response to stimulatory fuel levels regulates proton leak in the islet, in part, through the ANT. This leads to increased flux through the TCA cycle and the generation of TCA-cycle derived secretagogues. These metabolic species contribute to the amplifying pathway of insulin secretion. When chronic, high levels of nutrients are present, oscillations in this system no longer occur and the continuous generation of TCA-cycle derived secretagogues would lead to increased basal insulin secretion. Taken together, all of these results suggest that nutrient-induced disruption of mitochondrial fusion may underlie the metabolic dysfunctions that contribute to the development of diabetes.

Acknowledgments

This work was conducted at Tufts University in the Program of Pharmacology and Experimental Therapeutics (PPET) and at Boston University in the Department of Molecular Medicine during 2005-2011. During these years, I have had the privilege of working under the supervision of my advisor, Dr. Orian Shirihai. Under his guidance, I was able to explore the fields of obesity and diabetes and conduct cutting-edge research in the exciting field of mitochondrial physiology. I am deeply grateful for all the time Dr. Shirihai spent mentoring me over the years by answering my questions, providing insightful and inspiring conversation, and giving me guidance throughout my doctoral work. He has provided me with so many amazing opportunities and wonderful experience for which I am thankful. Without Dr. Shirihai, I would not be the mitochondriac that I am today.

I would also like to thank all of the past and present members of the Shirihai laboratory that I have had the pleasure of working with throughout my graduate school experience. I can not imagine that there is a better group of scientist to work with and I am thankful for all of their guidance and support. They have all taught me so much over the past 6 years. I do not just consider them co-workers, but instead close friends. I am especially indebted to Dr. Anthony Molina with who I worked closely with throughout my time in Dr. Shirihai's laboratory. He acted as an additional mentor to me and has proved endless guidance. I must also thank Sam Sereda for all of the support and the assistance he has contributed to the completion of this work. Sam has been a joy to work with and has taught me a lot in the few years I have worked with him. Additionally, Wuhbet Abraham

has provided a great amount of genotyping support for this project and I truly appreciate all of her hard work.

I am also very thankful for the support and education I have received from the PPET faculty and from members of the Department of Molecular Medicine at Boston University, especially Drs. Emmanuel Pothos, Theoharis Theoharides, Barbara Corkey and Jude Deeney; as well as Jerold Harmatz who provided statistical support. Additionally, my committee members Drs. Martin Beinborn, Richard Shader and John Castellot have provided a great deal of guidance throughout this process and I am grateful to all of them. Furthermore, the support staffs at both Tuft University and Boston University were instrumental in helping me over the years and I am thankful to them.

I am truly appreciative of the support given by my fellow students at Tufts, both in PPET and in other departments. In particular I would like to thank Katherine Malanson, Brenda Geiger, and Kristina Weisman for their support during graduate school. They have been there for me from the start of the 2005 academic year and I consider their friendship to have been invaluable. In addition, I would like to thank Dr. Michael Hanley for being an insufferable journal club partner and for always providing use of his office.

Last and most importantly, I want to thank my family for their love and continuous and unconditional support. I am incredibly thankful to my mother and father for always believing in me and encouraging me. I am lucky to have a wonderful brother, Michael, who has been very supportive and who can always make me laugh. I am also grateful to my grandmothers and grandfather for all of their support throughout the years. My family has always been there for me and has helped shape me into the person I am today and no words could ever truly convey how appreciative I am of them.

List of Original Articles

Findings discussed in this dissertation provided the basis for the following articles:

Molina AJ, Wikstrom JD, **Stiles L**, Las G, Mohamed H, Elorza A, Walzer G, Twig G, Katz S, Corkey BE, Shirihai OS (2009). Mitochondrial networking protects beta-cells from nutrient-induced apoptosis. *Diabetes*. 58: 2303-15.

Anthony J. A. Molina*, **Linsey Stiles***, Samuel B. Sereda, Marc Liesa, Jakob Wikstrom, David Chan, Barbara E. Corkey, and Orian S. Shirihai (2011). Reduction of Mfn2 mediates diet induced β-cell dysfunction in-vivo. In preparation
* These authors contributed equally to this manuscript.

Wikstrom JD , **Stiles L**, Sereda SB, Corkey BE, and Shirihai OS (2011). Islet respiratory leak is acutely regulated by nutrients and ROS and is dysregulated in the obese state. In preparation.

Additional articles that were written during the dissertation but are not directly related to doctoral work:

Twig G, Elorza A, Molina AJ, Mohamed H, Wikstrom JD, Walzer G, **Stiles L**, Haigh SE, Katz S, Las G, Alroy J, Wu M, Py BF, Yuan J, Deeney JT, Corkey BE, Shirihai OS (2008). Fission and selective fusion govern mitochondrial segregation and elimination by autophagy. *EMBO J*. 27:433-46.

Tagen M, **Stiles L**, Kalogeromitros D, Gregoriou S, Kempuraj D, Makris M, Donelan J, Vasiadi M, Staurianeas NG, Theoharides TC (2007). Skin corticotropin-releasing hormone receptor expression in psoriasis. *J Invest Dermatol*; 127: 1789-91.

Fulton S, Pissios P, Manchon RP, **Stiles L**, Frank L, Pothos EN, Maratos-Flier E, Flier JS(2006). Leptin regulation of the mesoaccumbens dopamine pathway. *Neuron.* 51: 811-22.

Table of Contents

List of Figures

List of Tables

List of Abbreviations

ANT	adenine nucleotide translocase
ATP	adenosine 5'-triphosphate
CMT2A	Charcot-Marie-Tooth neuropathy type 2A
DN	dominant negative
DNP	2,4- dinitrophenol
Drp1	dynamin related protein 1
ER	endoplasmic reticulum
ERK1/2	extracellular signal-regulated protein kinase 1/2
ETC	electron transport chain
FCCP	carbonylcyanide-p-trifluoromethoxyphenylhydrazone
GLT	glucolipotoxicity
Glc-6-Pase	glucose-6-phosphatase
GLUT 2	glucose transporter 2
GSIS	glucose-stimulated insulin secretion
GT	glucotoxicity
GTT	glucose tolerance test
H+	protons
HF	high fat
HFG	high fat and glucose
HG	high glucose
IMM	inner mitochondrial membrane
ITT	insulin tolerance test
LT	lipotoxicity
MAC	mitochondrial apoptosis-induced channel
Mfn1/2	mitofusin 1 and 2
mtDNA	mitochondrial DNA
mtPAGFP	mitochondrial photoactivatable green fluorescent protein
mtPTP	mitochondrial permeability transition pore
OCR	oxygen consumption rate
OMM	outer mitochondrial membrane
OPA1	optic atrophy protein 1
PAGFPmt	mitochondrial photoactivatable green fluorescent protein
PEPCK	phosphoenolpyruvate carboxykinase
PTT	pyruvate tolerance test
RER	respiratory exchange ratio
RIP	rat insulin promoter
ROS	reactive oxygen species
STZ	Streptozotocin
TCA	tricarboxylic acid cycle
TMRE	tetramethylrhodamine ethyl ester
ZDF	Zucker Diabetic fatty
ZDL	Zucker Diabetic lean
ZF	Zucker fatty
ZL	Zucker lean

βMfn2KO	Animal model of Mfn2 knockout in insulin producing cells

The Role of Mitochondrial Dynamics in β-Cell Function and the Development of Type 2 Diabetes

Chapter 1: Introduction

1.1 Pancreas Physiology and Type 2 Diabetes

1.1a Type 2 Diabetes Statistics

Type 2 Diabetes is a metabolic disease that has become a health crisis and financial burden in the United States and world wide. The Centers for Disease Control and Prevention reported that in 2011 approximately 26 million people in the U.S, or 8.3% of the population, were living with diabetes (http://www.cdc.gov/diabetes/statistics). Type 2 diabetes mellitus (T2D) accounts for approximately 90-95% of all diagnosed cases of diabetes. It is estimated that there are an additional 79 million Americans that have prediabetes, which is characterized by blood glucose levels that are elevated, but not high enough to diagnose diabetes (glucose levels >100 mg/dL to < 126 mg/dL) (http://www.cdc.gov/diabetes/pubs/pdf/ndfs_2011.pdf). The number of people with diabetes and prediabetes is rapidly increasing. This raise in prevalence includes populations that had previously had very low incidences of diabetes, such as children (Weiss and Caprio, 2006). T2D is not only a problem in the US, but also worldwide. A recent study in Lancet reveled that there were 347 million adults with diabetes worldwide in 2008. This is more than double the reported 153 million people in 1980 (Danaei *et al.*, 2011).

Type 2 diabetes is a severe and costly disease resulting in a cost of $174 billion annually, which includes both direct medical costs and indirect costs. It is the seventh leading cause of death in the U.S. and is associated with a number of serious complications (Knight, 2011). Diabetes leads to a greater risk of heart disease, stroke, and peripheral

neuropathy and is the leading cause of kidney failure, nontraumatic lower limb amputations, and new cases of blindness among adults in the United States. This results in large number of hospitalizations of diabetic patients due to both diabetes and complications resulting from diabetes.

1.1b The Pancreas with Emphasis on Endocrine Function

The pancreas is the organ that secretes a number of metabolic factors, including insulin, which contributes to the development and progression of diabetes. It is an elongated gland located behind the stomach that has dual roles: endocrine and exocrine functions. Acinar cells make up the exocrine pancreas and secrete digestive enzymes into the duodenum, which is in close proximity to the head of the pancreas. The endocrine pancreas is comprised of Islets of Langerhan, which make up approximately 1% of the total pancreas volume. It is in the islet that hormones are produced and secreted. It is estimated that C57BL/KsJ mice have 1,000 islets at one month of age and this number remains fairly constant until 18 months of age. Islets range in diameter from 50mm to 300mm in healthy mice.

Islets are groups of cells that include α-cells, which secrete glucagon, β-cells that secrete insulin and amylin, and δ-cells which secrete somatostatin. There are also PP cells and ε-cells, which secrete pancreatic peptide and ghrelin, respectively. In addition, there are capillaries to supply blood flow to the islet. Insulin secreting β-cells make up approximately 80% of the islet cells.

The main hormones secreted from islets that act to regulate blood glucose levels are glucagon and insulin. Glucagon is a hormone that increases glucose levels during periods

when blood glucose levels falls too low. It increases glucose by acting on the liver to first convert stored glycogen to glucose and then subsequently, when glycogen stores are depleted, glucagon promote gluconeogenesis. Insulin has the reverse effect, it promotes glucose uptake into cells during times with high circulating blood glucose levels and supports glycogen storage in the liver and inhibits gluconeogenesis. It has a central role in regulating whole body metabolism for instance by increasing lipid synthesis and esterification of fatty acids.

1.1c Pathogenesis of Type 2 Diabetes and Glucolipotoxicity: Evidence for the Detrimental Effect of High Fat and Glucose on β-Cells

Weir and Bonner-Weir proposed that there are five stages of β-cell dysfunction leading to the progression of diabetes. First, β-cells compensate for insulin resistance with increased insulin secretion, which is associated with an increase in β-cell mass. Stage 2 or stable adaptation occurs when β-cells can no longer compensate with increased insulin secretion and therefore, normal glucose levels can no longer be achieved. Unstable early decompensation (stage 3) is triggered by another increase in fasting blood glucose levels, an important step in the progression to diabetes. At this stage, β-cell mass becomes inadequate and causes glucose levels to rise rapidly over a short period of time. Stage 4 is stable decompensation and is characterized by high blood glucose and is considered to be full-blown diabetes at this point. Most people with type 2 diabetes never progress to stage 5 or severe decompensation that is associated with marked loss of β-cell mass. This point in diabetes leads to insulin-dependence.(Weir and Bonner-Weir, 2004)

Type 2 Diabetes is associated with metabolic dysfunction in both the insulin secreting β-cells and peripheral tissues. Decreased insulin sensitivity in muscle, termed insulin

resistance, is an early event in the development of diabetes. This decrease in insulin sensitivity leads to high fasting blood glucose levels. In this state, muscle mitochondria have a decreased capacity for fuels integration. β-cells compensate for the decreased sensitivity and high glucose levels by increasing insulin secretion. The constant high level of insulin secretion eventually leads to β-cell dysfunction and a failure of mitochondria to generate metabolic signals to trigger insulin secretion. In this state, insulin resistance can no longer be compensated for by an increase in secretion.

Glucolipotoxicity (GLT) is the combined adverse or toxic effect of excessive glucose and lipids on pancreatic β-cells. Additionally, glucotoxicity (GT) and lipotoxicity (LT) refer to toxicity due to glucose and lipids, respectfully. Since β-cells are equipped to handle nutrients and can utilize fat and lipids for normal insulin secretion function, toxicity generally arises from high concentrations and/or chronic exposure to these fuels. Originally it was shown that overstimulation of the β-cell by glucose led to an attenuated insulin secretion response to glucose due to depleted insulin stores, impaired insulin-mediated glucose transport, and a decline in β-cell function (Unger and Grundy, 1985). Likewise, over-exposure of the β-cell to lipids also has a detrimental effect on β-cells (Unger, 1995). Importantly the concept of GLT emerged from the observation that elevated glucose levels are required for the toxic effects of lipids to occur (Poitout and Robertson, 2008). GLT results in alterations to insulin secretion, insulin gene expression, ROS levels, and β-cell viability. Additionally, GLT does not appear to be an *in vitro* phenomenon given evidence that high glucose and lipids are evident in the human condition and contribute to the onset and progression of type 2 diabetes.

1.1d Current Treatments for Type 2 Diabetes

Type 2 Diabetes is a very complex disease; therefore, the treatment of diabetes can be problematic. In addition to the drugs that will be reviewed here, there are many more drugs for the treatment of diabetes. Tahrani *et al.* recently reviewed the most current treatment strategy for the management of type 2 diabetes (Tahrani *et al.*, 2011). Current treatments for T2D include sulfonylureas (SU) and non-SU insulin secretagogues. These compounds bind to and prevent opening of the K_{ATP} channel on the plasma membrane of β-cells; therefore, promoting insulin secretion (Aquilante, 2010). One of the problematic side effects of SU use is weight gain. In fact, weight gain is often associates with treatments that increase insulin secretion.

Thiazolidinediones are another commonly used drug in the fight to maintain normal blood glucose levels in diabetics. The mechanism of action of thiazolidinediones is to bind PPARγ and activate gene transcription of insulin-responsive genes that regulate lipid and carbohydrate metabolism. Thiazolidinediones require insulin to be present for their action. They primary effect is to increase insulin sensitivity in peripheral tissues, but they can also decrease gluconeogenesis in the liver (Schwanstecher and Schwanstecher, 2011). Additionally, alpha-glucosidase inhibitors, which decrease the absorption of carbohydrates from the intestine, are used to treat diabetes. The consequence of decreased carbohydrate absorption is decreased blood sugar because carbohydrates are metabolized to sugars.

The most recent drugs developed for diabetes include the glucagons-like peptide-1 (GLP-1) mimetics and dipeptidyl peptidase IV inhibitors, the enzyme responsible for the breakdown of GLP1. GLP-1 is a 30 amino acid peptide that is secreted from intestinal

enteroendocrine L cells after meal ingestion. The mechanism of action of these incretin is to increase GLP-1 levels that can subsequently bind to β-cells. These compounds promote oxidative phosphorylation and β-cell proliferation, while preventing apoptosis (Lund *et al.*, 2011).

Additionally, it has recently been shown that gastric bypass surgery may have a beneficial effect in the treatment for diabetes (Pories *et al.*, 1995). Interestingly, the benefits of bypass surgery seem to exceed those attributable entirely to weight loss. This effect has been observed with many different types of weight loss surgeries. The mechanism of action underlying this phenomenon is currently unknown.

1.2 The Role of Mitochondria in β-Cells

Insulin secretion is the most critical functions of the β-cell and mitochondria play a very important role in both the main triggering and supplementary amplifying pathways of insulin secretion. Mitochondria integrate different types of fuels and produce metabolic signals that can be used to trigger secretion in the β-cell. Mitochondria respond to free fatty acids, amino acids, and glucose, through metabolism to pyruvate, and then generate a number of different secretagogues through metabolism of these nutrients.

Insulin secretion in the β-cell begins when glucose is transported into the β-cell via glucose transporter 2 (GLUT 2). Glucose is then metabolized to pyruvate, which can enter the mitochondria. Once inside, the pyruvate can enter the TCA cycle and produce the reducing equivalents needed for oxidative phosphorylation. Increased oxidative phosphorylation will lead to an increase in mitochondrial membrane potential and the

generation of ATP. The ATP is transported to the cytoplasm via the adenine nucleotide translocase (ANT). The increase in the ATP/ADP ratio causes closure of the ATP-sensitive K^+ channel on the plasma membrane. This leads to depolarization of the plasma membrane and opening of voltage-gated Ca^{2+} channels, allowing Ca^{2+} influx and exocytosis of insulin granules. This pathway is considered the triggering pathway of insulin secretion, but there are also amplifying pathways of insulin secretion, which rely heavily on mitochondrial metabolism (Henquin, 2000).

The role of mitochondria in the β-cell can be further appreciated when examining mitochondrial membrane potential. In response to glucose, β-cell mitochondria increase their membrane potential. Heart *et al.* demonstrated that as glucose concentrations increase there is also a corresponding increase in mitochondrial membrane potential (Heart *et al.*, 2006) (Figure 1.1b). The increase in membrane potential occurred within 30 seconds of glucose addition to a single islet. They also showed that this increase in membrane potential positively correlates with an increase in insulin secretion. In figure 1.1c the x-axis represents increasing membrane potential on the same scale as that seen in figure 1.1b. On the Y-axis is insulin secretion represented as a percentage of basal secretion. Increasing membrane potential is associated with increased insulin secretion (Figure 1.1b). On the other hand, cytosolic Ca^{2+} levels did not display a graded response to stimulatory glucose concentrations (Figure 1.1a). These data demonstrated that the magnitude of insulin secretion and levels of Ca^{2+} do not always correlate and, therefore, provided evidence for amplifying pathways of insulin secretion. Additionally, it implied that mitochondrial metabolism may be a determining factor in explaining glucose concentration-dependent increases in insulin secretion that are not dependent on Ca^{2+}.

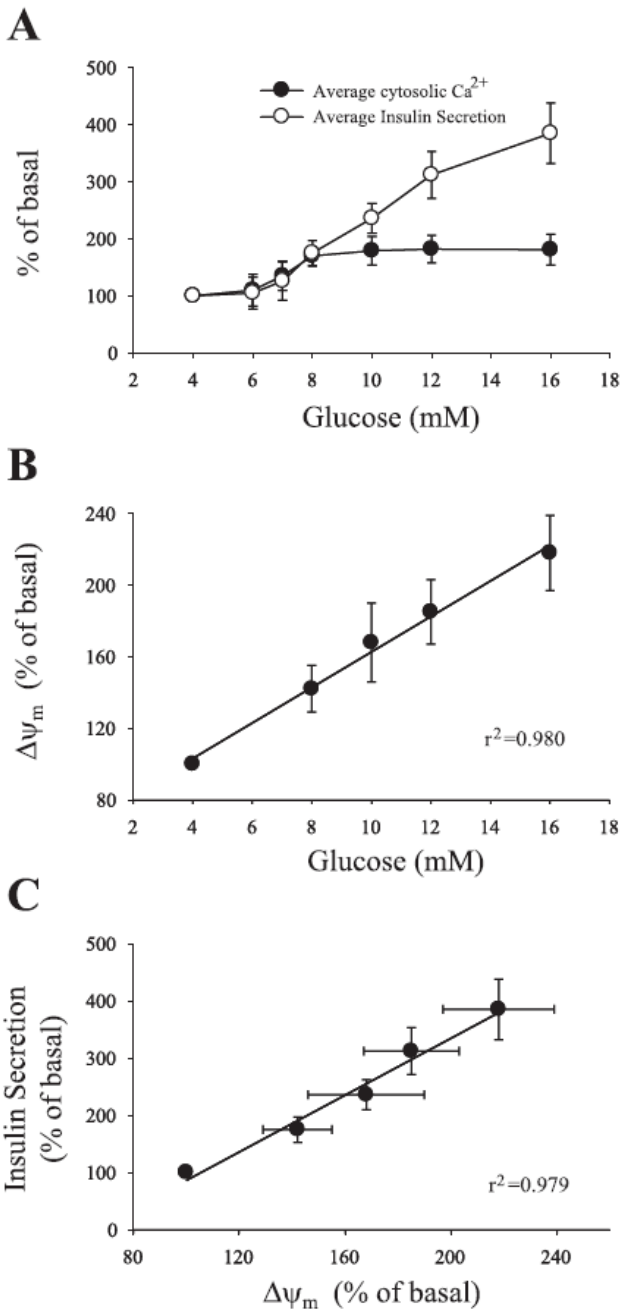

Figure 1.1 from (Heart *et al.*, 2006) Influence of glucose concentration on average value of $Ca2^{2+}$ responses and insulin secretion (*A*) and ΔΨmt (*B*). *C*: correlation between ΔΨmt and insulin secretion. Insulin secretion data are expressed as means ± SE from 4 independent measurements.

There are now known to be a number of signals that amplify insulin secretion. These include a number of mitochondrial metabolites including reactive oxygen species (ROS),

a byproduct of oxidative phosphorylation, GTP, which is generated in the tricarboxylic acid (TCA) cycle, NADPH, long-chain acyl-Co-A, glutamate, phosphoenolpyruvate (PEP), and malonyl CoA (Jitrapakdee *et al.*, 2010). These are often referred to as K_{ATP}-independent GSIS. All of these signals emerge from mitochondrial metabolism, yet they each play different roles in amplifying GSIS. The following is a short overview of some of the amplifying signals of insulin exocytosis that are relevant for this work. A more detailed descriptions of amplifying pathways of GSIS have been reviewed elsewhere (Henquin, 2000;Deeney *et al.*, 2000b;Maechler, 2002;Maechler *et al.*, 2006;Jitrapakdee *et al.*, 2010;Henquin, 2011).

ROS is known to be toxic to β-cells at high concentrations, this is because β-cells have low antioxidant capacity and are therefore more prone to damage (Tiedge *et al.*, 1997). Paradoxically, ROS, specifically H_2O_2, seems to be required for GSIS with acute stimulatory glucose concentrations (Pi *et al.*, 2007). Insulin secretion can be stimulated with either exogenous H_2O_2 or diethyl maleate, which raises intracellular H_2O_2 levels. The addition of exogenous H_2O_2 scavengers, catalase and N-acetyl-L-cysteine (NAC), inhibited GSIS. Therefore, the concentration of ROS that β-cells are exposed to determines whether ROS has a GSIS signaling effect or is toxicity and leads to impaired β-cell function (Maechler *et al.*, 1999).

The TCA cycle contributes many metabolic signals to GSIS. Pyruvate is imported into the mitochondrial matrix and converted to acetyl-CoA or oxaloacetate, which is shuttled into the TCA cycle. Interestingly, it has been shown that inhibition of pyruvate carboxylase (the enzyme that converts pyruvate to oxaloacetate) decreased GSIS.

Intermediates of the TCA cycle such as succinate, α-ketogluterate, and GTP also influence insulin exocytosis. Succinate induces hyperpolarization of the mitochondrial membrane potential and causes elevated Ca^{2+} levels and ATP production, both of which are important signals for GSIS. The increase in insulin secretion caused by succinate has been shown to be glucose-dependent (Attali *et al.*, 2006). Succinate is also involved in the control of proinsulin biosynthesis ((Maechler *et al.*, 2006).

GTP, unlike ATP, can induce insulin secretion in a Ca^{2+}-independent manner (Vallar *et al.*, 1987). However, it seems that the Ca^{2+}-dependence of this process is still not completely understood. Kibbey *et al.* demonstrated that siRNA suppression of the mitochondrial isoform of the GTP-producing pathway reduced GSIS by 50%. Insulin secretion correlated with increased cytosolic Ca^{2+} but not with changes in the ATP/ADP ratio. While the role of calcium still needs to be elucidated, these data imply an important role for GTP in mediating GSIS in β-cells by modulation of mitochondrial metabolism (Kibbey *et al.*, 2007).

Fatty acids also play an important role in insulin exocytosis. Fatty acid transport into the mitochondria is the rate-limiting step for fatty acid oxidation and is regulated by carnitine palmitoyltransferase I (CPTI). When β-cells are glucose stimulated, malonyl-CoA is synthesized from glucose metabolism and inhibits the CPTI, thereby regulating the metabolism of fatty acids by β-oxidation (Maechler, 2002). Since malonyl-CoA inhibits fatty acid transport and thus oxidation, the availability of long-chain acyl-CoA (LC-CoA) is increased. Long-chain acyl-CoA augment Ca^{2+}-induced insulin secretion (Deeney *et*

al., 2000a;Deeney *et al.*, 2000b). LC-CoA may act directly on the exocytotic machinery to stimulate insulin release (Deeney *et al.*, 2000a).

Mitochondria play a key role in generating signals for both the triggering and amplifying pathways of insulin secretion. Mitochondrial oxidative phosphorylation, TCA-cycle intermediates, fatty acid pathways, as well as shuttles, and the control of expression and activity of rate-deterring enzymes influence metabolism secretion coupling in β-cells.

1.3 Mitochondria Structure and Function

1.3a Mitochondrial Structure

Mitochondria are double membraned organelles that are approximately 0.5-10 μm in diameter based on electron microscopy images. The number of mitochondria per cell varies, ranging from hundreds to thousands mitochondria per cell, which is dependent upon cell type (Santos *et al.*, 2006). They consist of an outer mitochondria membrane (OMM), which is penetrable by solutes, proteins, and molecules 10000 Daltons or less in size, and an inner mitochondrial membrane (IMM), which is impermeable to molecules. The inner mitochondrial membrane forms folds, known as cristae, which act to increase the surface area of the inner membrane and provide internal compartments where proteins can be stored. Since small molecules can freely diffuse through the outer mitochondrial membrane, the intermembrane space, (the space between the outer and inner mitochondrial membrane) has a similar concentration of ions and small molecules as the cytosol. The mitochondrial matrix is the space within the inner mitochondrial membrane and here the concentration of ions and small molecules is tightly regulated by a number of channels and transporters.

It is in the matrix that mitochondrial DNA (mtDNA) is located. Mitochondria have their own double stranded, circular DNA that encodes for 37 total genes including: 13 proteins, 22 transfer RNA (tRNAs), and 2 for ribosomal RNA (rRNA). It is estimated that 2-10 copies of mtDNA are present per mitochondrion (Wiesner *et al.*, 1992;Santos *et al.*, 2006). All 13 proteins that mtDNA encode for are subunits of the electron transport chain (ETC), with genes encoding proteins for complex I, complex III, complex IV, and the ATP Synthase. Only complex II of the ETC is encoded for entirely by nuclear DNA.

It has been hypothesized that mitochondria have a decreased ability to repair their DNA compared to the mechanisms that are in place to repair nuclear DNA. This hypothesis was originally proposed when it was shown that cells treated with ultraviolet (UV) light to induce DNA damage could not repair their mitochondrial genome (Clayton *et al.*, 1974). This is because mitochondria lack a pyrimidine dimer repair mechanism. However, it has been show that they do have other repair mechanisms in place for DNA repair. Mitochondrial DNA repair mechanisms may not be as important as it is for nuclear DNA (nDNA) because of the large copy number of mtDNA per mitochondrion. It has been shown that a very high threshold is in place for mtDNA mutations to become pathogenic. Indeed approximately 65-95% of mtDNA have to be mutated, depending on the mutation and cell type, before functional changes and disease progression can be observed (Smith and Lightowlers, 2011).

1.3b Mitochondrial Respiratory Function

1.3b.1 Mitochondrial Bioenergetics

The number of mitochondria present per cell varies greatly with cell type and is, in large part, based on energy requirements. Most of the cellular energy production, in the form of adenosine 5'-triphosphate (ATP), is generated in mitochondria via oxidative phosphorylation. This is accomplished by using the proton motive force as the driving force for ATP synthesis. The ETC is located in the inner mitochondrial membrane and consists of four complexes: complex I or NADH dehydrogenase, complex II or succinate dehydrogenase, complex III or cytochrome c reductase, and complex IV or cytochrome c oxidase, as well as the ATP synthase. The ETC facilitates electron transfer from electron donors to electron acceptors, which is coupled to the transfer of protons (H+) across the inner membrane into the inner membrane space. Only complex II of the ETC does not act as a proton pump, although it is the site where the tricarboxylic acid (TCA) cycle feeds directly into the respiratory chain (Dudkina *et al.*, 2010). At complex IV, the electrons are passed to molecular oxygen to produce two molecules of water, making this an aerobic process that consumes oxygen. The pumping of protons across the inner membrane generates an electrochemical H+ gradient, or proton motive force, that drives ATP production. ATP is synthesized when H+ flow back to the matrix through the ATP synthase that promotes the phosphorylation of ADP to ATP. ATP is transported to the cytosol via the adenine nucleotide translocator.

Complete oxidation of glucose is calculated to yield a total of 38 ATP molecules: 8 from glycolysis to pyruvate and 30 from aerobic oxidation of pyruvate to CO_2 and water. However, due to proton leak and the energetic cost of shutting ADP and phosphate from

the cytoplasm into the mitochondrial matrix, the total yield of ATP is estimated to actually be 29-30 per glucose molecule (Rich, 2003). Oxygen consumption is usually tightly coupled to ATP synthesis, but there are instances where this is not the case. Proton leak is the process by which H+ are leaked back through the inner membrane to the matrix without being coupled to ATP production. This is the biological basis of thermogenesis, where energy is given off as heat. One of the best known examples of this is in brown adipose tissues where there is very low coupling efficiency in the mitochondria. Instead, proton leak through uncoupling protein-1 (UCP1) is utilized to generate heat, this process also relies on free fatty acids (Richard and Picard, 2011). Another example of uncoupling of the ETC occurs if the H+ is leaked to oxygen, this will lead to the production of reactive oxygen species (ROS) in the form of superoxide (O_2•). This occurs primarily at complex I and complex III. It is estimated that ROS production accounts for approximately 1-5% of oxygen consumption (Costa *et al.*, 2011).

1.3b.2 Monitoring Mitochondrial Bioenergetic in Intact Cells

Mitochondrial bioenergetic function can be measured by employing a number of approaches, including the measurement of membrane potential, pH, and oxygen consumption. Assessing mitochondrial bioenergetics in both isolated mitochondria and intact cells presents important information about the function and health of mitochondria. Analysis of bioenergetics makes it possible to distinguish what aspect of mitochondrial function is altered in response to a certain treatment or molecular modification. The Seahorse XF24 Extracellular Analyzer can be utilized to measure oxygen consumption and extracellular acidification rate in intact cells. The Seahorse respirometry platform allows for the measurement of oxygen consumption in a more physiological relevant

setting than classical approaches. This technology uses a piston to reversibly enclose the cells in a small volume where oxygen uptake can be monitored for short time periods (2-5 minutes). Rising the piston allows for the mixing and re-equilibration of oxygen into the cell medium, which allows for multiple measurements to be taken over time. Additionally, there are four injection ports that allow for addition of compounds to the cells during the experiments and allows for respiratory control to be measured (Ferrick *et al.*, 2008).

Bioenergetic analysis can provide a great deal of information about mitochondrial and cellular function. The use of different mitochondrial inhibitors can provide information on basal, maximal, uncoupled (proton leak), and non-mitochondrial respiration. Basal respiration is achieved before any inhibitor or stimulation to the cells and is controlled primarily by ATP turnover. An increase in basal respiration can be indicative of either increased ATP turnover or increased proton leak (Brand and Nicholls, 2011). Oligomycin is used to estimate proton leak or uncoupled respiration (also termed oligomycin-insensitive respiration), which is defined as oxygen consumption that is not coupled to ATP synthesis. Oligomycin is an inhibitor of ATP Synthase. Any remaining respiration after the addition of oligomycin is a combination of proton leak and non-mitochondrial respiration. Maximal respiration (also called reserve capacity) is calculated by the addition of an uncoupler, such as carbonylcyanide-p-trifluoromethoxyphenylhydrazone (FCCP) to the cells. Approximately 10% of respiration is obtained from non-mitochondrial sources, such as detoxification enzymes. Determination of the percentage of non-mitochondrial respiration is achieved by

inhibiting ETC complex I and III with rotenone and antimycin A (or myxothiazol), respectively (Brand *et al.*, 2011).

Monitoring bioenergetics in intact cells is a very useful tool for examining mitochondrial function. However, care must be taken in the interpretation of these data. Disadvantages to this technique include the lack of direct mitochondrial context, cell-impermeant substrates and reagents, and different interpretation of results based on normalization techniques (Brand *et al.*, 2011). Therefore, when possible, bioenergetic should also be measured in isolated mitochondria. The bioenergetic profile of isolated mitochondria provides the most information for studies on the mechanism underlying mitochondrial dysfunction. A combination of respirometry measurements on intact cells and isolated mitochondria would provide the optimal amount of data on bioenergetic function.

1.3c Mitochondrial ROS: A Vicious Cycle of Damage

Reactive oxygen species are a group of molecules, including peroxides and free radicals, that are produced from molecular oxygen and are reactive to biological molecules, including lipids, proteins, and nucleic acids (Maynard *et al.*, 2009). Mitochondria are both the main source and, due to their close proximity and less efficient DNA proofreading enzymes, target of ROS. Harman hypothesized in 1956 that ROS induces mitochondrial dysfunction and this mitochondrial dysfunction generates more ROS, leading to a vicious cycle of mitochondrial damage (HARMAN, 1956). It was hypothesized then, and is generally accepted today, that this vicious cycle of ROS could be involved with aging. Indeed, this vicious cycle of mitochondrial damage is the basis of the mitochondrial theory of aging. However, it is important to note that not all ROS is

deleterious, it also acts as a physiological cellular signal. For instance, as was already discussed, at low levels ROS is an amplifying signal of GSIS (Pi *et al.*, 2007). Additionally, low amounts of ROS can be a signal to stimulate ROS scavenging pathways, mitochondrial biogenesis, and mtPTP, which may lead to mitochondrial turnover (Valko *et al.*, 2007). This implies that ROS can have a role in mitochondrial quality control when present in minimal concentrations. As ROS levels and oxidative damage increase, a transition occurs from promoting survival of mitochondria to instead trigger release of factors that initiate apoptosis.

Increased ROS levels may also elevate mitochondrial DNA mutations. Mitochondria exhibit an increased incidence for DNA mutation compared to genomic DNA. This is due to a number of reasons; including, being in close proximity to higher levels of ROS and decreased repair mechanisms. Increased accumulation of mtDNA mutations has also been proposed as an aging mechanism and is a cause for heterogeneity in the mitochondrial population. Accumulation of mutated mtDNA is an indication that mitochondrial quality control mechanisms are dysfunctional. It has been hypothesized that certain mtDNA mutations that decrease mitochondrial respiration and therefore ROS production (a seemingly beneficial result in circumstances of mitochondrial damage and high ROS production) may also decrease mitochondrial turnover (Lemasters, 2005).

1.3d The Role of Mitochondria in Apoptosis

Two pathways are known to mediate apoptosis: the extrinsic pathway and the intrinsic or mitochondrial pathway. Both of these pathways lead to activation of caspases, which are cysteine proteases that mediate cellular destruction. The extrinsic pathway is mediated

by the cell surface receptors, FAS and tumor necrosis factor receptor 1 (TNFR1), while the mitochondrial pathway is controlled by the Bcl-2 family of proteins (Suen *et al.*, 2008). This family of proteins has both pro- (Bax and Bak) and anti-(Bcl-2, Bcl-xL, and Mcl-1) apoptotic members and is characterized by having between two and four Bcl-2 homology (BH) domains (Youle and Strasser, 2008). Their dual action in regulating apoptosis is mediated by the role of the anti-apoptotic members to control the pro-apoptotic members. An apoptotic signal induces the release of the pro-apoptotic members and the activation of apoptosis (Suen *et al.*, 2008). The mechanism underlying apoptosis induction is the ability of Bax and Bak to oligomerize on the mitochondria, upon release from anti-apoptotic members, and permeabilize the outer mitochondrial membrane (through the mitochondrial apoptosis-induced channel (MAC)). Permeabilization of the OMM leads to release of cytochrome c from cristae within the inner mitochondrial membrane. The released cytochrome *c* leads to propogation of the apoptotic cascade by activation of caspase 9 (Youle *et al.*, 2008;Suen *et al.*, 2008).

There are also BH-3 only members of this family, which refers to the fact that they only have one BH domain, the BH-3 domain. BH-3 only proteins include: Bad, Bid, Bik, Bim, Bmf, HRK/DP5, MULE, NOXA, and PUMA (Giam *et al.*, 2008). All of these proteins promote apoptosis. They act upstream of Bax and Bak and promote apoptosis by causing pro-apoptotic Bcl-2 members to be activated. This can be achieved by either directly activating Bax/Bak (Letai *et al.*, 2002;Kim *et al.*, 2006) or via inhibition of the anti-apoptotic members that will indirectly lead to release of Bax and Bak (Willis *et al.*, 2005;Willis *et al.*, 2007;Giam *et al.*, 2008).

Permeabilization of the OMM is a central step in the mitochondrial apoptotic cascade. There are two proposed mechanism by which permeabilization can occur: through the mitochondrial permeability transition pore (mtPTP) in the inner membrane and through MAC in the outer membrane (Kinnally and Antonsson, 2007;Rasola and Bernardi, 2007). Mitochondrial permeability transition is a sudden increase in permeability of the IMM to solutes. This is due to opening of a voltage-gated Ca^{2+} channel and can be transient. The mtPTP is induced by Ca^{2+} overload, high ROS levels, and other stressors. Opening of the mtPTP results in depolarization of the mitochondrial membrane, release of Ca^{2+} and cytochrome c stores, as well as mitochondrial swelling. Cytochrome c release can occur through cristae remodeling (Scorrano *et al.*, 2002). Additionally, there is also evidence that the Bcl-2 family of proteins can work through the PTP to release cytochrome c, in additiona to the known role of MAC (Rasola *et al.*, 2007).

Mitochondria are at the crossroads of life and death. They play major roles in metabolism and energy production, as well as the regulation of cell death. This highlights the important role mitochondria play in cells and demonstrates that the ability to maintain a fit mitochondrial population is critical for keeping cells healthy. Maintenance of the mitochondrial population is a highly balanced process that is regulated, in part, by mitochondrial dynamics (a more detailed review on mitochondrial quality control can be found in Appendix 1).

1.4 Mitochondrial Dynamics

1.4a Mitochondrial Dynamics Overview

Mitochondria function as heterogeneous networks that undergo frequent fusion and fission events, constituting mitochondrial dynamics, which regulate their morphology, number, and function (Bereiter-Hahn and Voth, 1994;Chen and Chan, 2005a). Mitochondrial dynamics have been demonstrated to contribute to mitochondrial function in a number of systems including budding yeast, pancreatic β-cells, muscle, and neurons (Liesa *et al.*, 2009). It has been established that mitochondrial dynamics can influence almost every aspect of the mitochondrion including biogenesis, bioenergetics, heterogeneity and elimination (Wikstrom *et al.*, 2009;Hyde *et al.*, 2010).

Proteins that mediate mitochondrial fusion and fission have been identified. In mammals, fusion is regulated by at least three mitochondrial localized GTPases: mitofusin 1 (Mfn1), mitofusin 2 (Mfn2), and optic atrophy protein 1 (Opa1) (Santel and Fuller, 2001;Misaka *et al.*, 2002). The yeast homologs of these proteins are Fzo1p (Mfn1/2) and Mgm1p (OPA1) (Merz *et al.*, 2007). Mfn1 and Mfn2 are localized to the outer mitochondrial membrane, while OPA1 is an inner mitochondrial membrane protein. Mitochondrial fusion is a two-step process where fusion of the inner and outer membranes occurs as separate events. Fission is mediated by the transmembrane protein Fis1 and the cytosolic GTPase dynamin related protein 1 (Drp1/DNM1L); with Fis1 as the rate limiting factor of fission in some models. Additionally, another outer mitochondrial membrane fission factor has recently been identified, Mff (Gandre-Babbe and van der Bliek, 2008). The yeast homologs to the fission proteins are Dnm1p (Drp1) and Fis1p (James *et al.*, 2003;Praefcke and McMahon, 2004). Drp1 translocates from the cytosol to scission sites

(Fis1 sites) on the outer mitochondrial membrane to initiate fission events. Mff is a mitochondrial fission factor that serves an essential factor in recruitment of Drp1 to mitochondria. Additionally, Mff-dependent mitochondrial fission is independent of Fis1 (Otera *et al.*, 2010).

Mitochondrial dynamics are essential to maintain a metabolically efficient mitochondrial population and disruption of either fusion or fission alters mitochondrial morphology and functionality. Both alterations to mitochondrial dynamics proteins and the balance between mitochondrial fusion and fission have been shown to contribute to a number of diseases.

1.4b Mitochondrial Fission

Mitochondrial fission is an important modulator of mitochondrial function. Fission has been shown to regulate the inheritance of mitochondria by daughter cells within dividing cells, cellular differentiation (neuronal, cardiac, and muscle cells), and the progression of apoptosis. Fission is also involved in the process of segregating dysfunctional mitochondria from the network so that they can be targeted for degradation (Twig *et al.*, 2008a). This is a very important process for mitochondrial quality control. Loss of fission results in increased mitochondrial connectivity, loss of mtDNA, bioenergetic deficiency and changes in apoptosis (Liesa *et al.*, 2009;Karbowski, 2010).

It has been well established that apoptosis and mitochondrial fragmentation are often simultaneous events. Frank *et al.* helped elucidate this phenomenon when they demonstrated that mitochondria fragment during apoptosis and showed that this is a tightly regulated process. They found that inhibition of Drp1 delays cytochrome c release

and cell death, indicating that mitochondrial fission is an important part of the progression of apoptosis (Frank *et al.*, 2001). This work demonstrated that mitochondrial fission is a regulated event during apoptosis that occurs before caspase activation.

Mitochondrial fission proteins have also been shown to have roles outside of the mitochondria. Fis1 and Drp1 are localized to peroxisomes and mediate peroxisomal fission in a similar manner to that of mitochondrial fission (Koch *et al.*, 2003;Koch *et al.*, 2005).

1.4c Mitochondrial Fusion with Emphasis on Mitofusin 2

Mitochondrial fusion contributes to maintenance of oxidative phosphorylation and mitochondrial membrane potential, with loss of fusion generally resulting in mitochondrial fragmentation, decreased mitochondrial membrane potential and oxygen consumption, and often increased reactive oxygen species (ROS) production and susceptibility to apoptosis (Chen and Chan, 2010;Zorzano *et al.*, 2010). Fusion allows for the generation of continuous membranes and matrix lumen, which subsequently allows for complementation of solutes, metabolites, and proteins. Complementation is thought to be a key mechanism by which mitochondria can rescue a damaged unit within the network.

Mitochondrial depend on the proteins OPA1, Mfn1, and Mfn2 for mitochondrial fusion. The gene, *OPA1,* encodes a highly conserved dynamin-related GTPase that is dispersed throughout the mitochondria. It is either localized to the inner mitochondrial membrane or it is present in the intermembrane space in a soluble form (Akepati *et al.*, 2008). OPA1 coordinates inner mitochondrial membrane fusion and participates in the

regulation of mitochondrial shape. Additionally, it has been shown to play a role in the regulation of cristae remodeling, which can be independent of its role in fusion (Frezza *et al.*, 2006). There are 8 different isoforms of OPA1 and it has been shown that the long form of OPA1 (L-OPA1) can undergo proteolytic cleavage by mitochondrial proteases (such as PARL, paraplegin, mAAA, and OMA1) under a number of conditions including cristae remodeling and apoptosis (Cipolat *et al.*, 2006;Duvezin-Caubet *et al.*, 2007;Akepati *et al.*, 2008;Ehses *et al.*, 2009). Downregulation of OPA1 also plays a role in the regulation of targeting dysfunctional mitochondria for degradation, which is reviewed in Appendix 1 and 2 (Twig *et al.*, 2008a).

Studies utilizing OPA1 overexpression and loss-of-function have demonstrated a role of OPA1 in the regulation of mitochondrial morphology. However, differing morphology results were obtained depending on the isoform of OPA1 targeted. Therefore, understanding the exact role of OPA1 can be complicated because it is based on the predominant form of OPA1 that is present, which can be further altered via proteolytic cleavage (Liesa *et al.*, 2009). The exact mechanism by which OPA1 promotes inner mitochondrial membrane fusion is not known. However, progress is being made in this area (Zhang and Chan, 2007;Meeusen and Nunnari, 2007;Rujiviphat *et al.*, 2009). Cipolate *et al.* demonstrated that OPA1 functionally requires Mfn1 to regulate mitochondrial fusion but not Mfn2 (Cipolat *et al.*, 2004).

Mfn1 and 2 are approximately 80% homologous and both participate in outer mitochondrial membrane fusion. They also have functionally diverse roles as demonstrated by their differential regulation of fusion (Cipolat *et al.*, 2004). The Mfns

can form both homo- and heterodimers to promote tethering of neighboring mitochondria, which is necessary for the first step of fusion. Whole body knockouts of both Mfn1 and Mfn2 are embryonically lethal midgestation. It was determined that Mfn2-deficiency is lethal due to dramatic disruptions in placental development, specifically in trophoblast giant cells (Chen *et al.*, 2003). While the role of Mfn1 is primarily in mitochondrial fusion, Mfn2 has a number of roles besides fusion. Mfn2 has been shown to play a role in the regulation of oxidative metabolism, cell cycle, cell death, and mitochondrial axonal transport (Liesa *et al.*, 2009). Additionally, it has been shown that Mfn2 is located on endoplasmic reticulum (ER), where it can regulate ER morphology and ER to mitochondria tethering. This process is required for efficient Ca^{2+} homeostasis and buffering (de Brito and Scorrano, 2008). Currently, it is unknown whether all of these functions are mediated through mitochondrial fusion or if they take advantage of another function of Mfn2. Knockdown of Mfn2 results in fibroblasts and L6E9 myotubes results in depolarization of mitochondrial membrane potential, as well as reduced oxygen consumption and substrate oxidation (Bach *et al.*, 2003;Pich *et al.*, 2005).

In vascular smooth muscle cells, overexpression of Mfn2 has been shown to cause growth arrest and inhibition of proliferation. Chen *et al.* found that Mfn2 expression was markedly reduced in hyper-proliferative vascular smooth muscle cells (VSMCs) from a number of different animal models of vascular proliferative disorders. Overexpression of Mfn2 suppressed VSMC proliferation in culture and blocked balloon injury induced VSMC proliferation and restenosis in rat carotid arteries (Chen *et al.*, 2004). Additionally, Mfn2 overexpression has been shown to inhibit atherosclerotic lesion

formation in rabbits (Guo *et al.*, 2007). Mfn2 regulation of the cell cycle is mediated by the interaction of Mfn2 and p21Ras. Mfn2 binds and sequesters Ras, which inhibits its downstream signaling pathway (Raf-MEK1/2-ERK1/2) and therefore its ability to regulate proliferation, differentiation, cell cycle progression (Chen *et al.*, 2004). Mfn2 plays a role in apoptosis in addition to proliferation. Mfn2 has been shown to interact with members of the Bcl-2 family that regulate the intrinsic mitochondrial death pathway. Mfn2 interacts with pro-apoptotic Bak and anti-apoptotic Bcl-2 and BclxL. Brooks *et al.* have shown that during apoptosis Bak dissociates from Mfn2 and enhances the association with Mfn1. Mutations in the BH3 domain of Bak prevent the dissociation of Bak and Mfn2 and thus the association of Bak with Mfn1. In this mutant, the fragmentation associated with apoptosis was also absent. Therefore, the association/dissociate seems to be an important point of regulation of apoptosis and the concomitant mitochondrial fragmentation (Brooks *et al.*, 2007).

All of this evidence demonstrates that mitochondrial fusion and the components that regulate fusion are important regulators of cellular functions. In particular, Mfn2 has been shown to contribute to a wide range of both mitochondrial and cellular processes. These functions of Mfn2 imply that it could be important in the pathogenesis of a number of diseases.

1.4d The Relationship between Mitochondrial Dynamics and Bioenergetics

There is some evidence that there is a relationship between mitochondrial dynamics and bioenergetics. For example, when mitochondrial membrane potential is depolarized there is altered mitochondrial fusion capacity. This is in part due to proteolytic cleavage of OPA1 that inhibits fusion ability (Duvezin-Caubet *et al.*, 2006). This is probably

occurring because depolarization is a signal for dysfunctional mitochondria that should be targeted for degradation. OPA1 degradation is a key point of regulation that prevents dysfunctional units from fusing back with the network (this is reviewed in detail Appendix 1) (Twig *et al.*, 2008a). Additionally, it has been shown that alterations in the expression of some mitochondrial dynamics proteins results in changes to oxygen consumption and energy production. Mfn2 deficiency in myotubes leads to reduced mitochondrial membrane potential and oxygen consumption (Pich *et al.*, 2005). Mitochondrial fission also seems to be associated with bioenergetic capacity. Downregulation of Drp1 expression impaired oxygen consumption and reduced the rate of ATP synthesis in HeLa cells (Benard and Rossignol, 2008). It has also been shown that the use of rotenone to inhibit ETC activity at complex I results in decreased membrane potential, increased ROS production, and fragmented mitochondrial morphology (Benard *et al.*, 2007). These data suggest that both mitochondrial fusion and fission can influence bioenergetics and that this could be a bidirectional relationship.

1.4e Mitochondrial Dynamics and Disease

Alterations to mitochondrial fusion and fission have been demonstrated in a number of conditions including neurodegeneration, obesity, and type 2 diabetes. Additionally, mutations in mitochondrial dynamics proteins have been identified in human pathologies. Mutations in OPA1 leads to autosomal dominant optic atrophy (ADOA), which is the most common form of hereditary optic neuropathy. It begins with impairment of vision during early childhood. The primary cell affected by ADOA is the retinal ganglion cell. Currently, 230 gene mutations have been identified in OPA1 (Ferre *et al.*, 2005).

Charcot-Marie-Tooth (CMT) disease is a group of genetically heterogeneous diseases of the peripheral nervous system, characterized by distal muscle atrophy. It is one of the most commonly diagnosed hereditary diseases and it is the most commonly diagnosed hereditary neuropathy (Skre, 1974). More than 40 mutations in Mfn2 have been identified that result in CMT Type 2A (Zuchner *et al.*, 2004). Interestingly, cultures of skin fibroblasts from four CMT2A patients with mutations in the Mfn2 gene did not display altered mitochondrial morphology. However, they did have increased in uncoupled oxygen consumption and decreased mitochondrial membrane potential (Loiseau *et al.*, 2007). This implies that the dysfunction observed in CMT2A may be due to a function of Mfn2 besides mitochondrial fusion.

Changes in mitochondrial morphology and mitochondrial function have also been identified in a number of disease states. These data implicate mitochondrial dynamics in the pathogenesis of a large number of diseases, not just the subset that arise from mutations in mitochondrial dynamics proteins. In particular there is mounting evidence that alterations in mitochondrial dynamics influence the development of metabolic and neurodegenerative diseases (Bossy-Wetzel *et al.*, 2003;Zorzano *et al.*, 2009;Schafer and Reichert, 2009;Han *et al.*, 2011). These data place mitochondrial dynamics and function at the crossroads of human pathologies.

1.4f Evidence that Mitochondria Contribute to the Development of Diabetes

There is growing data demonstrating that mitochondrial dynamics contribute to the pathogenesis of diabetes. Alterations in mitochondrial architecture and mitochondrial dynamics proteins have been found in both β-cells and peripheral tissues.

Mitochondrial dysfunction has been reported in skeletal muscle of obese subjects and diabetic patients. Reduced mitochondrial size is observed in skeletal muscle of obese (Toledo *et al.*, 2006) and type 2 diabetic patients (Kelley *et al.*, 2002) compared with control subjects. Additionally, Zucker Fatty (ZF) rats have decreased mitochondrial networking ability and reduced Mfn2 expression (Bach *et al.*, 2003). Skeletal muscle biopsies from control and obese patients indicate that Mfn2 gene and protein expression is decreased in obese muscle (Bach *et al.*, 2003;Bach *et al.*, 2005). Both obese and non-obese type 2 diabetic patients were also found to have decreased Mfn2 mRNA expression in skeletal muscle (Bach *et al.*, 2005). Interestingly, when obesity was treated with bilio-pacreatic diversion (Mingrone *et al.*, 2005) or Roux-en-Y gastric bypass (Gastaldi *et al.*, 2007), Mfn2 mRNA level was increased in skeletal muscle. Exercise is another intervention that has also been shown to increase skeletal muscle Mfn2 gene expression in healthy subjects (Cartoni *et al.*, 2005). All of these data suggest that alterations in mitochondrial morphology are a common occurrence in obesity and diabetes and that Mfn2 could be playing a specialized role in the development of these diseases.

Mitochondrial alterations have been found in β-cells of animal models of diabetes. Bindokas *et al.* demonstrated that there is an increase in mitochondrial superoxide in response to glucose in normal islets. In Zucker Diabetic Fatty (ZDF) rats, there was a significantly higher level of mitochondrial superoxide compared with lean controls. Moreover, they found that islets isolated from ZDF rats exhibit fragmented mitochondrial morphology (Bindokas *et al.*, 2003). Higa *et al.* have also demonstrated altered mitochondrial morphology in β-cells of ZDF rats. They observed large, swollen mitochondria with clear mitochondrial remodeling and altered cristae structure (Higa *et*

al., 1999). Additionally, they were able to prevent these alterations to mitochondria structure with the treatment of ZDF rats with troglitazone (Higa *et al.*, 1999). Changes in mitochondrial architecture have also been observed in animals fed a high fat diet and are in agreement with what was observed in ZDF animals. Mitochondrial area per β-cell was found to be approximately 2-fold greater in HFD compared to control β-cells (Fex *et al.*, 2007).

Diabetic islets from patients have reduced ATP levels, a lower ATP/ADP ratio and impaired hyperpolarization of the mitochondrial membrane. Increased protein expression of UCP-2, complex I and the ATP synthase of the respiratory chain, and a higher level of reactive nitrogen species were also found in type 2 diabetic islets. Additionally, diabetic β-cells displayed an increase in mitochondrial volume albeit a similar number of total mitochondria compared with control β-cells (Anello *et al.*, 2005). These β-cells also have a vastly different architecture than the control β-cells and appear to be fragmented with disrupted cristae morphology.

Evidence from both skeletal muscle and β-cells demonstrate that changes in mitochondrial function and morphology are a common occurrence in diabetic tissues. Whether changes in β-cell mitochondrial dynamics are a cause or consequence of diabetes is not currently known. Studies on the function of mitochondrial dynamics in β-cells are necessary to better understand the role of mitochondrial dynamics under normal physiological conditions and in the development of β-cell dysfunction in disease states.

1.5 Research Objectives and Organization of the Dissertation

Obesity and type 2 diabetes are a huge health and financial burden in the United States and worldwide. This seems especially significant considering the current trend for increased incidence and prevalence of obesity and type 2 diabetes in younger age demographics. A better understanding of the pathogenesis of these diseases could provide new potential drug targets to fight these epidemics. The work presented in this dissertation focuses on the role of mitochondrial dynamics and function in the pancreatic β-cell. This was investigated because while it has been long known that mitochondria play a critical role in fuel utilization and the generation of secretagogues in β-cells, the contribution of mitochondrial fusion and fission had not been studied. In fact, it had been proposed that mitochondrial dynamics may not be important in primary β-cells given their short length. The central hypothesis of this work is that proper control of mitochondrial functions, including mitochondrial dynamics, is critical for maintenance of nutrient sensing and response to both acute fuel challenges and high nutrient environments in β-cells. Moreover, we hypothesize that mitochondrial dysfunction contributes to impaired metabolic function, obesity, and diabetes. To test this hypothesis, we utilized a multilevel approach that incorporated work done *in vivo* to study whole body metabolic function in living animals and *in vitro* in clonal β-cell lines and isolated islets under various nutrient conditions. We utilized a number of different methods including live cell confocal imaging, whole body metabolic phenotyping, and respirometry in whole islets, which are presented throughout this dissertation.

Initially, we wanted to characterize mitochondrial dynamics in β-cells and understand the effect of nutrients on mitochondrial fusion and fission in β-cells. We focused on the

effects of glucolipotoxicity, an *in vitro* model of obesity and diabetes that is known to have a detrimental effect on β-cell function and viability. We demonstrated that β-cell mitochondria undergo continuous cycles of fusion and fission. We found that in response to a toxic nutrient environment, β-cells become fragmented, which was due to a decrease in mitochondrial fusion capacity. Maintaining mitochondrial morphology in a "fused" state by inhibiting mitochondrial fission prevented the effects of GLT on mitochondrial fusion and apoptosis. This demonstrated that mitochondria require a tight balance between mitochondrial fusion and fission in order to maintain both mitochondrial function and viability. Therefore, we conclude that disruptions in the balance of mitochondrial dynamics in the β-cell may lead to pathologic states, such as obesity and diabetes. All of this work can be found in Chapter 2: Characterization of Mitochondrial Dynamics in the Pancreatic Beta Cell: A Mechanism of Protection Against Nutrient-Induced Cell Death.

In Chapter 3: The Role of the Mitochondrial Fusion Protein, Mfn2, in β-Cell Control of Whole Body Nutrient Utilization, we sought to further investigate the role changes in mitochondrial fusion have in response to chronic exposure to high fuel surroundings. We first examined the levels of mitochondrial fusion proteins in islet isolated from animal models of obesity and diabetes. Mfn2 was decreased in islets of HFD and Zucker Diabetic fatty rats. To understand the role of mitochondrial fusion in β-cells, we generated a Mfn2KO mouse where Mfn2 excision was mediated by RIP-Cre. This resulted in Mfn2 knockout in β-cells and a subset of neurons in the hypothalamus. These mice exhibited severe metabolic dysfunction including hyperglycemia, impaired glucose tolerance, uncoordinated insulin secretion and obesity. Currently, we have not been able

to rule out that Mfn2 excision in the hypothalamus is driving the whole body metabolic phenotype in these mice. However, we do know that *ex vivo* excision of Mfn2 from the β-cell resulted in basal hypersecretion of insulin. Increased insulin secretion at unstimulatory glucose concentrations is emerging as a hallmark of diabetes and has been observed in animal models of obesity and diabetes, as well as obese and diabetic patients. Finally, we examined the mechanism behind increased basal hypersecretion in βMfn2KO islets, which led to a more general investigation of how nutrients affect bioenergetic efficiency in islets. Changes in insulin secretion were not due to cytosolic Ca^{2+} concentrations or ROS, which was, interestingly, lower in βMfn2KO islets compared to controls. However, we did find changes in stimulatory oxygen consumption and bioenergetic efficiency in βMfn2KO islets. Increased proton leak was determined to occur in islets in response to acute nutrient stimulation, chronic elevated fuel levels, high oxidative stress, and due to Mfn2 deficiency. We hypothesize that the induction of uncoupled respiration could be contributing to nutrient detoxification and/or basal insulin secretion, which is further expanded upon in Chapter 4: Islet Respiratory Proton Leak is Regulated by Nutrients, ROS, and Mfn2 Deficiency.

The finding of this research points to a prominent role for mitochondrial dynamics and bioenergetic function in the ability of β-cells to respond to nutrient stimulation in both physiologic and pathologic conditions. We present potential models by which increased alterations to mitochondrial function could be contributing to some of the metabolic dysfunction observed in obesity and diabetes. Understanding how β-cell mitochondrial dynamics and bioenergetic efficiency contribute to normal and pathologic β-cell function could provide further insight into the development and progression of metabolic diseases.

Furthermore, this work in combination with prospective studies could, in the future, provide new potential therapeutic targets. A full explanation of this work can be found in Chapter 5: Discussion, Implications, and Future Directions.

Two appendixes are also presented in this work: Appendix 1: Mitochondrial Dynamics and Autophagy and Appendix 2: Mitochondrial Fusion and Mitochondrial Fusion Proteins Represent Important Points of Regulation for Mitophagy. These are works that have been completely but do not fit strictly into the scope of the experimental work that has been completed. Appendix 1 is a chapter that was written for the text book: Mitochondrial Dynamics and Neurodegeneration and focuses on the role of mitochondrial fusion and fission in mitochondrial quality control and mitochondrial turnover. Most of this chapter is in the context of how dysregulation of mitochondrial dynamics and mitophagy contribute to neurodegeneration. Appendix 2 also focuses on the role of mitochondrial dynamics in mitochondrial quality control and mitochondrial degradation. However, in this review we take a more focused look at the role of mitochondrial fusion in mitophagy, with emphasis on the fusion protein, OPA1. This is of interest because it is generally thought that mitochondrial fission plays a more prominent role in mitochondrial autophagy. We proposed that a balance between mitochondrial fusion and fission is essential for this process. Mitochondrial quality control was not specifically addressed in our experimental work on the βMfn2KO mouse, but this would be an interesting avenue to peruse in the future.

Chapter 2: Characterization of Mitochondrial Dynamics in the Pancreatic Beta Cell: A Mechanism of Protection Against Nutrient-Induced Cell Death

Adapted from the publication: Molina AJ, Wikstrom JD, Stiles L, Las G, Mohamed H, Elorza A, Walzer G, Twig G, Katz S, Corkey BE, Shirihai OS (2009). Mitochondrial networking protects beta-cells from nutrient-induced apoptosis. *Diabetes.* 58, 2303-15. (Molina *et al.*, 2009)

In this data chapter I contributed to cell culture and viral transductions, western blot analyses, mitochondrial morphology determination, and insulin secretion experiments.

2.1 Abstract

Previous studies have reported that β-cell mitochondria exist as distinct organelles that exhibit heterogeneous bioenergetic capacity. However, mitochondrial networking activity and its role in mediating β-cell mitochondrial morphology and function had not been established. In this experimental series, we investigate mitochondrial fusion and fission in β-cells and whether morphology responds to changes in nutrient levels. Using matrix-targeted photoactivatable green fluorescent protein, mitochondria were tagged and tracked in β-cells within intact islets, as isolated cells and as cell lines, revealing frequent fusion and fission events. Manipulations of the key mitochondrial dynamics proteins OPA1, DRP1, and Fis1 were tested for their role in β-cell mitochondrial morphology. In addition, the combined effects of free fatty acid and glucose on β-cell survival, function, and mitochondrial morphology were explored with relation to alterations in fusion and fission capacity. Despite their short size, β-cell mitochondria undergo constant fusion and fission events that underlie their morphology. We found that mitochondrial networking activity is able to distribute matrix-localized green fluorescent protein signal throughout β-cells within an intact islet, isolated β-cells, and a β-cell line. Under toxic high nutrient conditions, we find that β-cell mitochondria become fragmented and lose

their ability to undergo fusion. Manipulations that shift the dynamic balance to favor fusion are able to prevent mitochondrial fragmentation, maintain mitochondrial dynamics, and prevent cell death. These data suggest that alterations in mitochondrial fusion and fission play a critical role in nutrient-induced β-cell apoptosis and may be involved in the pathophysiology of type 2 diabetes.

2.2 Introduction

β-cell mitochondria integrate signals, such as extracellular glucose in the form of pyruvate, and generate the ATP that triggers a cascade of events concluding with the release of insulin. Therefore, β-cell mitochondria have become an important target for investigations into β-cell physiology and the etiology of Type 2 Diabetes. Mitochondria are highly dynamic organelles whose morphology is regulated by cycles of fusion and fission (Amchenkova *et al.*, 1988;Bereiter-Hahn *et al.*, 1994;Skulachev, 2001;Otera and Mihara, 2011). Mitochondrial networks are formed when mitochondria undergo fusion events that cause the compartments of participating mitochondria to become continuous. As a result, the mitochondria that go through a fusion event share solutes, metabolites, and proteins (Nakada *et al.*, 2001;Arimura *et al.*, 2004;Chen *et al.*, 2005b) as well as a transmembrane electrochemical gradient (Skulachev, 2001;Twig *et al.*, 2006), this process is known as inter-mitochondrial complementation. The disruption of such networks, as displayed by fragmented mitochondrial network, has been shown to play an important role in the progression of cells to apoptosis, particularly in cases where ROS are involved (Yu *et al.*, 2006). As such, mitochondrial networking is thought to be a potential defense mechanism allowing for the buffering of mitochondrial ROS and calcium overload (Szabadkai *et al.*, 2004;Frieden *et al.*, 2004).

Chronically elevated levels of glucose and fatty acid, termed glucolipotoxicity, are thought to contribute to the progression of type 2 diabetes by adversely affecting β-cells and consequently leads to a decline in insulin secretion (El-Assaad *et al.*, 2003). *In vivo*, a reduction in insulin gene expression due to reduced binding of the transcription factor pancreatic and duodenal homeobox 1 (Pdx-1) has been observed in rats perifused with glucose and intralipids (Hagman *et al.*, 2008;Poitout, 2008). In addition, exposure to high levels of glucose and/or free fatty acid has been shown to affect β-cell viability by inducing mitochondrial-mediated cell death and has been linked to ROS-induced mitochondrial calcium overload and damage (Robertson, 2006;Robertson *et al.*, 2007). Recent studies indicate that nutrient-induced ROS increases subcellular mitochondrial membrane potential heterogeneity and fragmentation of the mitochondrial architecture (Karbowski *et al.*, 2004;Wikstrom *et al.*, 2007). These findings suggest that mitochondrial dynamics might play a role in the effects of noxious stimuli, through the regulation of mitochondrial morphology. Although the functional significance of these changes has not been studied in β-cells, studies of mitochondrial morphology in other cells have demonstrated that the ability of mitochondria to form networks influences both ROS and calcium handling (Szabadkai *et al.*, 2004;Frieden *et al.*, 2004;Yu *et al.*, 2006).

Mitochondria play an essential role in β-cell insulin secretion function, yet a complete study of mitochondrial fusion and fission has not yet been investigated in β-cells. The elucidation of this is particularly important given that previous studies have reported that mitochondria from primary β-cells form less elaborate network structures compared with other cell types, COS cells for example. This information has raised doubts as to the

existence of mitochondrial networking in β-cells. Until recently, technologies for examining and quantifying the ability of mitochondria to undergo fusion and fission were not readily available or physiologically relevant. Currently, mitochondrial fusion events can be measured using a polyethylene glycol (PEG) fusion assay, where whole cells have to be fused in order to measure mitochondrial fusion (Cipolat *et al.*, 2004) or by utilizing mitochondrial matrix-target photoactivatable green fluorescent protein (PA-GFPmt), which can also monitor fission events (Karbowski *et al.*, 2004). The use of PA-GFPmt to measure mitochondrial fusion will be further described in this chapter.

In this work, we show that the densely packed appearance of mitochondria in the β-cell represents the existence of multiple juxtaposed units that do not share continuous matrix lumen but do go through frequent fusion and fission events. We further demonstrate that mitochondrial dynamics are disrupted by exposure to the combination of high fat and glucose, gradually leading to the arrest of fusion activity and complete fragmentation of the mitochondrial architecture. Inhibiting mitochondrial fission preserved mitochondrial morphology and dynamics and prevented β-cell apoptosis.

2.3 Material and Methods

2.3.1 Islet isolation, primary cell and cell line culture

Islets of Langerhans from 10-12 week old male C57/Bl6 mice were isolated and dispersed as previously described (Heart *et al.*, 2006). Briefly, mice are asphyxiated with carbon dioxide and then opened to expose the abdominal cavity. A clamp is placed on common bile duct at the site where it enters the duodenum to occlude collagenase from entering the intestines. The pancreas is then filled with collagenase through the common

bile duct. The pancreas is digested by the collagenase until this process is stopped by the addition of Hanks Balance Salt Solution with 1% BSA. Islets are separated from other pancreatic cells by using a histopaque gradient. Once islets are collected, they are washed and allowed to incubate overnight.

Rat insulinoma cells (INS1; pancreatic tumor β-cells) were grown in monolayer cultures and kept at 37°C in a humidified (5% CO2, 95% air) atmosphere in 11mM glucose RPMI 1640 medium supplemented with 10mM HEPES, 10% FBS, 2mM L-glutamine, 1mM sodium pyruvate, and 50μM β-mercaptoethanol. B-cells were exposed to the following conditions: high glucose (HG), 20mM glucose and 1% FBS in the presence of 0.5% BSA; high fat (HF), 11mM glucose and 0.4mM Palmitate (Sigma, St. Louis, MO) bound to 0.5% BSA; high fat low glucose (HFLG), 5mM glucose and 0.4mM Palmitate bound to 0.5% BSA; and high fat and glucose (HFG), 20mM glucose and 0.4mM Palmitate bound to 0.5% BSA. 24 hour BSA binding was used for all conditions.

2.3.2 Generation of Fis1 RNAi and PAGFPmt constructs

Two complementary oligonucleotides were designed specifically for rat Fis1 silencing. They contain both MluI and ClaI sites at 5' and 3' ends respectively and a 5' phosphate modification. Sense: 5' cgc-gtg-ccc-agg-cat-cgt-gct-gct-gga-gtt-caa-gag-act-cca-gca-gca-cga-tgc-ctt-ttt-tgg-aaa-t 3', Antisense: 5' cga-ttt-cca-aaa-aag-gca-tcg-tgc-tgc-tgg-agt-ctc-ttg-aac-tcc-agc-agc-acg-atg-cct-ggg-ga. The primers were annealed and cloned into pLVCTH lentiviral vector (Trono lab, Lausanne, Switzerland) at the MluI and ClaI sites. The positive clone siFis1 – pLVCTH was verified by DNA sequencing. PAGFPmt design was described previously (Twig *et al.*, 2006).

The DRP1 DN (DRP1K38A) construct was generously provided by Gyorgy Hajnoczky (Saotome *et al.*, 2008) and cloned into a lentiviral vector as described above. OPA1 overexpression construct was generously provided by Luca Scorrano and recombinant adenovirus made using the AdEasy system according to manufacturer specifications (Cipolat *et al.*, 2004).

2.3.3 Lentivirus generation

Lentiviral particles were generated by transient transfection of 293T cells using fugene6 (Roche, Nutley, NJ) according to manufacturer's instructions and the three-plasmid system according to Tronolab's protocols (www.tronolab.com). This system is comprised of the packaging plasmid pCMV-dR8.91, the envelope coding plasmid pMD2.G and the transfer vector plasmid pLVCTH. The lentivirus was harvested from 293T cells for three consecutive days and concentrated by centrifugation as previously described (Rubinson *et al.*, 2003). Transduction efficiency was determined by the level of GFP expressed by the host cells and by western blot.

2.3.4 Mitochondrial dynamics assays

2.3.4a Confocal Imaging

Confocal microscopy was performed on live cells in glass bottom dishes (MatTek, Ashland, MA). A Zeiss LSM 510 Meta microscope with a plan apochromat 100x (NA = 1.4) oil immersion objective was used for experiments involving primary β-cells and time-lapse mitochondrial tracking experiment. Other experiments were performed on an inverted Leica TCS SP2 confocal microscope (Wetzlar, Germany) upgraded with an acousto-optical beam splitter system and configured for 2-photon microscopy using a Coherent Mira 900 femto second laser (Santa Clara, CA).

2.3.4b Tagging and tracking mitochondria with matrix-targeted photoactivatable green fluorescent protein

Primary β-cells and INS1 cells were transfected with PAGFPmt expressed under the insulin promoter and allowed to accumulate in the mitochondrial matrix for 48–72 h. Mitochondria were labeled with 7 nM TMRE (tetramethylrhodamine-ethyl-ester-perchlorate; Invitrogen, Eugene, OR) for 45 min prior to imaging to allow visualization. The transition to active GFP was achieved by photoisomerization using 2-photon laser 750 nm excitation to give a 375 nm photon equivalence at the focal plane. This allowed for selective activation of regions <0.5 μm2 (Zeiss LSM510) or >4 μm2 (Leica TCS SP2). In the absence of photoactivation, PAGFPmt protein molecules remained stable in preactivated form. The presence of preactivated PAGFPmt was detected using high-intensity excitation at 488 nm in combination with a fully opened collection pinhole.

2.3.4c Whole-cell mitochondrial fusion assay

We used the dilution of PAGFPmt into the mitochondrial web as an index for mitochondrial fusion (Karbowski *et al.*, 2004). A region of interest (ROI) occupying 10–15% of the cell in one confocal section was activated using a 2-photon laser (350 nm equivalence at the focal plane). The dilution of activated PAGFPmt within the mitochondrial web was assessed by repeatedly scanning the entire cell volume (six confocal z-axis section projection) at 3- to 10-min time intervals for 50 min.

Controls for laser or fluorophore induced toxicity in PAGFPmt fusion assay experiments were reported in detail previously (Twig *et al.*, 2006). Briefly, careful attention was devoted to determining the dye concentrations and laser parameters that would prevent photodamage-induced artifacts. Intense activation of TMRE can damage mitochondria,

causing depolarization or destruction. The minimum intensity and duration of laser exposure that initiated changes in ΔΨm and/or mitochondrial morphology in cells treated with TMRE was determined. The parameters utilized in the reported experiments were well below those thresholds. To determine the safety limits of 2-Photon laser stimulation in INS1 and β-cells, excitation was delivered over a wide range of intensities and durations. We find that excitation with 600 milliseconds/μm2 at 1mW laser intensity at the objective is the threshold dosage for both cell types above which a reduction in mitochondrial membrane potential can be observed. All experiments using 2-photon illumination were conducted with duration of 150 ms/μm2 and an intensity of 1mW.

2.3.4d Image analysis

Quantification of fusion was performed using Metamorph (Molecular Devices, Sunnyvale, CA) by measuring the average fluorescence intensity (FI) of the mitochondria that became PAGFPmt positive based on a fixed threshold. The GFP FI values of PAGFPmt dilution were normalized to the GFP FI value immediately after photoactivation and then fitted to a hyperbolic function: $F(t) = 1 - Fplateau \times t/(t + T50)$. F and Fplateau denote FI at time t and in the plateau phase. T50 denotes the time interval to a 50% decrease in normalized GFP FI ([1 − Fplateau]/2). All fitting procedures and statistical tests were conducted using Kaleida-Graph software (Synergy Software, Reading, PA). Paired Student's t tests were performed to calculate statistical significance. Prior to measuring FI, we used an integrated morphometry analysis function designed for these experiments to extract PAGFPmt-positive structures that were larger than 10 pixels. These areas were interpreted to be mitochondria, and their TMRE FIs were recorded. This procedure enabled the selection of mitochondrial structures using very low threshold

levels in the green channel (~10% of the image average intensity), assuring that >90% of the mitochondrial pixels were included for analysis. To set the threshold level, a test-threshold function first measured the average green FI of the mitochondria. The lower (inclusive) threshold was set at two-thirds of this average. Prior to analysis, all images were scanned to verify that all intensity measurements were below saturation; therefore, an upper threshold was not necessary.

2.3.5 Quantitative analysis of mitochondrial fragmentation

Confocal sections were obtained from β-cells and INS1 cells in order to analyze mitochondrial morphometry. Individual confocal sections were used to illustrate and quantify morphometry of β-cells and INS1 cells since z-projections of 3 dimensional reconstructions introduce significant overlap between separate mitochondria residing in different focal planes. For quantitative morphometric analysis performed in INS1 cells, each of 7 confocal sections was analyzed for each cell. The number and geometric properties of mitochondrial webs were measured using the 'particle analysis' feature of ImageJ (NIH, Bethesda, MD). A single web is defined as a continuous cluster of (at least 10) TMRE-positive pixels, regardless of matrix continuity. For each web, the perimeter, area maximal and minimal aspect length were measured and the aspect ratio (AR; maximal aspect divided by minimal aspect) was derived.

2.3.6 Immunostaining

Fis1 RNAi and empty vector RNAi expressing INS1 cells were plated on MatTek glass bottom dishes (MatTek) or poly-D-lysine coated cover slips and cultured in the presence or absence of HFG. After 24 hrs, the cells were washed once with PBS and fixed with

4% paraformaldehyde for 15 minutes. Cells were then washed three times with PBS, permeabilized in 0.2% Triton-X for 15 minutes, and washed three more times with PBS. Blocking was performed with 1% BSA/PBS for 15 minutes at room temperature. Cells were incubated in the presence of Cleaved Caspase-3 antibody (Cell Signaling Technology) diluted 1:100 or DLP-1 (DRP-1) antibody (BD transduction laboratories, Franklin Lakes, NJ) diluted 1:500 in 1%BSA/PBS for 1 hr at room temperature (secondary only controls were incubated in blocking solution). After incubation with primary antibody, cells were washed 3 times in 1%BSA/PBS. TRITC-conjugated goat anti-rabbit secondary antibody (Zymed/Invitrogen) diluted 1:100 in 1%BSA/PBS was then added to the cells for 1 hr at room temperature. Cells probed for DLP-1 were incubated with anti mouse secondary antibody conjugated with Alexa 488 (Zymed/Invitrogen), Cells were then washed 3 times with PBS at 37°C. Cells grown on cover slips were mounted onto Superfrost microscope slides with Mowiol mounting media. Imaging was performed on an Olympus BX-61 fluorescence microscope with a Photometrics CoolSnap HQ CCD camera (Roper Scientific, Trenton, NJ) or on an inverted Leica TCS SP2 confocal microscope (Wetzlar, Germany).

2.3.7 Western Blotting

Primary antibodies used include anti-Fis1 (BioVision, Mountain View, CA), anti-Beta-Actin (Novus Biologicals, Littleton, CO), anti-Akt (Cell Signaling Technology, Danvers, MA), anti-Phospho-Akt (Cell Signaling Technology), anti-DLP-1 (DRP1, BD Transduction Laboratories, Franklin Lakes, NJ), and anti-OPA1 (BD Transduction Laboratories, Franklin Lakes, NJ).

2.3.8 Insulin Secretion

INS1 cells infected with either Fis1 RNAi or empty vector pLKO.1 were cultured in RPMI media supplemented with 10% FBS, 10mM HEPES buffer, 1mM pyruvate, 50μM 2-ß-mercaptoethanol, 50U/ml penicillin and 50μg/ml streptomycin. Insulin secretion was run in quadruplicate and collected in a parallel fashion for basal (3mM glucose), stimulatory (15mM glucose), and stimulatory plus KCl conditions. In detail, prior to insulin secretion, cells were cultured for four hours in RPMI containing 1% pen/strep and 10% FCS with either 11mM glucose (control) or 20mM glucose with 0.4mM palmitate (GLT). This was followed by a 1 hour washout period in INS1 media containing 3mM glucose and then a 30 minute preincubation period in modified Krebs-Ringer bicarbonate buffer (KRB) containing (in mM) 119 NaCl, 4.6 KCl, 5 NaHCO3, 2 CaCl2, 1 MgSO4, 0.15 Na2HPO4, 0.4 KH2PO4, 20 HEPES, 0.05% BSA, pH 7.4, containing 3mM glucose. The INS1 cells were then washed and incubated with either 3mM glucose KRB, 15mM glucose KRB, or 15mM glucose plus KCl KRB. The samples were collected and stored at –20°C for insulin measurements. Insulin was measured by radioimmunoassay (LINCO RESEARCH INC., St. Charles, MO.).

2.3.9 Fluorescence-Activated Cell Sorting (FACS)

Apoptotic cells were detected by flow cytometry using fluorescent isothiocyanate-conjugated Annexin V (Molecular Probes) according to the manufacturer's protocol. Briefly, about 106 cells were harvested, washed with PBS by centrifugation at 200 x g for 5 minutes, and resuspended in 100 μl of Annexin-V-florescent labeling solution containing annexin V. Cells were incubated 10–15 minutes at 15–25°C and immediately

analyzed by flow cytometry on a Becton Dickinson FACS Calibur (Heidelberg, Germany).

2.4 Results

2.4.1 Characterizing Mitochondrial Architecture and Dynamics in β-cells

Since mitochondrial dynamics in primary β-cells had not been previously characterized, we first explored mitochondrial fusion and fission events, mitochondrial morphology and the effect of mitochondrial fusion and fission proteins in both primary and clonal β-cells. Additionally, we used a mitochondrial fusion assay to monitor mitochondrial fusion over time.

2.4.1a Mitochondrial Fusion and Fission in Primary β-cells

Primary β-cells isolated from mice exhibit dense mitochondrial architecture as revealed by confocal microscopy. A three-dimensional reconstruction of mitochondria within an entire β-cell has been projected onto a single plain to illustrate the density of these organelles (Figure 2.1A). This morphology suggests the presence of either large continuous networks throughout the cell or, alternatively, small discrete networks juxtaposed with one another. To decipher this complex architecture to its individual components, we double labeled the mitochondrial web with TMRE and PAGFPmt (Twig *et al.*, 2006). Because individual mitochondria are often in apposition with one another, tagging individual mitochondria with PAGFPmt targeted to the matrix allows morphological and biophysical studies of mitochondria within a complex web. In addition, this methodology takes into account organellar movement and mitochondrial dynamics that continuously change the size, shape, and location of the mitochondrion

(Twig *et al.*, 2006). With adenoviral delivery, PAGFPmt is expressed in all β-cell mitochondria but remains in its inactive form (nonfluorescent).

Precise (0.5 μm^2) photoactivation of PAGFPmt molecules was achieved using a 2-photon laser. Equilibration of activated PAGFPmt was immediate and revealed the boundaries of matrix continuity of individual mitochondria. Figure 2.1B shows five sequential photoactivations revealing the boundaries of multiple individual mitochondrial networks in a mouse β-cell. Whereas TMRE staining may show continuous mitochondrial structures, the spread of matrix PAGFPmt is limited to short segments, indicating that these segments do not form a continuous lumen. In 90 photoactivation events performed in nine different cells, we found that most (>95%) individual networks are rod-like in shape with 76% exhibiting a length <2 μm (Figure 2.1C). A series of control studies confirmed that laser intensity was kept at levels that did not affect mitochondrial function or morphology. These included time-lapse studies of $\Delta\Psi m$ in cells exposed to sequential laser scanning and dose-response studies with the 2-photon laser (Twig *et al.*, 2006). The small network size of β-cell mitochondria raises the possibility that mitochondrial fusion is absent in these cells or, alternatively, that fusion events are transient and brief. To address this issue, PAGFPmt was used to detect mitochondrial fusion events. Fusion events were identified by the transfer of PAGFPmt from a labeled mitochondrion to a previously unlabeled one when the two came in contact as shown in Figure 2.1D. Fusion events were commonly followed by fission (11 of 12 events) in a manner that reverted to pre-fusion size and morphology of the involved mitochondria. A similar pattern was observed in INS1 cells (Figure 2.1E).

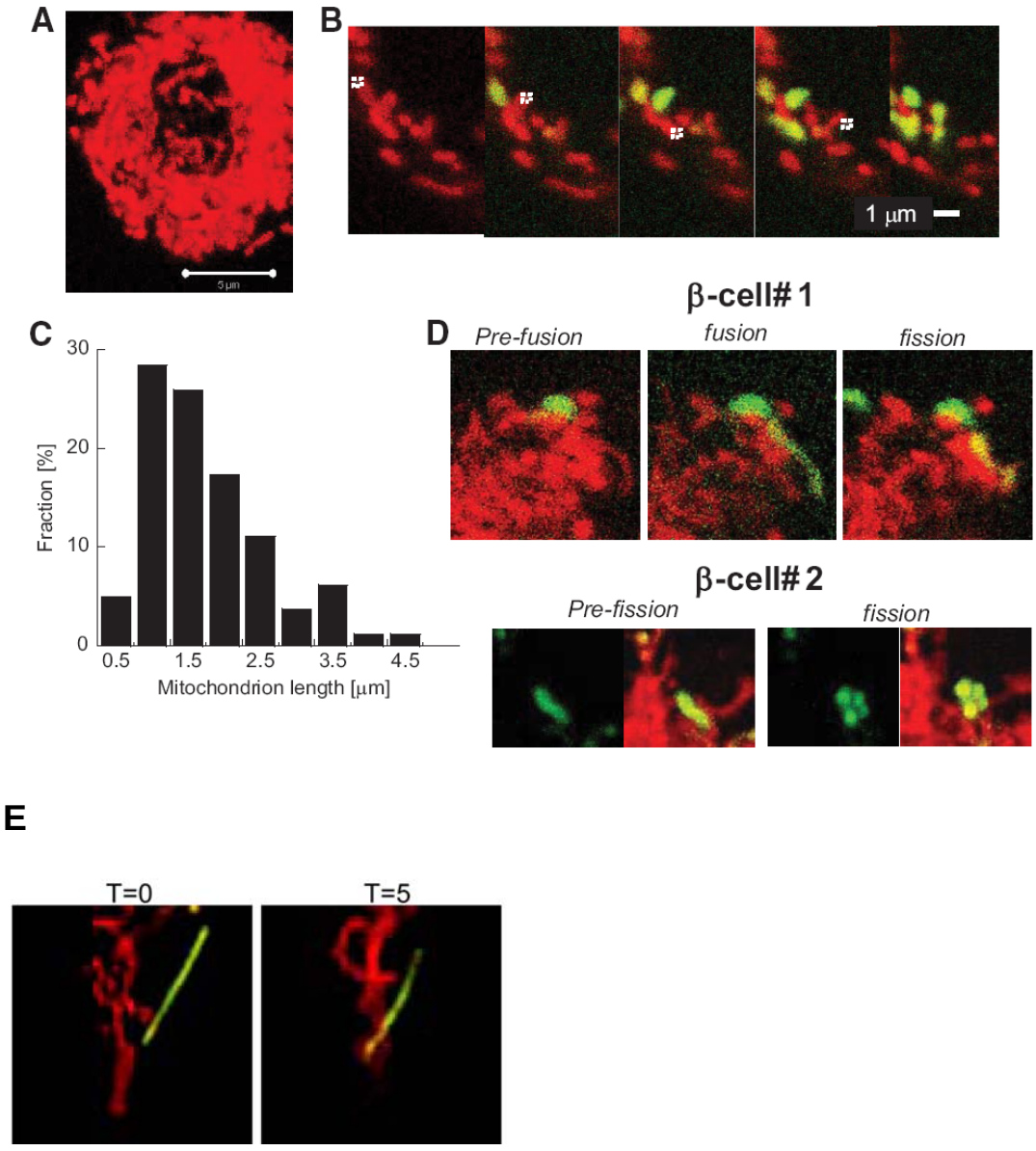

Figure 2.1: Characterization of mitochondrial size and networking in primary β-cells using PAGFPmt. **A.** Projection of confocal images of a cell stained with TMRE. Note that mitochondria are densely packed in β-cells. **B.** Sequential 2-photon laser photoactivation of individual mitochondria. **C.** Summary of mitochondrial size distribution performed by 90 photoactivation steps in 9 cells. **D.** Tagging and tracking individual mitochondria in primary β-cells reveals fusion events (transfer of activated PAGFPmt to juxtaposed unlabeled mitochondria) that are then followed by fission events (separation of previously connected mitochondria). **E.** A fusion event that is followed by a fission event in INS1 cells. Green: PAGFPmt, Red: TMRE. An individual mitochondrion was photolabeled by a short exposure to 2-Photon laser at 750nm resulting in conversion of PAGFPmt to fluorescent PAGFPmt. During a fusion event this

mitochondrion was sharing its PAGFPmt with a neighboring mitochondrion. This was then followed by a fission event.

2.4.1b The Effect of Manipulating Mitochondrial Dynamics Proteins on β-Cells

We undertook a series of experiments designed to manipulate the balance between fusion and fission to assess the consequence on mitochondrial architecture in primary and clonal β-cells. Of particular interest is the fusion protein OPA1 because transcriptom databases suggest its expression levels in the β-cell is uniquely high (www.t1dbase.org). To test the significance of OPA1 in modulating β-cell mitochondrial architecture, we overexpressed the protein by adenoviral transduction. Overexpression of OPA1 in primary β-cells caused mitochondria to fragment into even smaller units (Figure 2.2A). In INS1 cells, transduction with the same number of OPA1 adenoviral particles caused mild overexpression and increased density in mitochondrial architecture. Increasing the amount of virus further increased the expression level and led to fragmentation of the mitochondrial network (Figure 2.2B). These findings suggest that the increased degree of fusion may promote elongation; however, further increases in OPA1 levels can lead to fragmentation. GFP infections were performed to control for potential effects of viral transduction and normalized so that cells were exposed to the same number of viral particles. We found that expression of GFP did not affect mitochondrial morphology in any of the experiments performed.

An alternative approach to examining the consequences of a pro-fusion state is to prevent fission. We found that manipulating the pro-fission protein DRP1 also caused dramatic changes in mitochondrial architecture. Disruption of fission in primary β-cells by overexpressing dominant negative DRP1 (DRP1-DN) resulted in swelling of the

mitochondria and formation of large mitochondria that likely represent a superfused state (Figure 2.2C). In INS cells, similar treatment with DRP1- DN caused the formation of very elongated mitochondrial tubules along with the appearance of swollen sections of the mitochondrial networks (Figure 2.2D).

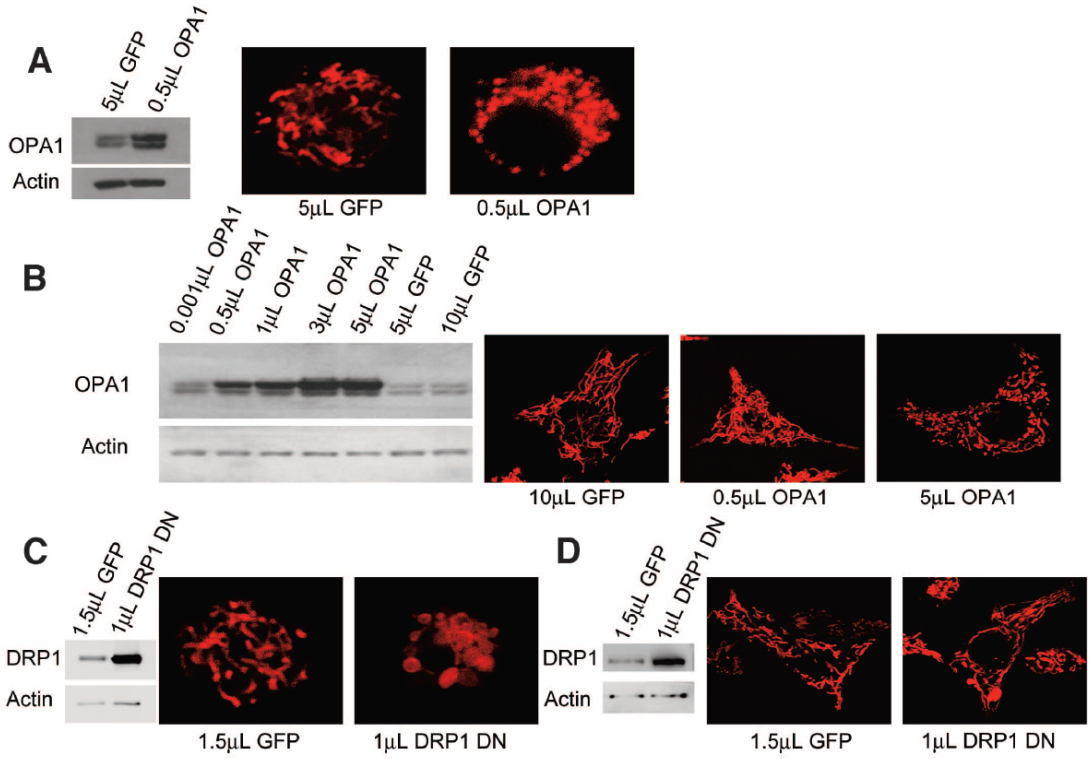

Figure 2.2: Mitochondrial fusion and fission proteins modulate mitochondrial morphology in primary and clonal β-cells. **A.** In primary β-cells, overexpression of the fusion protein OPA1 leads to mitochondrial fragmentation. Overexpression was achieved by adenoviral transduction of GFP or OPA1 at equal concentrations of viral particles. **B.** Level of OPA1 overexpression in INS1 cells was controlled by the dose of viral particles used. Mild overexpression causes mitochondria to take on a dense and elaborate morphology compared with controls. Further increases in OPA1 overexpression levels resulted in mitochondrial fragmentation. **C.** In primary β-cells, overexpression of DN DRP1 to reduce mitochondrial fission leads to mitochondrial swelling. **D.** In INS1 cells, overexpression of DN DRP1 leads to network superfusion and a limited amount of mitochondrial swelling. The number and concentration of viral particles used in **A, C,** and **D** was identical.

2.4.1c Assessing Mitochondrial Fusion in β-Cells with a Mitochondrial Fusion Assay

The overall rate of mitochondrial fusion activity within an isolated β-cell was assessed by photoactivating a subpopulation of mitochondria and monitoring the spread as well as the dilution of active PAGFPmt throughout the rest of the cell's mitochondria (Figure 2.3A). The gradual spread of PAGFPmt signal to other parts of the β-cell, which were not photoactivated, is accompanied by dilution of PAGFPmt (Figure 2.3A and B). As a result, the average PAGFPmt fluorescence intensity in mitochondria that contain photoactivated PAGFPmt gradually decreases as long as the process of spreading is in progress. When spreading of PAGFPmt reached equilibrium, FI was significantly lower and remained stable.

To rule out the possibility that decay in PAGFPmt FI was the result of either nonspecific leak of activated PAGFPmt from tagged mitochondria or bleaching of PAGFP by the laser, two experiments were conducted: GFP FI was measured over time *1*) in individual mitochondria that did not engage in fusion events and *2*) in the presence of FCCP, a mitochondrial inner membrane uncoupler that collapses $\Delta\psi_m$ and arrests mitochondrial dynamics. In both experiments GFP FI remained unchanged and stable over a period of 20 min, indicating a negligible component of nonspecific PAGFPmt leak or laser-induced bleach.

Individual β-cells within an islet were tested for mitochondrial fusion activity using PAGFPmt that is under the insulin promoter (Figure 2.3C). We found that fusion activity is functional and comparable with that in isolated β-cells. Interestingly, there is greater heterogeneity in the overall fusion activity among individual cells within intact islets

exhibiting varied rates of GFP dilution (Figure 2.3D). This is evident when comparing the standard deviations of GFP intensity at equilibrium.

2.4.2 Nutrient Effects on Primary β-cell Mitochondria

Exposure to increased levels of glucose and fatty acids has been shown to compromise β-cell function and viability (El-Assaad *et al.*, 2003). Incubation in 20 mmol/l glucose along with the fatty acid palmitate (0.4 mmol/l complexed with 0.5% BSA) for 48 h resulted in fragmentation of mitochondrial morphology and inhibition of mitochondrial dynamics in β-cells within mouse islets (Figure 2.3E), compared with controls in Figure 3. The mitochondrial fusion capability of β-cells decreased significantly under HFG (20 mmol/l glucose and 0.4 mmol/l palmitate) which was revealed by the decreased ability of cells to dilute the GFP signal 2 h after photoactivation (Figure 2.3F).

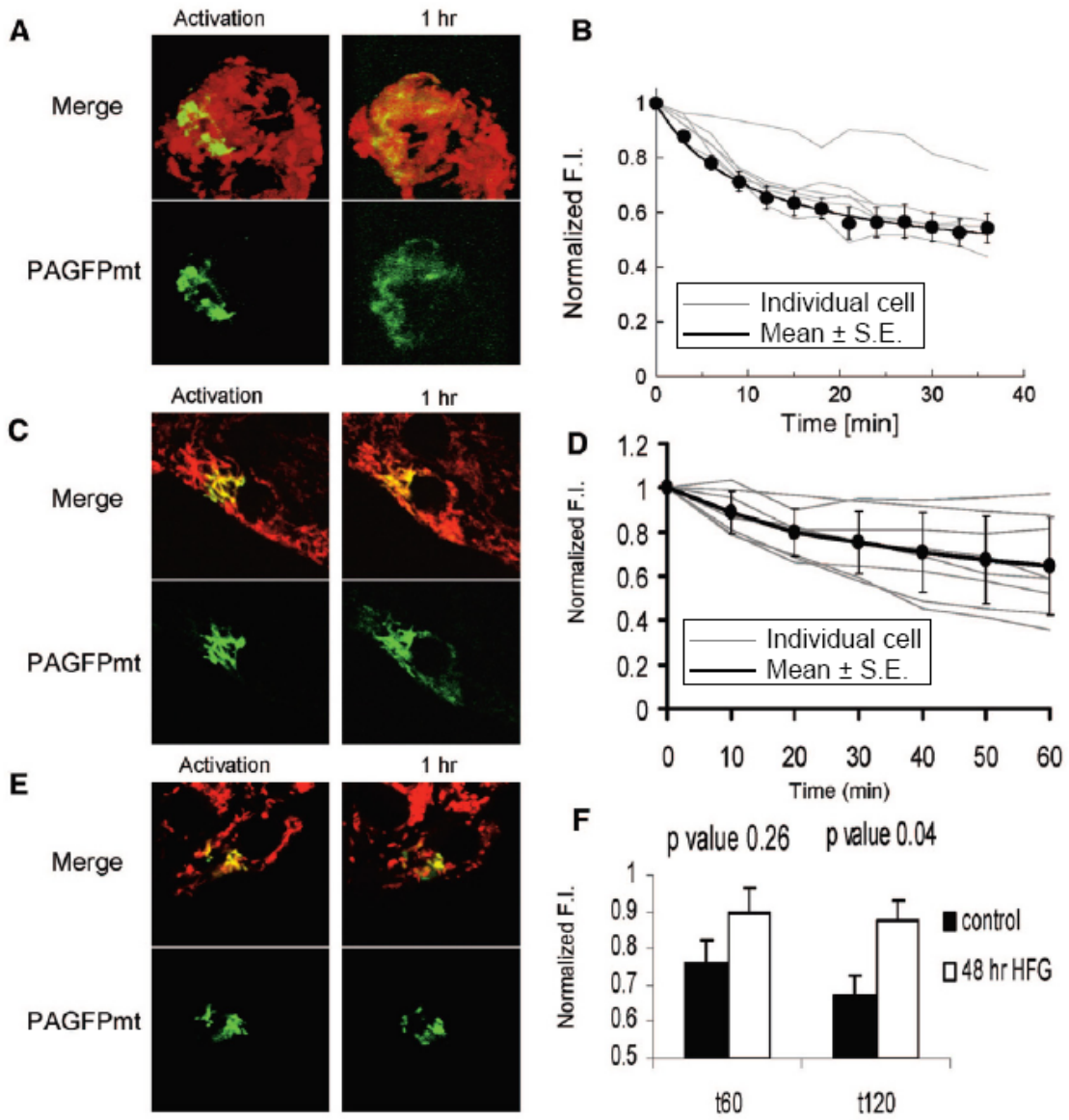

Figure 2.3: Mitochondrial fusion and fission in primary β-cells. **A.** Fusion of the photoactivated fraction (~10%) with the rest of the mitochondrial web dilutes activated PAGFPmt and leads to a reduction in fluorescence intensity. A plateau is reached within approximately 40 min. Images are representative Z-projections. (n =8; gray lines) **B.** Dilution of GFP FI is shown for individual cells (n =8; gray lines) and their average ± SE (●). The average dilution values were fitted (R=0.99) to a hyperbolic function yielding T50 of 12.1 min. **C** and **D.** β-Cells within an intact islet also exhibit mitochondrial dynamics as revealed by the diffusion of the activated PAGFPmt signal. **E.** Fusion activity in primary β-cells is reduced after 24 h in HFG media. Images taken during the assay show that the number of PAGFPmt-positive mitochondria and the FI of PAGFPmt remained unchanged. **F.** Quantitative summary of PAGFPmt dilution shown 60 and 120

min after photoactivation. The HFG-treated cells possess significantly brighter GFP intensity (P=0.04) than controls, indicating reduced mitochondrial fusion activity.

2.4.3 Individual and Combined Effects of Fatty Acids and High Glucose in INS1 Cells

El Assaad *et al.* showed that in INS1 cells, exposure to 20 mmol/l glucose and >0.2 mmol/l palmitate for 24 h leads to apoptosis and that caspase inhibitors do not rescue the cells from death (El-Assaad *et al.*, 2003). We used confocal imaging of mitochondria to examine alterations in morphology caused by alterations in nutrient level (Figure 2.4A). Cells were assessed visually, and those possessing >50% punctate mitochondria were considered fragmented. Exposure to 0.4 mmol/l palmitate in combination with 5, 11, or 20 mmol/l glucose (HFG) caused fragmentation in 40, 75, and 88% of cells after 4 h and in 51, 61, and 79% of cells after 24 h, respectively (Figure 2.4A). Only 16 and 28% of cells exposed to 20 mmol/l glucose without palmitate for 4 and 24 h, respectively, exhibited fragmented mitochondrial architecture. These data indicate that increasing levels of glucose in the presence of palmitate is deleterious to mitochondrial architecture. However, increased glucose alone has a minor effect on mitochondrial fragmentation.

2.4.4 HFG-Induced Fragmentation is Accompanied by Reduced Mitochondrial Fusion in INS1 Cells

To determine the effect of HFG on mitochondrial fusion, we measured the spread of PAGFPmt across the mitochondrial population by quantifying its dilution. As shown in Figure 2.4B and C, 24-h HFG–treated cells with fragmented mitochondria failed to share the activated PAGFPmt. GFP FI remained unchanged ($n = 5$; $p = 0.46$; Figure 2.4B) in HFG-treated cells 50 min after photoactivation, compared with a significant decrease observed in control cells ($n = 6$; $p \leq 0.05$; Figure 2.4C). Interestingly, 4-h exposure to HFG was sufficient to impair fusion ability (Figure 2.4E). These data reveal that fusion is

compromised in fragmented mitochondria observed under HFG and that the reduction in fusion activity is measurable long before apoptosis. Fusion activity was also monitored in cells exposed to palmitate or varying levels of glucose for 24 h. We found that similar to HFG, HF (11 mmol/l glucose and 0.4 mmol/l palmitate) inhibits the mitochondrial fusion ability, whereas HG (20 mmol/l glucose) and HFLG (5 mmol/l glucose and 0.4 mmol/l palmitate) leave fusion intact (Figure 2.4D).

It is conceivable that PAGFPmt bleaching or leakage may contribute to the decrease in PAGFPmt signal over time. This would present an artifact in the analysis and quantification of PAGFPmt dilution. Under HFG, when mitochondria are fragmented and fusion is inhibited, we report that the PAGFPmt signal remains stable over 50 minutes (Figure 2.3C). This shows that without fusion and sharing of PAGFPmt, there is no bleaching from repeated excitation and no loss of signal intensity.

We also sought to determine whether the observed decrease in fusion activity is specific to HFG-induced toxicity as opposed to a physiological response to glucose challenge that is part of the glucose-stimulated insulin secretion (GSIS) cascade (Figure 2.4E). INS1 cells were kept at 2 mmol/l glucose for 2 h before exposure to two different stimulatory conditions: 8 and 15 mmol/l glucose. In these experiments glucose concentration was switched immediately after a group of mitochondria had been labeled, and thus the effect of acute glucose challenge on fusion activity was tested within the first 30 min of the exposure. We find that neither of these conditions resulted in statistically significant changes in mitochondrial fusion capacity of the INS1 cells when compared with 2 mmol/l

glucose. These data suggest that mitochondrial fragmentation and loss of fusion capacity are specific to noxious external stimuli and are not altered during normal β-cell function. Although most INS1 cells exhibit fragmented mitochondria after exposure to HFG, there remains a population of cells with normal (elongated) mitochondrial morphology. We were interested to see if the rate of mitochondrial dynamics was affected in these cells as well. We found that although dynamics is not completely inhibited, as seen in cells with punctate mitochondria, the rate of dilution is significantly decreased (Figure 2.4F). After 30 minutes, comparison of the PAGFPmt dilution levels of normal cells, HFG exposed cells with ramified mitochondria, and HFG exposed cells with punctate mitochondria, shows significant differences between all groups (Figure 2.4G). There are two potential explanations for this finding. First is that the HFG exposed cells with ramified mitochondria are on their way to full fragmentation and abolishment of mitochondrial dynamics. It is possible that with longer HFG exposure, loss of mitochondrial dynamics would become evident. Another possibility is that these cells are at least partially protected from HFG. This would be a worthwhile topic for future studies.

A

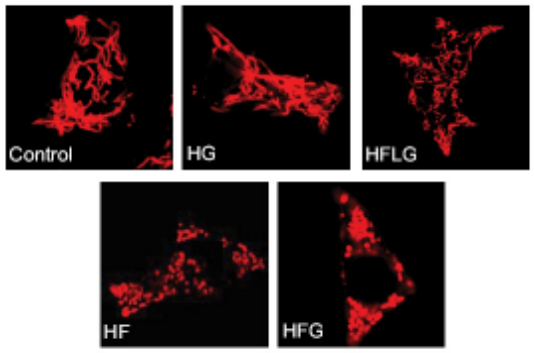

Condition	N	% Fragmented
Control (4 hours)	51	27
HG (4 hours)	54	16
HFLG (4 hours)	82	40
HF (4 hours)	51	75
HFG (4 hours)	51	88
Control (24 hours)	95	13
HG (24 hours)	149	28
HFLG (24 hours)	72	52
HF (24 hours)	147	61
HFG (24 hours)	138	79

B

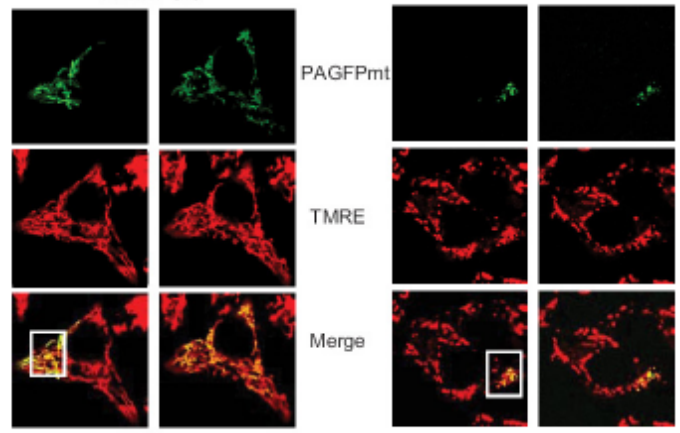

C

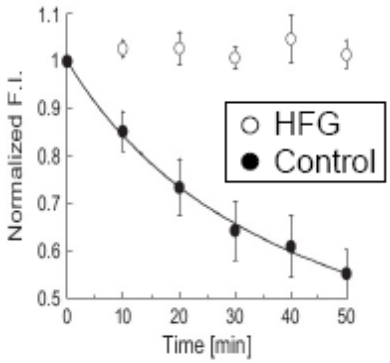

D

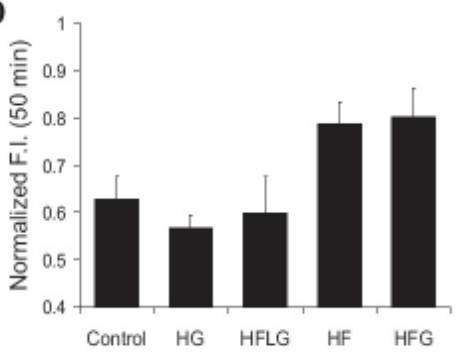

E

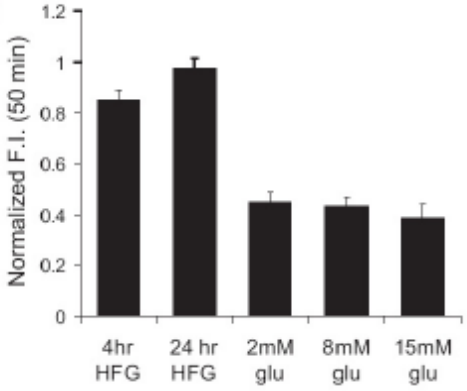

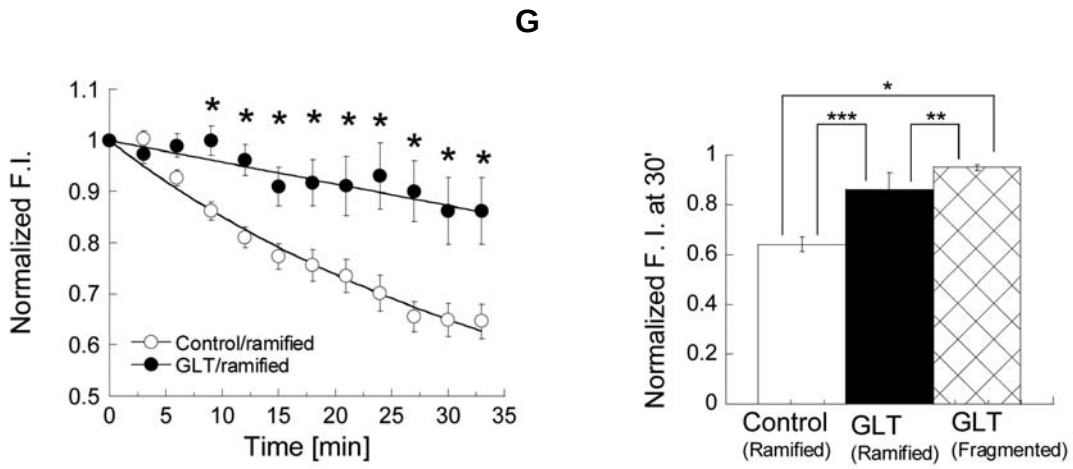

Figure 2.4: Culturing INS1 cells in media with high levels of fatty acids and glucose impairs mitochondrial morphology and dynamics. **A.** Confocal images of INS1 cells stained with TMRE after 24 h in control (11 mmol/l glucose), HG (20 mmol/l glucose), HFLG (5 mmol/l glucose and 0.4 mmol/l palmitate), HF (11 mmol/l glucose and 0.4 mmol/l palmitate), and HFG (20 mmol/l glucose and 0.4 mmol/l palmitate) media. HF and HFG induce mitochondrial fragmentation within 4 h as opposed to incubation with control, HFLG, and HG media, which induce little or no effect on morphology. Cells possessing >50% fragmented mitochondria were considered fragmented. **B.** Assessment of mitochondrial fusion activity using the mitochondrial fusion assay. A group of mitochondria were labeled using a 2-photon laser (□, *inset*). Through fusion events, photoactivated GFP distributed itself throughout the mitochondrial network within 50 min in cells treated with control media. Redistribution is accompanied by dilution of the photoactivated form of PAGFPmt, revealed by the decreased PAGFPmt FI. In cells pretreated with HFG for 24 h (*right panel*), the activated PAGFPmt remained segregated in the mitochondria where it was initially photoactivated; dilution does not occur and PAGFP FI remains elevated. (n=5) **C.** Average GFP dilution values were fitted ($R = 0.99$) to a hyperbolic function yielding T50 of 10.1 min only for the normal media group. (n=6) **D.** Mitochondrial fusion activity, measured by the ability to dilute PAGFPmt after 50 min. Histogram shows steady-state values of GFP FI obtained 50 min after photoactivation, when the PAGFPmt dilution reached equilibrium. HFG- and HF-treated cells show reduced fusion activity compared with control and HFLG- and HG-treated cells (*$p < 0.05$). **E.** A 4-h HFG treatment is sufficient to reduce the fusion activity of INS1 cell mitochondria to levels similar to those found with 24-h HFG treatment. Mitochondrial fusion activity is not affected by 30-min challenge with 8 and 15 mmol/l glucose. Glucose media was changed from 2 to 8 or 15 mmol/l 10 min prior to photoactivation. The plateau GFP FI level after 50 min is similar to that of the INS1 cells that remained in 2 mmol/l glucose. **F.** Mitochondrial fusion measured by PAGFPmt dilution. Black circles represent cells exposed to HFG for 24 hours that were able to

maintain a normal, elongated, mitochondrial morphology (n=8). Open circles represent INS1 cells in normal growth conditions (11mM glucose without palmitate, n=7; $p<0.05$). **G.** Normalized PAGFPmt fluorescence intensity after reaching steady state between control cells with normal mitochondria (n=8), HFG- treated cells that retained elongated mitochondrial architecture (n=7), and HFG treated cells with fragmented mitochondria (n=7, *$p<0.0001$; **, $p=0.01$***, $p=0.04$).

2.4.5 Role of Mitochondrial Fission Machinery in the Response to HFG

We hypothesized that the fragmented mitochondrial morphology that accompanies HFG is mediated by alterations in the balance between fusion and fission processes. Because these processes typically occur in a 1:1 ratio (Twig *et al.*, 2008a), our hypothesis predicts that reduction in fusion activity may be counteracted by reduced fission. We chose to reduce the expression levels of Fis1 because it plays a rate-limiting function in the recruitment of Drp1.

We were able to inhibit the expression of Fis1 using a shRNA sequence described previously (Stojanovski *et al.*, 2004;Arai *et al.*, 2004). Protein levels are reduced by ~90%, and RNA transcripts are reduced by an average of 83% (n = 5; Figure 2.5A). It is notable that in INS1 cells the knockdown of Fis1 does not cause noticeable alterations in mitochondrial morphology (Twig *et al.*, 2008a).

To determine the efficiency of Fis1 knockdown on the inhibition of fission machinery, we tested its effect on Drp1 recruitment to fission sites (Figure 2.5B). Colocalization of Drp1 puncta to mitochondria was visualized and quantified by immunofluorescence in control and lentivirally transduced Fis1 RNAi INS1 cells exposed to 4 h of HFG. This time period corresponds to the duration required to achieve full fragmentation of the mitochondrial web without apoptosis (Figure 2.4A). With Fis1 knockdown, the formation

of DRP1 puncta along mitochondria is prevented. Control cells transduced with empty vector exhibited numerous Drp1-positive puncta along every mitochondrial network after 4 h of HFG. Colocalization of Drp1 puncta with mitochondria was significantly higher in the empty vector control group compared with Fis1 RNAi ($P < 0.05$; Figure 2.5C). A Western blot was performed to test whether HFG, Fis1 knockdown, or a combination of both affected the expression of Drp1. We find that Drp1 expression levels did not change under these conditions, thereby supporting that Fis1 knockdown and HFG affected puncta formation alone without altering Drp1 expression (Figure 2.5D). In addition, immunostaining for Drp1 in control INS1 cells exposed to HFG for 4 h revealed the same staining pattern as cells not exposed to HFG (Figure 2.5E).

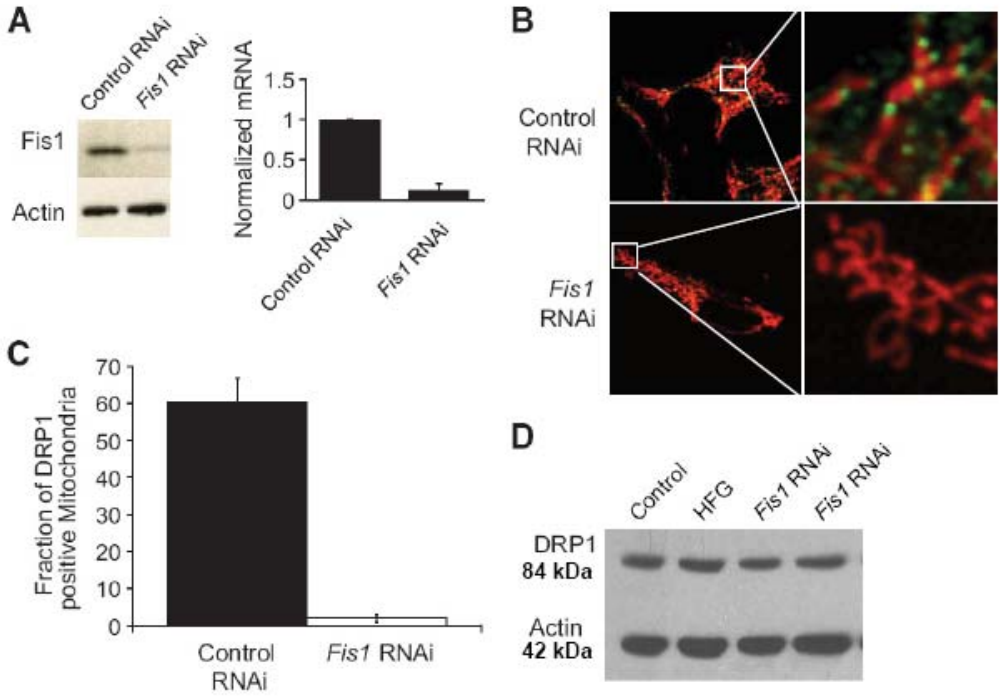

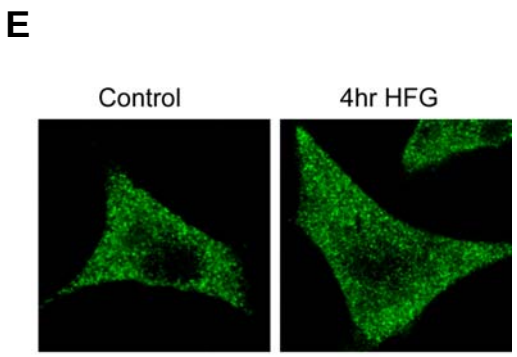

Figure 2.5: Recruitment of Drp1 to mitochondria under HFG is prevented by Fis1 knockdown. **A.** Western blot and qPCR analysis of INS1 cells infected with control or Fis1 RNAi lentivirus. Fis1 protein level was reduced by 80–90%, and RNA transcripts were reduced by an average of ~83% (n = 5). **B.** INS1 cells expressing mitochondrially targeted DsRed were stained for Drp1 (green). After 3.5 h of HFG incubation, Drp1 puncta are abundant in the control RNAi cells but not in the Fis1 RNAi cells. **C.** Quantification of Drp1 recruitment to mitochondria after 3.5-h exposure to HFG (n=7 for each group). **D.** Western blot analysis indicates that the changes in DRP1 recruitment observed were not due to changes in Drp1 expression levels because these remained the same in all the treatments tested. **E.** Drp1 immunofluorescence reveals that there is no appreciable difference in the appearance of puncta with and without the addition of HFG for 4 hours.

2.4.6 Effect of Fis1 on Mitochondrial Fragmentation and Mitochondrial Dynamics Under HFG

Inhibition of Drp1 recruitment to mitochondria suggests that *Fis1* shRNA can effectively prevent mitochondrial fission in β-cells. We next determined whether Fis1 knockdown can prevent HFG-induced fragmentation by performing morphometrical analysis of mitochondrial structures in INS1 cells infected with *Fis1* shRNA and control shRNA viruses.

INS1 cells infected with control virus were cultured in either 11 mmol/l (normal growth/culture conditions) glucose or with 20 mmol/l glucose and 0.4 mmol/l palmitate for 24 h and stained with TMRE. Under HFG, we observed a change from elongated and

elaborate networks to fragmented and punctate mitochondria (Figure 2.6A). The aspect ratio (AR) of all mitochondria in each cell was calculated by measuring the length and width of best fit ellipses (an AR of 4 represents a mitochondrion that is four times longer than it is wide). Organelles were classified according to AR values into those with short (AR $\leq$2), intermediate (2<AR$\leq$4), and long (AR >4) morphology. HFG treatment reduced the fraction of long mitochondria fivefold and doubled the fraction of short mitochondria. Fis1 knockdown significantly reduced the appearance of short mitochondria under HFG treatment. Furthermore, the number of long mitochondria was tripled. It is notable that *Fis1* RNAi alone did not alter the distribution of short, intermediate, and long mitochondria within a cell's mitochondrial population (Figure 2.6A).

In addition to rescuing mitochondrial architecture, Fis1 knockdown also preserved the capability of mitochondria to fuse after 24-h HFG treatment. Whereas cells transduced with control lentiviral treatment were unable to diffuse GFP after HFG treatment, those transduced with *Fis1* RNAi lentivirus reduced GFP intensity by 31%, similar to control cells not treated with HFG that exhibited a 29% decrease in GFP intensity (Figure 2.6B). Fis1 knockdown alone also caused a mild decrease in mitochondrial fusion ability, exhibiting a 14% intensity decrease after 50 min. This result suggests the importance of fission in mitochondrial dynamics. It is reasonable to infer that with decreased fission, mitochondrial dynamics may occur more slowly although the network morphology remains unchanged.

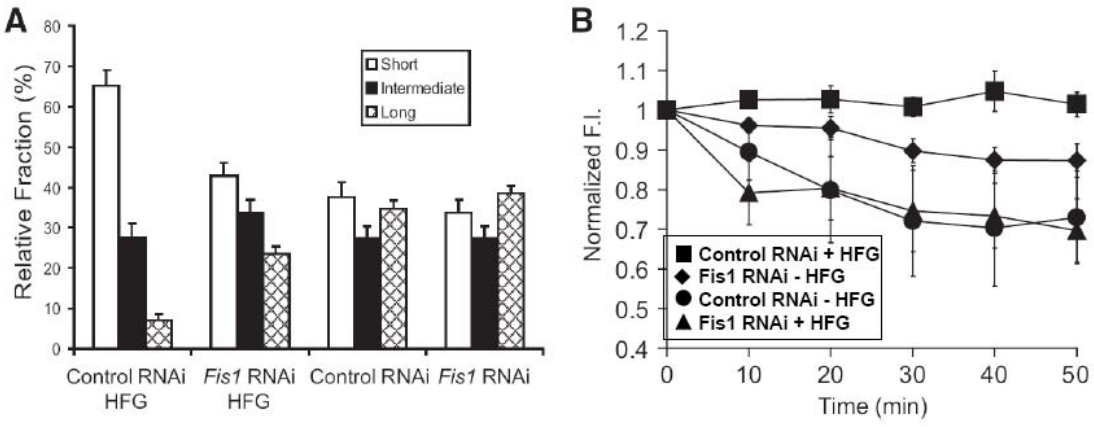

Figure 2.6: Fis1 RNAi restores mitochondrial morphology and dynamics under HFG in INS1 cells. **A.** Mitochondrial morphometry. Mitochondria were classified according to AR into short (AR <2), intermediate, (2<AR<4), and long (AR >4) length (n =8 cells per group). **B.** Whole-cell mitochondrial fusion assays (PAGFPmt dilution) in Fis1 RNAi INS1 cells exposed to HFG for 24 h (▲). A hyperbolic fitting yielded T50 =7.6 min Fis1 RNAi cells not exposed to HFG are also plotted (♦). Values of control RNAi cells with and without HFG treatment were imported from Figure 2.4C (■ and ●, respectively).

2.4.7 Reduced Fis1 Expression by RNAi Protects Against HFG-Induced Apoptosis

Previous studies have demonstrated that HFG induces β-cell apoptosis (El-Assaad *et al.*, 2003). We proceeded to examine the effect of Fis1 RNAi on HFG-induced apoptosis. Control and Fis1 RNAi INS1 cells were exposed to HFG for 24 h and tested for various molecular markers of apoptosis (Figure 2.7A–C). Immunostaining for cleaved caspase-3 as well as the 17 kDa and 19 kDa proapoptotic active forms of caspase-3 revealed a reduction back to basal levels in the Fis1 RNAi cells exposed to HFG. The percentage of control INS1 cells exhibiting staining for cleaved caspase-3 staining (78 ± 4%) was significantly greater compared with Fis1 RNAi–treated cells (25 ± 3%) when exposed to 24-h HFG (Figure 2.7A). Similar results were found when apoptosis was analyzed using transferase-mediated dUTP nick-end labeling staining (Figure 2.7B). Fis1 knockdown cells did not possess the dark nuclear staining, indicating that they are not undergoing

apoptosis. Consistent with the immunofluoresence and TUNEL data, fluorescence-activated cell sorter analysis using annexin V, another apoptotic marker, revealed a dramatic reduction in apoptotic cells in Fis1 RNAi–infected cells exposed to HFG (Figure 2.7C).

Phosphorylated Akt (pAkt) has been shown to protect a variety of cell types, including β-cells, from apoptosis through the inhibition of proapoptotic proteins including BAD and caspase-9 (Downward, 2004;Jetton *et al.*, 2005). Previous studies have found that β-cell survival under elevated glucose or fatty acid is dependent on Akt phosphorylation (Tuttle *et al.*, 2001;Wrede *et al.*, 2002;Srinivasan *et al.*, 2002). To determine whether Fis1 RNAi was upstream or downstream of Akt phosphorylation we examined the effect of HFG-induced apoptosis on the activation state of Akt (Figure 2.7D). Activated pAkt inhibits apoptosis by inactivating downstream proapoptotic targets (Wikstrom *et al.*, 2007). Control INS1 cells exposed to HFG, but not HG or HF, showed a marked decrease in the amount of pAkt (Ser 473), consistent with their progression through apoptosis. *Fis1* RNAi–expressing cells also exhibited a dramatic decrease in pAkt because Akt signaling in apoptosis is primarily upstream of the mitochondrial machinery and Fis1 action (Danial and Korsmeyer, 2004). Expression levels of Akt remained unchanged in both empty vector and *Fis1* RNAi–expressing cells under basal, HG, HF, and HFG culture conditions.

2.4.8 Insulin Secretion

Although restoration of mitochondrial fusion improved cell viability under HFG, it did not rescue GSIS (Figure 2.7E). We found that under HFG, insulin secretion in response

to 15 mmol/l glucose is significantly decreased by an average of 31% ($p = 0.023$). Fis1 knockdown cells exposed to similar HFG treatment exhibit the same levels of insulin secretion compared with control cells ($p = 0.43$).

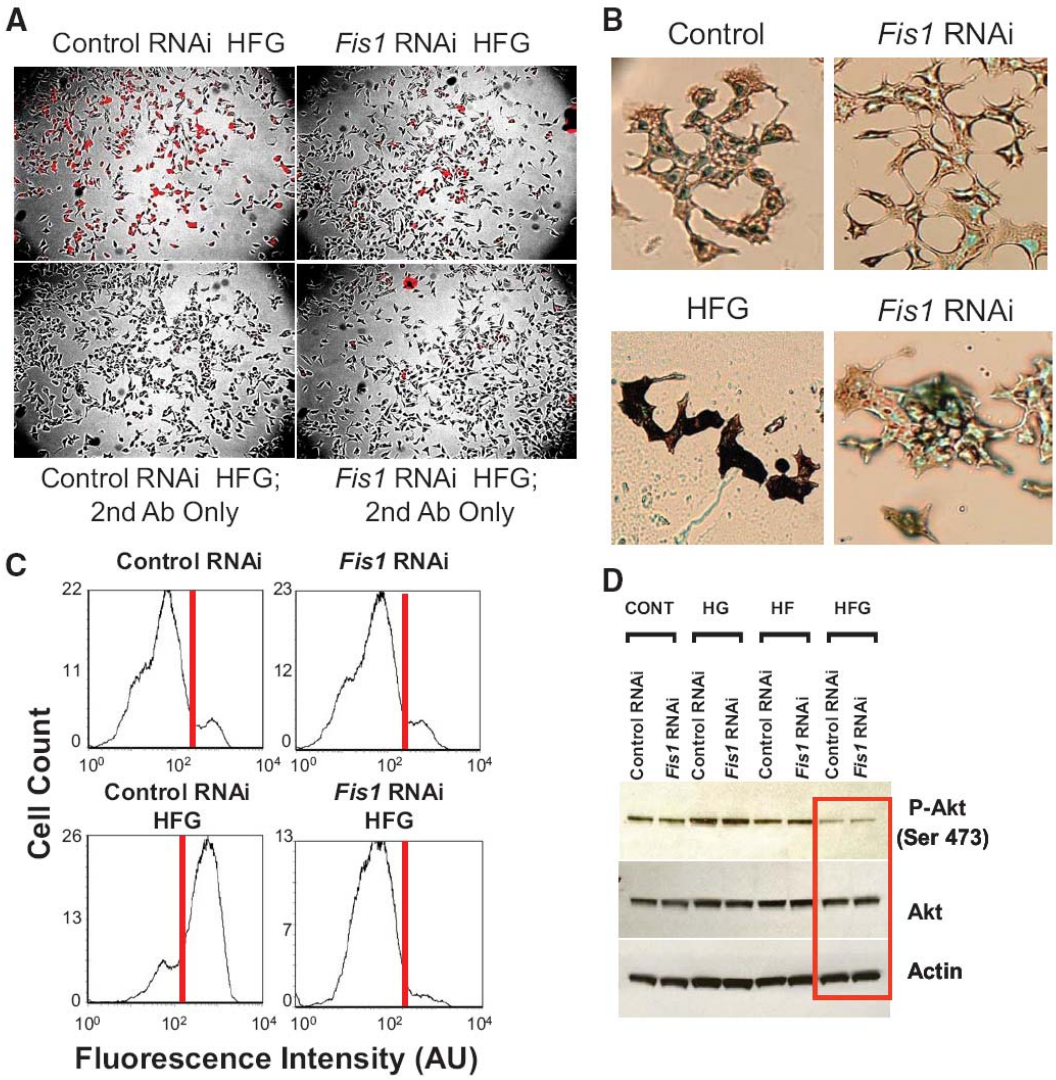

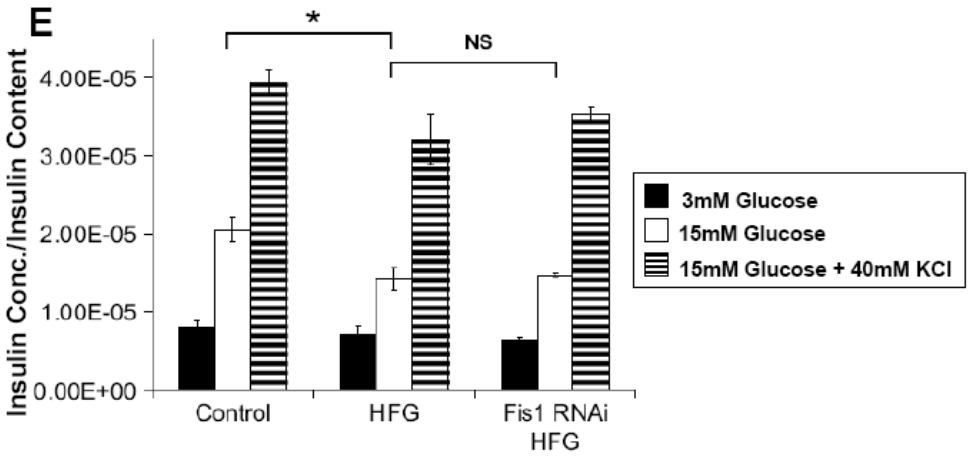

Figure 2.7: Effect of Fis1 RNAi on HFG-induced apoptosis in INS1 cells. **A:** Immunostaining for cleaved caspase-3 in Fis1 RNAi and control RNAi INS1 cells exposed to HFG for 24 h. *Lower panels* show the experiment repeated but with cells treated to secondary antibody only. **B:** Transferase mediated dUTP nick-end labeling staining of cells treated with the same conditions described in **A**. **C:** Fluorescence-activated cell sorter analysis for the apoptotic marker annexin V shows a reduction in cell death in Fis1 RNAi cells compared with control RNAi. Both groups were exposed to HFG for 24 h prior to analysis. **D:** Western blot analysis of Akt and its downstream target pAkt; β-actin serves as a loading control. **E:** Insulin secretion measurements were performed on INS1 cells infected with control or *Fis1* RNAi lentivirus. Cells were incubated for 4 h in 11 mmol/l glucose or HFG media, sufficient time to achieve mitochondrial fragmentation and impaired fusion capacity. After a 1-h washout period, cells were preincubated with 3 mmol/l glucose for 30 min. Insulin was measured after 30-min exposure to 3 mmol/l glucose (■), 15 mmol/l glucose (□), or 15 mmol/l glucose with 40 mmol/l KCl (≡). Incubation of control cells in HFG media resulted in a decrease in GSIS ($p = 0.023$), which is not restored by knockdown of Fis1 ($p=0.43$). (n=3)

2.5 Discussion

A number of studies have established that mitochondrial dysfunction plays a role in the development of type 2 diabetes and that exposure of β-cells to high levels of glucose and fatty acids may contribute to the development of the disease (Maechler and Wollheim, 2001;Lowell and Shulman, 2005;Poitout, 2008). Mitochondrial dysfunction in the form of increased superoxide generation and short and swollen mitochondrial morphology has been observed in the Zucker Diabetic fatty rat model (Bindokas *et al.*, 2003). We found

that exposure to toxic nutrient levels induces β-cell mitochondrial fragmentation, which is due to alterations in mitochondrial dynamics. Preserving mitochondrial dynamics prevented both fragmentation and cell death.

The presence of mitochondrial fusion and fission has been reported in a variety of cells, where this process has been demonstrated to generate elaborate networks of mitochondria. However, whether mitochondrial dynamics is relevant in β-cells had not been determined. In fact, given the dense appearance of β-cell mitochondria and their relatively short size, it was unclear whether fusion and fission events occur in β-cells and if mitochondrial dynamics play any role in the development of diabetes. In this work, we demonstrate that β-cells mitochondria undergo continuously fusion and fission cycles and that these interactions may function to counteract the damaging effects of long-term exposure to high levels of nutrients. Under normal nutrient conditions, the dynamic activity of mitochondria is evident in clonal β-cells, dispersed β-cells, and β-cells within an intact islet. Mitochondrial fusion assays performed within intact islets indicate that fusion rates vary from cell to cell. The intercellular variation appears to be greater between β-cells within an islet compared with dispersed β-cells. This may correlate to previous studies by Marsh and colleagues suggesting that differences in the level of mitochondrial branching between β-cells in an islet may reflect differences in secretory capacity (Noske *et al.*, 2008). Indeed, it is conceivable that cells with more branched mitochondrial networks will have a different PAGFPmt fusion rate than cells with less branched mitochondria.

Tagging individual mitochondria with matrix-targeted PAGFPmt enables quantitative dissection of mitochondrial architecture and dynamics. Mitochondria in primary β-cells are densely packed, which can lead to an overestimation of mitochondrial size and the impression of a continuous structure. However, when the matrix boundaries of each mitochondrial unit were determined by photoactivation of PAGFPmt, it is clear that many of the larger convoluted webs actually represent short units of mitochondria juxtaposed with one another without matrix continuity. For comparison, COS cells possess very elaborate mitochondrial structures that often appear to be interconnected within a complex web (Karbowski *et al.*, 2004). Although despite the appearance of connectivity, the average COS cell mitochondrion is only about 1% of the size of the entire web, which is revealed by PAGFPmt photoactivation of individual units (Twig *et al.*, 2006). Indeed, it has been reported that mitochondria are largely unconnected, as determined by utilizing fluorescence-recover after photobleaching (FRAP), even when they appear to have elongated, dense mitochondrial structures (Collins *et al.*, 2002). Furthermore, mitochondria have distinct boundaries that limit luminal continuity, which introduces functional heterogeneity in parameters such as $\Delta\Psi$mt, sequestration of Ca^{2+} signals, and the opening of the permeability transition pore in response to toxic stimuli (Collins *et al.*, 2002). With the PAGFPmt-based mitochondrial fusion assays, we have been able to observe that β-cell mitochondria undergo transient fusion events. Therefore, the relatively small size of these units is not the result of the inability of these mitochondria to undergo fusion, but that they, more likely, undergo rapid cycles of fusion followed by fission to maintain a smaller size (Twig *et al.*, 2008a). In fact, we show that these mitochondria frequently go undergo fusion events, demonstrated by their ability to completely

equilibrate PAGFPmt throughout the web in as little as one hour. Compared with other cell types, the time to equilibrium we report is similar to what has been observed in HeLa cells and several other cell types including rat hipoccampal neurons (Karbowski *et al.*, 2004).

Interestingly, INS1 cell mitochondria assemble into more elongated and convoluted networks than primary β-cells. Our data suggest that the mechanism underlying differences in mitochondrial morphology between cell types may be related to the levels of OPA1 expression. We report that overexpression of OPA1 leads to the appearance of short punctate mitochondria. Similarly, overexpression of another mitochondrial fusion protein, Mfn2, leads to the clustering of mitochondria into short fragments (Huang *et al.*, 2007). In INS1 cells, it takes larger increases in OPA1 to achieve similar fragmentation of the mitochondrial network. These findings suggest that INS1 cell mitochondria are better equipped to maintain networking ability when faced with disruptions in the balance between fusion and fission.

HFG, the synergistic combination of elevated glucose and fatty acid, is an *in vitro* model of type 2 diabetes described previously (Roduit *et al.*, 2000) and has been shown to cause progressive β-cell dysfunction and cell death (Poitout and Robertson, 2002). Previous studies have shown that HFG leads to an increased level of $\Delta\Psi$mt heterogeneity that is due in part by the appearance of a growing population of depolarized mitochondria (Wikstrom *et al.*, 2007). It is conceivable that these changes may be mediated by alterations in mitochondrial fusion and fission and network morphology. Indeed, we found dramatic differences in mitochondrial morphology between control (basal glucose)

and HFG-treated groups, where HFG caused the appearance of numerous punctate mitochondria and a generalized fragmentation of the mitochondrial network. When combined with palmitate, increasing concentrations of glucose (5, 11, and 20 mmol/l) lead to increasing levels of fragmentation in a dose-dependent manner. However, in the absence of palmitate, even 20 mmol/l glucose does not affect mitochondrial architecture. These data are congruent with the synergistic effects of palmitate and glucose that have been reported previously (El-Assaad *et al.*, 2003).

Interestingly, higher levels of glucose alone and with longer exposure has been shown to induce an increase in the expression of the mitochondrial fission protein DRP1 (Men *et al.*, 2009). This finding supports an important role for mitochondrial fission in nutrient-apoptosis given that the induction of DRP1 expression increased high glucose–induced apoptosis, while INS1 cells expressing a DRP1-DN were not able not undergo apoptosis in response to high glucose levels (Men *et al.*, 2009). Our results indicate that with the combination of high fat and glucose, mitochondrial fragmentation occurs within 4 h. Furthermore, we report that alterations in mitochondrial fusion mediate mitochondrial fragmentation, whereas DRP1 translocation is unaffected. Rescue of mitochondrial fusion ability was sufficient to prevent HFG-induced apoptosis.

Fragmentation of the mitochondrial network may be mediated by increased fission, decreased fusion, or conditions characterized by uniquely high expression levels of fusion proteins such as OPA1 or Mfn2. To determine which of these possibilities occurs under HFG, we quantified mitochondrial dynamics by studying the spread of photoconverted PAGFPmt across the mitochondrial web. We found a significant inhibition of

mitochondrial fusion in cells exposed to HFG compared with control (basal glucose). The disruption of mitochondrial dynamics in the presence of palmitate appears at 11 mmol/l glucose but is not apparent at 5 mmol/l glucose. As shown in the mitochondrial morphometry analysis, after 24-h HFG, there remains a small population of mitochondria that retains a relatively elongated morphology. Indeed, certain cells retain complex mitochondrial morphology that is comprised of a mixture of elongated and punctuate structures. This may represent an intermediate stage prior to full fragmentation. Future work will address whether these cells represent a population that is less susceptible to apoptosis. Cells under HFG that do not exhibit mitochondrial fragmentation are still capable of mitochondrial fusion, shown by PAGFPmt dilution. However, the kinetics of PAGFPmt sharing in these cells is reduced compared with control cells, indicating that fusion activity is compromised even before fragmentation is apparent.

The contribution of fission machinery to fragmentation was determined by analyzing the effect of HFG on Fis1 and Drp1. Analysis of Fis1 transcript as well as protein levels in cells treated with HFG did not reveal a statistically significant induction of this protein. Although expression does not change, we show that HFG is accompanied by recruitment of DRP1 to mitochondrial fission sites. This was inhibited in cells treated with Fis1 RNAi, indicating an essential role for Fis1. We rationalized that the inhibition of fission may balance reduced fusion activity observed under HFG. Indeed, Fis1 RNAi restored mitochondrial dynamics and morphology in HFG-treated cells, determined by the spreading and dilution of matrix PAGFPmt through the mitochondrial network.
In our studies, knockdown of the fission protein Fis1 did not result in robust morphological changes in INS1 cells. This finding suggests that INS1 cells are able to

counteract the effects of reduced fission by balancing the rate of fusion under physiological conditions. Indeed, our data indicate that Fis1 knockdown is accompanied by a reduction in the fusion rate reported by the PAGFPmt dilution assay. Because fusion and fission events are paired (Twig *et al.*, 2008a), it is conceivable that decreased fission activity may render the mitochondrial webs more static, suggesting that a certain level of fission is required for an optimal mitochondrial dynamics rate. Additionally, the lack of change in gross mitochondrial morphology with Fis1 knockdown may be due to the packed and entangled appearance of mitochondria in INS1 cells compared with other cell types such as fibroblasts. The density of mitochondria leads to a large percentage of juxtaposed mitochondria that are not necessarily fused. Under these conditions, alterations in the level of connectivity can produce a measurable shift in PAGFPmt dilution without necessarily altering the overall morphology.

The mechanism by which HFG leads to mitochondrial fragmentation may be related to an increase in ROS. HFG has been shown to increase superoxide levels (Brownlee, 2003). In a separate study, treatment of INS1 with H_2O_2 resulted in fragmentation of the mitochondrial network, suggesting that nutrient-induced ROS production can lead to mitochondrial fragmentation (Maechler *et al.*, 1999). On the other hand, other studies have shown that dynamic changes in mitochondrial morphology may influence glucose-induced overproduction of ROS (Yu *et al.*, 2006). In H9C2 (rat cardiomyoblast) and CRL-1439 (rat hepatocytes) cell lines, inhibition of mitochondrial fission with DRP1-DN attenuates ROS production and mitochondrial fragmentation induced by acute exposure to 50 mmol/l glucose. In neurons, inhibition of fission was found to mitigate NO-induced mitochondrial fragmentation and cell death (Bossy-Wetzel *et al.*, 2003). Thus, it is

conceivable that the effect of HFG on mitochondrial morphology may be due to increased ROS damage. The decrease in ROS production in Fis1 RNAi cells under HFG may be at least partially responsible for the protection from fragmentation and apoptosis. In a previous study, we demonstrate that Fis1 knockdown does not lower ROS levels in INS1 cells under growth conditions. However, a significant decrease was observed in INS1 cells incubated in 22 mmol/l glucose (Twig *et al.*, 2008a).

Inhibition of mitochondrial fission through Fis1 RNAi markedly reduced apoptosis compared with cells infected with control virus. This result demonstrates the importance of mitochondrial networking in β-cell physiology since preventing HFG-induced fragmentation through Fis1 RNAi reduces β-cell apoptosis. However, this does not indicate that fragmentation necessarily leads to apoptosis. Indeed, it has been shown that overexpression of hFis1 in INS1 cells only leads to nominal increased levels of apoptosis. Moreover, fragmentation caused by the expression of Mfn1-DN does not result in apoptosis in INS1 cells ((Park *et al.*, 2008)). Although it is possible to induce fragmentation and apoptosis by Fis1 overexpression in other cell types, it is also possible to prevent apoptosis without affecting mitochondrial fragmentation, which has been demonstrated with the overexpression of Bcl-X_L (James *et al.*, 2003).

Previous studies have raised a number of potential mechanisms by which inhibition of mitochondrial fragmentation can affect apoptosis (Frank *et al.*, 2001;Olichon *et al.*, 2003). Fragmentation occurs early in the cell death pathway (Frank *et al.*, 2001;Heath-Engel and Shore, 2006) and is thought to contribute to the release of cytochrome c into the cytosol, culminating in caspase-mediated apoptosis (Heath-Engel *et al.*, 2006). It is

notable that although a decrease in the translocation of Bax to mitochondria and the subsequent release of cytochrome c have been reported with Fis1 knockdown, DRP1-DN did not alter Bax translocation (Lee *et al.*, 2004). An article by Martinou and colleagues has shown that inhibition of fission machinery can prevent mitochondrial fragmentation and reduce cytochrome c release (Parone *et al.*, 2006). However, Bax/Bak-mediated apoptosis still occurs along with the release of Smac/DIABLO. A more recent article by Yuan et al. has reported that mitochondrial fission occurs upstream of Bax translocation in response to nitric oxide (Yuan *et al.*, 2007). Revealing the relevance and timing of these events in HFG-induced apoptosis in β-cells is a topic for future investigation. Activated Akt provides protection from apoptosis through phosphorylation and inhibition of proapoptotic proteins such as BAD (Tuttle *et al.*, 2001;Jetton *et al.*, 2005). Previous studies have indicated that β-cell survival under elevated glucose or fatty acid is dependent on Akt phosphorylation and that reduced level of pAkt is associated with β-cell loss (Tuttle *et al.*, 2001;Wrede *et al.*, 2002;Srinivasan *et al.*, 2002). Interestingly, in HFG-treated cells where Fis1 has been knocked down, reduced pAkt was not accompanied by cell death. Enhanced β-Cell survival accomplished by Fis1 knockdown indicates that the effect of Fis1 occurs downstream of the Akt signaling pathway and that the reduction in mitochondrial fragmentation bypasses the reduction in Akt activity.

Recent studies have also indicated that increased calcium influx plays a role in palmitate-mediated β-cell apoptosis (Choi *et al.*, 2007). Activation of calcineurin by calcium may regulate mitochondrial morphology by dephosphorylation of DRP1 (Cribbs and Strack, 2007;Cereghetti *et al.*, 2008). However, our results indicate that HFG-mediated mitochondrial fragmentation is not accompanied by an increased level of DRP1 assembly

on mitochondria and increased fission but rather a decrease in the level of fusion activity, demonstrated by mtPAGFP diffusion assays.

The role of mitochondrial dynamics in β-cell function and insulin secretion remains unclear. Our data indicate that the mitochondrial fusion rate is unchanged by acute stimulation by 15 mmol/l glucose. In addition, Fis1-mediated rescue from HFG is not accompanied by improvements in GSIS. Previous studies by our group and by Wollheim and colleagues indicate that altering mitochondrial dynamics proteins Mfn1 and Fis1 does not improve GSIS (Park *et al.*, 2008;Twig *et al.*, 2008a;Twig *et al.*, 2008b). It is interesting to note that both Fis1 overexpression and Fis1 knockdown lead to a decrease in GSIS. Together, these data suggest that any disturbance in the balance of fusion and fission can lead to β-cell dysfunction.

Chapter 3: The Role of the Mitochondrial Fusion Protein, Mfn2, in β-Cell Control of Whole Body Nutrient Utilization

I contributed to all of the experiments in this data chapter. I worked closely with Anthony Molina and Samuel Sereda on the work presented in this chapter. Additionally, the islet transplantation experiments were done in collaboration with Gordon Weir's laboratory at the Joslin Diabetes Center.

3.1 Abstract

β-cell mitochondria are dynamic and undergo cycles of fusion and fission. Previously, we reported that fusion capacity is abolished with exposure to fatty acids and elevated glucose levels. Here, we report that *in-vivo* a high fat diet and models of type 2 diabetes lead to a reduction in the mitochondrial fusion protein, Mfn2, in the pancreatic islet. To determine the functional role of reduced fusion in diet-induced obesity and diabetes, we excised Mfn2 from insulin producing cells. In the absence of Mfn2, β-cell mitochondria become fragmented while other islet cell types retain normal mitochondrial morphology. *In-vivo* metabolic dysfunction is evident in young animals while older animals become obese and diabetic. This occurs in the absence of changes in diet or feeding behavior and correlates with a decrease in metabolism. Basal insulin secretion is increased while glucose stimulated insulin secretion appears uncoordinated in βMfn2KO islets. These results suggest that nutrient-induced disruption of mitochondrial fusion may underlie the development of diabetes and metabolic dysfunction.

3.2 Introduction

Mitochondria are highly dynamic organelles whose morphology is regulated by continuous cycles of fusion and fission, collectively termed mitochondrial dynamics (Bereiter-Hahn *et al.*, 1994;Skulachev, 2001;Chen *et al.*, 2005a). Networks are formed when mitochondria undergo fusion events that cause the compartments of participating

mitochondria to become continuous. As a result, the constituents of each network are able to share solutes, metabolites and proteins (Nakada *et al.*, 2001;Arimura *et al.*, 2004;Chen *et al.*, 2005b) as well as a transmembrane electrochemical gradient (Skulachev, 2001;Twig *et al.*, 2006). Mediators of mitochondrial fusion include OPA1, Mfn1, and Mfn2. The disruption of mitochondrial networks has been shown to have a profound effect on the progression of cells to apoptosis, particularly in cases where reactive oxygen species (ROS) are involved (Yu *et al.*, 2006). Mfn2 in particular has been implicated to play an important role in mitochondrial function. Transfection with a Mfn2 antisense sequence results in reduced glucose oxidation and decreased oxygen consumption (Bach *et al.*, 2003). A reduction in the substrate oxidation and mitochondrial membrane potential have also been observed (Pich *et al.*, 2005). Overall, mitochondrial networking is thought to be a potential quality control mechanism, allowing for the buffering of mitochondrial ROS and calcium overload (Szabadkai *et al.*, 2004;Frieden *et al.*, 2004).

In the β-cell, mitochondria mediate responses to extracellular glucose by generating metabolites and initiating a cascade of events that culminate in the release of insulin. In chapter 2, we reported that β-cell mitochondria undergo continuous cycles of fusion and fission despite their short length. Furthermore, we reported that extended exposure to high levels of glucose and fatty acid leads to the fragmentation of mitochondria (Molina *et al.*, 2009). Similar changes in mitochondrial morphology have been reported in the β-cells isolated from T2D patients, Zucker Diabetic Fatty rats, and in diet induced obesity (Higa *et al.*, 1999;Bindokas *et al.*, 2003;Anello *et al.*, 2005;Fex *et al.*, 2007). By selectively photolabeling mitochondria, we found that fragmentation due to extended

exposure to high levels of nutrients stems from nutrient-induced inhibition of mitochondrial fusion (Molina *et al.*, 2009).

To address the role of nutrient induced inhibition of mitochondrial fusion in the development of β-cell dysfunction and diabetes, we undertook the investigation of mitochondrial fusion proteins in-vivo. Here we report that under high fat diet, the levels of mitochondrial fusion protein, Mfn2 are reduced in beta cells. Deletion of Mfn2 from the β-cell results in a phenotype that resembles the effects of high fat diet and the development of marked obesity.

3.3 Materials and Methods

3.3.1 Generation and genotyping of βMfn2KO mice

The generation of $Mfn2^{loxP}$ mice has been previously described by Hsiuchen Chen (Chen et al., 2007). Briefly, ES clones (129 strain) carrying targeted mutations were injected into C57BL/6 blastocysts. Founder chimeric mice were bred to Black Swiss mice, and agouti offspring were bred to FLPeR mice to remove the neomycin resistance cassette. Resulting mice were maintained as homozygous stocks (Farley et al., 2000). B6.Cg-Tg(Ins2-cre)25Mgn/J mice (RIP-Cre) were obtained from JAX mice (Bar Harbor, ME.) and bred with homozygous $Mfn2^{loxP}$ to generate F1, double heterozygous mice. F1 mice were then bred with the original $Mfn2^{loxP}$ mice in order to generate the βMfn2KO mice. Littermates include $Mfn2^{loxP}$ +/+ RIP-Cre -/- and Mfn2 +/- RIP-Cre -/- which were used at WT controls. In addition, $Mfn2^{loxP}$ +/- RIP-Cre +/- were tested and found to possess a mild phenotype.

Genotyping was performed by PCR of tail snip lysates (Viagen, DirectPCR, Los Angeles, CA.) obtained during the weaning of pups. Floxed Mfn2 transgene was detected using GoTaq Green Master Mix (Promega, Madison, WI.) and the following primers: gaa gta ggc agt ctc cat cg and ccc aag aag agc atg tgt gc. The unexcised conditional band is 810bp and the WT is 710 bp. Cre transgene was detected in the same samples by following the genotyping protocol provided by JAX Mice using the following primers: gcg gtc tgg cag taa aaa cta tc and gtg aaa cag cat tgc tgt cac tt.

3.3.2 Confocal Microscopy

Confocal microscopy was performed on live cells in glass bottom dishes (MatTek, Ashland, MA) using an inverted Leica TCS SP2 confocal microscope or Zeiss LSM 710 DUO with a plan apochromat 100x (NA = 1.4) oil immersion objectives. Mitochondria were stained with 3.5nM TMRE (Invitrogen, Eugene, OR.) for 45 minutes prior to imaging. Insulin promoter mediated paGFP expression in the mitochondrial matrix was induced by lentiviral transduction. The generation of these constructs was previously described in detail (Molina and Shirihai, 2009).

3.3.3 Metabolic Phenotyping

Body composition was measured non-invasively at the Boston University Animal Research Resource Center using the EchoMRI 900 system (Echo Medical Systems, Houston, TX.). Spatial Distribution of fat tissue was measured by CT scan using the LaThetaT LCT-100 scanner (Echo Medical Systems). In-vivo metabolic parameters were measured using Comprehensive Laboratory Animal monitoring System (CLAMS, Columbus Instruments, Columbus, OH.) metabolic cages.

3.3.4 Insulin Tolerance Test (ITT)

Mice were fasted (with ad libidum water) for four hours prior to an ITT. The volume (μL) of insulin stock (0.1 U/mL) injected into each mouse was determined by multiplying the mouse weight (in grams) by 10. Initial time zero blood glucose measurements are taken using a FreeStyle glucometer with a drop of blood obtained from the tail prior to the intraperitoneal (IP) insulin injection. The appropriate amount of insulin was then injected and blood glucose measurements were taken at 15, 30, 60, 90, and 120 minutes. Mice were fed once the last glucose measurement was taken.

3.3.5 Glucose Tolerance Test (GTT) and Pyruvate Tolerance Test (PTT)

Mice are fasted (supplied with water ad libidum) overnight prior to the GTT and PTT. For GTT's, the volume (μL) of 10% glucose to be injected per mouse is determined by multiplying mouse weight (in grams) by 5. Initial time zero blood glucose measurements were taken using a glucometer with a drop of blood obtained from the tail. For PTT's. Sodium pyruvate (Sigma) is injected at a concentration of 2g/kg. After blood glucose for time zero is taken, the mice are given an intraperitoneal (IP) glucose or pyruvate injection and blood glucose measurements were taken at 15, 30, 60, 90, and 120 minutes. Lab chow was reinstated to cages once the last glucose measurement and blood sample was taken. To measure insulin production during GTT, blood samples were taken at 0, 5, 15, and 30 minutes during the assay. Serum insulin was measured using an ultra sensitive mouse insulin ELISA (Mercodia). In order to measure glucagon production during PTT, blood samples were taken at 0, 15, and 30 minutes during the PTT. Serum glucagon was measured by ELISA (ALPCO).

3.3.6 Histology

Whole pancreata were excised, placed in a tissue cassette, and submerged in 4% paraformaldehyde for at least 24 hours. Tissues were embedded in paraffin, sectioned (5μm), and stained with Hematoxylin and Eosin for visualization. Images were taken using an inverted Olympus IX71 microscope equipped with a 40X dry objective and color camera.

3.3.7 Batch Insulin Secretion

Islets were cultured in RPMI 1640 media supplemented with 10% FBS and 50 U/ml penicillin and 50 μg/ml streptomycin overnight prior to insulin secretion assay. Insulin secretion was run in quintuplicate and collected in a parallel fashion. Islets were washed and preincubated for 30 min in modified Krebs-Ringer bicarbonate buffer (KRB) containing (in mM) 119 NaCl, 4.6 KCl, 5 $NaHCO_3$, 2 $CaCl_2$, 1 $MgSO_4$, 0.15 Na_2HPO_4, 0.4 KH_2PO_4, 20 HEPES, 2 glucose, 0.05% BSA, pH 7.4. This was followed by a 30 min incubation in media containing either 3 mM or 15 mM glucose. Media was collected and stored at –20°C for insulin measurement. Insulin was measured by radioimmunoassay (LINCO RESEARCH INC., St. Charles, MO.). Normalization was performed by lysing the cells and measuring total insulin content. In order to measure insulin content, islets from three different animals were measured per genotype. For each animal, islet insulin content was measured in triplicate. For each measurement, six islets were lysed and diluted for insulin and protein measurements. Insulin was measured using the HTRF Insulin Assay (Cisbio Bioassays). Total protein was measured using the Bio-Rad Protein Assay, which is based on the Bradford method. Insulin content is presented as nanograms of insulin per milligram of total protein.

3.3.8 Islet Perifusion

Islets were perifused in a column as described (Cunningham et al., 1996). A collection of 50 islets was laid between 2 layers of Cytodex microcarrier beads (Sigma). The column used was 0.4 cm in diameter and 4 cm high and contained in a temperature controlled environment at 37 °C. Perifusion reagents were pumped through the column at 0.3 ml/minute using an analog tubing pump (Ismatech REGLO pump, type ISM 827, model 78,016–30; Cole-Parmer Instrument Co., Chicago, IL). Islets were perifused with Krebs-Ringer Bicarbonate buffer with added 0.5 % BSA for 30 minutes to allow for equilibrium. Eluted samples were collected at 30 second intervals for 48 minutes. Basal levels of insulin were determined with 3mM glucose perifusion for 6 minutes, response to 15mM glucose was measured for 32 minutes and 15mM glucose with KCl was perifused for 10 minutes.

3.3.9 Western Blot

Primary antibodies used include anti-Mfn2 (AbCam, Cambridge, MA), anti-Beta-Actin (Novus Biologicals, Littleton, CO), and anti-porin (AbCam, Cambridge, MA).

3.3.10 qPCR

Total RNA was isolated from islets using the Qiagen RNesay Plus Mini Kit. cDNA was obtained from RNA by a reverse transcriptase reaction using Applied Biosystems High Capacity cDNA Reverse Transcription Kit. Changes in gene expression were detected with SYBR Green. All samples were normalized to 18S content, which served as an endogenous control.

3.3.11 Islet Transplantation

Male immune-deficient athymic Swiss nude mice (8 weeks old) were used as graft recipients. Islets were isolated from βMfn2KO and control mice and subsequently approximately 100 islets were transplanted under the kidney capsules of Swiss nude mice. Aliquots of islets were sedimented in a PE-50 polyethylene tube attached to a 1-ml Hamilton syringe, which allowed the injection of an islet pellet under the kidney capsule (Davalli *et al.*, 1995). Then the islet pellets were transplanted beneath the left kidney capsule under methoxyflurane anesthesia. After transplantation, nonfasting blood glucose levels and body weights were measured weekly. A GTT was performed during the eighth week after the transplantation. Blood glucose was measured with a portable glucose meter after tail snipping. Nonfasting plasma insulin levels were measured after 15 weeks. Nonfasting blood samples were collected into heparinized capillary tubes, and plasma insulin was determined by ELISA. (Kaneto *et al.*, 2002)

3.3.12 Streptozotocin Treatment

STZ treatment was a single dose of 140mg/kg administered IP. This dose is on the low end of standard dose ranges used for C57Bl6 animals. Weight was measured one weekly for three weeks. Three weeks after administration of STZ, blood glucose measurements were taken and mice were euthanized and their pancreata were harvested. Histology was performed as described in methods section 3.3.6.

3.3.13 Data Analysis

All results are presented as mean ± S.E unless it otherwise stated. Statistical analysis was performed using the unpaired Student's *t* test.

3.4 Results

3.4.1 Mfn2 is Reduced Under High Fat Diet and in the ZDF Rat

In chapter 2, we showed that exposure of β-cells to a high fat and glucose environment resulted in the arrest of mitochondrial fusion *in vitro*. To determine the effects of nutrients on mitochondrial dynamics *in vivo*, we examined the levels of the mitochondrial fusion protein, Mfn2, in high fat diet fed mice, a model of diet-induced diabetes and obesity and in the Zucker diabetic animal model. Mfn2 was investigated because it has been shown to be altered in both obesity and diabetes in skeletal muscle, but had not been studied in β-cells. Bach *et al.* demonstrated that Mfn2 mRNA levels are decreased in human skeletal muscle of obese patients and that there is decreased mitochondrial networking in obese Zucker rats (Bach *et al.*, 2003). Additionally, there is a decrease in Mfn2 gene expression and protein levels in diabetic patients and animal models (Bach *et al.*, 2003;Bach *et al.*, 2005). They also show that muscle Mfn2 mRNA levels in skeletal muscle are inversely proportional to BMI and directly proportional to insulin sensitivity (Bach *et al.*, 2005). For these reasons, we determined that Mfn2 would be a good candidate in the β-cell for a mitochondrial fusion protein that could be altered in diabetes.

C57Bl6 mice were placed on a high fat diet (HFD, 58% kcal from fat, New Brunswick, NJ.) for 12 weeks. Glucose tolerance tests were performed weekly from weeks 8-12. Impaired glucose tolerance became evident at week 12. Islets were isolated from three mice per group at weeks 1, 2, 3, 5, and 7. Western blot analysis of Mfn2 revealed that during weeks 1-5 there were no significant changes in Mfn2 protein levels (Figure 3.1A). However, at week seven, a statistically significant decrease of 27% was observed. By week 12, when hyperglycemia and impaired glucose tolerance became evident, Mfn2

expression levels were reduced by 67 % compared with control mice (Figure 3.1B). Interestingly, islet MFN2 mRNA from the same animals is not decreased indicating that the change in Mfn2 protein may be due to increased degradation (Figure 3.1B). These results suggest that either weight, poor glycemic control or both contribute to reduction in Mfn2 levels.

We have previously shown that the mild inhibitory effect of fatty acids on mitochondrial fusion is strongly exacerbated and leads to full inhibition when fatty acids are joined by high glucose concentrations. To determine the isolated contribution of weight gain, insulin resistance and hyperglycemia on Mfn2 levels, we examined islets isolated from Zucker rats (Figs. 3.1C, & D). Three animals from each experimental group (Zucker Lean, Zucker Fatty, Zucker Diabetic Lean, and Zucker Diabetic Fatty) were assayed at eight weeks of age. Comparison of the Zucker fatty and the Zucker diabetic to their corresponding lean control showed that Mfn2 was significantly reduced by 41% in the Zucker diabetic but not in the Zucker fatty. This indicates that obesity alone is not sufficient to decrease islet Mfn2. Together with the information obtained from the HFD model these data suggest that reduction in Mfn2 is linked to hyperglycemia.

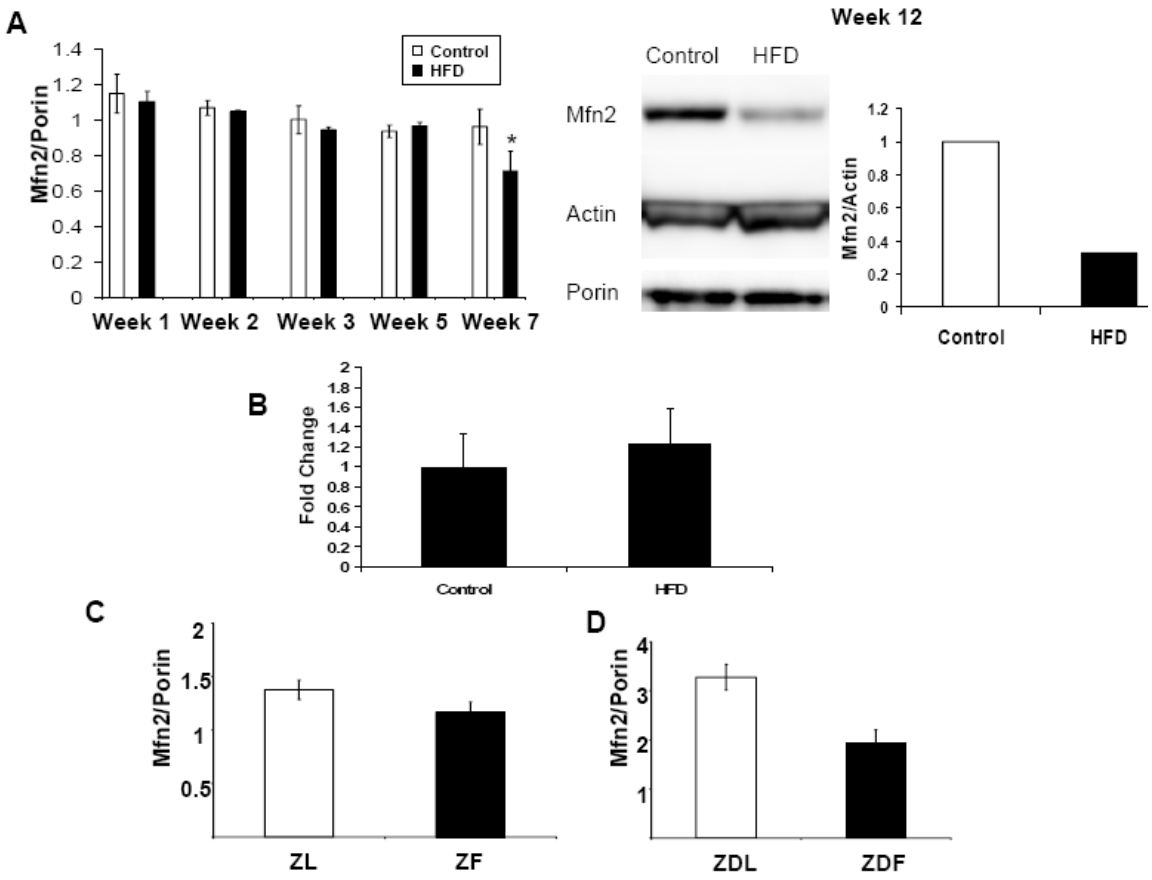

Figure 3.1: Mfn2 protein levels are decreased in pancreatic islets isolated from animal models of obesity and diabetes. **A.** Male C57Bl6 mice were administered either HFD, containing 58% of kcal from fat, or a control diet consisting of 6% of kcal from fat for 12 weeks. Western blot analysis of protein lysates obtained from islets isolated from HFD mice reveals a significant decrease in Mfn2. Actin and Porin expression were equal in both sets of mouse islets tested, indicating this is not due to changes in mitochondrial mass (n=3). **B.** Islet Mfn2 mRNA from HFD and control mice was measured by real time PCR. No significant difference was measured between the groups displayed as mean ± standard deviation. (n=3; p=0.06) **C,D.** Islets were isolated from 8 week old Zucker Lean (ZL), Zucker Fatty (ZF), Zucker Diabetic Lean (ZDL), and Zucker Diabetic Fatty (ZDF) and tested for Mfn2 protein expression by western blot (n=3 per group). Densitometric analyses of Mfn2/porin indicates that there is a 41% decrease in Mfn2 expression in ZDF rats compared to ZDL control ($p<0.05$) and no difference between ZF and ZL mice.

3.4.2 Generation of a β-Cell Specific Mfn2 Null Animal Model

In order to investigate the significance of the reduction in islet Mfn2 in diabetes and obesity, we created a mouse lacking Mfn2 in insulin secreting cells by using the

Cre/LoxP system. Rat Insulin Promoter (RIP)-mediated Cre expression produced excision of Mfn2 (βMfn2KO) in β-cells of the islets of Langerhans. Tissue specific excision of Mfn2 from isolated pancreatic islets was confirmed by PCR and western blot (Figure3.2A and B). Comparison of Mfn2 expression in other tissues (liver, muscle, heart, fat, thymus, and brain) obtained from βMfn2KO mice indicates that these tissues are not significantly affected (Figure 3.2C). The amount of mitochondria per cell varies greatly between different tissue types, therefore loading an equal amount of total protein leads to differential amounts of mitochondria. Therefore, in this western blot, we used porin, an outer mitochondrial membrane protein, as a mitochondrial loading control to ensure that mitochondria were present in each sample.

βMfn2KO animals are viable and there is no difference in survival between βMfn2KO mice and littermate controls. The number of βMfn2KO pups born per litter is similar to those of other littermates (LoxP homozygous, LoxP heterozygous, and Double Heterozygous pups). In this study, all experiments were performed on male mice that were characterized at the F2 generation, which have a mixed genetic background of C57Bl6 and S129. We are in the process of backcrossing to the C57Bl6 genetic background. Unless otherwise stated, all characterization of βMfn2KO mice was done in animals fed normal lab chow.

The origin of insulin in the central nervous system is still controversial, although there is evidence that both pancreatic and local sources of insulin are present in the brain (Clarke *et al.*, 1986;Schechter *et al.*, 1996;Banks and Kastin, 1998;Grunblatt *et al.*, 2007). In accordance with the evidence that insulin can be produced in the brain, Cre expression

driven by the RIP promoter has been shown to display brain expression in addition to the expected β-cell expression (Lin *et al.*, 2004;Choudhury *et al.*, 2005;Covey *et al.*, 2006;Mori *et al.*, 2009;Song *et al.*, 2010). This has also been found with other Cre lines thought to be pancreas specific including neurogenin 3 promoter (Ngn3-Cre mice) and pancreas-duodenum homeobox 1 promoter (Pdx1-Cre) (Song *et al.*, 2010). Song *et al.* demonstrated that the expression of GFP that was dependent on RIP-Cre activity was found to the largest extent in the arcuate nucleus of the hypothalamus, but was also scattered in the cortex, striatum, and other hypothalamic regions including the suprachiasmatic nucleus (SCN), the ventral medial hypothalamus (VMH), the dorsal medial hypothalamus (DMH), and the medial tuberal region (mTu). Consequently, it is expected that these cells are also targeted for Mfn2 excision (Song *et al.*, 2010).

Western blot analysis of Mfn2 expression, shown in Figure 3.2C, demonstrates that there is Mfn2 present in the brain. However, our samples were derived from whole brain lysates, whereas Mfn2 excision has only been reported in a small subset of cells primarily in the hypothalamus. Therefore, any excision of Mfn2 from the arcuate nucleus or other hypothalamic neurons would be masked by Mfn2 expression in the rest of the brain. To address this, we attempted to utilize immunohistochemistry (IHC) to examine Mfn2 protein expression in histological slices from βMfn2KO and control brains. Unfortunately, we were unable to obtain a signal for Mfn2 due to the quality of the antibody we used. In the future, it would be worthwhile to attempt this again if a better antibody is developed or by using another technique, such as *in situ* hybridization to investigate mRNA expression in the brain. Therefore, it is important to keep in mind that

the interpretation of any results obtained from the characterization of βMfn2KO mice could be due to either β-cell or hypothalamic Mfn2 excision or a combination of both.

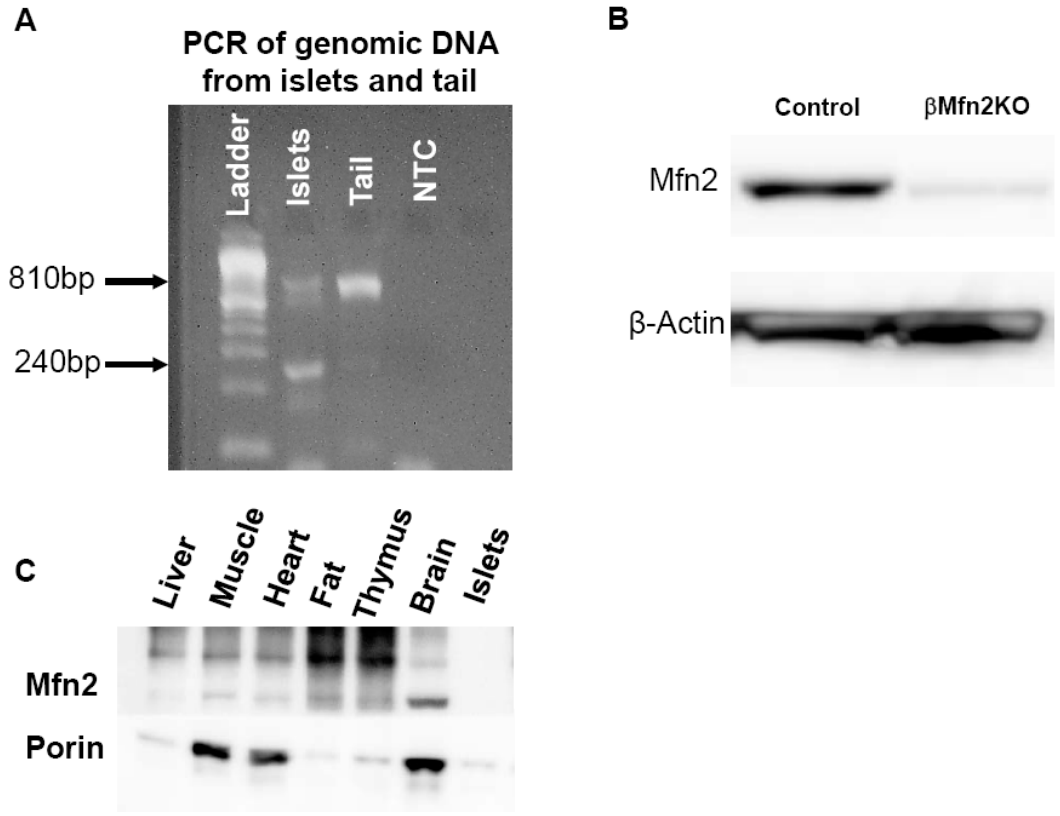

Figure 3.2: Validation of β-cell specific Mfn2 knockout. **A.** PCR analysis for Mfn2 LoxP of genomic DNA obtained from a tail sample and islets from a βMfn2KO animal. Lane 1 is the DNA ladder. Lane 2 is the PCR product obtained using islet DNA as the template; the band is present at a 240bp, which is the size of the excised gene, demonstrating knockout of Mfn2. Any residual unexcised 810bp band is contributed by other islet cell types (alpha cells, delta cells, etc) in the islet that would not have Mfn2 excised under the insulin promoter. Lane 3 is the PCR product obtained using tail lysates and is present as the unexcised 810bp band. Lane 4 is the no template control demonstrating that no bands are present when no DNA template is added to the PCR reaction. **B.** Western blot of protein samples obtained from βMfn2KO and control littermate islets. Mfn2 protein is largely reduced in the islets of βMfn2KO islets. Any Mfn2 expression is attributed to non-β-cell islet cells. **C.** Represenative western blot for the tissue specificity of Mfn2 excision using the RIP-Cre promoter (n=3 samples per genotype). . Mfn2 was present in all tissues measured expect from islets. Porin was used as a mitochondrial loading control.

3.4.3 Deletion of Mfn2 Impairs β-Cell Mitochondrial Morphology

To determine whether Mfn2 deficiency is sufficient to lead to a fragmented mitochondrial network, confocal imaging was undertaken in order to visualize mitochondrial architecture. Islets isolated from βMfn2KO and control littermates were dispersed and imaged. Dispersed islets were infected with a mitochondrial targeted PAGFP adenovirus that was expressed under the RIP promoter; this made it possible to distinguish β-cells from the population of dispersed islet cells. Cells were first stained with TMRE in order to visualize all polarized mitochondria. Then a pulse of UV light was delivered using a 2 photon laser in order to induce photoconversion of mitochondrial PAGFP into its fluorescent form in cells expressing insulin. We find that β-cells isolated from βMfn2KO mice display fragmented mitochondrial architecture (Figure 3.3A). On the other hand, in images that contain both β-cells and non-β-cells, we find that only PAGFP positive cells from dispersed βMfn2KO islets possessed altered mitochondrial morphology (Figure 3.3B).

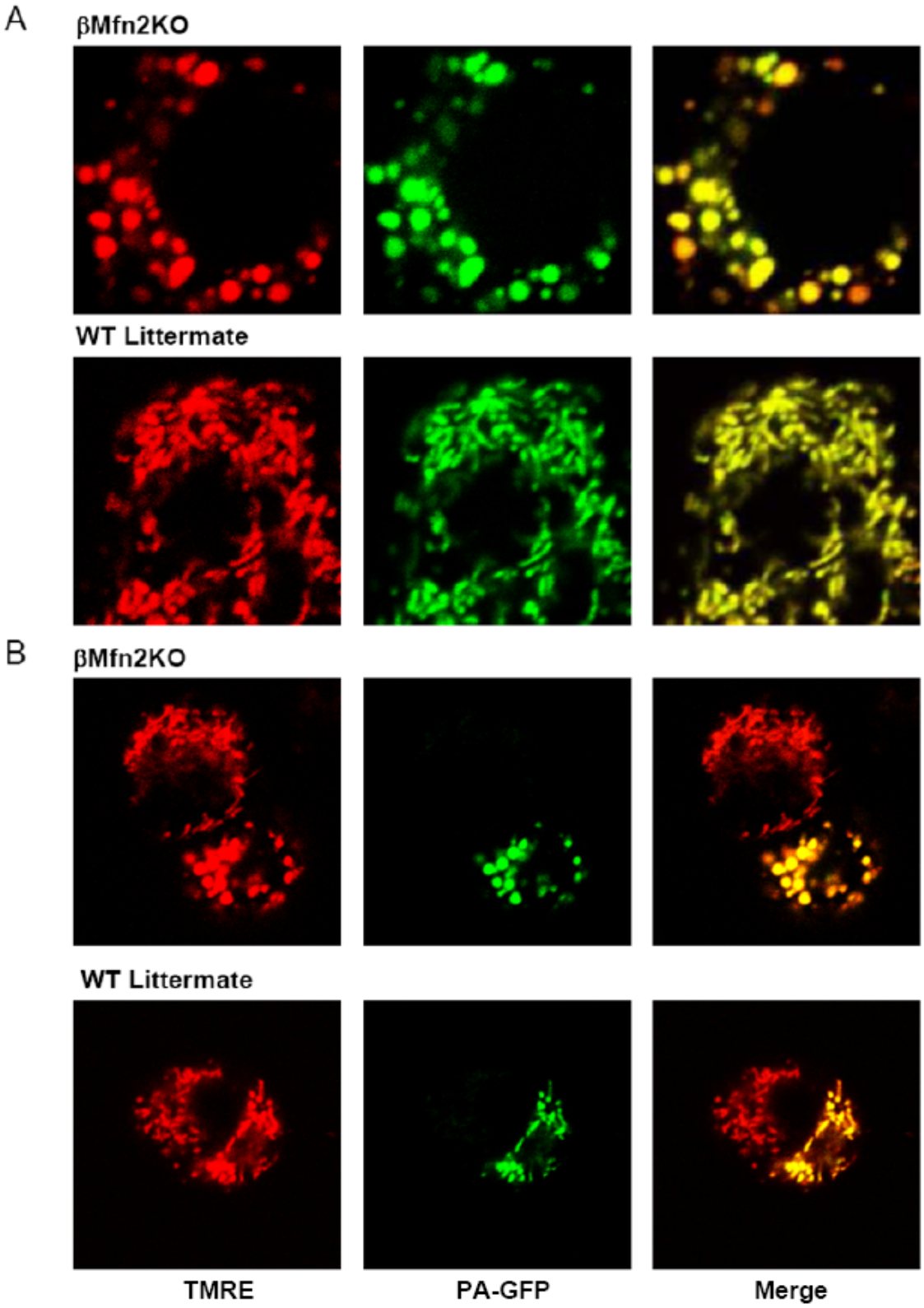

Figure 3.3: Excision of Mfn2 leads to β-cell mitochondrial fragmentation without causing alterations in the morphology of non-β-cell islet cells. **A**. Confocal imaging was

performed on β-cell mitochondria that were labeled with TMRE and mitochondrial matrix targeted PAGFP under control of the insulin promoter. β-cell mitochondria were identified by expression of PAGFP and were found to have fragmented mitochondria in βMfn2KO β-cells. **B**. Representative images showing β-cells and non-β-cells from dispersed islets in the same field of view. Mitochondrial fragmentation is only evident in the β-cell obtained from βMfn2KO samples. Cells from βMfn2KO islets that do not contain insulin promoter-driven PAGFP expression display normal mitochondrial architecture.

3.4.4 βMfn2 Null Animals Develop Obesity on Normal Chow

βMfn2KO mice maintained on regular chow (Teklad Global 18% protein rodent diet, Indianapolis, IN) begin to exhibit dramatic weight gain compared to control littermates within 3 months after birth (Figure 3.4 A,B,C). The generation of βMfn2KO mice also yields double heterozygous (Dbl Het) mice as littermates. These animals have one copy of both RIP-Cre and the floxed Mfn2 gene. Thus, these animals can be used to report phenotypes associated with the expression of RIP-Cre when compared to βMfn2KO and control littermates. At 94 days of age, βMfn2KO weigh 32.2g ($\pm$ 1.6g) on average while control and double heterozygous littermates weigh an average of 26.7g ($\pm$0.6g) and 27.1g ($\pm$1.3g) respectively. The difference in body weight was progressive and at one year of age βMfn2KO mice were approximately 50% heavier than control littermates (Figure 3.4B). Whole body MRI measurements reveal that weight gain in βMfn2KO animals is due to an increase in fat mass, rather than lean tissue mass (Figure 3.4D). Moreover, the increase in fat mass is evident in both visceral and subcutaneous deposits and is seen even at early time points when βMfn2KO and control animals are weight-matched (Figure 3.4E&F). Lean tissue mass was mildly decreased in βMfn2KO mice.

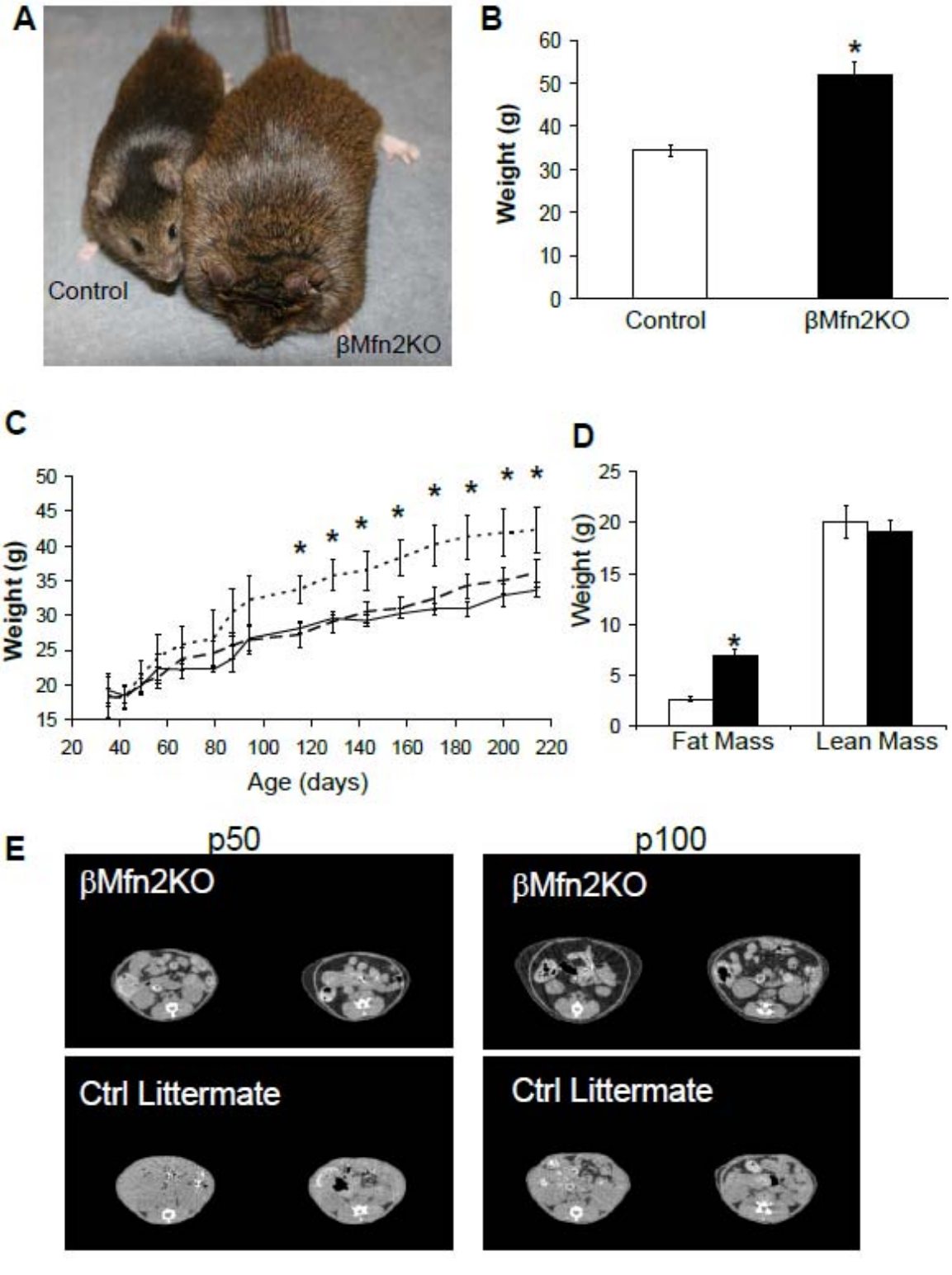
A
Control
βMfn2KO
B
Weight (g)
60
50
40
30
20
10
0
*
Control
βMfn2KO
C
Weight (g)
50
45
40
35
30
25
20
15
20 40 60 80 100 120 140 160 180 200 220
Age (days)
D
Weight (g)
25
20
15
10
5
0
*
Fat Mass
Lean Mass
E
p50
p100
βMfn2KO
βMfn2KO
Ctrl Littermate
Ctrl Littermate

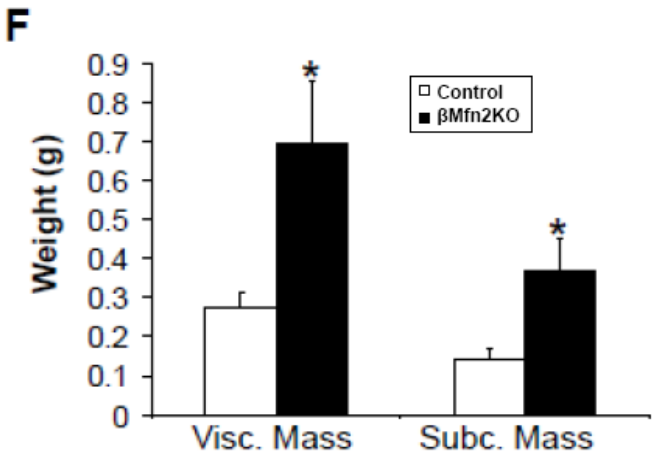

Figure 3.4: βMfn2KO animals display dramatic obesity without any change in diet. **A.** Dramtic obesity is evident in one year old male littermates. A βMfn2KO mouse is displayed on the right and a control littermate on the left. **B.** Average body weight of 1 year old male animals indicate that βMfn2KO mice are significantly heavier (n=6; *p≤0.05). **C.** βMfn2KO (dotted), double heterozygous (dashed), and control mice (solid) were weighed every 2 weeks for 214 days (n=10 per genotype; *p≤0.05). Immediately after weaning, there is no difference in body weights between the groups. Obesity begins to develop in the βMfn2KO animals around 2 months of age and continues throughout all tested time points thereafter. **D.** Comparison of fat mass and lean mass in 50 day old βMfn2KO mice and control littermates (n=6; *p≤0.05). This is a time point before the development of obesity in βMfn2KO mice. Relative fat mass is significantly greater in the βMfn2KO mice (black bars). **E.** CT scans through sequential abdominal sections taken in βMfn2KO mice and littermate controls at 50 and 100 days old. Black areas are indicative of fat tissue. Even in young, weight matched animals βMfn2KO mice accumulate significantly more fat than in littermate control mice. Fat accumulation progresses with time and additional weight gain. **F.** Sequential CT scans through the abdomen of the 50 day old mice were analyzed in order to compare visceral and subcutaneous fat depots. βMfn2KO mice display a significant increase in mass in both fat depots (n=4; *p≤0.05).

3.4.5 βMfn2 Null Mice Store More and Expend Less Energy

To determine whether weight gain was a result of increased food intake or reduced metabolism, we next examined feeding behavior and quantified animal movement and oxygen consumption. Feeding behavior was examined at 50 days of age, before the onset of differences in body weight (Figure 3.5A, B, and C). Over a one week period, βMfn2KO animals gain 1.9. ± 0.4g on average compared to control littermates that gain

an average of 0.5g ± 0.3g. During this period, there was no difference in total food intake; 41±2g for βMfn2KO animals compared with 39g ± 2g for littermate controls.

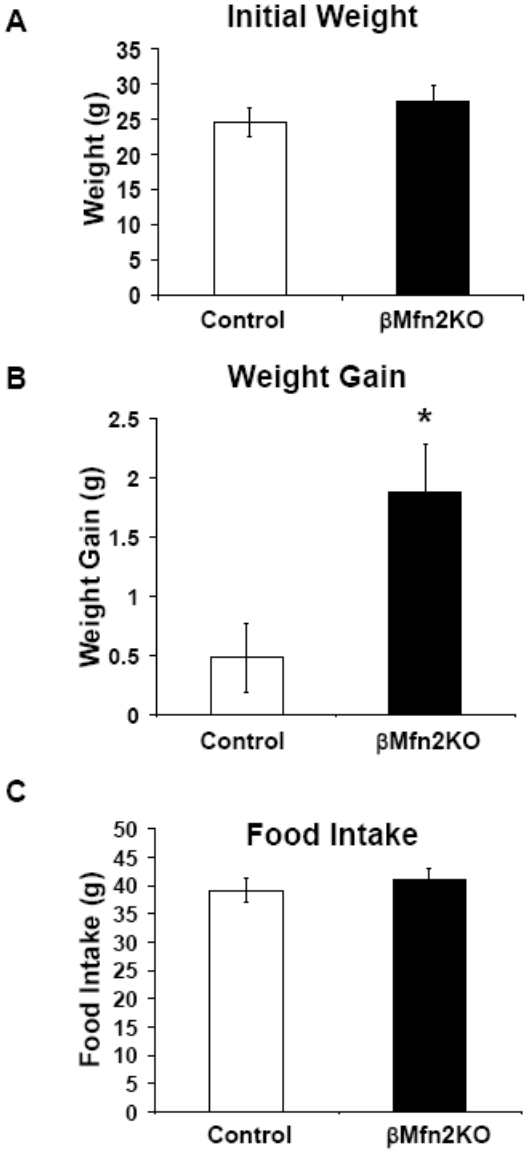

Figure 3. 5: Weight gain in βMfn2KO is not due to increased food intake. Comparison of initial weight, one week weight gain, and one week food intake in a cohort βMfn2KO and WT littermates (n=6 per group). **A.** At 50 days of age, no significant difference in body weight is evident between groups. **B.** Over a one week period, βMfn2KO mice gain significantly more weight (four times) compared to control littermates. **C.** Total food intake over the one week measurement period was not statistically different between the two groups of animals. *p≤0.05.

Having ruled out hyperphagia as the cause of weight gain, we sought to examine the contribution of whole body metabolism and activity. In order to measure these parameters, we placed mice in a Complete Lab Animal Monitoring Systems (CLAMS) (Columbus, OH.). Our results indicate that respiratory exchange ratio (RER) and oxygen consumption are both lower in the βMfn2KO mice compared to controls (Figure 3.6A & B). Over a 48 hour period, the average RER was 0.86 $\pm$ 0.03 for βMfn2KOs and 0.97 $\pm$ 0.01 for controls. A lower RER suggests that βMfn2KO mice utilize a mix of fat and charbohydrate as fuel sources compared to control mice, which preferentially utilize carbohydrates as fuel. Locomotive activity was measured by counting laser line crossings within the metabolic cage. We find that βMfn2KO animals trend towards a decrease in the amount of times they cross the laser line, an average of 1019 $\pm$129 times per hour, compared to control littermates that exhibit more activity with 1350 $\pm$ line crossing per hour; although this was not significant (Figure 3.6C).

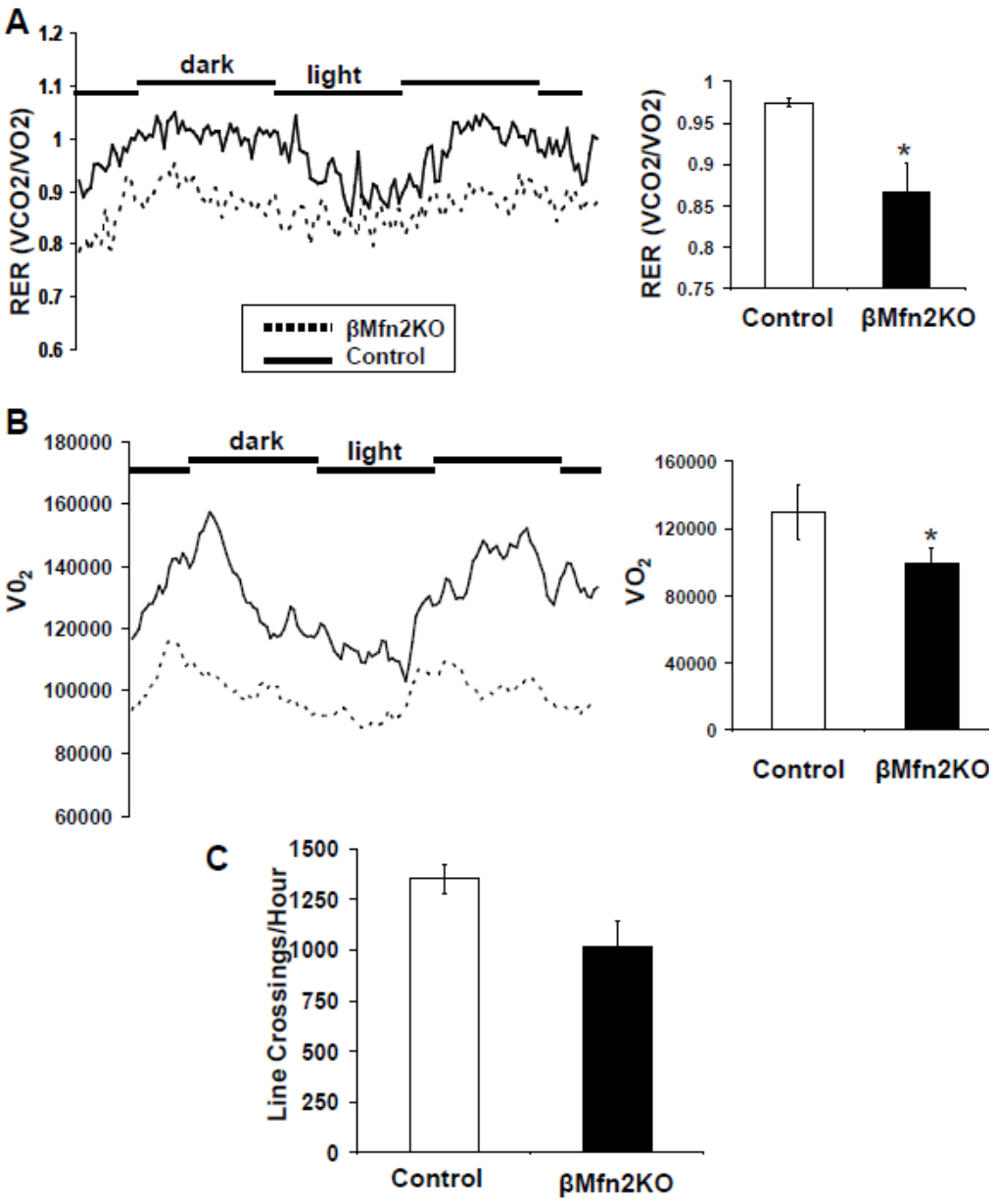

Figure 3.6: βMfn2KO mice display decreased whole body metabolism compared to littermate controls. **A.** Respiratory exchange ratio (RER) is decreased in βMfn2KO animals (dotted line) compared to control littermates (solid line) over a 48 hour recording period. Bar graphs present the average RER ± standard deviation (SD) over the entire recording period (n=4; *p≤0.05). **B.** Whole animal oxygen consumption rate measured over 48 hours is lower in βMfn2KO animals (dotted line) compared to control littermates (solid line). Bar graphs represent the average oxygen consumption (± SD) over the recording period (n=5; *p≤0.05). **C.** Physical activity measured by average laser line crossings per hour (± SD) over a 48 hour recording period. βMfn2KO animals trend

towards being less active than littermate controls (n=3 for control and n=5 for βMfn2KO mice; p=0.065).

3.4.6 βMfn2 Null Mice Display Impaired Glycemic Control

3.4.6a Fasting Blood Glucose and Glucose Handling

Blood glucose was tested after an overnight fast every 2 weeks from 94-214 days of age. At most time points tested, fasting blood glucose levels were significantly higher in βMfn2KO mice versus control littermates (Fig 3.7A). Interestingly, βMfn2KO mice display glucose intolerance before and after the onset of obesity. Specifically, glucose tolerance tests (GTT) reveal significantly larger blood glucose excursions upon injection of glucose into βMfn2KO animals (Figure 3.7B). The blood glucose level does not return to baseline even after 2 hours of monitoring. Glucose clearance was determined by measuring the area under the curve (AUC) through the course of the GTT, corresponding to the integrated value of blood glucose over a period of 2 hours. At 50 days of age, insulin AUC for control animals is 18641± 2220 while the βMfn2KO exhibit an AUC of 35848 ± 5823 (Figure 3.7C). Serum insulin was measured at 0, 5, 15, and 30 minutes during the GTT to determine insulin secretion in response to glucose (Figure 3.7D). βMfn2KO mice had significantly higher serum insulin levels ($p<0.05$) at 15 minutes (0.368 ug/l) compared to control mice (0.254 ug/l). There was no significant difference in insulin concentration at any other time point during the GTT. βMfn2KO animals at 10 months of age continue to display glucose intolerance; Control AUC: 20555 ± 1895; βMfn2KO AUC: 40259 ± 1405 (Figure 3.7E and F).

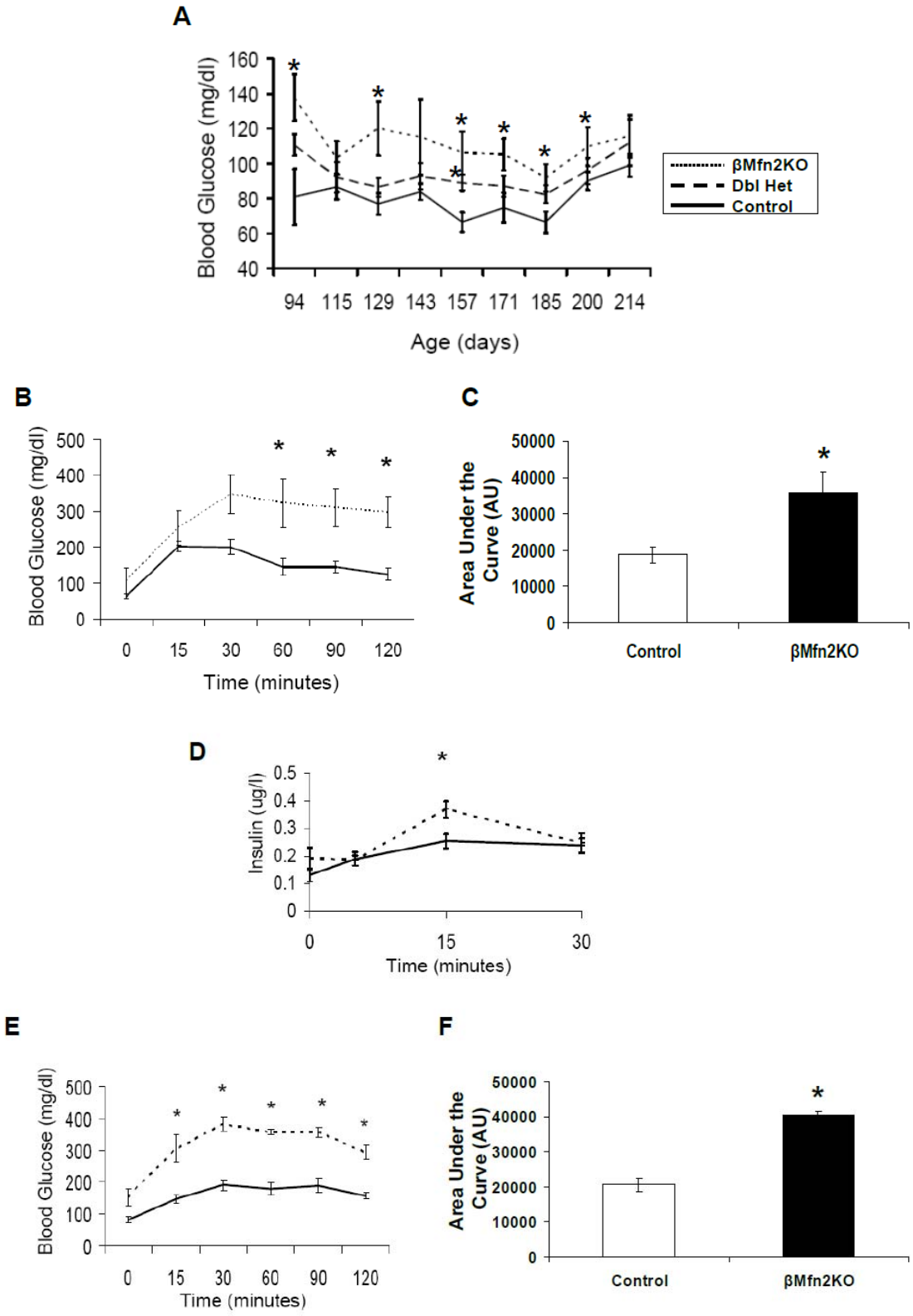

Figure 3.7 Young βMfn2KO mice display impaired glucose tolerance before the onset of weight gain. βMfn2KO mice are represented by the dotted line and/or black bar in the

bar graph and control littermates are shown with the solid black line and unfilled bar. **A.** Fasting blood glucose was measured biweekly for 30 weeks. βMfn2KO mice (dotted) display hyperglycemia compared with littermate controls (solid line) at most time points. Double heterozygous mice (dashed) display an intermediate phenotype (n=10; *$p \leq 0.05$ compared with control). **B.** Glucose tolerance tests (GTT) were performed on βMfn2KO and control animals at age p50. At this young age, βMfn2KO animals already have impaired glucose tolerance compared with controls (n=4; *$p \leq 0.05$). **C.** Area under the curve of the GTT graphs. AUCs demonstrate that there is a significant increase in integrated glucose levels in βMfn2 KO mice. **D.** Blood samples were taken during the GTT in p50 mice. βMfn2KO mice display an increase in serum insulin levels 15 minutes after glucose injection compared with control mice (n=4; *$p \leq 0.05$). **E. and F.** GTT and corresponding AUC of βMfn2KO mice and control littermates at 10 months of age when obesity is prominent. βMfn2KO mice have impaired glucose tolerance compared with controls (n=4; *$p \leq 0.05$).

3.4.6b Peripheral Insulin Resistance

To determine if impaired glucose tolerance was due to insulin resistance, we performed IP Insulin Tolerance Tests (ITT) before and after the onset of obesity (Figure 3.8A and C). This test targets the muscle and adipose tissue primarily. IP insulin tolerance tests reveal that insulin resistance develops over time and becomes evident after the onset of obesity. At 50 days of age, the integrated values of glucose over the course of two hours after the injection of insulin (ITT AUC), is 10991 ± 613 for control animals while βMfn2KO animals exhibit similar values of 9580 ± 848 (Figure 3.8B). This demonstrates that insulin resistance of the fat and muscle are not apparent even though impaired glucose tolerance is already present. At 10 months of age, ITT AUC is 8596 ± 1176 for controls and 17874 ± 1512 for βMfn2KO mice indicative of insulin resistance (Figure 3.8D). Taken together, these data demonstrate that βMfn2KO mice display impaired glucose clearance before the development of whole body insulin resistance.

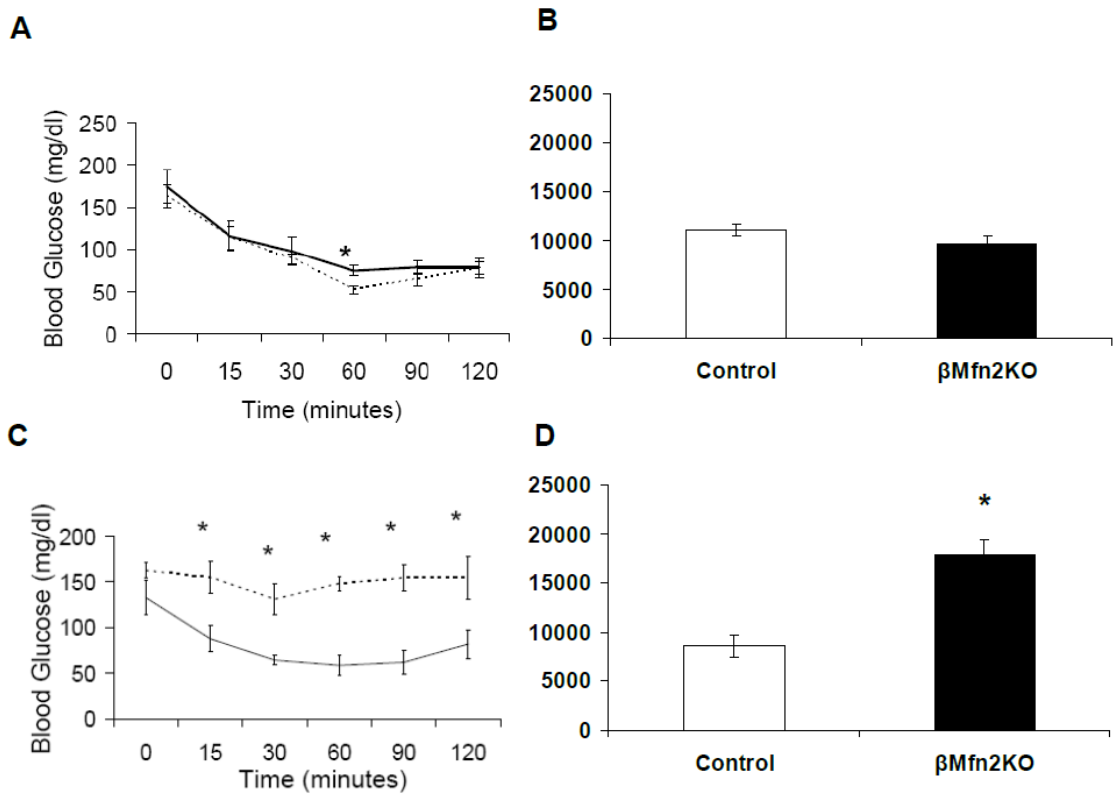

Figure 3.8 Peripheral insulin resistance is not present in young, weight matched βMfn2KO mice but develops with age and weight gain. βMfn2KO mice are represented by the dotted line and/or black bar in the bar graph and control littermates are shown with the solid black line and unfilled bar. **A. and B.** ITT with corresponding AUC. Young βMfn2KO mice that are weight matched to littermate controls do not display insulin resistnace at 2 months of age (n=4 for control and n=5 for βMfn2KO mice; one control mouse was removed due to technical issues). The ITT demonstrates that young βMfn2KO mice can response to insulin by decreasing blood gluoce levels. **C and D.** ITT and corresponding AUC for 10 month old βMfn2KO mice. Old βMfn2KO mice no longer respond to an IP insulin injection by decreasing blood glucose levels, demonstrating peripheral insulin resistance (n=4; *p≤0.05).

3.4.6c In Vivo Insulin Secretion Measurements

Insulin secretion was determined *in vivo* by measuring both insulin as well as c-peptide in blood. These measurements reveal that c-peptide levels are higher in βMfn2KO animals starting at 50 days of age, prior to the development of obesity (βMfn2KO: 1533 ±252 pM; control: 997 ±113 pM without fasting) (Figure 3.9A). This is also in agreement with

blood chemistry analysis that was performed on control and βMfn2KO mice (Table 1). Interestingly, hyperinsulinemia does not become evident as early as high circulating c-peptide (Figure 3.9B). These findings indicate that higher levels of insulin secretion in βMfn2KO animals are compensated for by increased insulin clearance by the liver, suggesting the presence of portal vein hyperinsulinemia Overall, these findings reveal that islets lacking Mfn2 secrete more insulin and that this hypersecretion is not in response to insulin resistance.

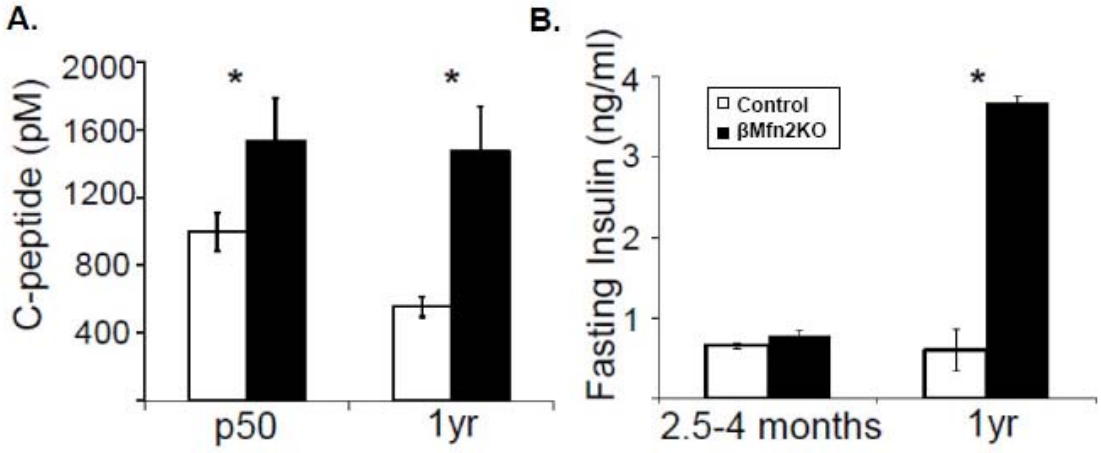

Figure 3.9 βMfn2KO mice secrete more insulin *in vivo*. **A.** Serum C-peptide levels, measured by ELISA, were obtained after an overnight fast. βMfn2KO mice at both 50 days (p50) and 1 year of age have increased circulating C-peptide concentrations. **B.** Development of hyperinsulinemia with age. At 2.5-4 months of age, no significant difference in blood insulin is apparent. At one year of age, fasting blood insulin is dramatically increased.

	4-5 Month Old Animals		One Year Old Animals	
	Control	βMfn2KO	Control	βMfn2KO
Insulin (ng/ml)	-	-	0.24±0.1	2.47±1.2
C-Peptide (pM/l)	226.7±125	583±172	554.2±57.9	1472±255.2
Leptin (ng/ml)	0.98±0.6	8.3±3.1	5.2±0.8	9.3±0.8
Glucagon (pg/ml)	135±42	148±48	45.4±3.5	47.4±9.5
Free Fatty Acids (µmol/l)	1995.3±700	4328±157	1804.5±295	2682.7±1211.6
Triglycerides (mg/dl)	136.7±1.9	342.7±46.8	158±16	244±83.2
Total Cholesterol (mg/dl)	126.7±16.7	160.3±17.2	120±7	121.3±12
HDL (mg/dl)	67.7±20	14±10	74±8	68±9.3
LDL (mg/dl)	35±31	31±6	4.5±1.5	8.3±1.9

Table 3.1 Blood chemistry profiles of young and old βMfn2KO mice compared with age matched controls (n=3 animals per group; except n=2 in one year control).

3.4.7 Insulin Hypersecretion in the βMfn2KO is Accompanied by Increased Insulin Clearance and Liver Insulin Resistance

Previous studies have shown that the liver can respond to alterations in insulin secretion by changing the rate of insulin clearance as well as its sensitivity to insulin. Since peripheral insulin concentration is a result of a balance between secretion (measured as C peptide) and clearance, any change in insulin secretion that is not met with a parallel change in insulin concentration suggests a change in clearance. As shown in figure 3.9, measurements of insulin concentration revealed that the increased level of insulin secretion was not accompanied by an increase in blood insulin. These findings indicate that higher levels of insulin secretion in βMfn2KO animals are compensated for by increased insulin clearance by the liver, suggesting the presence of portal vein hyperinsulinemia.

To determine if insulin hypersecretion affects liver insulin sensitivity in the βMfn2KO mice we studied the rate of gluconeogenesis by conducting pyruvate tolerance tests (PTT) (Figure 3.10A and B). Sodium pyruvate was injected IP after an overnight fast and

gluconeogenesis was measured by tracking the blood glucose concentration over time. PTT indicate a higher level of hepatic glucose production or gluconeogenesis in the young, non-obese and weight matched, βMfn2KO mice (AUC: 14445 ± 63.8) compared to littermate controls (AUC: 21176 ± 2226) (Figure 3.10B). Serum glucagon concentrations were also measured during the PTT to determine the potential contribution of pancreatic α-cells to gluconeogenesis (Figure 3.10C). There was no difference in secretion of glucagon in response to pyruvate at any time point tested, suggesting that changes in gluconeogesis would be emerging from the liver.

We also looked at the hepatic expression of some of the key enzymes of gluconeogesis to verify that there is an increase in gluconeogenesis in βMfn2KO mice. We probed for phosphoenolpyruvate carboxykinase (PEPCK), the enzyme that converts oxaloacetate into phosphoenolpyruvate and carbon dioxide and is a rate-controlling step of gluconeogenesis, and glucose-6-phosphatase (Glc-6-Pase), the enzyme that hydrolyzes glucose-6-phosphate to generate free glucose, consequently executing the final step of gluconeogenesis. We found that there was no difference in hepatic expression of these enzymes in βMfn2KO liver lysates compared with control lysates (Figure 3.10D). This result suggests that there is no difference in gluconeogenesis in these animals, although this may not be the case. Most enzymes are present in excess and therefore it would be beneficial to measure enzyme activity in these samples instead of protein expression. Enzyme activity would be a much better indicator of any changes in gluconeogenesis.

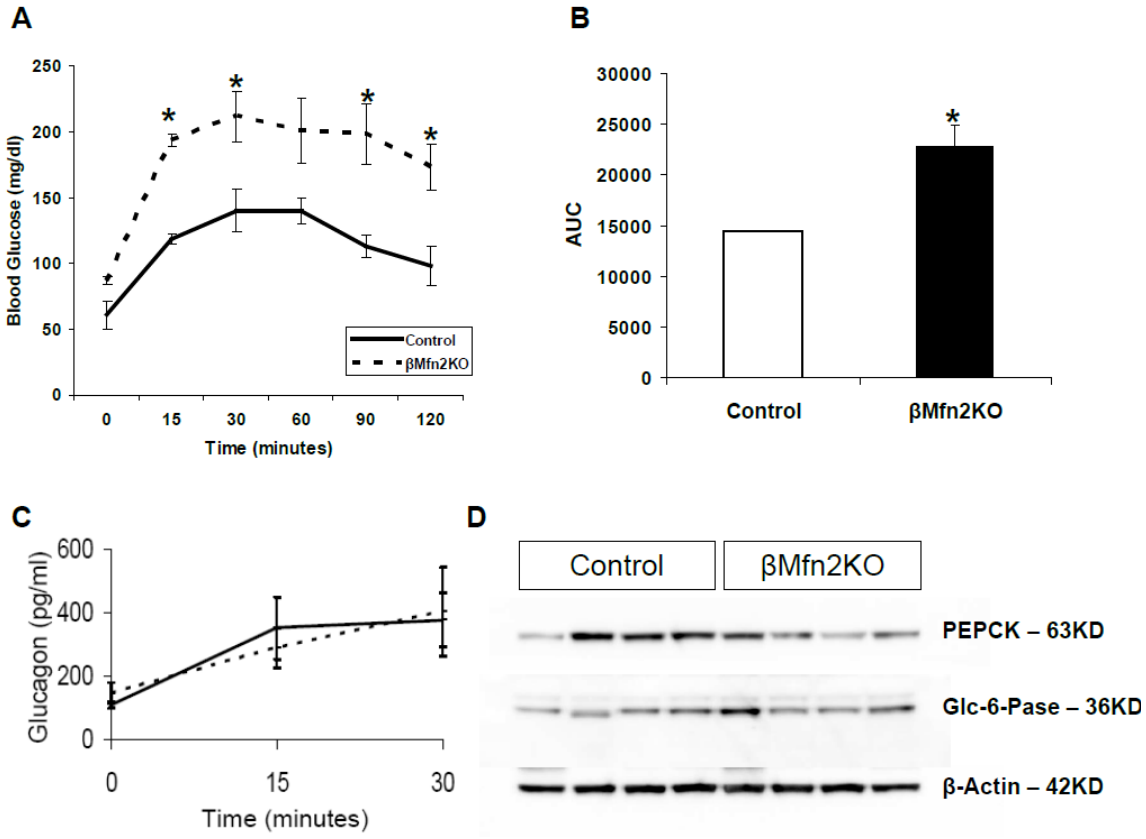

Figure 3.10 Increased gluconeogenesis in βMfn2KO mice without accompanying changes in protein expression of key gluconeogenic enzymes. **A.** Pyruvate tolerance tests indicate that male 2 month old βMfn2KO mice exhibit higher gluconeogenesis compared to control littermates (n=3; *p≤0.05). **B.** Area under the curve analysis also demonstrates a significant increase in integrated blood glucose in response to sodium pyruvate in βMfn2KO mice compared with littermate controls (n=3; *p≤0.05). **C.** Glucagon concentrations were measured during the PTT of p50 mice. There were no significant changes in serum glucagon levels observed between βMfn2KO mice and controls (n=3; *p≤0.05). **D.** Western blot analysis for PEPCK and glucose-6-phosphatase in livers from control and βMfn2KO livers reveal no change in the expression of these enzymes. β-actin was used as a loading control (n=4 samples per genotype).

3.4.8 Insulin Secretion in βMfn2KO Mice In Vitro

3.4.8a βMfn2KO Islets Display Iincreased Insulin Secretion at Non-Stimulating Glucose Levels

To determine if hyper secretion is endogenous to the islets lacking Mfn2, islets isolated from βMfn2KO mice were analyzed. When normalized to insulin content, islets isolated from βMfn2KO mice displayed a greater than 2.5 fold increase in basal insulin secretion

under 3mM glucose ($5.99*10^{-4} \pm 1.8*10^{-4}$) compared with control islets ($2.24*10^{-4} \pm 6.8*10^{-5}$) (Figure 3.11A). Glucose stimulated insulin secretion (GSIS) from isolated islets can be induced by exposure to 15mM glucose. We found that insulin secretion during a 30 minute exposure to 15mM glucose was not different in βMfn2KO islets ($1.74*10^{-4} \pm 3.19*10^{-4}$) compared with control islets ($1.7*10^{-4} \pm 5.1*10^{-4}$). Insulin content was measured to verify that changes in insulin secretion are not due to changes in insulin content (Figure 3.11C). There was no significant change in insulin content between size matched control (3196 ng insulin/mg protein) and βMfn2KO (2763 ng insulin/mg protein) islets ($p= 0.193$). This is especially important considering that H&E analysis of pancreas slices revealed islets hyperplasia in βMfn2KO islets compared with control islets, which becomes more evident with age and obesity (Figure 3.11D). Upon further investigation of islet composition by immunohistochemical labeling of alpha cells and beta cells, we find that both populations increase in number. However, the ratio of the abundance of the two cell types does not change (Figure 3.11E).

Factors related to the excision of Mfn2 during development may affect the function of islets isolated from βMfn2KO animals. To evaluate the contribution of the long term deficiency of Mfn2 into the increase in insulin secretion at unstimulating glucose concentrations, insulin secretion was measured in islets from which Mfn2 was acutely excised *ex vivo*. Islets were isolated from control Mfn2 LoxP animals, dispersed, and embedded in matrigel (BD biosciences, San Jose, CA.) containing adenoviral particles for expression of either Cre-GFP or GFP alone. Insulin secretion was measured from these preparations and a similar increase in basal insulin secretion was observed with Mfn2 excision (Figure 3.11B). This suggests that changes in Mfn2 mediate basal

hypersecretion and that this is not a hypothalamic occurrence. Cre infected and control islets had similar response to glucose, although this response was diminished compared to un-infected islets.

3.4.8b βMfn2 Knockout Islets have Diminished 1st Phase and Elevated 2nd Phase Secretion

Islet perifusion experiments were conducted in order to examine the time course of insulin secretion in response to glucose (Figure 3.11F). Islets from βMfn2KO and control littermates were first perifused with 3mM glucose. The same increase in basal insulin secretion in βMfn2KO islets versus control islet was evident and consistent with what we had measured in the batch insulin secretion studies. Upon increasing the glucose concentration to 15mM, control islets exhibit a short dip, followed by a large 5 fold spike in secretion consistent with normal phase I insulin secretion. This was followed by a rapid decrease in secretion and the initiation second phase secretion with continued exposure to high glucose as is typical of mouse islets. βMfn2KO islets exhibit no dip in insulin secretion upon stimulation with 15mM glucose and a more modest, slow rising, first phase peak. The insulin secretion remains significantly higher for the duration of exposure to high glucose. Subsequent exposure to 40mM KCl caused a similar excursion in insulin secretion between both groups although the βMfn2KO islets continued to secrete at a higher rate overall.

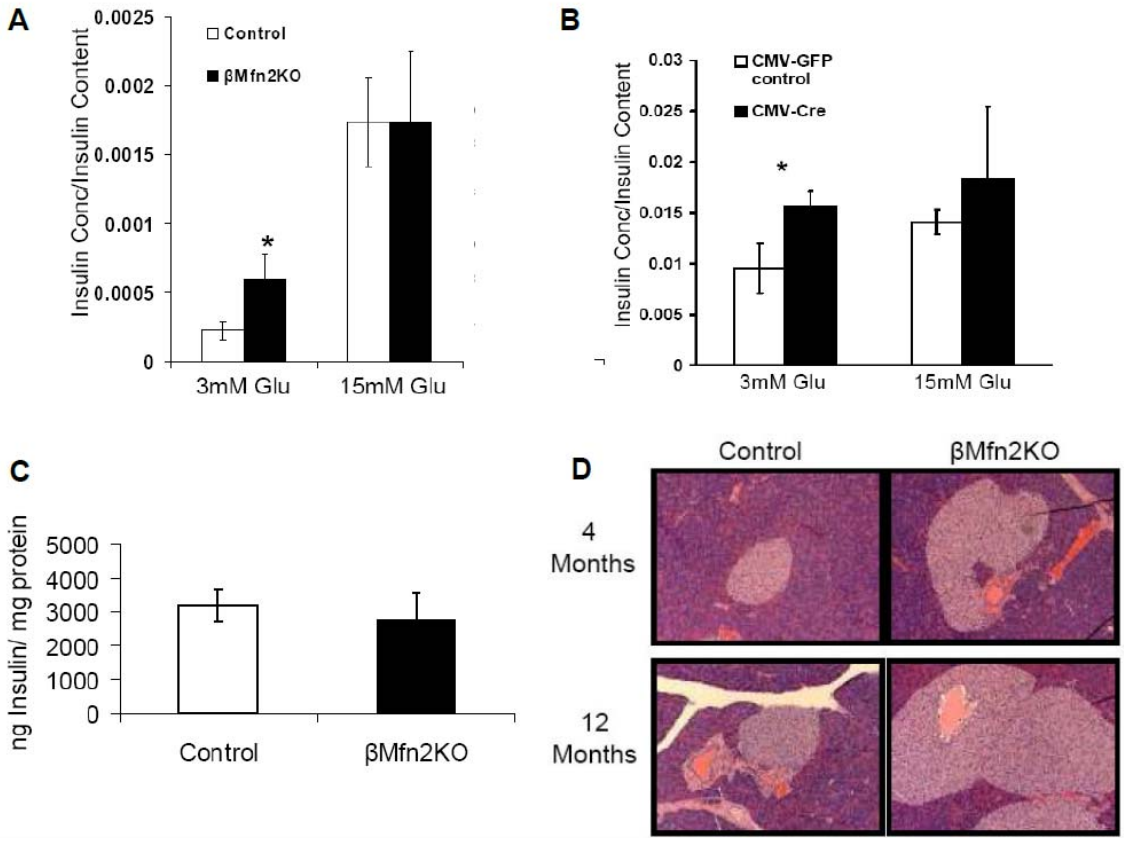
A
Insulin Conc/Insulin Content
0.0025
0.002
0.0015
0.001
0.0005
0
Control
βMfn2KO
*
3mM Glu
15mM Glu
B
Insulin Conc/Insulin Content
0.03
0.025
0.02
0.015
0.01
0.005
0
CMV-GFP control
CMV-Cre
*
3mM Glu
15mM Glu
C
ng Insulin/ mg protein
5000
4000
3000
2000
1000
0
Control
βMfn2KO
D
Control
βMfn2KO
4 Months
12 Months

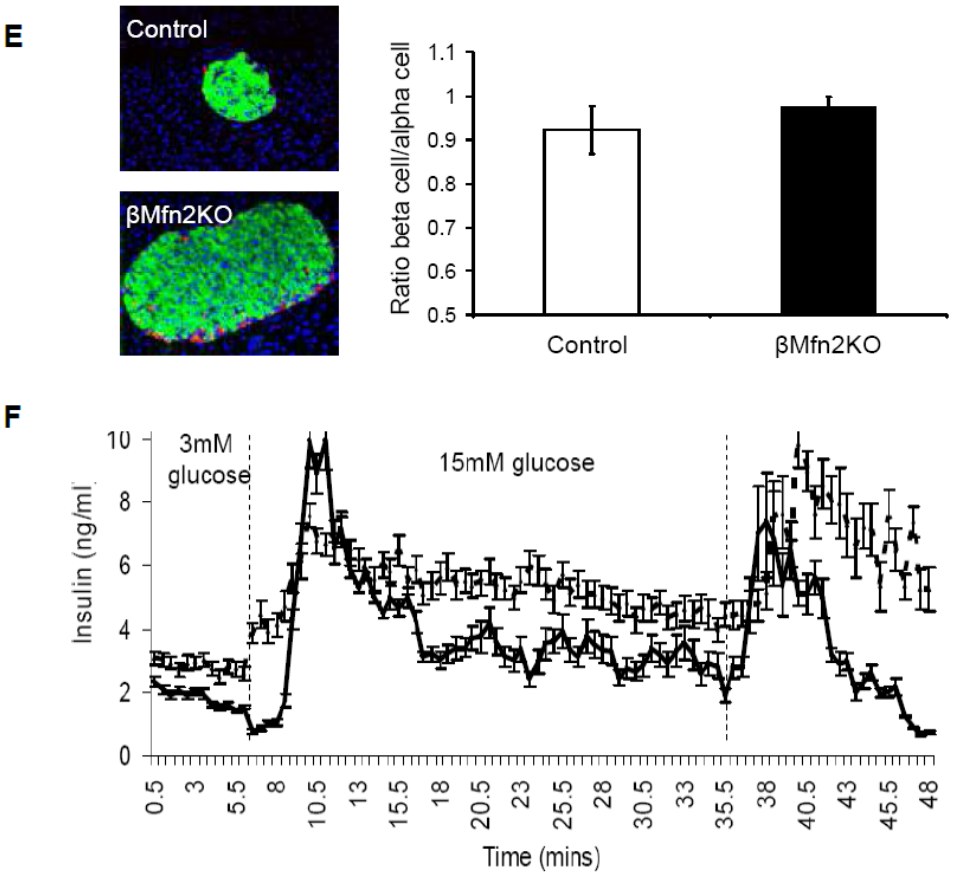

Figure 3.11 Insulin secretion is altered in βMfn2KO mice. **A**. Thirty minute secretion assays demonstrate that βMfn2KO islets have an increase in basal insulin secretion with no change in GSIS. (n=3 animals per genotype, performed in triplicate; *p≤0.05). **B**. Acute excision of Mfn2 *in vitro* alters insulin secretion. Dispersed LoxP homozygous islets were infected with GFP control and Cre-adenovirus and insulin secretion was measured after 48 hours. CMV-Cre infected β-cells displayed increased basal insulin secretion with no significant change in GSIS compared with CMV-GFP control infected β-cells (n= 3 animals per genotype; performed in triplicate). **C**. Insulin content was measured in isolated islets from βMfn2KO and control mice. No difference in insulin content was observed in βMfn2KO islets compared with control islets. **D.** H&E staining of pancreas sections from control and βMfn2KO mice at 4 months (top row) and 1 year of age (bottom row). As compared to control, islets from βMfn2KO mice are larger. **E.** Immunohistochemistry staining of pancreata sections reveal that the ratio of β-cells stained with anti-insulin (green) compared to α-cells stained with anti-glucagon antibody (red) in βMfn2KO sections is not changed in comparison to control; nuclei are stained with DAPI (blue). IHC also demonstrates the increase in islet size in the βMfn2KO sections. **F**. Islet perifusions were run on βMfn2KO and control islets. Basal, 3mM glucose, Krebs buffer was perifused through islets for 3 minutes, followed by 15mM glucose Krebs buffer for 30 minutes, and finally 15mM glucose + 40mM KCl solution

for 15 minutes. βMfn2KO islets (dashed line) have increased basal insulin secretion, a more prolonged increase in insulin secretion upon addition of stimulating concentrations of glucose, and display disrupted oscillatory patterns of secretion compared with control islets (n=4).

3.4.9 βMfn2KO Mice Fed a High Fat Diet do not Display any Additive Metabolic Dysfunction

Thus far, all the metabolic effects we have observed from Mfn2 deficiency in β-cells and/or hypothalamus have developed in mice fed normal lab chow. We wanted to know if any additional metabolic dysfunction would develop when we placed βMfn2KO mice on a HFD. Interestingly, we found that βMfn2KO mice placed on a HFD had very minimal changes to fasting blood glucose levels, weight, or glucose tolerance (Figure 3.12). Control animals placed on a HFD display an increase in body weight similar to the weight observed in βMfn2KO mice. On the other hand, the weight of βMfn2KO mice on HFD compared to those on normal chow is almost identical. There is still a small, yet insignificant, difference in weight between βMfn2KO mice on HFD compared to littermates on HFD (Figure 3.12A). Fasting blood glucose (Figure 3.12B) and glucose tolerance tests (Figure 3.12C) are also almost identical between βMfn2KO mice fed a HFD and those on a normal diet, while control mice on a HFD have a similar GTT profile and blood glucose measurements to βMfn2KO mice. These results demonstrate that control mice fed a HFD display a similar phenotype to βMfn2KO mice fed normal chow. Moreover, when placed on a HFD βMfn2KO mice do not have any additional alterations to their metabolic function. While this is still very preliminary and needs to be repeated on a larger cohort of animals, it suggests that downregulation of Mfn2 may play a central role in the development of nutrient-mediated obesity and diabetes.

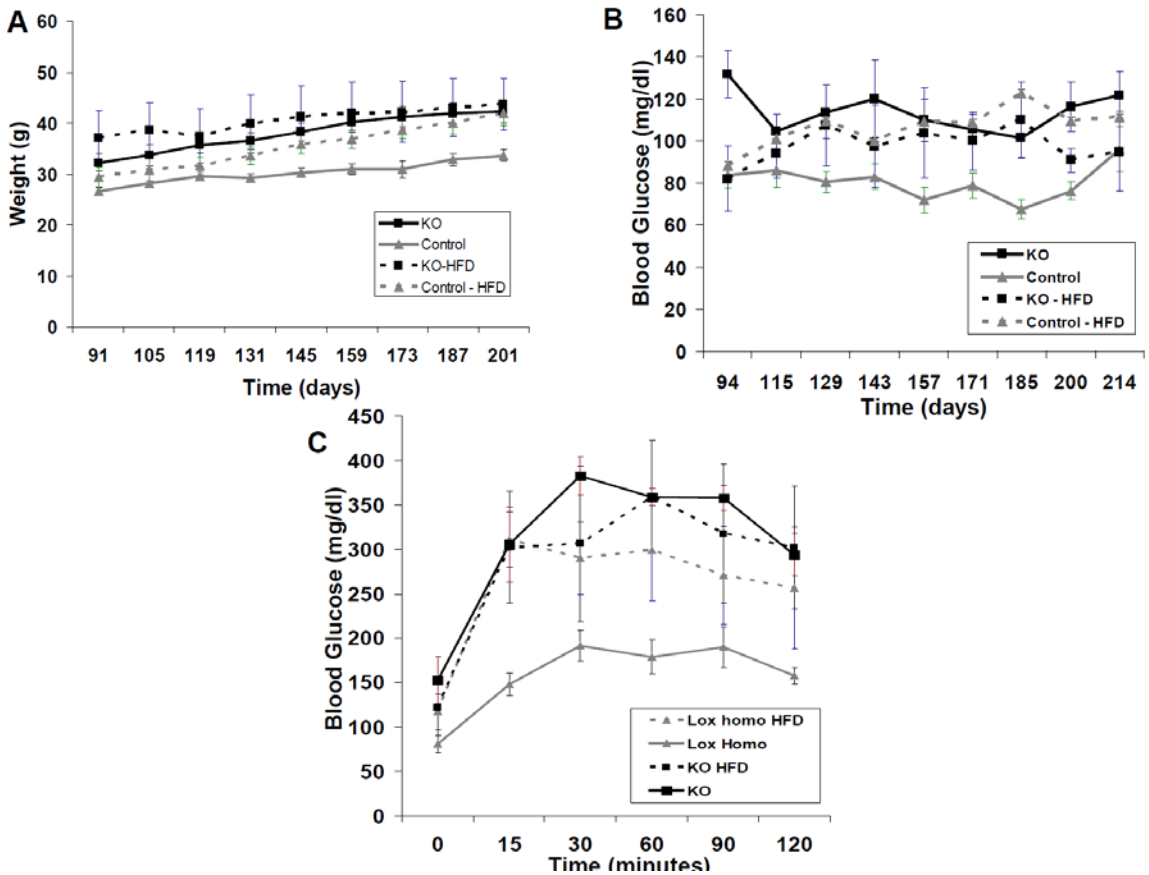

Figure 3.12 βMfn2KO mice on high fat diet do not display any further metabolic phenotype deterioration. **A.** Body weight of control and βMfn2KO mice on control and HFD. Control mice on a HFD gain a significant amount of weight compared with control mice on a normal lab chow. This bring their weight up to the level observed in βMfn2KO mice on normal chow. βMfn2KO mice on HFD do not gain any additional weight (n=3 mice per genotype). **B.** Fasting blood glucose levels measured in control and βMfn2KO mice on control and HFD. Control mice on a HFD display a significant increase in fasting blood glucose concentrations compared with control mice fed a control diet, and this increase in blood glucose is similar to the concentration observed in βMfn2KO mice on normal chow. βMfn2KO mice on HFD do not display any further deterioration in glycemia (n=3 mice per genotype). **C.** GTT performed on control and βMfn2KO mice on control and HFD. There were no differences between βMfn2KO mice on HFD, βMfn2KO on control diet, or control mice on a HFD. All of these exhibited impaired glucose toleranc compared with control mice on a normal diet (n=3 mice per genotype).

3.4.10 Addressing Mfn2 Excision in the Brain

We took two different approaches to address the effect that Mfn2 excision in the hypothalamus has on the whole body phenotype we obsesrved in the βMfn2KO mice. Our first approach utilized an islet transplantation model and secondly we administered young βMfn2KO mice with streptozotocin (STZ) to eliminate their endogenous β-cells.

3.4.10a Mice that Received βMfn2KO Islet Transplantation do not Develop Obesity

We first addressed the role of insulin producing cells in the brain with an islet transplantation experiment. This allowed us to examine the role of Mfn2 in just the β-cell because βMfn2KO islets were transplanted into mice that had intact Mfn2 expression in the hypothalamus. When βMfn2KO islets were transplanted into the kidney capsule of immunodeficient mice, we found no difference between the KO islet transplantation and control groups (Figure 3.13). There were also no differences in weight (Figure 3.13A), fasting blood glucose levels (Figure 3.13B), plasma insulin levels (Figure 3.13C), or glucose tolerance (Figure 3.13D). We measured body composition with dual-emission X-ray absorptiometry (DEXA) and found no difference in fat mass percentage, lean mass percentage, or the fat/lean ratio between any of the three groups (Figure 11.13E).

These results suggest that the brain is the major contributing factor to metabolic dysfunction in the βMfn2KO mice because transplantation of βMfn2-deficient islets resulted in a completely normal metabolic phenotype. While no weight gain was observed in the KO transplant group, this does not necessarily rule out the β-cells as being the origin of the observed phenotype in the βMfn2KO mice. In this experiment, the islet recipients were not first made diabetic by STZ treatment. Since the endogenous

islets of the immune-deficient mice were not destroyed by STZ treatment, it is possible that the endogenous islets were compensating for or masking any effects of the transplanted islets. In addition, because of the limited number of βMfn2KO mice that can be generated, we only transplanted 100 islets per mouse, which may not have been a sufficient amount.

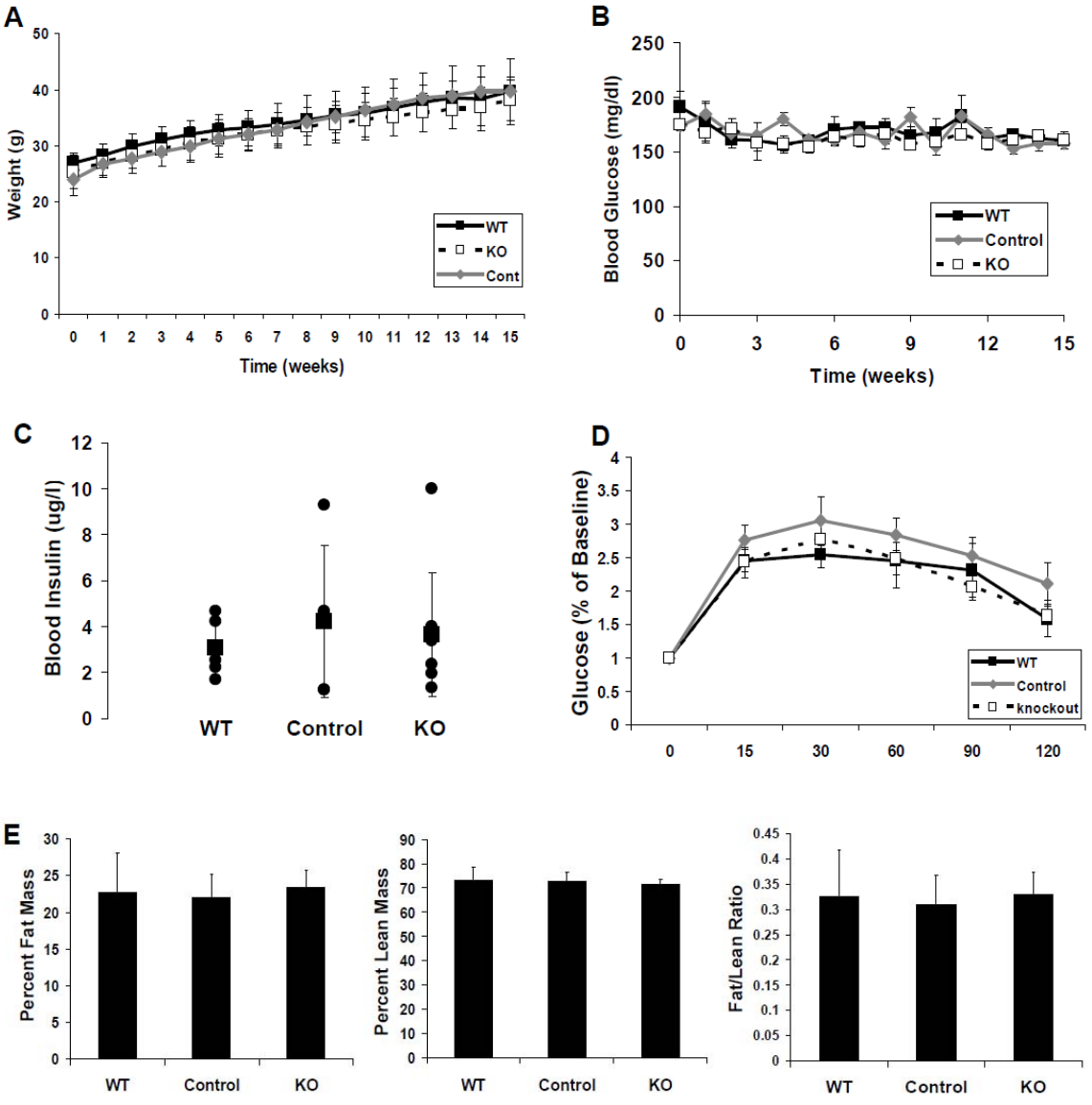

Figure 3.13 Mice transplanted with islets from βMfn2KO mice do not develop obesity or diabetes. **A.** Body weight taken weekly for 15 weeks. No difference in weight gain developed in mice transplanted with βMfn2KO islets compared with WT and control

groups (n=5 for WT and Control, n=9 for KO). **B.** Nonfasted blood glucose measurements were taken with a glucometer every week for 15 weeks. Mice transplanted with βMfn2KO islets exhibit normal glycemia (n=5 for WT and Control, n=9 for KO). **C.** Serum insulin levels from transplant animals. No differences were found between any of the groups (n=5 for WT and Control, n=8 for KO). **D.** Glucose tolerance test demonstrates normal glucose tolerance in mice transplanted with βMfn2KO islets (n=5 for WT and Control, n=9 for KO). **E.** DEXA was utilized to measure body composition. There was no change in percent fat mass, percent lean mass, or the fat mass/lean mass ratio between any of the groups (n=3 animals per group).

3.4.10b βMfn2KO Mice are Protected from the Toxic Effects of STZ

The second experiment we performed to address the role of Mfn2 excision in the brain was an experiments where STZ was injected into βMfn2KO mice and control littermates. Weight and blood glucose were then monitored. STZ is a drug that is toxic to the β-cell; the mechanism of action is entry of STZ into the β-cell cell through the GLUT2 transporters and subsequent DNA alkylation and β-cell necrosis (Bolzan and Bianchi, 2002). The aim of this experiment was to destroy the β-cell while maintaining KO of Mfn2 in hypothalamic insulin producing cells intact. The STZ experiment provided an interesting result but not one that furthered our understanding of the metabolic consequence of Mfn2 knockout in a subpopulation of cells in the hypothalamus. STZ administration is known to cause weight loss and interestingly we found that the βMfn2KO mice were protected from weight loss (Figure 3.14A and B). They were also protected from the hyperglycemia caused by STZ (Figure 3.14C and D). This implies that the brain Mfn2 deficiency is leading to weight gain and metabolic dysfunction in βMfn2KOmice. However, when we looked further into what was happening to the islets in STZ treated mice, we found that islets in βMfn2KO mice were protected from the diabetogenicity of STZ. Histology sections of these animals demonstrate that βMfn2KO islets remain intact, which is in stark contrast to the total destruction of islets observed in

control islets (Figure 3.14E). The mechanism by which the βMfn2KO islets are protected from STZ still needs to be elucidated. Some possibilities worth investigating include altered sensitivity to mitochondrial permeability pore opening, altered reactive oxygen species production, or decreased GLUT2 expression.

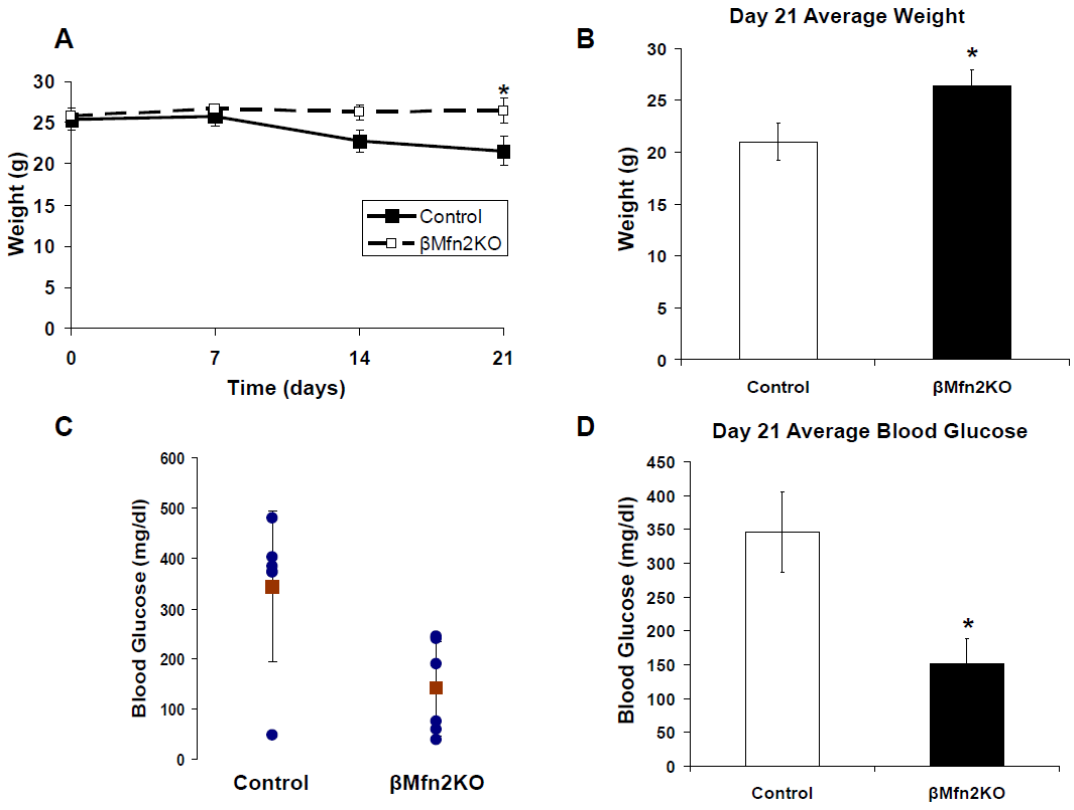

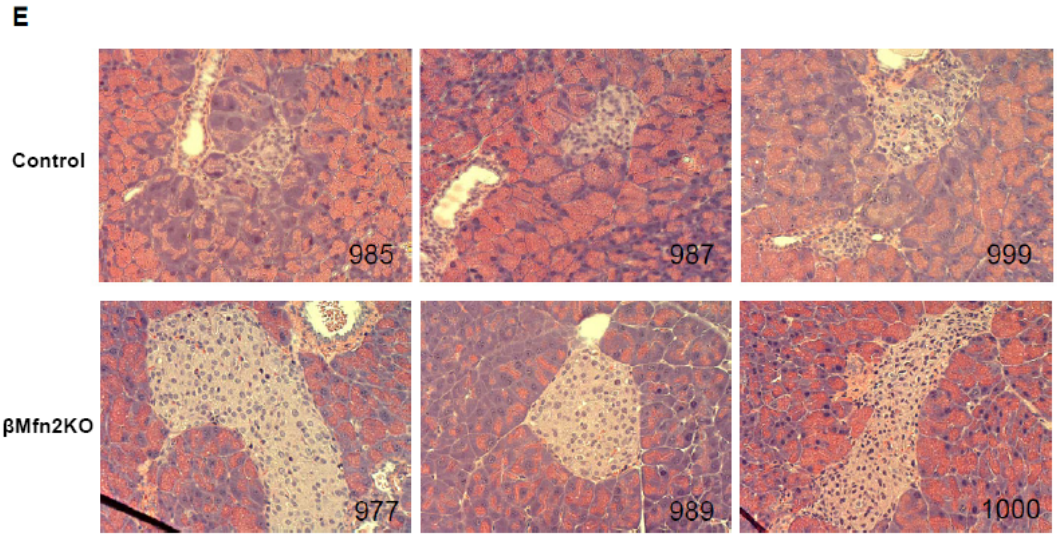

Figure 3.14 βMfn2KO mice are protected from the diabetegenic effects of STZ. **A.** Body weights of control and βMfn2KO mice treated with a single IP injection of STZ. Body weight measurements were taken once per week for 3 weeks. Control mice exhibited a decrease in weight in response to STZ, while the weight of βMfn2KO mice was maintained at a constant level (n=5; *p≤0.05). **B.** Weights of control and βMfn2KO mice 3 weeks after STZ treatment. βMfn2KO mice have a significantly higher weight than control mice treated with STZ (n=5; *p≤0.05). **C.** and **D.** Fasting blood glucose measurements of control and βMfn2KO mice 3 weeks after STZ treatment. βMfn2KO mice have significantly decreased fasting blood glucose compared with control mice. Blue circles represent individual blood glucose measurements, while the red square signifies the mean ± standard deviation. There was very little variability in the response to STZ except for one control mouse that did not respond and was able to maintained low fasting blood glucose levels (n=5; *p≤0.05). **E.** Representative images of H&E histology pancreas sections containing islets from control and βMfn2KO mice treated with STZ. βMfn2KO mice display largely intact islet morphology while in control pancreata the STZ treatment resulted in highly damaged islets.

3.5 Discussion

In chapter 2, it was reported that the application of high fat and glucose *in vitro* abolishes the ability mitochondria to undergo fusion events and leads to dramatic fragmentation of mitochondrial networks. However, there was previously no evidence that mitochondrial fusion was impaired *in vivo*. In this study, we show for the first time that high fat diet feeding in mice, an *in vivo* model of the combination of high fat and glucose (hyperglycemia and obesity), resulted in a reduction in Mfn2 content and therefore mitochondrial fusion in the β-cell. Knockout of Mfn2 in insulin secreting cells, including pancreatic β-cells and a subpopulation of cells in the hypothalamus, led to fragmentation of β-cell mitochondrial networks, whole body metabolic dysfunction, and altered β-cell endocrine function, in particular high basal insulin secretion. This work establishes a role for Mfn2 and mitochondrial fusion in the development of metabolic dysfunction in response to a high nutrient environment *in vivo*.

In the past decade, it has become increasingly apparent that changes in mitochondrial morphology underlie β-cell dysfunction both *in vivo* and *in vitro* (Higa *et al.*, 1999;Bindokas *et al.*, 2003;Anello *et al.*, 2005;Fex *et al.*, 2007;Park *et al.*, 2008;Molina *et al.*, 2009). Here, we propose that alterations in Mfn2, which we observe in two different models of diabetes and obesity, may underlie the changes in β-cell mitochondrial morphology, mitochondrial function, and insulin secretion that have been observed in diabetes. Hypersecretion of insulin is thought to be a response to the greater demand for insulin caused by insulin resistance. In early stages of insulin resistance, this leads to hyperinsulinemia which strives to maintain euglycaemia. In individuals with advanced type 2 diabetes, hypersecretion is no longer able to cope with the high demand for insulin and leads to hyperglycemia, its consequences, and eventual β-cell apoptosis. *In vitro* studies of insulin secretion indicate that islets isolated from mice maintained on a high fat diet secrete more insulin under basal, non-stimulating glucose concentrations (Fex *et al.*, 2007). Fex *et al.* attribute the elevated secretion of insulin to enhanced mitochondrial metabolism. Our results indicate that mitochondria may indeed be involved in the development of hypersecretion, although through a different mechanism, the reduction of Mfn2. Knockout of Mfn2 in the β-cell induced complete mitochondrial fragmentation in β-cells but not other islet cell types. The resulting mitochondrial fragmentation and changes in mitochondrial fusion may underlie the changes in β-cell function we report, however, Mfn2 is also known to have other functions, such as ER tethering, that may also play a role (de Brito *et al.*, 2008).

We report that βMfn2KO animals develop dramatic obesity with age. It is interesting to consider that the effects of Mfn2 KO on β-cells may contribute to the development of

whole body metabolic dysfunction, obesity, and diabetes. It is notable that weight gain in βMfn2KO mice is evident in the absence of alterations in diet and changes in feeding behavior. Our data support the hypothesis that hypersecretion of insulin can lead to an increase in energy storage in the form of fat. The link between hyperinsulinemia and obesity was predicted by Coleman in 1978 in the early characterizations of the *ob/ob* and *db/db* mouse models of leptin mediated obesity (Coleman, 1978). Over the years, evidence for this hypothesis has been emerging. Results from the Quebec Family Study indicate that increased insulin secretion strongly predicts an increase in body weight, particularly in individuals on a low fat diet (Chaput *et al.*, 2008). In addition, an earlier study by LeStunff and Bougnares showed that the early stages of obesity are characterized by an increase in insulin secretion prior to the development of insulin resistance (Le and Bougneres, 1994;Le *et al.*, 2000). Type 2 diabetes can also be predicted by high fasting blood insulin levels as shown in a study of the Pima Indian population (Weyer *et al.*, 2000).

While β-cell Mfn2 deficiency is an attractive mechanism for nutrient-induced obesity and metabolic dysfunction, excision of Mfn2 in insulin positive cells in the brain should also be considered as an explanation for obesity and/or diabetes in βMfn2KO animals (Lee *et al.*, 2006;Song *et al.*, 2010). It has been well established that the RIP-mediated excision of genes from β-cells will also lead to excision in some areas of the brain, therefore, central Mfn2 deficiency could very well be the contributing factor in the metabolic phenotype found in the βMfn2KO mice. Until recently the brain was considered to be insulin-insensitive; therefore, the effect of insulin in the brain is just beginning to be elucidated. While the source of insulin in the central nervous system (CNS) is still

controversial, it is now known that insulin functions as a neuropetide, which plays an important functional role in the brain, including the control of feeding behavior, development, neuroendocrine actions, and learning and memory. Additionally, CNS insulin has been implicated in a number of pathologies including obesity, diabetes, and neurodegeneration.

CNS insulin and insulin receptors were first discovered by Havrankova *et al.* in rat brains in the late 1970s (Havrankova *et al.*, 1978a;Havrankova *et al.*, 1978b). They discovered that insulin, indistinguishable from pancreatic insulin, is present in whole rat brain extracts in concentrations 25 times higher, on average, than plasma insulin levels. Insulin receptor mRNA was localized to neuronal somata, while insulin receptor protein is found in cell bodies and synapses (Gerozissis, 2008). The source of cerebral insulin is still a topic of debate yet, it appears both pancreatic and local sources of insulin are present in the brain. Iodinated insulin injected into the carotid artery of mice was used to show that insulin can cross the blood brain barrier via receptor mediated active transport (Banks *et al.*, 1998). Insulin passage across the blood-brain barrier was found to be greatest in the pons-medulla and the hypothalamus. In addition to insulin from the periphery, there is also evidence that insulin is synthesized locally in the CNS. Evidence for *de novo* synthesis of insulin in the brain comes from both *in vitro* and *in vivo* approaches. Preproinsulin mRNA, a precursor of insulin, has been shown to be expressed in both neuronal cell lines and in fetal rat brains at 15, 17, and 19 days of gestation (Schechter *et al.*, 1996;Grunblatt *et al.*, 2007). It was demonstrated by Clarke *et al.* that insulin can be released from neuronal cell cultures (Clarke *et al.*, 1986). Additionally, it has been shown by RT-PCR and *in situ* hybridization that insulin transcripts are present in the

adult teleost fish, the Nile Tilapia (Oreochromis niloticus) (Hrytsenko *et al.*, 2007). All of this evidence points to a local source of insulin in the brain that accounts for some of the CNS insulin, although there are still a number of investigators that credit the insulin uptake across the blood-brain barrier as the sole source of insulin in the CNS.

The fact that Cre recombinase is expressed under the rat insulin promoter primarily in the hypothalamus, the area of the brain where there is also a high number of insulin receptors is in agreement with the hypothesis that insulin is produced locally in the brain. Although, it is also possible that brain RIP-Cre expression is driven by leakiness and is not due to insulin promoter activity. Regardless, this makes understanding the role brain insulin plays in glucose homeostatis, metabolism, and the development of obesity and diabetes critical in interpreting the results obtained in the βMfn2KO mice. We carried out two independent experiments (islet transplantation and STZ treatment) to address whether the observed phenotype in the βMfn2KO mice was due to β-cell or hypothalamic Mfn2 deletion. Unfortunately, we were unable to achieve a definitive result with either experimental approach. This means that additional work needs to be done in order to dissect the role of Mfn2 in controlling whole body metabolism and fuel utilization in the β-cell and hypothalamus. One approach would be to generate a colony of β-cell specific Mfn2 knockout mice using the newly developed MIP-Cre trasgenic mouse. In this mouse, Cre is driven by the mouse insulin-1 promoter instead of the rat insulin-2 promoter utilized for the RIP-Cre mouse (Wicksteed *et al.*, 2010). β-cell specificity in the MIP-Cre line is achieved since mouse *Ins1* gene is not expressed in the hypothalamus (Madadi *et al.*, 2008). If a similar phenotype was observed in a βMfn2KO colony

generated with Cre expression driven by MIP, this would provide evidence that it is β-cell Mfn2 deficiency that is driving the metabolic phenotype.

Weight gain has been observed in other mouse models where gene excision was achieved using RIP-Cre. In most of these cases, weight gain was caused by increased food intake. For example, RIP-Cre mediated excision of STAT-3 or insulin receptor substrate (IRS) leads to weight gain (Lin *et al.*, 2004;Cui *et al.*, 2004). In both of these models, increased weight gain was attributable to hyperphagia. The role CNS plays in the control of feeding behavior has been widely studied, in particular its interaction with the anorexigenic peptide hormone, leptin. Hypothalamic insulin has been known to reduce food intake and body weight in a dose-dependent manner for over twenty years (Brief and Davis, 1984). These effects of central insulin on feeding behavior and body weight have been shown to occur in both the short and long term. Defective insulin signaling has been proposed as a link between obesity and diabetes. Koch *et al.* created a transgenic mouse where the insulin receptor can be inducibly inactivated. They found that central insulin regulates glucose and fat metabolism in the periphery (Koch *et al.*, 2008). These mice exhibited more pronounced hyperglycemia when the insulin receptor was inactivated in both the brain and the periphery compared with the periphery alone. Additionally, Bruning *et al.* created a conditional knockout of the insulin receptor in neurons alone (NIRKO mice) and demonstrated that the absence of neuronal insulin receptor causes whole body insulin resistance and dyslipidemia, as well as obesity (Bruning *et al.*, 2000). This obesity was correlated with an increase in food intake and plasma leptin concentrations. Additionally, there is data demonstrating that obesity and diabetes induced by HFD in rats leads to alterations in insulin signaling and changes in

the expression of central insulin and insulin receptors in the hypothalamus but not the hippocampus (Banas *et al.*, 2009).

Our finding, that βMfn2KO mice do not exhibit increased feeding behavior, suggests that alterations in brain insulin may be not involved in the development of obesity in the βMfn2KO mice. Moreover, if the loss of Mfn2 leads to a similar increase in insulin in the brain as we observe in the periphery, one would expect weight loss due to decreased feeding behavior in the βMfn2KO model. However, this could also be explained by central insulin resistance. Indeed, central insulin resistance has been implicated in the response to high fat diet and obesity. It was found that obese humans have an impaired response to insulin, indicative of insulin resistance, in cortical neurons and that this effect may be related to changes in IRS signaling (Tschritter *et al.*, 2006). Therefore at this point we cannot rule out whether the loss of Mfn2 in insulin positive neurons may lead to alterations in function that are related to central insulin signaling. Indeed, these changes may still underlie the obese phenotype of the βMfn2KO mouse.

In addition to the development of obesity, our data indicate that there are several gross metabolic changes that result from the excision of Mfn2. Namely, there are decreases in oxygen consumption and respiratory exchange rate. The decrease in RER indicates that βMfn2KO mice rely on a combination of carbohydrate and fat metabolism in contrast to control animals that utilize carbohydrates primarily. We also found decreased movement, which could be contribute to these metabolic changes, and may be a result of changes in body composition. These parameters were all measured at 50 days of age, before differences in body weight are observed. However, CT scans and body

composition analysis by NMR reveals that there is already a significant increase in fat mass at this age. Therefore, we cannot determine if these whole body metabolic changes are the cause or consequence of increased fat mass.

We demonstrate that even in the presence of hypersecretion of insulin, βMfn2KO mice display mild hyperglycemia compared with control littermates. One possible explanation for this is portal vein insulin resistance resulting in increased gluconeogenesis. In the β-cell, insulin is made when pro-insulin is processed to generate both C-peptide and insulin, which are secreted in equimolar amounts in response to increased glucose. While insulin levels are influenced by hepatic clearance and peripheral receptor internalization leading to a very short half-life, C-peptide has a longer half-life (since it is not cleared by the liver) and is considered a more reliable measure of insulin secretion. For this reason, circulating levels of C- peptide provide a better indication of insulin secretion than insulin itself. We find that βMfn2KO mice display increased serum C-peptide concentrations prior to the onset of obesity and hyperinsulinemia, suggesting that islets from βMfn2KO mice secrete more insulin compared to those in control littermates. This was further confirmed by measurements of insulin secretion from isolated islets. Despite increased insulin secretion and clearance in the liver, we report that βMfn2KO animals exhibit hyperglycemia at all time points tested. Pyruvate tolerance tests indicate that this may be attributable to increased gluconeogenesis prior to obesity. Previous work by Kim *et al.* demonstrated that hepatic insulin resistance plays a primary role in the development of impaired glucose tolerance associated with obesity, in part due to the diminished capability of insulin to suppress liver gluconeogenesis (Kim *et al.*, 2003).

Perifusion and batch insulin secretion demonstrate that βMfn2KO islets hypersecrete *in vitro*. It is interesting to note that batch insulin secretion experiments were only able to report basal hypersecretion while perifusion experiments reported changes in insulin secretion under both basal and stimulatory conditions. This may be due to feedback inhibition leading to a suppression of continued secretion by the islets in the batch assay where insulin is not cleared for 30 minutes. We hypothesize that this basal hypersecretion could arise from changes in mitochondrial respiratory function. This will be explored further in Chaper 4.

The interrelationship between obesity and diabetes is often considered unidirectional, as obesity is thought to be a major contributing factor to the development of diabetes. Increasingly, this view is changing as the role of insulin signaling and β-cell function in the development of type 2 diabetes is becoming more apparent. We demonstrate that Mfn2, a mediator of mitochondrial fusion and interorganellar tethering plays an important role in mediating coordinated insulin secretion in response to glucose stimulation. This work provides evidence that nutrient induced alterations in mitochondrial dynamics in β-cells and/or neurons in the hypothalamus can affect insulin secretion as well as whole body fuel utilization and storage, thereby contributing to the development of obesity and diabetes.

Chapter 4: Islet Respiratory Proton Leak is Regulated by Nutrients, ROS, and Mfn2 Deficiency

In this data chapter, I contributed to all of the calcium, ROS, and insulin secretion experiments and many of the oxygen consumption experiments. Anthony Molina and Samuel Sereda also contributed to the calcium and ROS experiments. Additionally, I worked closely with Jakob Wikstrom and Samuel Sereda on this project; they performed the experiments showing that acute nutrient stimulation results in uncoupling in islets and that this is reversed by antioxidants. They also contributed to the experiments demonstrating that chronic high nutrient levels further increase bioenergetic inefficiency and that this is controlled, in part, by the ANT. Furthermore, Jakob Wikstrom and Alvaro Elorza developed the islet plate for the Seahorse XF24 Extracellular Flux Analyzer.

4.1 Abstract

β-cell mitochondrial dysfunction is thought to play a role in the development of Type 2 Diabetes. We have previously shown that mitochondrial fusion is altered in response to a high nutrient environment. Additionally, β-cells that are deficient in the mitochondrial fusion protein, Mfn2, display fragmented mitochondrial morphology and changes in insulin secretion similar to that seen in islets of mice fed a HFD. However, the mechanism behind this increased basal insulin secretion is still unclear. The goal of this study was to identify alterations in mitochondrial physiological and bioenergetic functions in the islet that can explain the transition towards the dysregulated insulin secretion that occurs with obesity and diabetes. This study utilized the Seahorse XF24 Extracellular Flux Analyzer to measure respiratory function in islets and INS1 cells. Insulin secretion was measured also to correlate how different treatments affect both mitochondrial bioenergetic function and insulin secretion. We find that conditions that lead to basal hypersecretion of insulin result in increased proton leak, or oxygen consumption that is not coupled to ATP production, in islets. Proton leak was regulated by both acute stimulatory fuel challenges and chronic, high nutrients levels. Pro-oxidants

also increase proton leak and basal insulin secretion, while antioxidants prevent leak in response to acute nutrient stimulation. Proton leak was found to be induced, in part, throught the adenine nucleotide translocase (ANT). We hypothesize that ROS generation in response to stimulatory fuel regulates proton leak in the islet. An increase in proton leak could increase flux through the TCA cyle and generate amplifying signals for insulin secretion. In a normal physiological state where there are nutrient oscillations, this may be protective and act as a nutrient detoxification mechanism in β-cells. On the other hand, when fuel levels are constantly high in obesity and diabetes, proton leak remains elevated potentially leading to increased basal hypersecretion, which promotes further metabolic dysfunction.

4.2 Introduction

β-cell mitochondria serve as the fuel integrator of the β-cell and generate signals for insulin secretion. Insulin secretion signals such as ATP, reactive oxygen species (ROS), GTP, α-ketoglutarate and malonyl-CoA are all directly or indirectly influenced by mitochondrial respiratory chain activity. The ETC generates the proton gradient that fuels oxidative phosphorylation and the generation of ATP. Thus, oxygen is generally tightly coupled to ATP synthesis. Although, under certain circumstances, protons may return to the matrix through other routes than the ATP synthase; therefore, uncoupling oxygen consumption from ATP synthesis, which is termed proton leak or uncoupling (Brand *et al.*, 1999). An increase in proton leak is reflected by an increase in uncoupled respiration, which may be assessed experimentally by inhibiting the ATP synthase with oligomycin. The level of uncoupling is an important biological phenomenon as it reflects bioenergetic efficiency (Affourtit and Brand, 2008a).

In β-cells, uncoupling may play an important role in insulin secretion function. It has been suggested that the role of β-cell proton leak may be to allow higher flux through the TCA cycle, thereby increasing levels of TCA cycle-derived signals for insulin secretion (Affourtit *et al.*, 2008a). Recently, it was shown that clonal INS1 β-cells exhibit considerably high levels of proton leak. Seventy five percent of the respiration measured from INS1 cells was reported to be uncoupled in comparison to 20% in myoblasts (Affourtit and Brand, 2008b). Considering the importance of mitochondrial ATP-production for insulin secretion this finding is certainly intriguing. The Shirihai laboratory has shown that islets also exhibit high levels of basal uncoupled respiration, which increases in response to acute nutrient exposure (Figure 4.6.1A; unpublished data). Interesting, acute nutrient stimulation also correlates with an increase in ROS (Figure 4.6.1B; unpublished data). However, the effects of chronic high nutrient levels and antioxidants on β-cell proton leak and how this effects β-cell insulin secretion has not been investigated.

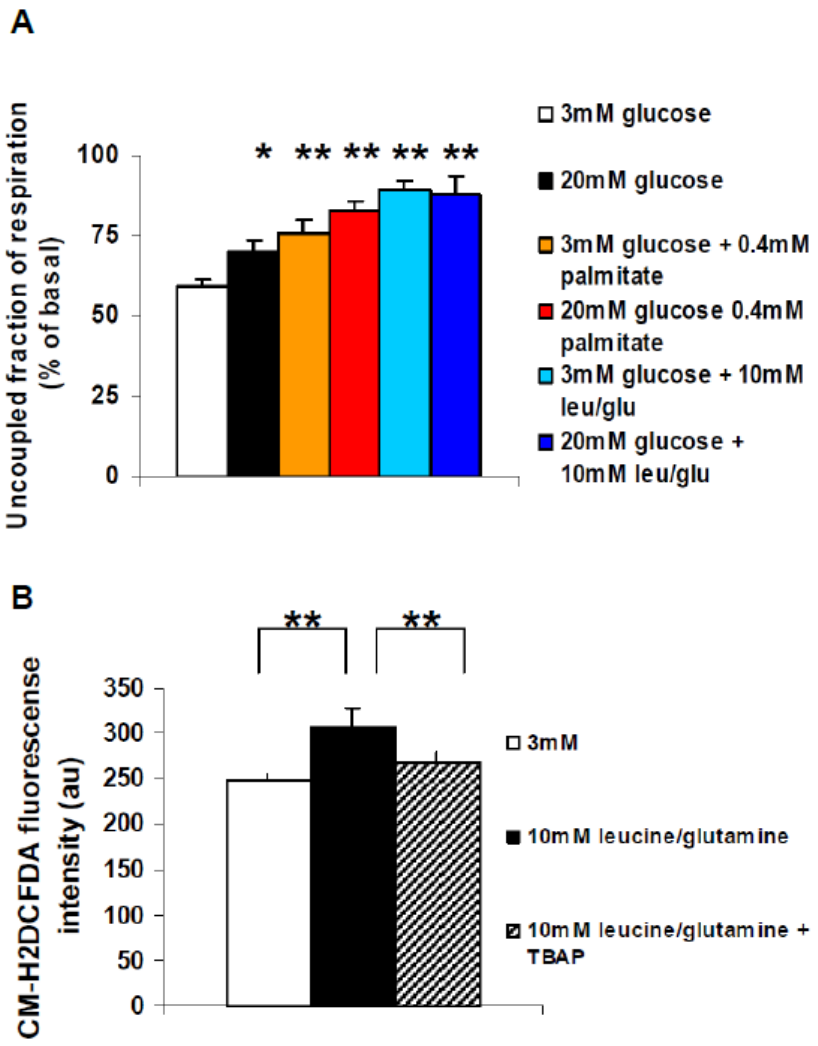

Figure 4.1 Isolated islets exhibit a high degree of uncoupled respiration, which is amplified in response to acute nutrient stimulation. **A.** Basal,uncoupled fraction of respiration in response to acute nutrient stimulation. At basal glucose concentration, isolated islets have an uncoupled fraction of respiration of approximately 60% of baseline. Stimulation with different types of nutrients leads to a further increase in proton leak. Interestingly, amino acids were found to induce the highest degree of uncoupling (89%). **B.** ROS levels measured by DCFDA fluorescence in response to 10mM leucine and glutamine, which are know to induce proton leak in islets. ROS levels increase in response to these amino acids and this can be reversed with treatment with the antioxidant, TBAP.

β-cells are unique in that they respond to glucose by increasing their respiratory rate. We have shown that OCR/min/islet is increased in response to different concentrations of glucose (Figure 4.2; unpublished data). At basal glucose levels OCR remains steady over

time. With increasing glucose concentrations there is a dose-dependent increase in respiration. In the presence of 6mM glucose, there is an increase in OCR, which is further increased with stimulatory levels of glucose. This increase in oxygen consumption rates correlates with an increase in mitochondrial membrane potential. Additionally, it has been shown that hyperpolarization of mitochondrial membrane potential in response to acute stimulation with nutrients also correlated with increased insulin secretion (Heart *et al.*, 2006).

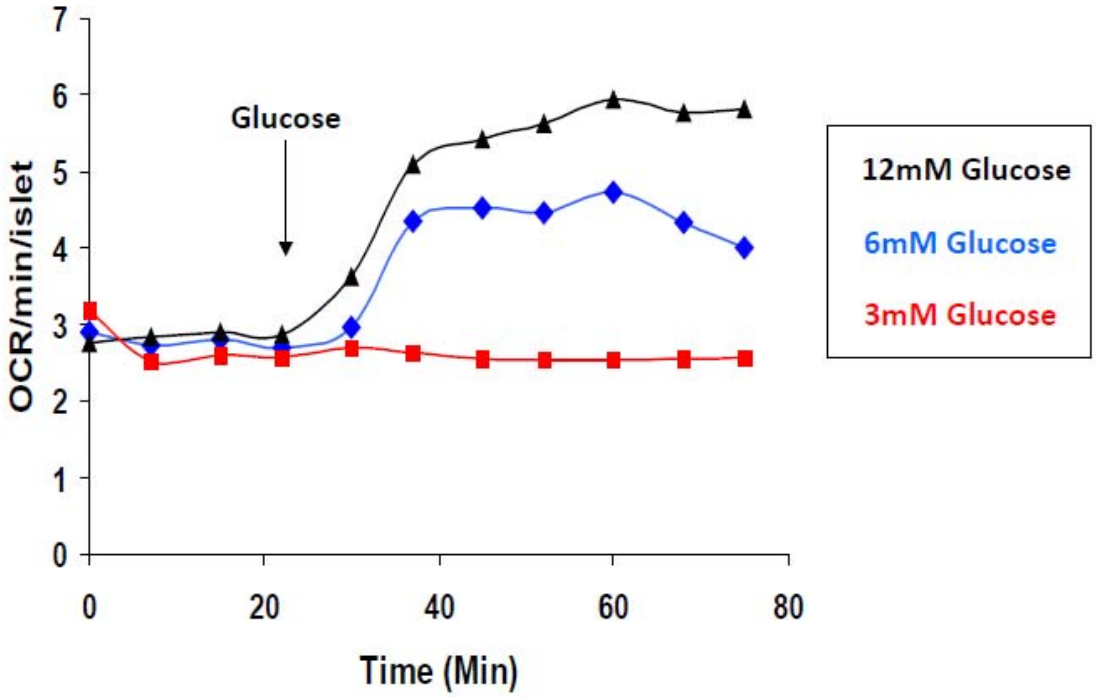

Figure 4.2 The oxygen consumption rate in islets increases in response to glucose. OCR remains steady in response to basal glucose concentrations (red line) over the length of the experiment. A does-dependent increase in OCR can be seen in response to increased glucose concentrations. An intermediate 6mM glucose concentration (blue line) increases OCR above basal levels. A stimulatory concentration of 12mM glucose (black line) further increases OCR.

A central characteristic of diet induced diabetes models is dysregulated insulin secretion with hypersecretion at low glucose levels (Surwit *et al.*, 1988;Zhou *et al.*, 1999;Fex *et al.*, 2007;Getty-Kaushik *et al.*, 2009). This phenotype was also found in mice with the Mfn2

deficient β-cells (Figure 3.6.11). The mechanism behind increased basal insulin secretion in βMfn2KO mice and mice fed a HFD is currently unknown. Recently it was suggested that transient increases in ROS levels that occur with fuel stimulation may acutely increase insulin secretion, while chronically elevated ROS may have deleterious effects on secretion (Pi *et al.*, 2007).

In this study we examine what changes in βMfn2KO mice may be leading to an increase in basal insulin secretion. We find that βMfn2KO mice actually exhibit decreased islet ROS levels and high proton leak. Therefore, bioenergetic efficiency was a major focus of this work in an attempt to understand what is occurring in islets of both high nutrient conditions and in the βMfn2KO mice that are leading to alterations in metabolic function. We found that diabetic islets exhibit higher levels of basal oxygen consumption that is associated with inefficient respiratory function. Exploring the mechanism behind this we found that normal islets exhibit high levels of uncoupled respiration which is further increased in diabetic rodent islets. Moreover we describe the molecular regulation of uncoupled respiration which includes ROS and the adenine nucleotide translocase. Finally, we examined the relationship between the levels of proton leaks and basal insulin secretion.

4.3 Materials and Methods

4.3.1 Chemicals

Chemicals not mentioned elsewhere: Tetrakis (4-benzoic acid) porphyrin manganese (TBAP) (Oxis international, Beverly Hills, CA); bongkrekic acid (Calbiochem, La Jolla,

CA); cyclosporin A (LC lab., Woburn, MA); L-leucine, L-glutamine, and menadione (Sigma, St. Louis, MO).

4.3.2 Experimental animals for HFD

10 to 14-week-old male wild type C57BL6/J mice (Jackson lab., Bar Harbor, ME) were used. Animals were fed normal chow or high fat diet (HFD) (DIO HFD; 45% fat; Research diets Inc, New Brunswick, NJ) starting at 3 weeks of age. At 12 weeks, mice we euthanized by CO2 asphyxiation and islets were isolated. All procedures were performed in accordance with the Boston University Institutional Guidelines for Animal Care (IACUC no. 1104) in compliance with U.S. Public Health Service Regulation.

4.3.3 Islet isolation and culture

Islets of Langerhans were isolated as previously described by collagenase injection into the bile duct (Lacy and Kostianovsky, 1967). After isolation, intact islets were cultured overnight in RPMI-1640 culture media supplemented with 10mM glucose, 10% FBS, 100IU/ml penicillin, and 100µg/ml streptomycin; all from Invitrogen (Carlsbad, CA). In GLT experiments, islets were incubated for 48h in medium supplemented with 1% FBS and 0.4mM palmitate, complexed 1:5 to BSA, and 20mM glucose or similar control media.

4.3.4 Cell culture

Clonal INS1 β-cells were cultured in RPMI-1640 media supplemented with 10% FBS, 10mM HEPES buffer, 1mM pyruvate, 50µM 2-ß-mercaptoethanol, 50U/ml penicillin and 50µg/ml streptomycin. 10^5 cells were seeded per V7 cell culture plate well the day prior to experiment. In cases where INS1 cells were infected with Mfn2 miRNA adenovirus,

75,000 cells were plated in a Seahorse cell culture plate and the next day, INS1 cells were infected with the virus. INS1 cells were transfected with a micro RNA against Mfn2 delivered by adenovirus at a MOI of 500. Oxygen consumption experiments were performed 48 hours post infection.

4.3.5 Calcium Imaging

Primary β-cells were dissociated with 0.25% trypsin and allowed to recover for several hours. Imaging of intracellular calcium was performed as previously described by Heart and colleagues (Heart *et al.*, 2006). Briefly, cells were loaded for 30 min at 37° C with 0.5 μmol/l fura 2/AM (acetoxymethyl ester) (Invitrogen) in KRB buffer containing 5 mmol/l glucose and 0.05%BSA. After loading, cells were washed twice and incubated for 15 min to allow cleavage of intracellular fura 2/AM by cytosolic esterases. Imaging was performed on a Zeiss IM 35 inverted microscope using a 40× glycerine objective in a temperature-controlled cabinet heated to 37° C. Fura 2 was excited using a xenon lamp and a dual-wavelength Ionoptix (Milton, MA.) synchronized chopper mirror at 340 and 380 nm. Fluorescence excitation intensity at 380 nm was equalized with that at 340 nm using a neutral-density filter. The fura 2 emission signal at 510 nm was recorded by an intensified CCD Ionoptix camera. Images were collected at 5 s intervals.

4.3.6 ROS imaging

Reactive oxygen species were detected with CM-H_2DCFDA (Invitrogen, 5-(and-6)-chloromethyl-2',7'-dichlorodihydrofluorescein diacetate, acetyl ester), a molecular probe for hydrogen peroxide. CM-H_2DCFDA fluoresces at 520 nm and an increased fluorescence corresponds to an increase in hydrogen peroxide. Islets were dispersed and

seeded in matrigel (BD Matrigel™ Basement Membrane Matrix) at 5,000 cells per well. Dispersed islets were kept overnight in beta cell medium (RPMI 1640 with 10% FBS, 5% Pen-Strep) and loaded the next day for one hour in 10 μM CM-H_2DCFDA dissolved in β-cell medium. Loading was done in a 37 °C, 5 % CO_2 incubator. Wells were washed with β-cell media without DCFDA twice, both followed by 15 minute incubations. Two washes with experimental media were performed, consisting of Krebs-Ringer buffer with basal concentrations of glucose. Fluorescence was read with a plate reader (Tecan Infinite® M1000) for one hour at 37 °C at a wavelength of 520 nm. Negative controls were done with unstained wells and positive controls were performed with tert-butyl hydrogen peroxide.

OxyblotTM protein oxidation detection kit (Chemicon International) was performed on cell lysates from islets isolated from βMfn2KO and mice. The kit was used according to manufacturer's manual. The technique is based on detection of carbonyl groups which are introduced into protein side chains when proteins are exposed to oxidative stress.

4.3.7 Respirometry

Respirometry of whole murine islets and clonal INS1 cell were performed using the Seahorse Bioscience XF 24 platform (Seahorse Bioscience, Billerica, MA) as previously described (Ferrick et al., 2008). βMfn2KO and control islets or C57Bl6 islets were isolated and allowed to culture overnight before respirometry was performed. Islet respirometry was measured in a specialized islet plate that was developed in the Shirihai laboratory (Figure 4.3A). Islets were transferred by pipetting to 50ml conical tubes with warm assay media containing 3mM glucose, 0.8mM Mg^{2+}, 1.8mM Ca^{2+}, 143mM NaCl,

5.4mM KCl, 0.91mM NaH2PO4, Phenol red 15mg/ml (Seahorse Bioscience, Billerica, MA); and maintained in this media throughout the experiment. In order to prevent islets from sticking to the plate, the media was supplemented with 1% FBS. After one wash islets were resuspended in 2ml of media. 50 to 80 islets were plated into the islet plate by pipetting 2x50 µl of stirred islet mix into each of the 20 wells, loaded previously with 400 µl of media. 4 wells were kept as controls in every experiment. The addition of an 80 micron screen kept islets in place directly over the oxygen sensors and still allows for mixing of the media in between measurements. By using tweezers, screens were carefully put on top of the depression of all wells. To avoid bubble formation in the net, screens were pre-wetted in media. The islet plate was then incubated 60min at 37°C before loaded into the XF24 respirometry machine (Seahorse Bioscience). During this time a cartridge with the injection compounds (50µl/port) used during the experiment was prepared and the machine programmed.

Oxygen consumption rates (OCR) were typically measured at low and high fuel levels as well as with drugs acting on the respiratory chain; oligomycin (5µM), FCCP (1µM), rotenone (5µM) and antimycin A (5µM); all from Sigma; and myxothiazol (5µM; Calbiochem, La Jolla, CA). In total, the preparation time before starting the measurements was 2-3h.

For oxygen consumption measurements, INS1 cells were switched to assay media (3mM glucose but no FBS), and further processed as described above.
Proton leak or the uncoupled fraction of respiration is calculated by subtracting the non-mitochondrial oxygen consumption (OCR as a percent of basal under rotenone and

antimycin A) from total uncoupled respiration (OCR as a percent of baseline basal under oligomycin to inhibit ATP Synthase. This is represented graphically in figure 4.6.3 obtained from the Seahorse XF24 Extracellular Flux Analyzer brochure (Figure 4.3B; www.seahorsebio.com).

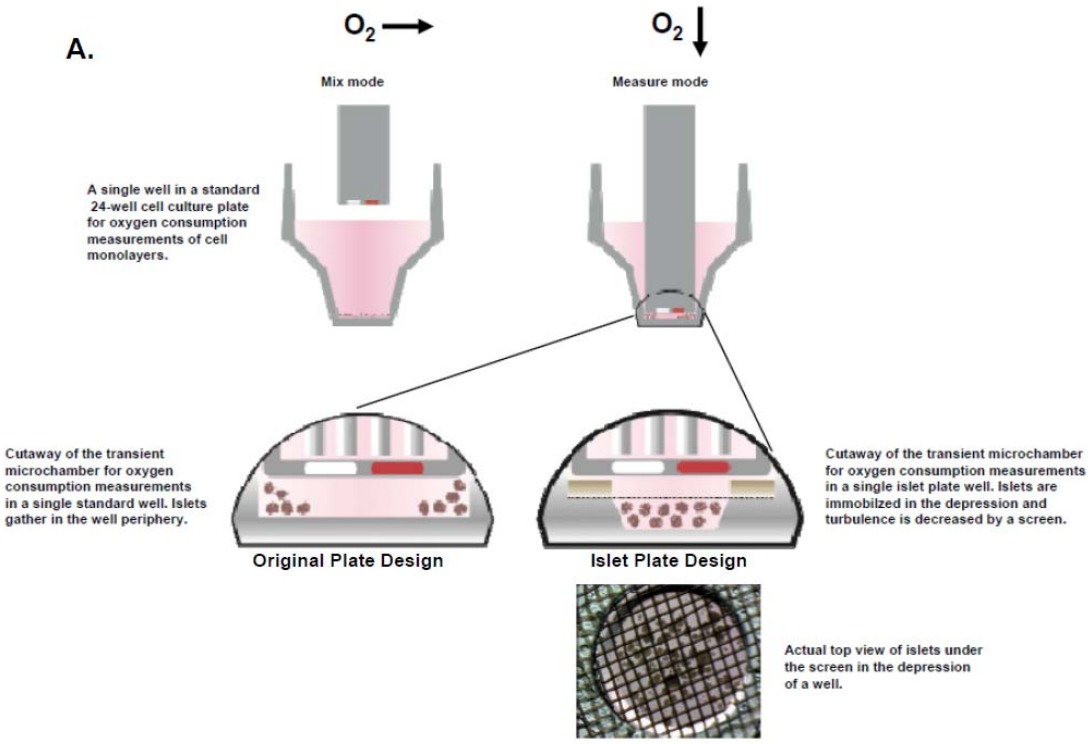

B.

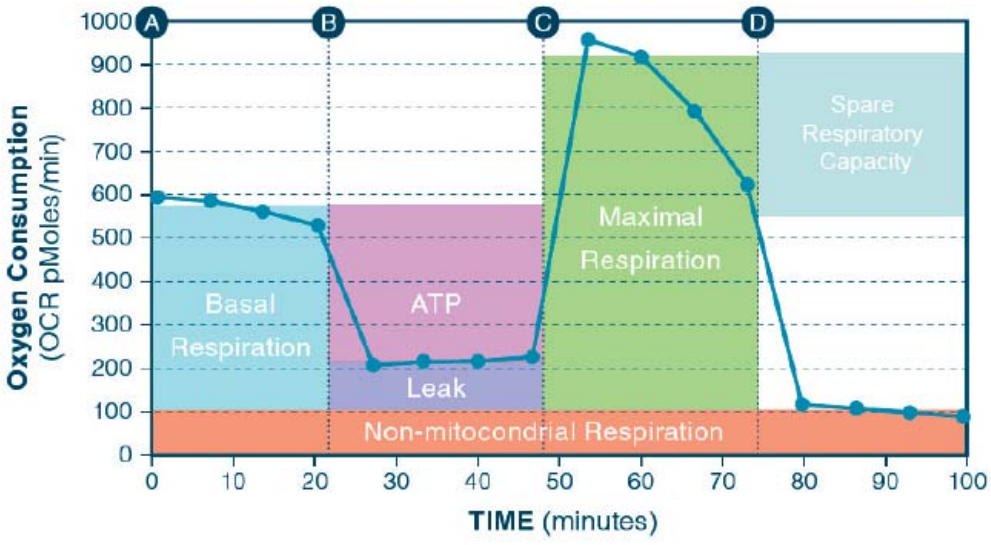

Figure 4.3: The Seahorse islet plate and bioenergetic profiling. **A.** A novel, specialized plate was developed for isolated islets based off of the existing plate. This Seahorse plate has an additional depression close to the probe head to keep islets in the center of the plate. At the top of the figure, the mechanics of the technique is shown with the probe head forming microwells (right) followed by re-equilibration of the media by mixing (left). The original plate is displayed on the bottom left, while the new islet plate with the addition of a smaller well to hold islets and a screen is shown on the lower right. A screen is place over the islet well to protect them from the turbulence created by probe-head mixing. The screen consists of a polycarbonate ring attached to a nylon net with 50μm pore size. **B.** A combination of chemicals can be used to determine a large amount of information from cells with the Seahorse Extracellular Flux Analyzer. Injections: point A is control media, B is oligomycin to inhibit ATP Synthase, C is FCCP, a chemical uncoupler that disrupts the proton circuit, and D is a cocktail of myxothiazol and rotenone to inhibit complex I and complex III of the ETC chain, thus inhibiting mitochondrial respiration (antimycin A is often used as an alternative to myxothiazol). Non-mitochondrial respiration is subtracted from oxygen consumption under basal media to determine basal oxygen consumption, from oxygen consumption under oligomycin to calculate proton leak, and from oxygen consumption under FCCP to determine maximal respiration, which is also known as reserve capacity (Ferrick *et al.*, 2008;Brand *et al.*, 2011)(www.seahorsebio.com).

4.3.8 Batch Insulin Secretion

Insulin secretion was run in quintuplicate and collected in a parallel fashion. Islets were washed and preincubated for 30 min in modified Krebs-Ringer bicarbonate buffer (KRB) containing (in mM) 119 NaCl, 4.6 KCl, 5 NaHCO3, 2 CaCl2, 1 MgSO4, 0.15 Na2HPO4, 0.4 KH2PO4, 20 HEPES, 2 glucose, 0.05% BSA, pH 7.4. This was followed by a 30 min incubation in media containing either 3 mM, 15 mM glucose, or 15mM glucose and 40mM KCl. Media was collected and stored at –20°C for insulin measurement. Insulin concentration was measured using the ratiometric HTRF insulin assay (Cisbio, Bedford, MA). Drug concentrations used for batch insulin secretion experiments were: 200nM FCCP (DMSO was used as the vehicle control), 10μM menadione (ethanol was used as the vehicle control).

4.3.9 Statistics

The Student's t-test was used to compare an experimental group to control in situations where this was appropriate. When multiple comparisons were made, an ANOVA followed by a Bonferroni test was utilized. Significant is considered $p \leq 0.05$.

4.4 Results

4.4.1 βMfn2KO Islets have Normal Cytosolic Calcium Release and Concentrations

As reported in chapter 3, βMfn2KO islets are deficient in β-cell Mfn2 and display a severe metabolic phenotypic, including basal hyperinsulin secretion. We hypothesize that increased basal insulin secretion could underlie the weight gain and obesity we observed in the βMfn2KO mice. Therefore, we sought to determine the mechanism behind increased basal hypersecretion in the βMfnKO islets. There are several potential mechanisms for increased basal insulin secretion that can shed light on the role of Mfn2 in insulin secretion. Calcium buffering has been shown to be regulated by Mfn2 and plays a critical role on the docking of vesicles for the secretion of insulin (de Brito *et al.*, 2008). We measured intracellular calcium in β-cells from dispersed islets isolated from βMfn2KO and control animals using the ratiometric dye, Fura-2. Figure 4.4A displays ratiometric Ca^{2+} traces from both βMfn2KO and control islets. We find that there were no differences in the basal level of intracellular calcium at 3mM glucose or with stimulated calcium with 15mM glucose and 40mM KCl (Figure 4.4B). Mitochondria play an important role in Ca^{2+} buffering and Mfn2, in particular, has been shown to be involved in this process by tethering mitochondria and ER together. Therefore, measuring mitochondrial Ca^{2+} may be an interesting avenue to pursue in the future.

However, our current data suggests that increased cytosolic calcium is not responsible for increased insulin secretion in the βMfn2KO mice.

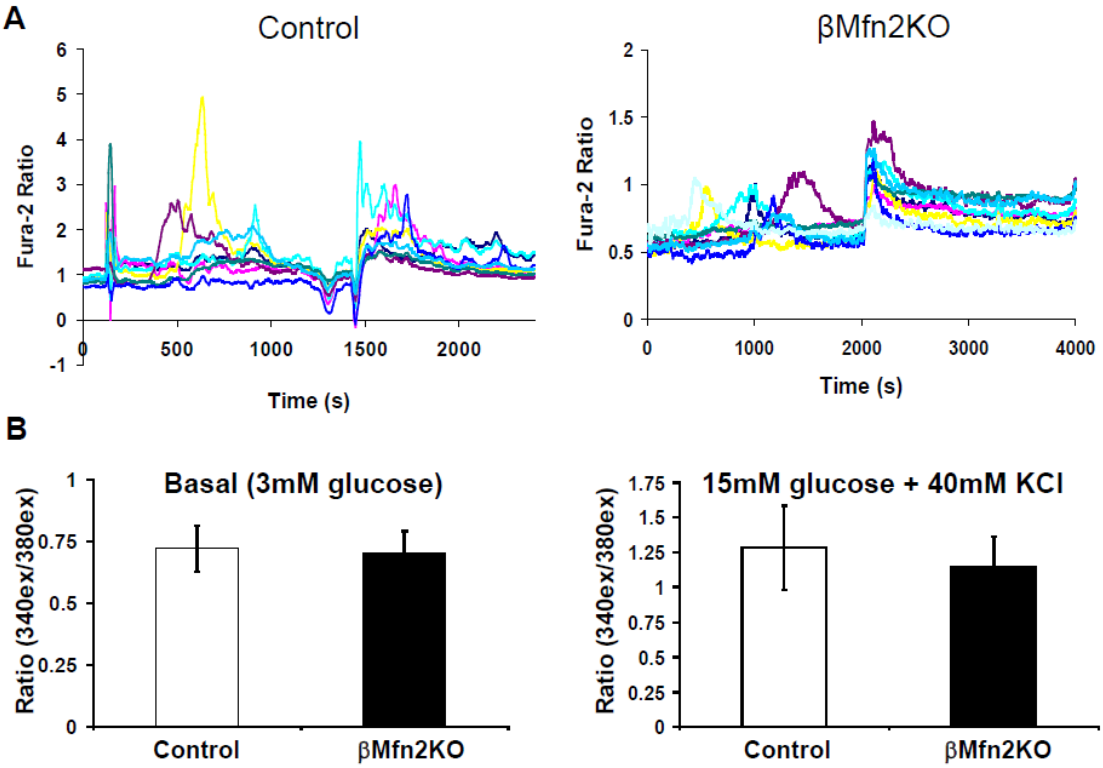

Figure 4.4: Cytosolic Ca^{2+} levels are not Altered in βMfn2KO islets. **A.** Ratiometric Fura-2 traces obtained from βMfn2KO and control islets. Each trace represents a single β-cell. **B.** Quantification of intracellular Ca^{2+} in control and βMfn2KO islets from traces in **A**. There was no difference in Ca^{2+} at basal glucose levels or after stimulation with 15mM glucose and 40mM KCl to induce Ca^{2+} release. (n=8)

4.4.2 βMfn2KO Islets have Decreased ROS Levels

Insulin secretion has been linked to oxidative metabolism and to the production of ROS. Additionally, ROS have also been shown to contribute to GSIS at low concentration, even as it is toxic to β-cells at high levels (Pi *et al.*, 2007). Interestingly, we found that βMfn2KO islet have decreased ROS levels compared with control islets. A representative oxyblot demonstrates a slight decrease in oxidized protein in βMfn2KO islets (Figure 4.5A). We investigated basal hydrogen peroxide (H_2O_2) levels using the

fluorescence probe DCFDA. There was a significant decrease in basal H_2O_2 levels in Mfn2-deficient islets (Figure 4.5B). This implies that high ROS levels are not the cause of increased basal insulin secretion in the βMfn2KO mice. However, these results suggested that ROS could still be playing an indirect role in basal hyperinsulin secretion. Since high levels of circulating free fatty acids and glucose similar to those in βMfn2KO mice are know to increase ROS levels, we concluded that an intrinsic characteristic of the βMfn2KO islets were leading to decreased ROS levels. Since one of the main sources of ROS is the electron transport chain, we next investigated mitochondrial bioenergetic function in βMfn2KO islets and whether alterations in oxygen consumption could be leading to decreased ROS levels.

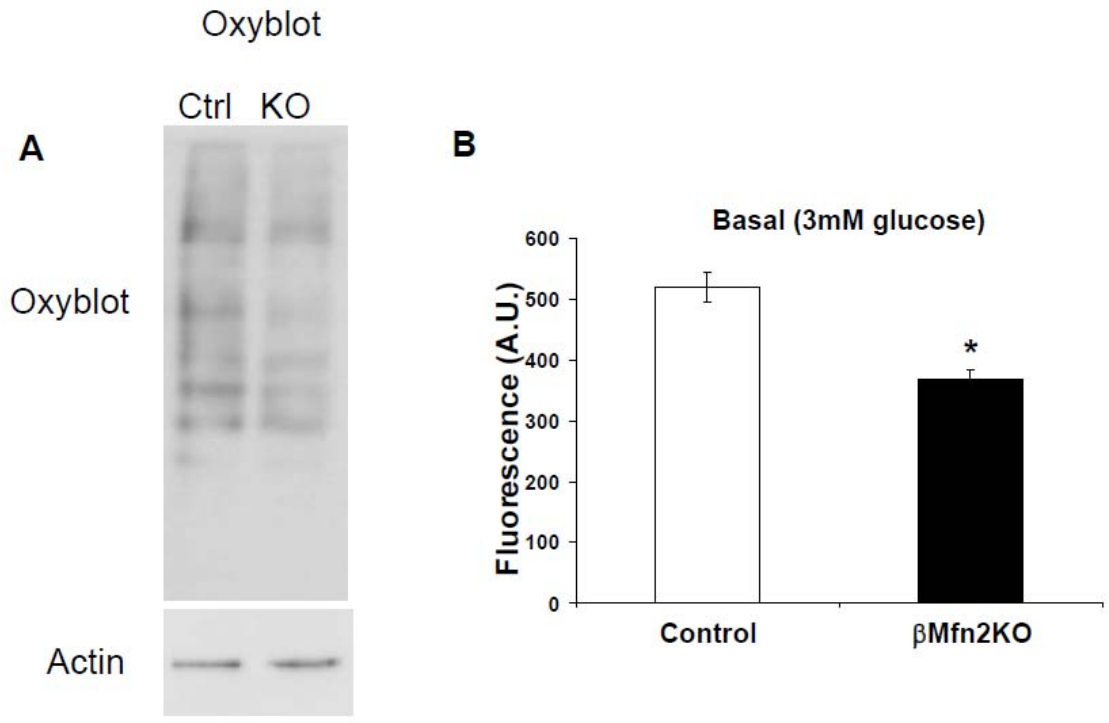

Figure 4.5: βMfn2KO islets present decreased oxidative stress compared with control islets. **A.** Representative oxyblot showing a mild decrease in oxidized protein in βMfn2KO islets. **B.** ROS in the form of H_2O_2 was measured at basal glucose levels in βMfn2KO and control islets. DCFDA fluorescence indicates decreased H_2O_2 in

βMfn2KO islets (n= 2 animals per genotype, replicates were performed in quadruplicate; *p≤0.05).

4.4.3 βMfn2KO Islets Display Alterations in Mitochondrial Respiratory Function

Loss of Mfn2 has been shown to decrease maximal oxygen consumption in muscle cells, indicative of decreased respiratory capacity (Bach et al., 2003). We tested the bioenergetic capacity of whole islets isolated from the βMfn2KO mice by measuring their oxygen consumption using the XF24 respirometer. We find that the surge in oxygen consumption, typically observed with the acute increase in glucose concentrations (from 3mM to 20mM), is significantly blunted in islets isolated from βMfn2KO mice (Figure 4.6 A). Moreover, βMfn2KO islets exhibited higher basal respiration ($p<0.05$) when normalized to size and number between groups. In the basal state, βMfn2KO islets respire a two fold higher compared to control (Figure 4.6B). Respiration not coupled to ATP synthesis (also termed proton leak or oligomycin-resistant respiration) was significantly increased by 10 percent in the βMfn2KO islets (Figure 4.6C). Measurements were normalized to basal respiration levels. This increased leak could account for the decrease in ROS levels in βMfn2KO islets. High leak would keep mitochondrial membrane potential low and prevent the flow of protons back through complex I or complex III to generate ROS. This should be further investigated by measuring mitochondrial membrane potential in βMfn2KO islets.

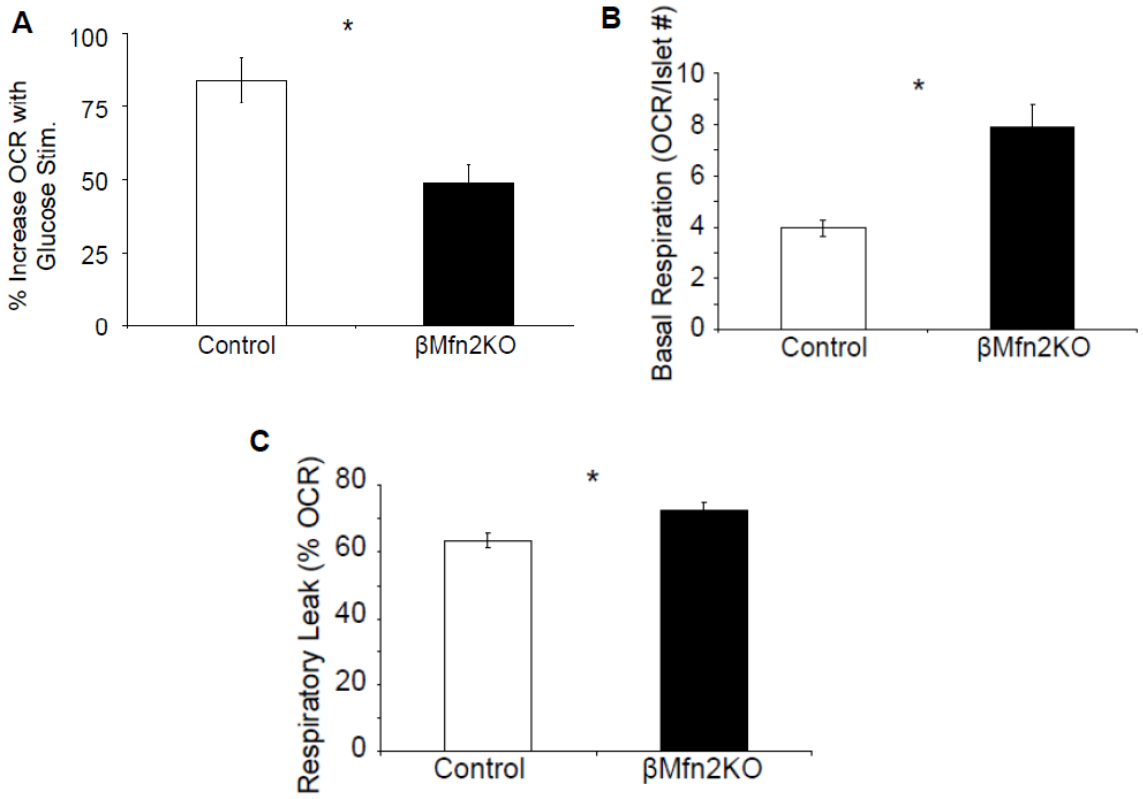

Figure 4.6 βMfn2KO islets have increased basal oxygen consumption and increased proton leak indicative of bioenergetic inefficiency. **A.** Oxygen consumption measured in whole islets. The bar graph depicts the percent increase in oxygen consumption when extracellular media is changed from 3mM to 20mM glucose. The normal increase in oxygen consumption is significantly blunted in the islets lacking beta cell Mfn2 (*p≤ 0.05, n=4). **B.** Basal oxygen consumption greater in islets lacking Mfn2 compared to controls (*p≤0.05, n=4). **C.** Respiratory leak under 5μM oligomycin, to block ATP Synthase, is 10% greater in islets lacking Mfn2 compared to control (*p≤0.05, n=4).

4.4.4 High Nutrient Environments Induce Proton Leak in Islets

The increase in proton leak in the βMfn2KO mouse is especially interesting given the already high level of uncoupled respiration in β-cells. We had already shown that proton leak is induced in islets in response to acute nutrient stimulation. Therefore, wanted to explore how changes in bioenergetic efficiency could be related to obesity and diabetes; for that reason, we examined how islets respond bioenergetically to chronic, high nutrient levels. To investigate bioenergetic changes in response to chronic exposure to high

nutrients levels, mice were fed a HFD for 8 weeks. Oxygen consumption was measured in intact islets isolated from these mice using the Seahorse respirometer. We found that high nutrient environments do, in fact, induce changes in bioenergetics (Figure 4.7). Basal respiration, which is strongly controlled by ATP turnover, is increased by about 25% in mice fed a HFD (Figure 4.7A). This is indicative of a harder working ETC. Although, increased OCR may also be a result of an increase in mitochondrial mass. This was tested for by western blotting for the mitochondrial protein porin. No increase in porin expression was observed; suggesting differences in basal respiration was not due to increase mitochondrial mass.

Uncoupled respiration was also measure in HFD islets and those treated with high free fatty acids and glucose. In the presence of 5μM oligomycin, control islets have approximately 50% leak. This is typical for islets, which have been well documented to have high levels of uncoupling. Islets from HFD animals have an even further increased basal leak, approaching 65% (Figure 4.7B). Interestingly, stimulating oxygen consumption by adding 20mM glucose further increases leak in HFD islet. To examine the effect of high fat alone on uncoupled respiration, islets were incubated for 48 hours in media with 0.4mM palmitate followed by respirometry. Under basal 3mM glucose concentrations, there was no significant difference in OCR under oligomycin (Fig 4.7C). However, at higher glucose (20mM) palmitate-incubated islets showed significantly higher proton leak. Thus, exogenous fuels could affect the level of uncoupling and interesting this again implies that it is the combination of free fatty acids and glucose that is the most detrimental to mitochondria.

Examining oxygen consumption in islets treated with chronic high nutrients has provided some interesting insight into fuel regulation of bioenergetics. Both HFD and βMfn2KO mice have increased oxygen consumption at basal glucose levels, indicative of increased electron transport chain activity at non-stimulatory levels. Respirometry data also suggests that chronic exposure to a high nutrient environment leads to bioenergetic inefficiency in islets. All of this data implies that increased fuel exposure leads to hard working mitochondria that are less efficient at making ATP.

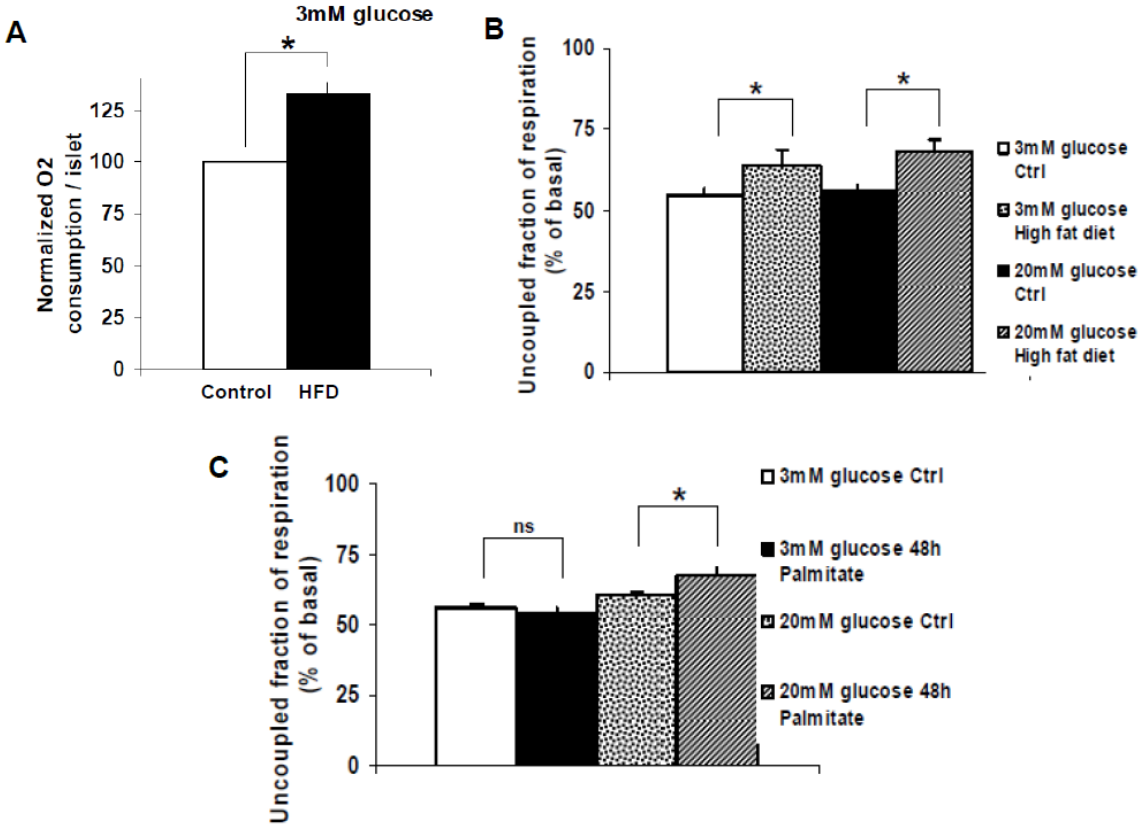

Figure 4.7 Chronic levels of elevated fuels leads to bioenergetic inefficiency. **A.** Mice were maintained on control or HFD for 8 weeks. Basal oxygen consumption was measured in islets from mice on control or high fat diet. There was a significant increase in basal oxygen consumption normalized to islet number in HFD islets compared with control islets (*$p<0.05$; n= 3 independent experiments). **B.** HFD islets have increased uncoupled respiration at both basal and stimulatory glucose concentrations (*$p<0.05$; n= 3 independent experiments). **C.** The contribution of free fatty acids to leak. Islets were treated with palmitate for 48 hours and respirometry was performed. At basal glucose concentrations there is no significant difference in oligomycin-resistant respiration

between control and palmitate treated islets. At stimulatory glucose concentration, palmitate treated cells display a significant increase in proton leak compared with control islets. This demonstrates that it is the combination of fat and glucose that is leading to decreased bioenergetic efficiency in islets chronically treated with high nutrient levels (*$p<0.05$; n= 3 independent experiments).

4.4.5 Effect of GLT on Mfn2 Deficient INS1 Cells

We previously showed that a high nutrient environment does not augment the metabolic phenotype of βMfn2KO mice (Figure 3.12). With this knowledge and the fact that both βMfn2KO islets and islets exposed to high nutrients have increased proton leak, we wanted to determine what would happen to bioenergetics when Mfn2 deficient INS1 cells were exposed to GLT. Interestingly, we found that Mfn2 deficient INS1 cells have a higher oxygen consumption rate (normalized to baseline rates) at basal levels and in response to stimulatory 15mM glucose levels (Figure 4.8). The graph from the respirometry run shows that at 3mM glucose levels there is a large OCR response in the Mfn2KD INS1 cells (Figure 4.8A; red plot). It appears that decreased Mfn2 expression is playing a protective role in response to high nutrients. The respirometry graph clearly displays that control cells exposed to GLT do not exhibit increased OCR in response to nutrients (pink plot = control at basal levels; cyan = control at stimulatory glucose levels); in fact, it appears that these cells are undergoing cell death characterized by a steady decrease in OCR. Mfn2KD INS1 cells do not respond to stimulatory glucose concentration as vigorously as they do basal levels (dark blue plot). This data is represented in bar graph form in figure 4.8B. Mfn2KD INS1 cells have a significant increase in OCR compared with control cells at both basal and stimulatory glucose concentrations; although, this effect is much more prominent at basal concentrations. This fits well with respirometry on βMfn2KO islets where we see increased basal (3mM

glucose) OCRs but a decrease in OCR in response to stimulatory glucose concentrations compared with control littermates (Figure 4.6). Although, it is also possible that the high glucose concentrations are toxic in these cells, but that the Mfn2KD is acting as a protective mechanism and delaying cell death (as we also see in response to STZ; figure 3.14). It would therefore be interesting to further study the protective role of decreased Mfn2 expression in response to nutrients and verify that GLT is causing apoptosis in the control cells and that this is being prevented or delayed in Mfn2 deficient cells.

Basal proton leak is significantly increased Mfn2KD cells under GLT compared with control GLT INS1 cells (Figure 4.8C). It should be noted that all of these INS1 cells were exposed to GLT, but it would be interesting to determine whether there is any difference in proton leak between Mfn2KD cells exposed to control or GLT media. In response to glucose stimulation, Mfn2KD cells maintain proton leak at approximately 70% uncoupled respiration. This is significantly higher than control GLT cells stimulated with glucose (Figure 4.8C). There is a decrease in glucose stimulated proton leak compared with basal leak in control GLT cells. Although, it is difficult to determine whether this is an actual bioenergetic response or if it is due to cell death in control GLT cells exposed to 20mM glucose levels. This needs to be further investigated before a definitive conclusion can be made regarding altered proton leak in control cells treated with GLT. Additionally, this was only one independent experiment, so should be repeated twice more to verify these results.

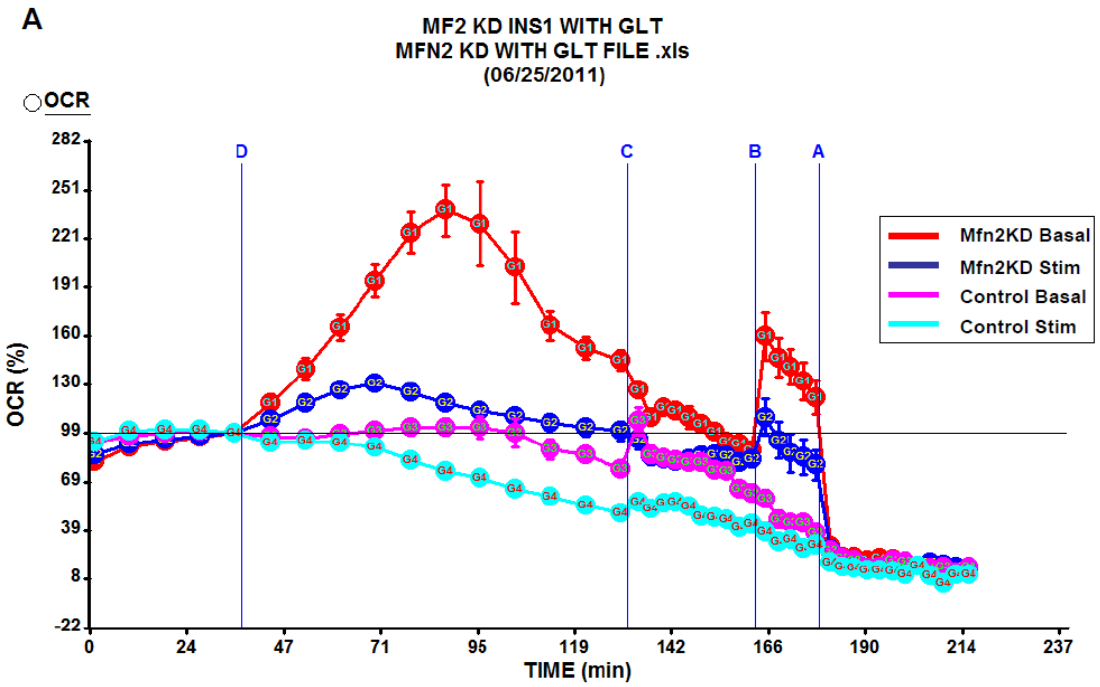
A
MF2 KD INS1 WITH GLT
MFN2 KD WITH GLT FILE .xls
(06/25/2011)
OCR
D
C
B
A
Mfn2KD Basal
Mfn2KD Stim
Control Basal
Control Stim
OCR (%)
TIME (min)

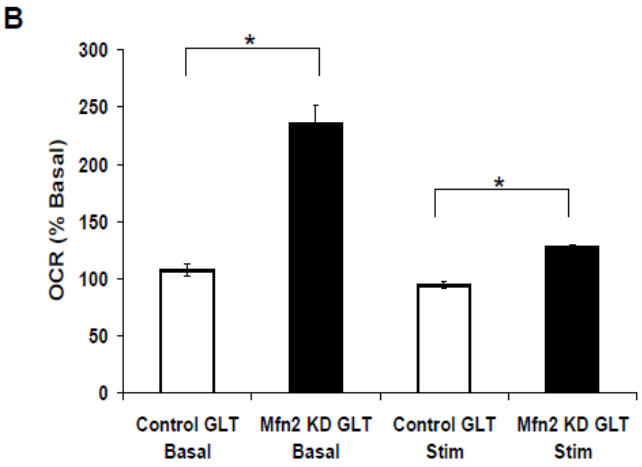
B
OCR (% Basal)
Control GLT Basal
Mfn2 KD GLT Basal
Control GLT Stim
Mfn2 KD GLT Stim

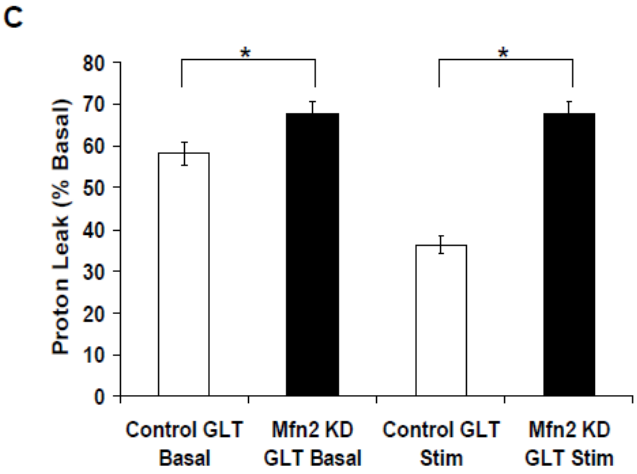
C
Proton Leak (% Basal)
Control GLT Basal
Mfn2 KD GLT Basal
Control GLT Stim
Mfn2 KD GLT Stim

Figure 4.8 The role of Mfn2KD in bioenergetic efficiency in response to a high nutrient environment. **A.** Seahorse plot of INS1 cells infected with either control or miRNA against Mfn2. All of the cells were treated with GLT for 48 hours. Oxygen consumption was measured under basal and stimulatory conditions. The red line represents Mfn2KD INS1 cells under basal conditions, dark blue is Mfn2KD INS1 cells under stimulatory glucose conditions; the pink plot is control INS1 cells under basal conditions and the cyan line is control cells at stimulatory glucose concentrations. The injections were as followed: D: either 3mM or 20mM glucose; C: 2 μM oligomycin; B: 5μM FCCP; A: 5μM Rotenone and Antimycin A cocktail. (n=1 independent experiment, 5 wells per condition). It appears that while Mfn2KD INS1 cells still respire, control INS1 cells are undergoing cell death. **B.** OCR in response to either basal or stimulatory glucose concentrations. Mfn2KD INS1 cells have increased OCR at both basal and stimulatory glucose concentrations (*$p \leq 0.05$). **C.** Uncoupled respiration in GLT treated Mfn2KD and control INS1 cells under basal and stimulatory conditions. Mfn2KD INS1 cells have increased proton leak as a percentage of basal compared with control cells at both 3mM and 20mM glucose concentrations.

4.4.6 Pro-oxidants Induce Proton Leak and Increase Basal Respiration in Islets

It has been shown that increased ROS contributes to the detrimental effect of HFD and GLT in β-cells. In β-cells, ROS have been shown to acutely increase in response to fuel stimulation and to act as a stimulant of insulin secretion (Pi *et al.*, 2007), whereas high oxidative stress are toxic to β-cells. Interestingly, while ROS is high in islets exposed to nutrients, it is lower in βMfn2KO islets. It has long been hypothesized that since ROS generation is elevated during times of increased mitochondrial activity (Sohal and Allen, 1985;Perez-Campo *et al.*, 1998) characterized by mitochondrial membrane potential hyperpolarization, that this would be involved in the regulation of proton leak (Echtay *et al.*, 2002;Kadenbach, 2003). Increased proton leak would decrease membrane potential and the generation of additional ROS hence makes a ROS/leak feedback loop (Brookes, 2005). Therefore, we next aimed to further explore the role of ROS in the regulation of bioenergetic efficiency in β-cells.

We first used the pro-oxidant menadione to determine how high ROS levels affect proton leak in isolated islets. Menadione is a naphthoquinone that forms a conjugate with glutathione (GSH) by reacting with thiol groups, thereby depleting GSH from the cell (Orrenius, 1985;Castro *et al.*, 2008). Since GSH is an antioxidant enzyme, this leads to an indirect increase in oxidative stress. It can also directly generate ROS via one-electron reduction pathways (Orrenius, 1985). When a quinone undergoes a one electron a semiquinone radical is formed, which under aerobic conditions can participate in redox cycling to generate ROS (Castro *et al.*, 2008). We found that menadione treatment leads to an increase in basal proton leak as a percentage of basal in islets (Figure 4.9A). The increase in uncoupled respiration was 20%, which is a larger increase than what we see under high nutrient levels. An increase in uncoupled respiration in response to ROS is in agreement with other cell types.

We next investigated whether there was a correlation between increased proton leak induced by elevated ROS levels and insulin secretion. We performed a batch insulin secretion assay in islets acutely treated with 10μM menadione. We found that there is a significant increase in basal insulin secretion in menadione treated islets compared with vehicle treated control islets with no difference in glucose stimulated insulin secretion (GSIS) (Figure 4.9B). This suggests that the increase in ROS levels, the increase in proton leak, or both are contributing to basal hypersecretion.

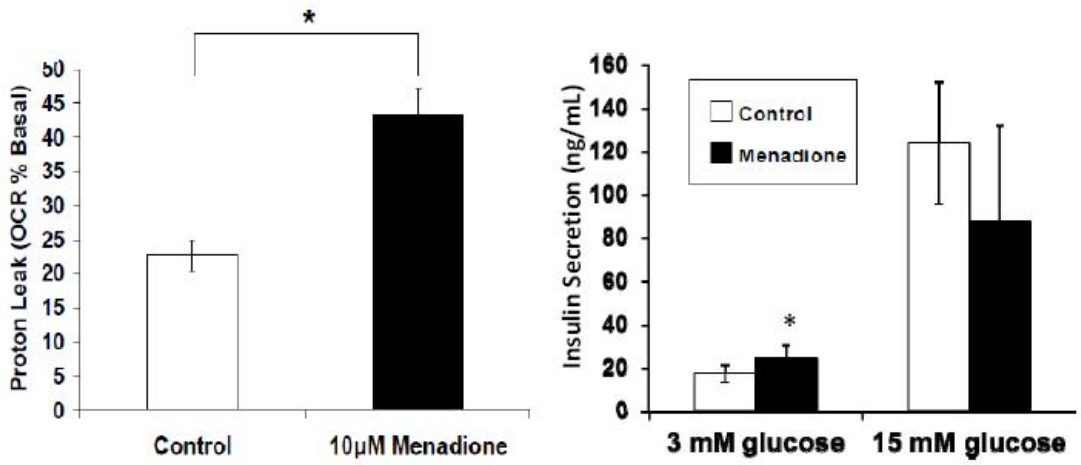

Figure 4.9 The pro-oxidant menadione alters both proton leak and insulin secretion in islets. **A.** Uncoupled respiration in islets in response to menadione. Acute injection of 10 μM induces a significant increase in proton leak in islets. (n= 2 independent experiments; 5 wells per condition per experiment; *$p \leq 0.05$). **B.** Insulin secretion in response to menadione treatment. Addition of 10 μM menadione to islets during batch insulin secretion experiments resulted in increased basal insulin secretion with no significant difference in GSIS. (n= 3 independent experiment; 5 replicates per condition per treatment for each experiment *$p<0.05$).

4.4.7 Regulation of Leak by Antioxidants

To understand whether ROS is a true regulator of proton leak in β-cells, we investigated if we could prevent leak in response to nutrients with antioxidants. We utilized the antioxidant, TBAP, a cell–permeable compound that has both superoxide dismutase (SOD) and catalase activity (Patel and Day, 1999).

4.4.76a Antioxidant Regulation of Proton Leak in Acute Nutrient Stimulation

We investigated the role antioxidants had on uncoupled respiration in response to acute stimulation with leucine and glutamine, the condition we found to induce the highest degree of proton leak in islets. Islets were acutely treated with the combination of TBAP (20μM) and amino acids (10mM leucine/glutamine with 3mM glucose) or control treatment (3mM glucose). TBAP significantly decreased proton leak at both basal levels

and completely prevented leak in response to amino acid stimulation (Figure 4.10A). This suggests that ROS play a role in acute fuel-induced uncoupling in islets.

4.4.7b Antioxidant Regulation of Proton Leak in Chronic Nutrient Stimulation

The effect of ROS on chronic fuel-induced proton leak was examined by treating islets with GLT for 24 hours and measuring oxygen consumption with and without TBAP. We find that there is no difference in proton leak with antioxidant compared with islets treated with GLT alone (Figure 4.10B). While this should be repeated because it was only one independent experiment, this implies than ROS is not involved with the regulation of leak in states of chronic high nutrient environments.

4.4.6c Antioxidant Regulation of Proton Leak in Mfn2 Deficient INS1 Cells

We also examined how Mfn2 deficient INS1 cells respond to antioxidants in response to high nutrients. We treated control and Mfn2KD INS1 cells with either palmitate alone or palmitate and TBAP (Figure 4.10C). We found that Mfn2 KD cells respire in response to palmitate significantly more than control INS1 cells. When TBAP is injected in addition to palmitate there is no significant difference in the OCR between control and Mfn2KD cells. This is mainly due to an increase in OCR rate in the palmitate and TBAP treated group. This implies that control cells are more sensitive to the antioxidant capacity of TBAP than Mfn2KD cells in the context of increasing respiration in response to acute nutrient stimulation. This is in agreement with our data showing that Mfn2 deficient islets have decrease ROS levels compared to control islets and therefore should be less sensitive to antioxidants.

Since we have shown that ROS can induce proton leak, we also wanted to know whether uncoupled respiration was sensitive to antioxidants in Mfn2KD INS1 cells (Figure 4.10D) to further understand the role of ROS in regulation leak. We find that while there is a trend towards an increase in uncoupled respiration in Mfn2KD cells treated with palmitate compared with control cells, the increase is not significant. However, this data only represents two independent experiments, so an additional experiment should be run to determine if there is a significant difference. TBAP treatment resulted in a trend towards decreased proton leak in both Mfn2KD and control INS1 cells, but again this was not significant. Therefore, while it appears that proton leak is regulated by ROS in both control and Mfn2KD INSl cells, a definitive answer can not be concluded from the current data.

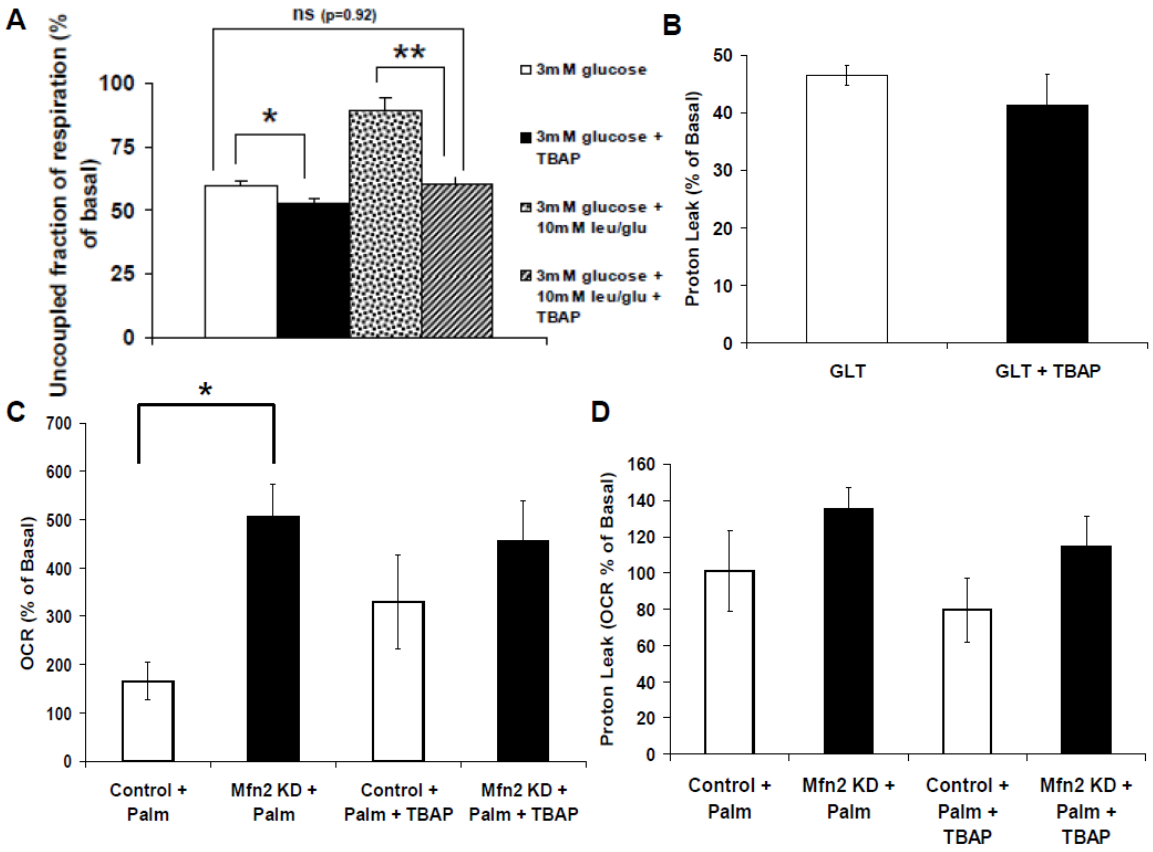

Figure 4.10 The effect of antioxidants in β-cells in response to acute and chronic nutrient stimulation. **A.** Uncoupled fraction of respiration in response to acute 10mM leucine and glutamine stimulation with and without antioxidant. TBAP decreased leak in basal glucose levels and completely reversed the increase in leak expected with amino acid stimulation. (n=3) **B.** Proton leak in GLT treated islets with and without antioxidant. Isolated islets were treated with GLT for 24 hours before respirometry was measured. TBAP did not decrease proton leak in islets treated with GLT. (n=1 independent experiment; 4 wells per treatment) **C.** OCR in response to stimulatory 0.4mM palmitate in control and Mfn2KD INS1 cells with and without TBAP. Mfn2KD INS1 cells have a significantly increased OCR as a percentage of basal respiration in response to palmitate compared with control INS1 cells. There is no difference in OCR between control and Mfn2KD cells treated with palmitate after the addition of the antioxidant, TBAP (n= 2 independent experiments; 5 wells per condition per experiment; *$p<0.05$). **D.** Uncoupled respiration in response to 0.4mM palmitate in control and Mfn2KD INS1 cells with and without TBAP. While there is a trend towards increased proton leak in Mfn2KD cells in both palmitate and palmitate plus TBAP treated cells, there is no significant difference in proton leak between any of the groups (n= 2 independent experiments; 5 wells per condition per experiment).

4.4.8 The Adenine Nucleotide Translocase is Involved in Inducing Leak in Islets

It is generally thought that ROS induces uncoupling through the activation of uncoupling proteins in the mitochondria (Echtay and Brand, 2007;Heuett and Periwal, 2010). Indeed, this has been shown in a number of different systems. However, our lab has found that UCP2, the main uncoupling protein thought to be involved in β-cell function does not regulate leak in response to nutrients (unpublished data demonstrated in UCP2KO islets). The adenine nucleotide translocase (ANT) is the most abundant mitochondrial inner membrane protein (Lee *et al.*, 2009b). It has been shown to account for a major portion of the proton leak, for example in muscle (Lee *et al.*, 2009a). To test for the contribution of ANT under basal and fuel stimulated conditions, we used the pharmacological ANT inhibitor, bongkrekic acid. In islets that were treated simultaneously with bongkrekic acid and amino acids, we found decreased proton leak under both basal and stimulated conditions (Figure 4.11A).

We also examined the role of ANT in ROS-induced proton leak. We treated islets with either menadione or menadione with bongkrekic acid. In agreement with what we found previously, menadione induced an approximate 20% increase in uncoupled respiration. This was significantly greater than control cells (Figure 4.11B). Bongkrekic acid resulted in a significant decrease in proton leak in menadione treated cells. However bongkrekic acid did not bring leak down to control levels since there was still a significant increase in uncoupled respiration in the menadione plus bongkrekic acid treated islets compared with control islets. This suggests that while the ANT is involved with inducing leak in high ROS environment, it is not the only uncoupling mechanism in place.

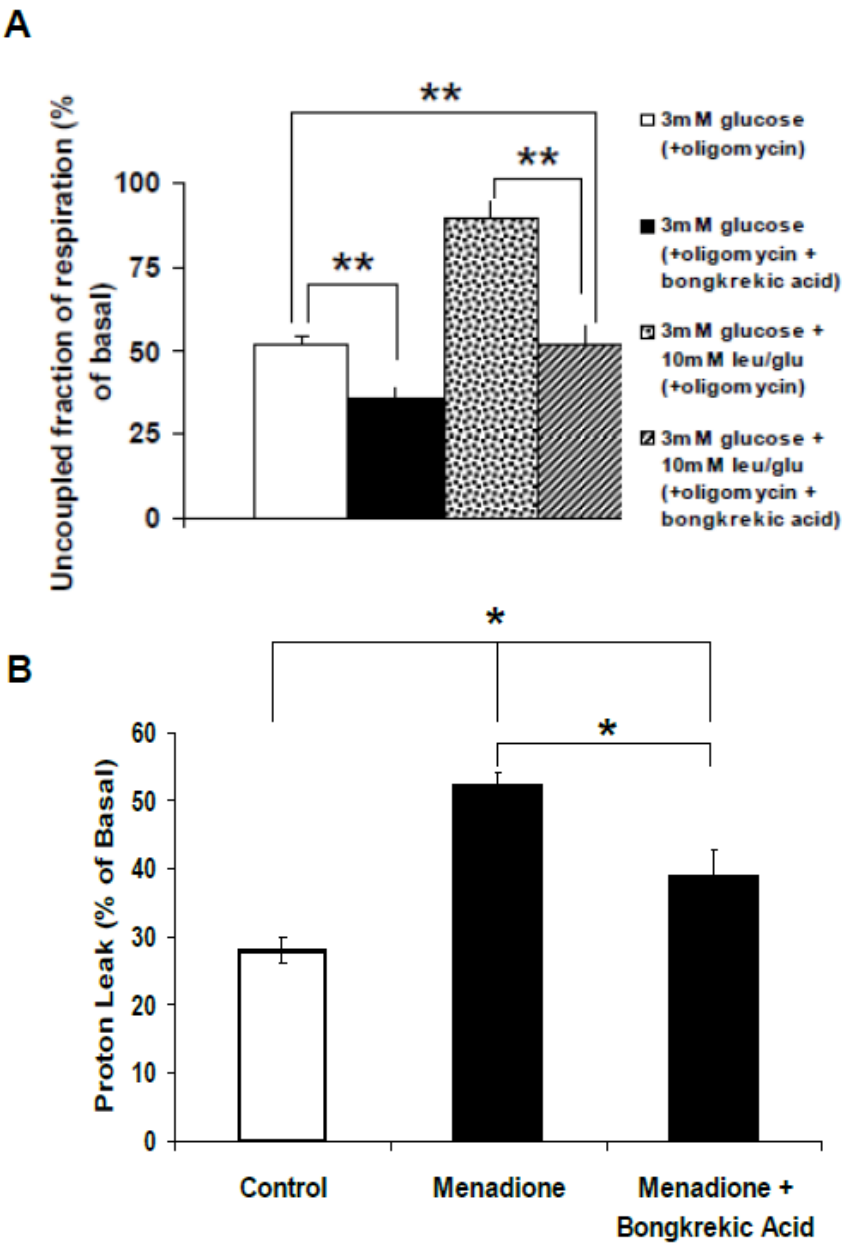

Figure 4.11 The ANT regulates proton leak in both acute amino acid stimulation and high ROS conditions. **A**. To test for the contribution of ANT under basal and fuel stimulated conditions, we used the pharmacological ANT inhibitor, bongkrekic acid, at a saturating concentration. Islets were treated simultaneously with bongkrekic acid and amino acids. Uncoupled respiration both under basal and stimulated conditions decreased under bongkrekic acid treatment (n=3; *p<0.05). **B.** Bongkrekic acid decreased leak in response to menadione. 10μM menadione injection results in a significant increase in proton leak in islets. Bongkrekic acid significantly decreases proton leak induced by menadione. (n= 2 independent experiments; *p<0.05).

4.4.9 Effect of Chemical Uncoupling of the Electron Transport Chain on Insulin Secretion

To investigate the functional role of increased proton leak in β-cells, we acutely treated islets with a low FCCP concentration (200nM) to induce uncoupling, without fully depolarizing the mitochondria, and measured insulin secretion. FCCP did not cause any changes in insulin secretion implying that uncoupling does not generate the basal hypersecretion of insulin we see in HFD and βMfn2KO islets (Figure 4.12). While, it is possible that leak is not contributing to basal insulin secretion, this should not yet be completely ruled out. Experimental conditions for this experiment should be optimized to explore the connection between proton leak and uncoupling. For example, we did not use oligomycin to inhibit ATP Synthase in this experiment. The use of oligomycin would prevent potential ATP loss in FCCP treated islets that could result in artificially lower insulin secretion. Additionally, the concentration and incubation period should be further optimized. It is possible that either 200nM FCCP was too low (of note: titrations were performed to determine a FCCP concentration that induced leak to a similar extend of nutrient stimulation) or that treatment with FCCP for the 30 minutes incubation time in the batch insulin secretion experiment was not enough time. Therefore, a preincubation with FCCP may be necessary for future experiments. Additionally another uncoupler could be more appropriate for this experiment, for instance *2,4*-dinitrophenol (DNP).
It is also possible that high proton leak does not lead to increased basal insulin secretion through the generation of amplifying signals for insulin secretion. Other potential roles for high levels of uncoupled respiration will be discussed in the discussion secretion (Section 4.5).

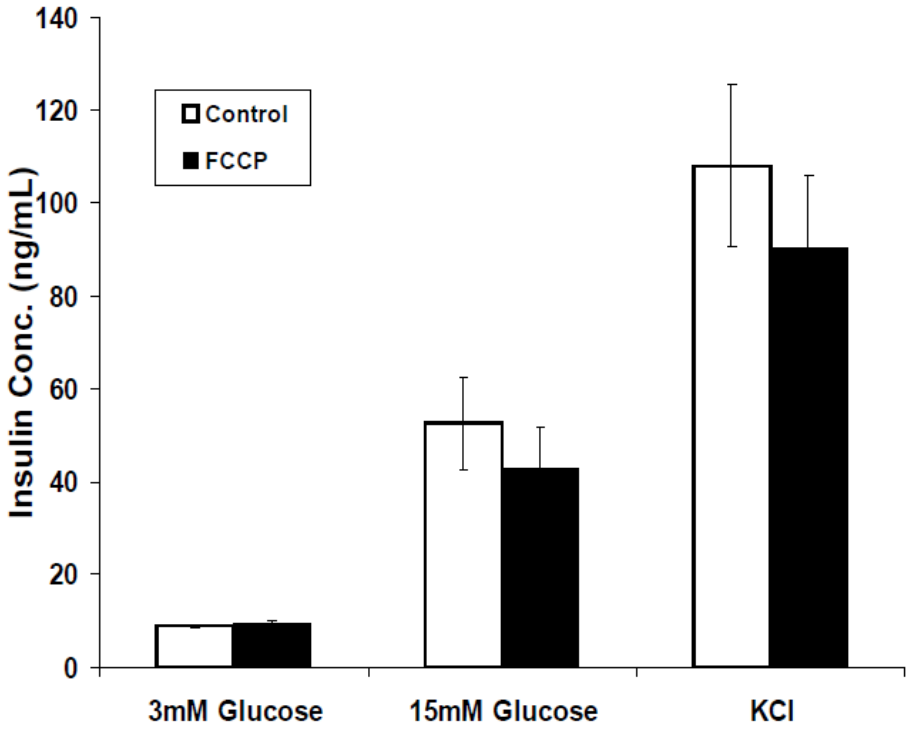

Figure 4.12 Chemical uncoupling does not induce basal hypersecretion of insulin. Islets were treated 200nM FCCP or vehicle control during the test incubation period of the batch insulin secretion. There were no significant changes between FCCP and control in basal, stimulatory, or KCl induced insulin secretion (n=3 independent experiments).

4.5 Discussion

This focus of this study was to determine mechanisms behind basal hypersecretion in βMfn2KO and HFD islets. While the exactly mechanism of basal hypersecretion was not determined, we did find a number of interesting results about the regulation and mechanism behind proton leak in β-cells. We were the first to use the Seahorse Extracellular Flux Analyzer to measure respiration in intact islets. This was achieved by developing a new plate specialized for islets to be used in the instrument. We found that differential regulation of proton leak by free fatty acids, amino acids, and ROS seems to play an important functional role in the β-cell.

Proton leak is a major contributing factor to energy homeostasis (Rolfe and Brand, 1996;Rolfe and Brand, 1997). In principle, the level of uncoupled respiration reflects cellular bioenergetic efficiency. Mouse islets are highly uncoupled, with approximately 50% of respiration as a result of uncoupling. A recent study in INS1 cells measured uncoupled respiration at 75% (Affourtit *et al.*, 2008b). This is in contrast with our measurements of uncoupled respiration in INS1 cells of about 38% (Fig 3). This difference is unlikely due to methodology differences as our measurements of uncoupled respiration in C2C12 myotubes (~22%) were similar to the results of Affourtit and colleagues. We suspect that this is more likely due to the known diversity in the behavior of different clones of INS1 cells.

A high level of uncoupling in β-cells is of interest since they integrate nutrients signals that are used to generate ATP for insulin secretion. Since uncoupling will decrease bioenergetic efficiency, the percentage of high leak seems counterproductive. Therefore, we sought to determine the effect of nutrients on β-cell bioenergetics. We found increased leak in response to acute nutrient stimulations, which is increased even further with chronic high nutrient exposure. The induction of proton leak in response to fatty acids is in agreement with previous studies. Free fatty acids were previously shown to induce uncoupling in rat islets (Carlsson *et al.*, 1999) as well as in isolated mitochondria (Esteves *et al.*, 2006) and intact cells (Nobes *et al.*, 1990), which is in accord with our finding that chronic palmitate treatment induces uncoupling (Figure 4.7C). Therefore, it appears that proton leak could be playing an important functional role in response to fuels in β-cells. Additionally, we find that βMfn2KO islets also display increase leak even though they have low levels of ROS. Since ROS induces leak and leak decreases ROS,

this suggests that Mfn2 could play a role in regulating leak. This is hypothesized because Mfn2 deficient β-cells have a persistent increase in leak, which could be leading to decreased ROS levels in these islets considering that ROS are generated from high ETC activity. While still a preliminary hypothesis, this would place regulation of Mfn2 after ROS generation but before the increase in uncoupled respiration. The role of Mfn2 in the generation of proton leak should be further investigated in the future.

We propose that nutrient-induced leak may provide a functional role in β-cells. We suggest this could be occurring through 3 mechanisms. First, uncoupled respiration may enhance the production of insulin secretagogues that are generated in metabolism prior to mitochondrial ATP-synthesis. For instance, high levels of uncoupling will require the TCA cycle, β-oxidation and amino acid metabolism to work at a higher rate. This increased rate may function to generate a large number of amplifying signals for insulin secretion from the metabolism preceding oxidative phosphorylation. Amplifying signals can be generated from pyruvate shuttle traffic; NADPH, α-ketoglutarate and GTP (Jensen *et al.*, 2008) as well as TCA cycle derived GTP (Kibbey *et al.*, 2007). We explored this by using low concentrations of FCCP to generate uncoupling in islets and then measured insulin secretion. We found no difference in basal insulin secretion between vehicle control and FCCP treated islets (Figure 4.12). While this data did not agree with our hypothesis, we still believe that high proton leak could be contributing to basal insulin hypersecretion. As discussed in the results secretion, a number of experimental conditions could have affected the outcome of this experiment and therefore optimization needs to be performed to determine the best approach for studying the connection between proton leak and basal insulin secretion.

Second, high levels of uncoupled respiration may provide the β-cell protection from fuel toxicity. Since the β-cell serve as a fuel sensor, it imports more fuel than is required for maintaining the ATP concentration. These fuels however may render them sensitive to fuel toxicity, as shown by studies on glucolipotoxicity. Increased mitochondrial uncoupling may allow excess fuel to be dissipated without causing damage to the mitochondria. This nutrient-detoxification mechanism is of particular interest when we take results from Mfn2 deficient β-cells into consideration. We find that Mfn2 deficient INS1 cells appear to be less sensitive to GLT than control cells, suggesting that the continuous high level of proton leak observed in βMfn2KO islets could be paradoxically serving as a mechanism of protect even though it is also resulting in metabolic dysfunction. The role of Mfn2 degradation as a survival mechanism in β-cells is an intriguing hypothesis that deserves further attention.

Finally, the obvious question arises as to whether the increased uncoupling due to obesity and diabetes should be viewed as a dysfunction or a compensatory mechanism. We demonstrated that islets from HFD fed mice have a further increase in uncoupling at basal levels compared with controls and this is elevated more in response to glucose stimulation (Figure 4.7B). Additionally HFD islets have increased OCR compared to control islets at basal glucose levels, but do not display a difference in OCR in response to glucose stimulation compared to control islets. This difference in respiration at basal levels is consistent with basal hypersecretion of insulin that has been well documented from islets of diabetic animals (Fex *et al.*, 2007). In a normal physiological state, leak will oscillate with oscillations in the fuels to which the β-cells are exposed. In this scenario, when nutrients are high and the ETC chain is working harder and producing

more ROS, uncoupling will be induced in order to decrease mitochondrial membrane potential and consequently ROS production, therefore detoxifying high nutrients. Additionally, high levels of leak at stimulatory levels of nutrients may also function to produce amplifying signals for insulin secretion (as discussed previously). On the other hand in conditions such as obesity and diabetes, where fuel levels are always elevated, leak will no longer be able to oscillate but instead will remain high. This will lead to changes in nutrient-sensitivity, thereby right shifting the insulin response curve to make islets less sensitive to stimulatory glucose levels while increasing basal insulin secretion. This would explain increased basal insulin secretion in chronic states of high nutrient exposure without corresponding increases in glucose stimulated insulin secretion.

We also wanted to determine how leak is induced in islets. It is generally accepted that proteins contribute to a major portion of the mitochondrial proton leak (Kadenbach, 2003;Brand *et al.*, 2005). While the identity of the major mediators of proton leak has been a subject of controversy, numerous studies support a role for ROS as a regulator of the amplitude of leak conductance (Echtay *et al.*, 2002). Unpublished data from our lab demonstrated that UCP2 does not seem to significantly contribute to uncoupling in isles (Jakob Wikstrom; unpublished data from UCP2KO islets). However there is evidence in INS1 cells that UCP2 may be contributing to leak in these clonal β-cells (Affourtit *et al.*, 2008b). The role and regulation of UCP2 in β-cells is still widely controversial and it remains largely unclear what is the function of UCP2 in the β-cell. Since we knew that UCP2 was not regulating the induction of leak in islets, we decided to focus on two other known inducers of leak: ANT and ROS.

In β-cells, low levels of hydrogen peroxide derived from glucose metabolism serve as signals for insulin secretion and antioxidants reduce insulin secretion (Pi *et al.*, 2007). However, the mechanism by which ROS increase insulin secretion is yet unknown. Here we show that antioxidants reduce the level of uncoupled respiration to basal levels in response to acute nutrient stimulation, suggesting a mechanism by which ROS could regulate insulin secretion. However, in chronic nutrient conditions, we were unable to demonstrate that antioxidants reduce uncoupled respiration (Figure 4.10). This could mean that ROS play a differential role in regulating leak in physiological conditions compared with disease states. This should be further investigated. Nevertheless, our study indicates that under physiological conditions reducing ROS improves mitochondrial bioenergetic efficiency and that this could also affect insulin secretion. Thus, the mitochondrial uncoupling may appear inefficient but may serve an important physiological role

The molecular target of ROS is unclear, but may involve ANT as its uncoupling activity appears to increase with acute fuel challenges (Figure 4.11). Indeed, we found that in addition to inducing leak at both basal and acute amino acid stimulation, the ANT also is involved with generating leak in response to elevated ROS. By using bongkrekic acid, an inhibitor of ANT (Klingenberg and Buchholz, 1973), in combination with oligomycin, the contribution of ANT to the basal level of uncoupled respiration was estimated to ~31% (Figure 4.6.11A). Under fuel stimulated conditions (leucine/glutamine) the contribution of ANT to uncoupled respiration increased to 42% (Figure 4. 11A). This suggests the possibility that a significant part of the fuel induced uncoupling may be due to increased nucleotide shuttling. We also demonstrated that inhibition of ANT results in

a significant decrease in the leak-induced by menadione, a pro-oxidant (figure 4.11B). Furthermore, it was shown in a fly model that ANT may be negatively regulated buy ROS (Yan and Sohal, 1998). In isolated liver mitochondria, it was demonstrated that the lipid peroxidation product 4-hydroxynonenal induces uncoupling through interaction with ANT (Azzu *et al.*, 2008). Interestingly, this was dependent on $\Delta\psi_m$ as more hyperpolarized $\Delta\psi_m$ promoted a greater effect of 4-hydroxynonenal. Hence, the $\Delta\psi_m$ hyperpolarization induced by fuels in β-cells (Katzman *et al.*, 2004;Wikstrom *et al.*, 2007) may play a similar role.

In conclusion, about one third of uncoupling appears mediated by the ANT. It is currently unknown what is contributing to the remaining proton leak. Other potential leak mechanisms may include endogenous leak of the phospholipid membrane, however liposomes (without proteins) made from inner membrane of liver mitochondria show low levels of proton leak (Wikstrom *et al.*, 2007). Thus, proteins are more likely to contribute the major part of the proton leak. Besides ANT these may include ion channels, e.g. mitochondrial Ca^{2+} channels, or metabolite transporters.

While more work needs to be completeled to fully understand the connection between nutrient-regulation of uncoupled respiration in islets and how this effects β-cell function, this work has contributed to elucidating some pieces of this puzzle. Further work must also be devoted to determining if Mfn2 somehow triggers proton leak. We hypotesize that high levels of uncoupled respiration in islets may effect cellular functions including ROS regulation, nutrient sensitivity, and insulin secretion. Therefore, unregulated proton leak could be contributing to the development or progression of diabetes and obesity.

Chapter 5: Discussion, Implications, and Future Directions

5.1 Summary and Implications of Key Findings

The work presented in this dissertation focused on how nutrients affect β-cell mitochondrial dynamics and bioenergetics and, in turn, how mitochondrial fusion and fission and mitochondrial function influence the metabolic response to a high nutrient environment. This is important because β-cells integrate nutrients and generate signals for insulin secretion, wherein mitochondria play a critical role. A number of different approaches were utilized to investigate how β-cell mitochondrial dynamics affect both islet and whole body metabolic function and survival. We conclude that β-cell mitochondrial dynamics could be contributing to whole body metabolic regulation of fuel availability and storage; although, some of the results we obtained could be a results of changes in the mitochondrial fusion protein, Mfn2, in the brain. We focused a majority of our work on Mfn2 because its expression has previously been shown to be altered in skeletal muscle of obese and diabetic animal models and patients and because we have shown that it is down regulated in islets of mice fed a HFD. An overview of our main finding and their significance in the context of β-cell and mitochondrial function are discussed.

5.1.1 Phenotypic Similarities Between HFD and βMfn2KO Mice

This work has begun to elucidate the role mitochondrial dynamics have in normal β-cell physiology and the development of Type 2 Diabetes. We demonstrate that under normal conditions β-cell mitochondria undergo continuous fusion and fission events despite their

small size. Under high nutrient conditions these mitochondria undergo fragmentation due to decreased fusion capacity. We found that this is caused, in part, by a decrease in the mitochondrial fusion protein, Mfn2. Excision of Mfn2 in β-cells demonstrated that there are a number of phenotypic similarities between these mice on a normal diet and wild type mice fed a high fat diet, which is summarized in Table 5.1.

	HFD	βMfn2KO
Weight	↑	↑
Fasting Blood Glucose	↑	↑
Glucose Tolerance	Impaired	Impaired
Insulin Secretion	↑ Basal	↑ Basal
Reactive Oxygen Species	↑	↓
Mitochondrial Morphology	Fragmented/Inhibited Fusion Ability	Fragmented
Heterogeneity	↑	↑
Basal Oxygen Consumption Rate	↑	↑
Uncoupled Respiration	↑	↑

Table 5.1 Overview of metabolic and mitochondrial characteristics of HFD and βMfn2KO mice. All data from βMfn2KO mice we collected over the course of this work, results from HFD animals represents a combination of data we collected and previously published and accepted data.

Both βMfn2KO and HFD mice gain weight, are hyperglycemic with impaired glucose tolerance, and display increased basal insulin secretion. Additionally, islets from these animals exhibit fragmented mitochondrial morphology, increased heterogeneity, and decreased bioenergetic efficiency. To date, the main difference we have found is in ROS levels. It is generally believed that high nutrient environments lead to increased ROS production, this characteristic is not present in Mfn2 deficient islets, which actually have decreased ROS levels. However, a recent study may be in agreement with our finding. Valle *et al.* report that islets from rats fed a HFD produce less ROS than control islets (Valle *et al.*, 2011). This suggests that ROS is decreased in islets exposed to high nutrients and could explain why we found that antioxidants could decrease leak with

acute nutrient stimulation but not in islets that were exposed to chronic high nutrients levels.

The phenotypic similarities between βMfn2KO mice and those fed a HFD are very interesting and require further investigation. This is intriguing because we have shown that Mfn2 is downregulated in the islets of mice fed a HFD. Moreover, we have preliminary evidence demonstrating that βMfn2KO mice on a high fat diet do not exhibit any further metabolic dysfunction in any of the parameters we have tested thus far (weight, fasting blood glucose, glucose tolerance). This implies that downregulation of β-cell Mfn2 could be a major contributor to the whole body metabolic consequences of HFD. However, as we have already discussed in chapter 3, we cannot rule out the possibility that Mfn2 deficiency in the hypothalamus is driving this phenotype. Either possibility presents an interesting insight into the possible mechanism driving the phenotype observed in mice fed a HFD. It also highlights the role of mitochondrial fusion in the regulation of whole body metabolism, whether it is arising from the brain or the β-cell. The Shirihai laboratory is currently generating an Mfn2 overexpression mouse; it will be interesting to see how these animals respond to HFD.

5.1.2 Potential Role of Mfn2 Downregulation as a Protective Mechanism to Combat a High Nutrient Environment in β-Cells

The possibility that decreased Mfn2 expression in the β-cell largely contributes to the metabolic phenotype of mice fed a HFD, leads to the question of what purpose or benefit this would provide the cell. It is possible that this decrease in Mfn2 expression is a compensatory mechanism that allows islets to survive a high nutrient environment. Preliminary evidence indicates that decreased Mfn2 expression in INS1 cells provides

protection from GLT. Mfn2 deficient INS1 cells have an improved ability to respire in response to nutrients when exposed to GLT. It also appears that Mfn2 deficient β-cells have a delayed apoptotic response to GLT compared with control cells. Additionally, βMfn2KO mice treated with STZ, a toxin that leads to β-cell necrosis, are protected from the noxious effects and are able to maintain their weight, normal blood glucose levels, and islet integrity. This provides evidence that downregulation of Mfn2 is providing a protective role in the β-cell in an *in vivo* environment. A possible mechanism of how this may be occurring is that Mfn2 deficiency could be postponing opening of the mitochondrial permeability transition pore. However, how Mfn2 would be regulating mtPTP sensitivity is still unknown, although there is evidence in other cell types that this could be the case. It was shown that Mfn2-deficient cardiomyocytes have delayed permeability transition in response to Ca^{2+} or ROS generation; two known inducers of mtPTP opening. Additionally these Mfn2-deficient cardiomyocytes display improved recovery from reperfusion injury (Papanicolaou *et al.*, 2011).

Much more work needs to be completed to fully understand the effect Mfn2 has in regulating sensitivity to mtPTP and therefore providing protective from noxious stimuli. The extent of mitochondrial swelling, a hallmark of mtPTP opening should be assessed in Mfn2-deficient cells. If it is the case that Mfn2 plays a role in regulating sensitivity to permeability transition, it could provide a connection between why decreased Mfn2 expression is beneficial even though it is leading to marked metabolic dysfunction.

5.1.3 Model of Proton Leak Regulation in the β-cell and how this Contributes to β-cell Function

We hypothesize that uncoordinated insulin secretion, namely an increase in basal insulin secretion, plays a significant role in the metabolic dysfunction observed in HFD mice and βMfn2KO mice. The mechanism behind increased basal insulin secretion is not fully understood, but this work has provided some novels insights into what could be leading to basal hypersecretion. We found that a high nutrient environment leads to an increase in respiratory proton leak. We hypothesize that this increase in proton leak can act as a detoxification mechanism in response to the high nutrient levels that can be toxic to the β-cell. Stimulation with an acute nutrient challenge will lead to an increase in ETC activity and hyperpolarization of mitochondrial membrane potential, which consequently increases ROS production. The increased ROS levels can induce proton leak in β-cells, in part via the ANT. Increased uncoupling will then result in decreased ETC activity, mitochondrial membrane potential, and ROS production. Therefore, the induction of proton leak is acting to protect the mitochondria against the detrimental effects of high nutrient load. Once this process is complete, proton leak would return to basal level. We also suggest that this effects oscillations in insulin secretion. Increased uncoupled respiration results in a less efficient ETC; meaning that the mitochondria have to work harder to produce the same amount of ATP. This would result in increased flux through the TCA cycle, which is known to contribute to amplifying signals of insulin secretion. Therefore in addition to acting as a nutrient detoxification mechanism, proton leak could also contribute to insulin secretion. Taken as a whole, in a normal physiologic state this mechanism would connect oscillation in nutrients with oscillations in membrane potential and insulin secretion.

When nutrients become chronically elevated the oscillations in this system would be lost. This leads to a constant high level of uncoupling that requires the mitochondria to work harder all the time, demonstrated by an increase in basal oxygen consumption. We hypothesize that this proton leak and increase in flux through the TCA cycle can also influence both basal and glucose stimulated insulin secretion. High leak should lead to situation where there is an increased fuel requirement for the induction of GSIS in the β-cell. Additionally, stable increased flux through the TCA cycle would still lead to elevated secretagogues, but, again, without the oscillations that would be present in a normal state. Taken together, this chronic elevation in proton leak could lead to increased insulin secretion at basal levels while at the same time leaving β-cells less sensitive to normal stimulatory glucose concentrations. Diagram 1 summarizes how increased leak can act as a detoxification mechanism and subsequently alter insulin secretion under normal and pathophysiological conditions. While we have some evidence for this pathway, more work needs to be completed to link uncoupled respiration to basal insulin secretion.

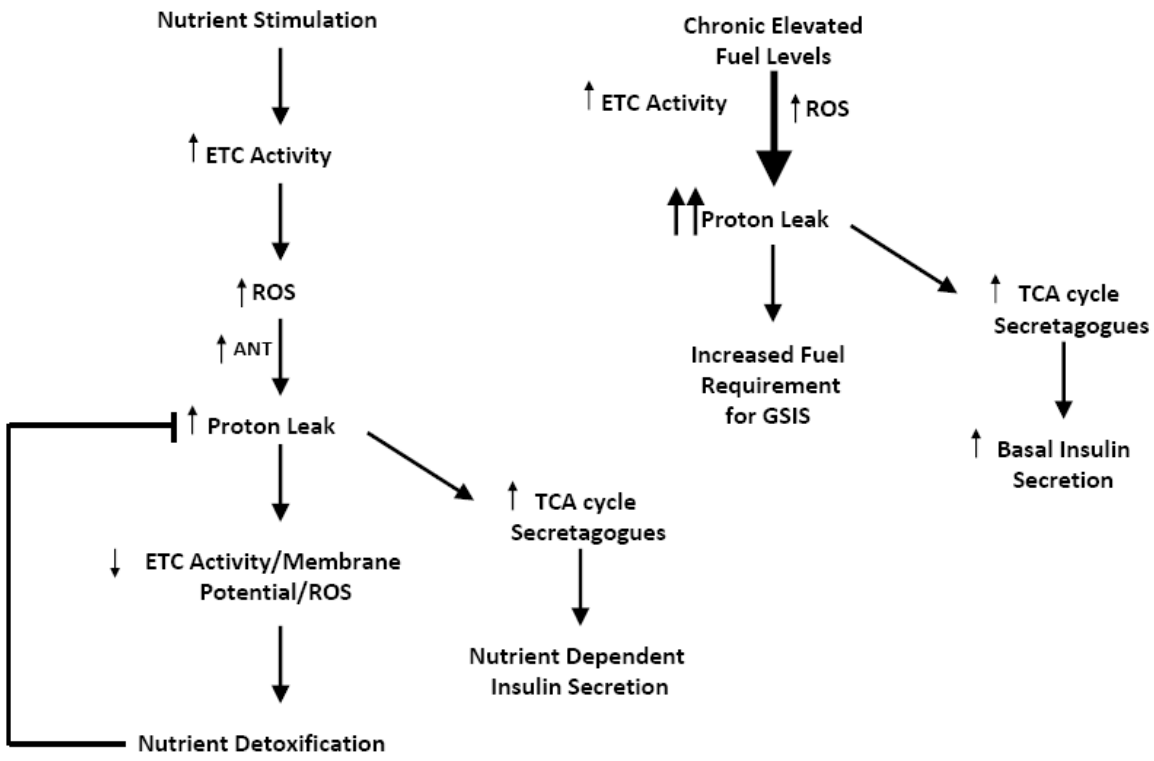

Figure 5.1 Schematic outline of our hypothesized role of β-cell proton leak in regulating fuel integration and insulin secretion in a normal, physiologic state and when nutrient oscillations no longer occur and the β-cell. The latter would result in an environment where the β-cell is always exposed to high fuel conditions.

Downregulation of Mfn2 may also be playing a role as a switch between bioenergetic efficiency and uncoupling in response to high nutrient levels in the β-cell. This hypothesis stems from our experimental data demonstrating that islets from βMfn2KO mice are highly uncoupled under normal nutrients levels to a similar extent to wild type islets exposed to a high nutrient environment. It is currently unknown whether decreased Mfn2 expression or activity is necessary for the transition between coupling efficiency and increased leak when high levels of nutrients are present, and accordingly needs to be further investigated. It is unlikely that Mfn2 would be able to directly generate proton leak, but it is possible that it is indirectly acting as a trigger for proton leak. It may do this by functioning as a nutrient sensor, where decreased Mfn2 expression or activity indicates the need for increased uncoupling. Additionally, given the possible role for

Mfn2 in survival as well as proton leak, the mtPTP could be a possible mechanism of uncoupling and should be examined as a possible candidate for the regulation of proton leak through Mfn2.

5.1.4 Therapeutic Implications and Potential

Obesity and diabetes is a serious health and financial burden and, with rates rapidly increasing all over the world, presents a challenge on how to efficiently diagnose and treat patients with these diseases. While for many, diet and exercise could be the answer to the reversal or prevention of metabolic dysfunction; this is not always the case. Therefore, a better understanding of the development and progression of these diseases can establish new drug targets for treatment. Mfn2 presents an intriguing point of regulation for whole body metabolic control and may provide an interesting target. However, before this is possible the differential roles and targets of Mfn2 in β-cells need to be further elucidated. For example, Mfn2 already has known roles in mitochondrial fusion and Ca^{2+} buffering and has proposed roles in mtPTP sensitivity and now in the regulation of mitochondrial bioenergetic efficiency. Which of these functions is contributing to maintenance of fuel utilization and storage and which are providing protection from cell death is critical to understanding if and/or how it could be utilized therapeutically.

5.2 Future Directions

This body of work has uncovered a number of interesting observations regarding the role of mitochondrial dynamics and mitochondrial function in β-cells. However, with every question answered many more questions were generated. The following is a brief

description of some of our current interests and where we would like to take this research in the future.

5.2.1 The Effect of Mitochondrial Proton Leak on Basal Hypersecretion of Insulin

As discussed extensively above, we suggest that uncoupling could be driving increased basal insulin secretion in β-cells. Our initial experiment to investigate this provided a negative result, but we hypothesize this could be due to technical issues. Therefore, a full experimental workup should be conducted to determine definitively if increased proton leak promotes basal hypersecretion. First, we would like to take advantage of different chemical uncouplers. In our batch insulin experiment, we used FCCP, an uncoupler that acts as an ionophore. It permeabilizes the inner mitochondrial membrane to protons thereby destroying the proton gradient. DNP (2,4-dinitrophenol) is another uncoupler that we could utilize. In addition concentrations, exposure time, and whether oligomycin should be co-administered for insulin secretion experiments needs to be further optimized. We will also consider the approach we take to measuring insulin secretion (i.e. would islet perifusion experiments be more informative than batch insulin secretion).

5.2.2 Understanding the Mechanism Underlying Mfn2 Degradation in Response to High Nutrient Environments

It is known that Mfn2 degradation is mediated by the ubiquitin-proteasome system. In mitophagy, or the autophagic degradation of mitochondria, Mfn2 is down regulated via the PINK1/parkin pathway. PTEN-induced putative kinase 1 (PINK1) is a mitochondrial serine/threonine kinase that recruits the E3 ubiquitin ligase, parkin, to dysfunctional mitochondria, for example depolarized mitochondria (Narendra *et al.*, 2008;Matsuda *et*

al., 2010). This scenario where mitochondria have to be depolarized for parkin recruitment and Mfn2 degradation is unlikely to happen in response to high nutrients, which would hyperpolarize mitochondrial membrane potential. Therefore, another mechanism must be regulating Mfn2 degradation in response to elevated nutrient concentration. We suspect that DJ-1, a ubiquitously expressed protein with links to the protease and chaperone functions, may be regulating Mfn2 expression in response to ROS (Nagakubo *et al.*, 1997;Lev *et al.*, 2008).

It has been shown that β-cells express DJ-1 and that its expression can be induced by cellular stressors. Inberg and Linial demonstrated that DJ-1 protein was induced following exposure to oxidative stress and ER stress in MIN6 cells, βTC-6 cells, and mouse islets. In pancreatic MIN6 cells, oxidized DJ-1 protein was induced by high glucose concentrations. Knockdown of DJ-1 by siRNA accelerated cell death whereas overexpression of DJ-1 attenuated cell death, induced by hydrogen peroxide or thapsigargin (Inberg and Linial, 2010). This work taken together with our understanding of how high nutrient environments and Mfn2 deficiency effect β-cell survival, ROS production and bioenergetics efficiency suggests that DJ-1 may be a good candidate as a physiological regulator of Mfn2 expression.

DJ1 is a cytosolic protein that translocates to mitochondria in response to ROS and regulates parkin recruitment (Moore *et al.*, 2005). We hypothesize that high nutrient environments lead to increased ROS and Mfn2 degradation through translocation of DJ-1 to the mitochondria and subsequent activation of parkin. We rationalize that DJ-1 serves as a physiological sensor of ROS that protects the cell from mitochondrial hyperactivity

by limiting fusion capacity and generating uncoupling through promoting Mfn2 degradation. This mechanism would prevent ROS damage during periods of increased mitochondrial activity due to elevated nutrient concentrations while also providing a possible quality control mechanism by isolating damaged mitochondria that produce high levels of ROS.

5.2.3 The Role Mfn2 Plays in Protection from Nutritional Insults

We know that the βMfn2KO mouse is protected from STZ treatment compared with littermate control animals. The KO mice are able to maintain normal glucose levels, body weight, and their β-cell mass is protected. Additionally, Mfn2 deficient cells seem better equipped to deal with the toxic effects of GLT. Therefore it is important to determine if Mfn2 is playing a protective role and, if so, the mechanism behind this protection needs to be elucidated. First, a complete analysis of whether Mfn2 deficiency protects β-cells from different cellular insults, especially nutrient toxicity, should be conducted. Next, potential mechanisms should be explored, for example protection due to diminished ROS levels or decreased mtPTP sensitivity. We have shown that βMfn2KO islets produce less ROS than control islets, which suggest decreased apoptosis could be due to lowered ROS production. This can be tested using antioxidants. However, our hypothesis is that Mfn2 is conferring protecting by decreasing the sensitivity to mtPTP opening. A number of tools can also be utilized to study the role of the mtPTP in protection. The ability to induce permeability transition can be measured by monitoring swelling in response to Ca^{2+} or increased ROS levels. Additionally, drugs such as cyclosporine A that decrease the sensitivity for mtPTP opening can be used to test if decreased sensitivity is playing a role in protection.

5.2.4 The Effect of Mfn2 Overexpression on the Development of Metabolic Dysfunction in Response to a High Fat Diet

Given that Mfn2 is decreased in HFD islets, mice with β-cell Mfn2 deficiency show a very similar phenotype to animals fed HFD, and placing these mice on HFD does not provide further dysfunction, which indicates that Mfn2 may be an attractive candidate as regulator of the metabolic phenotype presented with HFD. Therefore, the role of Mfn2 deficiency in HFD needs to be studied in more depth. The generation of a β-cell specific Mfn2 overexpression mouse would be an important tool for this study. Preferably an inducible expression could be achieved so that overexpression of Mfn2 could be turned on and off at different ages and under different conditions. Investigating how these animals respond to a HFD could be instrumental in determining whether Mfn2 downregulation is essential in the mechanism of HFD-induced obesity and diabetes or if it is a byproduct of this process.

5.2.5 Dissecting the Role of Mfn2 in the Brain and the β-Cell in the Control of Metabolic Function

Currently we do not know if Mfn2 excision in the β-cell, hypothalamus, or a combination of both is driving the metabolic phenotype observed in the βMfn2KO mice. Therefore, it is essential to determine the contribution of these areas to the phenotype. One possible approach would be to use the MIP-Cre mouse to conduct a similar study to what was presented in Chapter 3. MIP-Cre is expressed under the mouse insulin-1 promoter instead of the rat insulin-2 promoter used for the RIP-Cre mouse (Wicksteed *et al.*, 2010). This means that β-cell specificity is achieved in the MIP-Cre line. This is because the mouse *Ins1* gene is not expressed in the hypothalamus (Madadi *et al.*, 2008). If a similar phenotype was observed in a βMfn2KO colony generated with Cre expression driven by

MIP, this would provide evidence that it is β-cell Mfn2 deficiency that is driving the metabolic phenotype.

5.3 Overall Conclusions

Mitochondria play a critical role in integrating and generating signals that are required for β-cell function, including both the triggering and amplifying phases of insulin secretion. Therefore maintaining a functional mitochondrial population is necessary to retain proper control of β-cell metabolic function. Alterations in mitochondrial function including disturbances to morphology, ROS levels, and respiratory function can result in whole body metabolic dysfunction and contributes to the pathogenesis of diabetes and obesity. Deciphering how mitochondrial dynamics contribute to both the compensation to and survival from the high nutrient environment characteristic of obesity and diabetes will provide further understanding into the patholophysiology of these epidemics. Modulating mitochondrial function and preserving mitochondrial networks may provide an intriguing drug target in the fight against metabolic diseases.

Appendix 1: Mitochondrial Dynamics and Autophagy

Linsey Stiles[1,2], Andrew Ferree[1], Orian Shirihai[1]

1. Department of Medicine, Section of Molecular Medicine, Boston University School of Medicine, Boston, MA, USA.

2. Department of Pharmacology and Experimental Therapeutics, Tufts University School of Medicine, Boston, MA, USA.

This chapter was completed for the book Mitochondrial Dynamics and Neurodegeneration, which was published in June of 2011: **Linsey Stiles**, Andrew Ferree, Orian Shirihai. (2011) Mitochondrial Dyanmics and Autophagy. Bingwei Lu (editor), Mitochondrial Dynamics and Neurodegeneration. Springer.

Acknowledgements:

We are grateful to Drs. Marc Liesa, Gilad Twig, and Dani Dagan for insightful comments during the writing of this chapter.

Abbreviations:

A9-DA	A9-subtype dopaminergic neurons of the substantia nigra pars compacta
AD	Alzheimer's disease
ALS	amyotrophic lateral sclerosis
AMPK	5'adenosine-monophosphate activated protein kinase
ATG	autophagy-related genes
CA	constitutively active
CCCP	carbonyl cyanide m-chlorophenylhydrazone
CMA	chaperone-mediated autophagy
CMT2A	Charcot-Marie-Tooth neuropathy type 2A
Cvt	cytoplasmic to vacuole targeting
DA	dopaminergic
DLB	dementia with Lewy Bodies
DN	dominant negative
DNM1L	dynamin 1-like
Drp1	dynamin related protein 1
ER	endoplasmic reticulum
ERK1/2	extracellular signal-regulated protein kinase 1/2
ETC	electron transport chain
Fzo1p	fuzzy onions protein
GAP	GTPase-activating protein
HIF	hypoxia-inducing factor
LAMP-2A	lysosomal-assosiated membrane protein 2A
LC3;(MAP)LC3	miccrotubule-associated protein light chain 3;
MAO	monoamine oxidase

Mfn1/2	mitofusin 1 and 2
mPTP	mitochondrial permeability transition pore
MPTP	1-methyl-4-phenyl-1,2,3,6-tetrahydropyridine
mtDNA	mitochondrial DNA
mTOR	mammalian target of Rapamycin
mtPA-GFP	mitochondrial photoactivatable green fluorescent protein
NGF	nerve growth factor
OPA1	optic atrophy protein 1
PBMC	peripheral blood mononuclear cells
PD	Parkinson's disease
PE	phosphatidylethanolamine
PI	phosphatidylinositol
PINK1	PTEN-induced kinase 1
RGC	retinal ganglion cells
Rheb	Ras homolog enriched in brain
ROS	reactive oxygen species
TMRE	tetramethylrhodamine ethyl ester
TOR	target of Rapamycin
TORC1/2	TOR complex 1 and 2
Ulk-1/2	Unc-51-like kinase 1 and 2
VDAC1	voltage-dependent anion channel 1
Vps	vacuolar protein-sorting

A1.1 Abstract

Efficient mitochondrial quality control is critical for maintenance of a healthy mitochondrial population. Both mitochondrial dynamics and selective mitochondrial autophagy, termed mitophagy, contribute to mitochondrial turnover and quality control. Mitochondrial fusion and fission allow for complementation of mitochondrial solutes, proteins, and DNA but also for generation of unequal daughter organelles. Selective fusion is utilized for incorporation of polarized mitochondria back into the network, while a depolarized mitochondrion will not fuse, but instead will be targeted for elimination by mitophagy. Mitophagy is dependent on mitochondrial dysfunction, such as depolarization, and a number of proteins that are required for core autophagic machinery, signaling, and mitochondrial segregation and targeting. The relationship between mitochondrial dynamics and autophagy and how they may contribute to both

mitochondrial and cellular quality control is beginning to be elucidated. Even with the questions that remain in regards to the regulation and interdependence of mitochondrial dynamics and mitophagy, it is clear that alterations in these processes lead to mitochondrial dysfunction and pathological states such as neurodegeneration.

A1.2 A Brief Overview of Mitochondrial Dynamics

Mitochondria function as heterogeneous networks that undergo frequent fusion and fission events, constituting mitochondrial dynamics, which regulate their morphology, number, and function (Bereiter-Hahn *et al.*, 1994;Chen *et al.*, 2005a). Mitochondrial dynamics have been demonstrated to contribute to mitochondrial function in a number of systems including budding yeast, pancreatic β-cells, muscle, and neurons (Liesa *et al.*, 2009). It has been established that mitochondrial dynamics can influence almost every aspect of the mitochondrion including biogenesis, bioenergetics, heterogeneity and elimination (Wikstrom *et al.*, 2009;Hyde *et al.*, 2010).

Proteins that mediate mitochondrial fusion and fission have been identified. In mammals, fusion is regulated by at least three mitochondrial localized GTPases: mitofusin 1 (Mfn1), mitofusin 2 (Mfn2), and optic atrophy protein 1 (Opa1) (Santel *et al.*, 2001;Misaka *et al.*, 2002). The yeast homologs of these proteins are Fzo1p (Mfn1/2) and Mgm1p (OPA1) (Merz *et al.*, 2007). Mfn1 and Mfn2 are localized to the outer mitochondrial membrane, while OPA1 is an inner mitochondrial membrane protein. Mitochondrial fusion is a two step process where fusion of the inner and outer membranes occurs as separate events. Fission is mediated by the transmembrane protein Fis1 and cytosolic GTPase dynamin related protein 1 (Drp1/DNM1L); with Fis1 as the rate limiting factor in fission in some models. The yeast homologs to the fission proteins are Dnm1p (Drp1) and Fis1p (James

et al., 2003;Praefcke *et al.*, 2004). Drp1 translocates from the cytosol to scission sites on the outer mitochondrial membrane to initiate fission events. It should be noted that many of these proteins have roles outside of mitochondrial fusion and fission. For instance, it has been shown that Mfn2 is located on endoplasmic reticulum (ER), where it can regulate ER morphology and ER to mitochondria tethering; a process required for efficient Ca^{2+} homeostasis(de Brito *et al.*, 2008). Fis1 and Drp1 are localized to peroxisomes and have been shown to mediate peroxisomal fission in a similar manner to that of mitochondrial fission (Koch *et al.*, 2003;Koch *et al.*, 2005).

Mitochondrial dynamics are essential to maintain a metabolically efficient mitochondrial population and disruption of either fusion or fission alters mitochondrial morphology and functionality. Fusion contributes to maintenance of oxidative phosphorylation and mitochondrial membrane potential, with loss of fusion generally resulting in mitochondrial fragmentation, decreased mitochondrial membrane potential and oxygen consumption, and often increased reactive oxygen species (ROS) production and susceptibility to apoptosis (Chen *et al.*, 2010;Zorzano *et al.*, 2010). Fusion allows for the generation of continuous membranes and matrix lumen, which subsequently allows for complementation of solutes, metabolites, and proteins. Complementation is thought to be a key mechanism by which mitochondria can rescue a damaged unit within the network. Mitochondrial fission is also a modulator of mitochondrial function. Fission regulates inheritance of mitochondria by daughter cells within dividing cells, cellular differentiation (neuronal, cardiac, and muscle cells), and progression of apoptosis. Loss of fission results in increased mitochondrial connectivity, loss of mtDNA, bioenergetic deficiency and changes in apoptosis (Liesa *et al.*, 2009;Karbowski, 2010).

Alterations to mitochondrial fusion and fission have been demonstrated in a number of conditions including neurodegeneration, obesity, and type II diabetes. Additionally, mutations in mitochondrial dynamics proteins have been identified in human pathologies. Mutations in OPA1 lead to autosomal dominant optic atrophy, which is the most common form of hereditary optic neuropathy (Alexander *et al.*, 2000). Charcot-Marie-Tooth (CMT) disease is a group of genetically heterogeneous diseases of the peripheral nervous system, characterized by distal muscle atrophy. Mutations in Mfn2 have been identified that result in CMT Type 2A (Zuchner *et al.*, 2004). These data place mitochondrial dynamics and function at the crossroads of human pathologies, in particular neurodegenerative diseases.

A1.3 Autophagy

Christian de Duve coined the term 'autophagy' meaning 'self-eating' in 1963 (Klionsky, 2007). In 1967, he published work showing that mitochondria are located within lysosomes when rat liver was perfused with glucagon (Deter and De, 1967;Deter *et al.*, 1967). Recently, the field of autophagy has rapidly expanded with research demonstrating that autophagy contributes to survival in the face of starvation (nutrient-deprivation) and to turnover of damaged organelles and proteins with long half-lives. Autophagy is a key regulator of human health and aging, as it has been implicated in a number of diseases including type II diabetes, cardiomyopathies, and neurodegeneration (Fujitani *et al.*, 2010;Essick and Sam, 2010). There are three broad classifications of autophagy: chaperone-mediated autophagy, microautophagy, and macroautophagy. All three forms of autophagy promote proteolytic degradation of cytosolic components within the lysosome. In chaperone-mediated autophagy (CMA), individual proteins with

a consensus binding sequence (KFERQ) are recognized and delivered to the lysosome by a complex of chaperone proteins, such as heat shock cognate protein of 70 kDa (hsc70). The CMA targeted proteins then cross the lysosomal membrane via a translocation complex that includes lysosomal-associated membrane protein 2A, LAMP-2A (Orenstein and Cuervo, 2010). During microautophagy, cytosolic components are directly taken up via invagination of the lysosomal membrane. In contrast, macroautophagy is the process by which macromolecular cytosolic components are degraded via sequestration in a double-membrane structure, which fuses with the lysosome to deliver the enclosed material for degradation (Goldman *et al.*, 2010;Glick *et al.*, 2010;Yang and Klionsky, 2010b). Macroautophagy, herein referred to as autophagy, is the process by which mitochondria amongst other organelles (such as endoplasmic reticulum, ribosomes, and peroxisomes) are degraded for recycling and elimination.

A1.3a Autophagic Machinery

The process of autophagy (Figure A.1.1) begins with an isolation membrane derived from a lipid bilayer contributed by ER and/or trans-Golgi, endosomes, and possibly mitochondria (Hailey *et al.*, 2010); although the exact origin of the isolation membrane, also known as the phagophore, is controversial (Eskelinen, 2008). The membrane expands to engulf its cargo, which is then contained within a double-membraned structure known as the autophagosome. The autophagosome fuses with the lysosome to form an autolysosome, also called an autophagolysosome, which degrades its contents via lysosomal acidic hydrolases. The resulting breakdown products are delivered back to the cytosol by lysosomal permeases and transporters where they can be reused (Yang and Klionsky, 2010a).

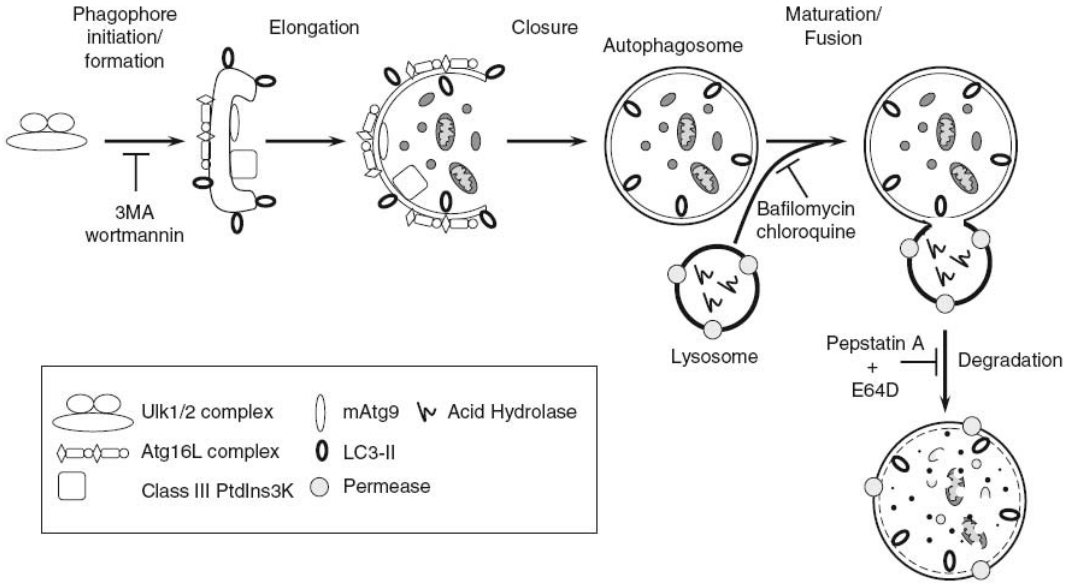

Figure A1.1: Overview of the mammalian autophagic machinery. Autophagy is a multi-step process that is initiated by the formation of the phagophore. This step can be blocked by using the chemical PI3-kinase inhibitors 3-methyladenine (3MA), LY294002, or, wortmannin. Phagophore formation is followed by elongation, and closure of the phagophore to form the autophagosome. Maturation of the autophagosome occurs upon fusion with a lysosome, generating the autophagolysosome. The maturation step can be inhibited by bafilomycin, an inhibitor of vacuolar H + ATPase (V-ATPase), and the lysosomotropic agent, chloroquine. Acid hydrolases degrade the cargo within the autophagolysosome, which can be blocked by the lysosomal protease inhibitors, pepstatin A and E64D. Breakdown products can be transported out of the autophagolysosome through permeases for recycling. Adapted from (Yang and Klionsky 2010a). (Originally published in **Linsey Stiles**, Andrew Ferree, Orian Shirihai. (2011) Mitochondrial Dyanmics and Autophagy. Bingwei Lu (editor), Mitochondrial Dynamics and Neurodegeneration. Springer.)

A1.3b Molecular Mechanism of Autophagy in Yeast

Major advancements in understanding molecular mechanisms of autophagy came from the discovery of several autophagy-related genes (ATG) in *Saccharomyces cerevisiae* yeast. Many mammalian homologs exist and a subset of these Atg proteins are considered the core components required for autophagosome formation (Yang *et al.*, 2010b).

In yeast, Atg1 exists in a complex, with Atg13 and Atg17, which is required for initial phagophore formation. Atg13 is phosphorylated in a Target of Rapamycin (TOR) kinase dependent manner, which prevents its binding to Atg1 and Atg17. Inactivation of TOR kinase complex 1 (TORC1) leads to dephosphorylation of Atg13, thereby promoting Atg1-Atg-13-Atg17 complex formation, generation of the phagophore, and autophagy. There are two complexes that incorporate Vps34, the only PI 3-kinase in yeast. Complex I consists of the proteins Vps34, Vps15, Atg6, and Atg14; this complex is necessary for the initiation of autophagy. Vps34 uses phosphatidylinositol (PI) as a substrate to generate phosphatidylinositol triphosphate, which is required for elongation of the phagophore as well as recruitment of other Atg proteins to the phagophore assembly site. The function of Vps34 is dependent on Vps15, a serine/threonine kinase, that modulates membrane recruitment and stimulation of the PI 3-kinase activity of Vps34 (Stack *et al.*, 1995). Complex II, consisting of Vps34, Vps15, Atg6, and Vps38, is involved in vacuolar sorting.

Two ubiquitin-like systems are essential for autophagy in yeast: Atg5-Atg12 conjugation and Atg8 processing. These two conjugation systems are evolutionary conserved from yeast to mammals and the nomenclature is essentially the same, except for Atg8. A number of mammalian homologs to Atg8 have been identified, the most prominent being microtubule associated protein light chain 3A (LC3). Additional Atg8 homologs include: GATE16, GABARAP, and Atg8L, all of which are processed in the same manner as Atg8 is in yeast (Tanida *et al.*, 2006). See the mammalian molecular mechanisms of autophagy section below for more detailed information on the Atg5-Atg12 and LC3 conjugation systems.

A1.3c Mammalian Homologs and Molecular Mechanism of Autophagy

Ulk-1 and Ulk-2 are homologous to yeast Atg1 and participate in complex formation with mAtg13 and FIP200 (the mammalian homolog of yeast Atg17). Unlike the yeast complex, mAtg13 interacts with Ulk-1, Ulk-2, and FIP200 independently of its phosphorylation state. A great deal about how the phosphorylation requirements relate to autophagic activity is beginning to be elucidated. For example, it is currently known that mAtg13, Ulk-1, Ulk-2, FIP200, and mTOR are all phosphorylated/dephosphorylated within the complex and that this is regulated by nutritional state and modulates autophagic activity. Interestingly, one study demonstrated a role for Ulk-1 in neurotrophic signaling (Zhou *et al.*, 2007). Activation of TrkA receptors by nerve growth factor (NGF) leads to ubiquitination of Ulk-1, subsequent association with p62, and binding to the NGF/TrkA complex. Through interactions with synaptic mediators of endocytosis, Ulk-1 facilitated trafficking of the ligand-receptor complex into endosomes. This novel role of Ulk-1 represents an important potential mechanism for axonal membrane homeostasis via autophagic and endosomal crosstalk (Komatsu *et al.*, 2007).

The role of the class III PI-3 kinase Vps34 and its binding partner beclin-1 (homolog of yeast Atg6) have been studied extensively. The complex of Vps34, beclin-1, and other regulatory proteins, such as p150 (homolog of Vps15), is required for the induction of autophagy. The role of Vps34 in complex I is conserved in yeast and mammals. UVRAG, BIF-1, Atg14L, Ambra, Rubicon, and Bcl-2 are additional regulatory proteins that complex with Vps34 and Beclin-1. UVRAG, BIF-1, Atg14L, and Ambra promote autophagy while Rubicon and Bcl-2 inhibit autophagy.

The two ubiquitin-like conjugation systems that are essential for autophagy in mammals are Atg5-Atg12 conjugation and LC3 processing. In the Atg5-Atg12 system, Atg7 acts as an E1-like ubiquitin activating enzyme, which activates Atg12 by binding to its carboxyterminal glycine residue in an ATP-dependent manner. Atg12 is transferred to the E2-like carrier protein Atg10, which increases the efficiency of covalent binding of Atg12 to Atg5 (on lysine 130). The conjugated Atg5-Atg12 interacts noncovalently with Atg16L, which oligomerizes to form the Atg16L complex: a large multimeric complex that associates with the extending phagophore. This association is thought to induce curvature in the expanding phagophore through recruitment of processed Atg8/LC3. The Atg16L complex dissociates from the phagophore membrane once the autophagosome is formed.

Microtubule-associated protein light chain 3 (LC3) is encoded for by the mammalian homolog of yeast Atg8. LC3 is expressed as a full-length cytosolic protein, which is proteolytically cleaved to LC3-I by Atg4, a cysteine protease, upon induction of autophagy. This cleavage exposes a glycine, which is subsequently activated by Atg7, an E1-like enzyme, in an ATP-dependent manner. Activated LC3-I is transferred to Atg3, an E2-like carrier protein, before phosphatidylethanolamine (PE) is conjugated to the glycine to generate LC3-II. This lipidated form of LC3 is integrated into both internal and external faces of the phagophore membrane, where it is involved in fusion of membranes. LC3-II may also act as a 'receptor' on the phagophore surface that can interact with target material via adaptor molecules, such as ubiquitinated proteins and p62, to induce selective cargo uptake.

The two conjugation systems (Atg5-Atg12 and LC3) are closely connected with Atg16L, which acts as an E3-like enzyme and determines the sites of LC3 recruitment and lipidation. In addition, it has been proposed that formation of the Atg16L complex may be dependent on Atg8/LC3 machinery given that mice lacking the ability to process LC3 (via knockout of Atg3) have reduced Atg5-Atg12 conjugation (Sou *et al.*, 2008). Sou et al. have also demonstrated that autophagosomes from Atg3-deficient animals are smaller and 'open-ended', providing evidence that the conjugation systems are involved in elongations and closure of the growing phagophore. This is further supported by experiments showing that autophagosomes are not closed in cells where LC3 lipidation is inhibited by overexpression of an inactive mutant of Atg4 (Fujita *et al.*, 2008).
The autophagosome is generated when the expanding ends of the phagophore fuse; although before the autophagosome is ready to fuse with the lysosome, it must first go through additional maturation steps by undergoing fusion events with early and late endosomes. It is thought that this connects endocytic and autophagic pathways to deliver both cargo and membrane fusion machinery to the autophagosome and to lower the pH of the vesicle. The lower pH of the autophagic vesicle makes it more suitable to house the lysosomal proteases that will breakdown the engulfed cargo.

The source of lipid used for autophagosome formation and the process by which this lipid is moved to the site of assembly remains largely unknown. mAtg9 is a transmembrane protein that is required for mammalian autophagy and is hypothesized to act as a 'membrane carrier'. Located in the trans-Golgi network and late endosomes, mAtg9 overlaps with LC3-positive autophagosomes upon starvation or rapamycin induction of autophagy. During starvation, the cycling of mAtg9 has been shown to require Ulk-1 and

hVps34 (Reggiori *et al.*, 2004;Young *et al.*, 2006). It has been proposed that mAtg9 may contribute to the formation of the autophagosome by delivering membrane components. This hypothesis is based on its function in yeast, yet this still remains to be demonstrated in mammalian cells.

Nishida et al. have shown that there is the possibility of an alternative macroautophagy pathway (Nishida *et al.*, 2009). They found that mouse cells lacking Atg5 or Atg7 can still form autophagosomes and autolysosomes and perform autophagy-mediated protein and mitochondrial degradation. Interestingly, lipidation of LC3 did not occur in the Atg5/Atg7-independent process of 'macroautophagy'. The alternative autophagy pathway still utilized and was regulated by known autophagic proteins, such as Ulk1 and beclin1. This implies that there may more than one pathway in which mammalian macroautophagy can occur, including an Atg5/Atg7-dependent conventional pathway and an Atg5/Atg7-independent alternative pathway.

A1.3d Signal Transduction Regulation of Autophagy

Autophagy occurs both at a basal level to maintain cellular homeostasis and at a stimulated level when induced by cellular stressors, such as nutrient starvation, oxidative stress, and hypoxia. A number of signaling pathways upstream of the 'Atg' machinery, or the mammalian equivalents (Yang *et al.*, 2010a), modulate autophagy in response to intracellular and extracellular stresses as shown in Figure A1.2.

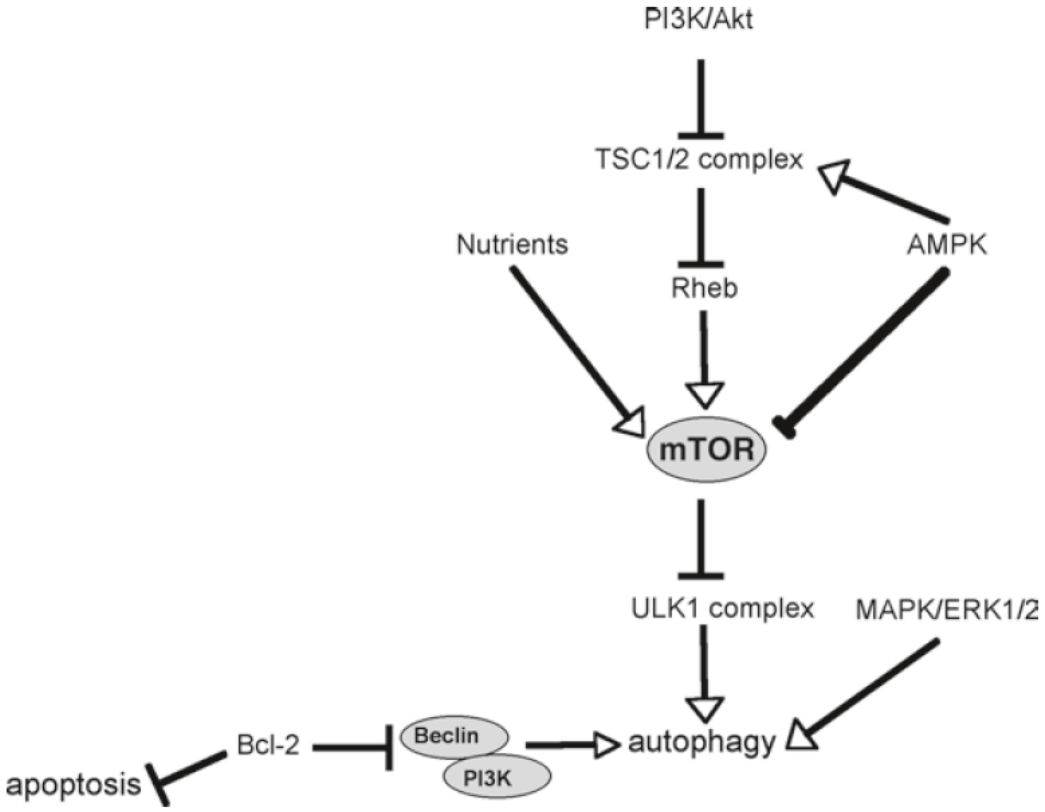

Figure A1. 2: Signal Regulation of Autophagy in Mammalian Cells. Autophagy is highly regulated by signaling networks, with mTOR as a common downstream target of many of the signal transduction regulators of autophagy. When mTOR is activated in conditions such as nutrient availability or Akt signaling, autophagy is inhibited. Activation of AMPK upon energy depletion causes inhibition of mTOR and stimulation of autophagy. ERK1/2 signaling and PI3K III/Beclin 1 complex formation induce autophagy. The anti-apoptotic protein Bcl-2 prevents the association of Beclin 1 and PI3K III. (Originally published in **Linsey Stiles**, Andrew Ferree, Orian Shirihai. (2011) Mitochondrial Dyanmics and Autophagy. Bingwei Lu (editor), Mitochondrial Dynamics and Neurodegeneration. Springer.)

In yeast there are two functionally distinct protein complexes for the protein target of rapamycin (TOR): TOR complex 1 and 2 (TORC1 and TORC2). TORC1 has the primary role in regulating autophagy in response to nutrient availability. The mammalian homology of TOR (mTOR) is a highly conserved serine/threonine protein kinase which acts as a key regulator of autophagy by sensing nutrient availability, growth factors, and

cellular energy. mTOR activation inhibits autophagy under conditions where nutrients are readily available and is a downstream signal of PI 3-kinase, insulin signaling, growth factor receptor signaling, and the Akt pathways (Young *et al.*, 2009). For instance, Akt signaling leads to phosphorylation and inhibition of the heterodimer Tsc1/Tsc2, which is a GTPase-activating protein (GAP) for the GTPase Ras homolog enriched in brain (Rheb). Rheb is required for mTOR activity, with the GDP-bound form inhibiting mTOR, while the GTP-bound form of Rheb stimulates mTOR. Akt inhibition of the Tsc1/Tsc2 complex activates mTOR signaling and thus has an inhibitory effect on autophagy. When mTOR is inhibited by stress conditions, such as hypoxia and starvation, autophagy is induced. Upstream signals of mTOR in this scenario include 5'adenosine-monophosphate activated protein kinase (AMPK), which is activated by depleted ATP levels. Activation of AMPK promotes the activity of the Tsc1/Tsc2 complex, which favors the GDP-bound form of Rheb, leading to inhibition of mTOR and induction of autophagy. In response to hypoxia, autophagy is induced in part by TOR inhibition and in part by hypoxia-inducing factor (HIF), which acts independently of mTOR. HIF induces autophagy by targeting BNIP3 and BNIP3L, which are members of the Bcl-2 family of cell death regulators (Mazure and Pouyssegur, 2009;Glick *et al.*, 2010). In both the neonatal and adult brain, hypoxia induces a rapid and extensive autophagic induction (Adhami *et al.*, 2006). It appears this response may not be entirely beneficial as mice lacking Atg7 are almost completely protected from ischemia-induced neurodegeneration. While much remains to be elucidated, this striking result suggests that modulation or temporary inhibition of neuronal autophagy may be a potential treatment strategy for ischemic stroke victims (Yue *et al.*, 2009). One important effector

of autophagy with connections to neurodegeneration is extracellular signal-regulated protein kinase 1/2 (ERK1/2). Brains from Parkinson's disease patients exhibit phosphorylated ERK2 granules that colocalize with autophagocytosed mitochondria (Zhu *et al.*, 2003). In a neuroblastoma model, expression of either constitutively active (CA) or wildtype ERK2 was sufficient to promote activation of autophagy with CA-ERK2 inducing mitophagy to a greater extent than wildtype (Dagda *et al.*, 2008).

Another protein family that plays a prominent role in regulating both autophagy and mitophagy is the Bcl-2 proteins. Inhibition of autophagy occurs via the antiapoptotic members such as Bcl-2, Bcl-X_L, and Bcl-w, while proapoptotic BH3-only proteins, such as BNIP3, Bad, Bix, and BimEL can induce autophagy. These proteins seem to play a more prominent role in regulating mitophagy.

A1.4 Mitophagy

Mitochondria are essential for a number of critical cellular processes. They are also the main source and target of reactive oxygen species (ROS); therefore, it is essential that the pool of mitochondria within a cell remain functional and energetically efficient. Mitochondrial autophagy, or mitophagy, refers to the selective removal of mitochondria by the autophagic machinery and is another method utilized for quality control by promoting turnover (autophagy of dysfunctional mitochondria in conjunction with biogenesis). Mitophagy serves to degrade mitochondria, effectively removing them from the dynamic network. Several questions remain regarding exactly how defective mitochondria are specifically targeted for degradation via autophagy. This section will overview mitophagy and what is known about whether and how mitochondrial are selectively targeted for autophagy.

It has been know since 1957 that mammalian mitochondria are degraded by autophagy with Clark's discovery that mitochondria are located in autophagosomes in the kidney of newborn mice. Since then mitophagy has been documented in a number of different tissues including brain, heart, liver, reticulocytes, and pancreatic β-cells. Mitophagy has been shown to be involved in cellular quality control, differentiation, and disease pathogenesis. Initially, it was thought that autophagy was a nonselective process, arbitrarily engulfing cytosolic components, but this notion is changing with evidence that specific, defective cargo is targeted for degradation. Certain proteins that are involved with targeting mitochondria for sequestration into autophagosomes have been discovered in yeast. While this process remains largely unclear in mammalian cells, potential tags are beginning to be identified, including mitochondrial depolarization and opening of the mitochondrial permeability transition pore (MPTP).

A1.4a Mitophagy in yeast

Takeshige et al. were the first to show in yeast that an induction of autophagy occurs when yeast are subjected to a stressful environment, such as starvation. This was also the first work to demonstrate that autophagy in yeast was similar to mammalian autophagy. They proposed a mechanism by which autophagy could remove cytosolic components, such as mitochondria, although they believed this to be an unselective process (Takeshige *et al.*, 1992;Goldman *et al.*, 2010).

Evidence for selective mitochondrial autophagy was first provided by Campbell and Thorsness using an experimental design that was able to distinguish mitochondria in an acidic compartment. This technique was used to demonstrate increased mitochondrial

degradation under conditions such as loss of mitochondrial membrane potential and mtDNA (Campbell and Thorsness, 1998). Their work provided a connection between mitochondrial damage and increased degradation, although did not provide direct evidence for mitochondrial quality control via autophagy. Early experimental evidence for this came from Kissova *et al*. when they demonstrated that knockout of the gene UTH1, which encodes for a yeast outer mitochondrial membrane protein, resulted in a loss of mitophagy, while other kinds of macroautophagy remained intact (Kissova *et al.*, 2004). In addition, autophagy deficient yeast display defects in mitochondrial biogenesis, decreased oxygen consumption and mitochondrial membrane potential, and increased ROS (Zhang *et al.*, 2007).This work highlights the role of mitophagy as a quality control mechanism that is required for maintenance of mitochondrial integrity. Further evidence for this role in quality control is provided by studies showing that mitochondrial dysfunction resulting from loss of specific proteins or pharmacologic treatments also increase mitophagy of damaged mitochondria. Removal of functionally damaged mitochondria helps maintain the mitochondrial network by keeping the systemenergetically efficient and removing both the major source and target of cellular ROS and, therefore, protects mtDNA.

Recently, a large amount of work has gone into identifying ‘mitophagy receptors’ in both yeast and mammalian systems. Since mitophagy is a subset of macroautophagy, it utilizes the basic core autophagic machinery common with autophagy described above. On the other hand, mitophagy does utilize some additional ATG genes that are required for other pathways. Atg11, Atg 20, and Atg24, which are proteins involved in the cytoplasmic to vacuole targeting (Cvt) pathway have been shown to be required for

mitochondrial autophagy (Nice *et al.*, 2002;Kanki and Klionsky, 2010). This may demonstrate that these proteins are a general requirement for selective autophagy. ATG32 and ATG33 were identified as mitophagy-related genes in yeast by using genomic screens for mutants defective in selective mitochondrial autophagy (Kanki *et al.*, 2009a;Kanki *et al.*, 2010). Atg32 is an outer mitochondrial membrane protein that has emerged as a mitochondrial receptor by interacting with Atg proteins that are essential for autophagosome formation. Atg32 binds to Atg11 during mitophagy and uses it as an adaptor protein to recruit mitochondria to the phagophore assembly site (Kanki *et al.*, 2009b;Okamoto *et al.*, 2009b). In addition, Atg32 has a binding motif (WXXI/L/V) for binding to Atg8/LC3 family members; this binding motif is also present in Atg19 and the mammalian protein p62 (Okamoto *et al.*, 2009a). Okamoto et al. showed through studies using mutations in the WXXI/L/V binding motif of Atg32 that the binding of Atg32 to Atg8 is required for sequestration of mitochondria by the phagophore. Atg33 is also localized to the outer mitochondrial membrane and may detect or present aged mitochondria for selective mitochondrial autophagy when cells have reached the stationary phase (Kanki *et al.*, 2010).

While Atg32 and Uth1 have been identified as the main proteins involved with regulating mitophagy in yeast; other proteins that play a role have been established. Nowikovsky et al. demonstrate that knockout of DMN1, the yeast homology of Drp1, was found to have an inhibitory effect on mitophagy in a strain (mdm38 conditional knockout) known to induce mitophagy. This study also demonstrated that osmotic swelling of mitochondria induces selective mitochondrial autophagy in yeast (Nowikovsky *et al.*, 2007). Another protein that was demonstrated to be required for mitophagy in yeast is Aup1p. This

mitochondrial intermembrane space protein is necessary for efficient targeted degradation of mitochondria via autophagy during the stationary phase of yeast (Tal *et al.*, 2007). Interestingly, mitochondrial membrane potential depolarization induced by the oxidative phosphorylation uncoupler, carbonyl cyanide m-chlorophenylhydrazone (CCCP), does not stimulate mitochondrial autophagy in yeast (Kissova *et al.*, 2004;Kanki *et al.*, 2009a), yet mitochondrial depolarization is a necessary, although not sufficient, requirement for mitophagy in mammals.

A1.4b Mitophagy in Mammalian Cells

Mitophagy has been shown to play a key physiological role in a number of different mammalian tissues. While no mammalian homologs of ATG32 and UTH1 genes have been identified, selective removal of mitochondria does occur in mammalian cells and is mediated by mitochondrial membrane potential as well as a number of required proteins. It was first demonstrated in hepatocytes that disturbances in mitochondrial membrane potential by mitochondrial permeability transition pore (MPTP) stimulates degradation of mitochondria via autophagy (Lemasters *et al.*, 1998;Elmore *et al.*, 2001). This work contributed to the knowledge that mitophagy functions to maintain cellular homeostasis by removing damaged mitochondria from healthy cells. It also acts as a mechanism to remove increased levels of ROS generated by dysfunctional mitochondria and keep cells energetically efficient (Goldman *et al.*, 2010).

Certain cell-type specific proteins that are required for mitochondrial targeting to the autophagosome have been identified. For instance, the protein Ulk1 has been shown to be necessary for autophagy during erythropoiesis. Reticulocyte maturation is an example of

a specialized system that demonstrates the role of autophagic degradation of mitochondria in cellular maintenance and physiology. During the final step of erythrocyte differentiation, mitophagy is utilized to remove reticulocyte mitochondria and other organelles to create a mature red blood cell. It has been shown that Unc51-like kinase (Ulk1) is not necessary for general autophagic activity outside of the reticulocyte, but is required to selectively remove ribosomes and mitochondria during red blood cell differentiation (Kundu *et al.*, 2008). This is in contrast with what was already reported about Ulk1 in previous sections. The discrepancy may be due to the fact that the work showing Ulk1 is a nonessential mechanistic component of mammalian autophagy was done in a Ulk1 conditional knockout where Ulk2 compensation is a possible confounding factor. Interestingly, in the Ulk1 knockout mice, not only are mitochondria not removed by autophagy during reticulocyte maturation but they also maintain their membrane potential (Zhang *et al.*, 2009). Nix is another protein that may be required for red blood cell mitophagy, which is upstream of Ulk1. It is located on the outer mitochondrial membrane and is a member of the Bcl-2 family of proteins, specifically the BH3-only proapoptotic subfamily. Nix deficient blood contains a large number of erythrocytes that retain their mitochondria, although in this system ribosomes are cleared, providing evidence that it is a mitophagy specific protein (Zhang and Ney, 2008). Nix is required for mobilization of autophagic machinery and mitochondrial depolarization following CCCP treatment (Ding *et al.*, 2010). The mechanism behind how Nix is involved in mitophagy is still controversial, but it may play a role in mitochondrial membrane potential destabilization, which is a trigger for mitophagy. Although, some studies have

reported that Nix has a membrane potential independent role in mitophagy. These findings suggest there are multiple pathways that lead to mitophagy in mammals. Nix, also known as Bnip3L, is not the only member of the Bcl-2 family of proteins that has been shown to play a role in mitophagy. Bnip3 is also a member of this family that is hypothesized to trigger autophagy by causing mitochondrial depolarization. Bnip3 has been shown to be activated following ischemia-reperfusion in cardiac myocytes, where it induces autophagy as a protective response to apoptotic signaling (Gottlieb and Carreira, 2010). It is important to note that both Nix and Bnip3 play a dual role in autophagy and apoptosis. Autophagy in this system can be both protective or associated with autophagic cell death depending on the conditions (Zhang and Ney, 2009). A number of mechanisms have been proposed for how Bnip3 induces autophagy including mitochondria permeability transition (MPT), mitochondrial depolarization, and/or inhibition of mitochondrial dynamics machinery.

A1.4c Mitophagy in Neurons

Under normal conditions a very small amount of autophagosomes can be detected in neurons by electron or light microscopy. However inhibition of autophagic clearance by pharmacologic or genetic tools results in a dramatic accumulation of autophagosomes, many of which contain mitochondria. These findings indicate that not only does mitophagy occur in neurons but also the normal flux from autophagosome formation to degradation is very rapid and efficient.

In fact, proper autophagic processing is absolutely crucial for neuronal survival. The dependence on autophagy for clearance of damaged macromolecules is less drastic in

dividing cells as cellular debris can be diluted in the daughter cells. This protective mechanism is not an option for long-lived post-mitotic cells. Thus neurons must have functional autophagic clearance mechanisms to avoid the accumulation of hazardous waste material such as damaged mitochondria and protein aggregates. It is not surprising therefore that strong evidence exists linking defects in autophagy with neurodegeneration.

To date the clearest evidence demonstrating a causal role of autophagic impairment leading to neuronal loss comes from transgenic animal models. Mice with neuronal-specific Atg5 or Atg7 deficiency display massive accumulation of polyubiquitinated protein aggregates and severe neurodegeneration (Hara *et al.*, 2006;Komatsu *et al.*, 2006). It is noteworthy that the neuronal loss and protein aggregates occur without additional stresses used to model neurodegeneration, such as exposure to neurotoxins or protein overexpression (Cuervo, 2006). Therefore the phenotypes of these mice emphasize the essential role of basal autophagy in maintaining quality control for neuronal maintenance.

The importance of autophagy in the human brain is underscored by autophagic abnormalities seen in several neurodegenerative diseases, including Alzheimer's disease (Nixon *et al.*, 2005;Nixon, 2006) frontotemporal dementia (Lee and Gao, 2008;Ju and Weihl, 2010) Parkinson's disease (Anglade *et al.*, 1997;Dehay *et al.*, 2010), and Dementia with Lewy Bodies (Zhu *et al.*, 2003). The autopsied brains from patients with these chronic diseases exhibit increased numbers of autophagic vesicles, protein aggregates, and dysfunctional mitochondria. In isolation the finding of increased

autophagosome number has different viable potential explanations. First, the observed vesicles could result from an increase in activation and thus increased formation of autophagosomes. Alternatively the increased autophagic vesicles could represent a loss of clearance capacity through the lysosome leading to an accumulation of autophagosomes. A third possibility is a combination of increased activation in the presence of impaired degradation. At the time of autopsy the latter possibility seems most likely, as patients tend to be at late stages of a chronic disease progression spanning years to decades.

It is likely to be the case in many age-related neurodegenerative diseases that impaired lysosomal degradation capacity leads to the accumulation of intracellular debris, such as damaged mitochondria and protein aggregates. This accumulation in turn signals the activation of autophagy and further increase in autophagosome number. While it is far from clear what comes first in this feed forward scenario, future therapeutics targeting enhancement of autophagic function should consider all stages of autophagosome maturation and seek to improve complete clearance of autophagosomal cargo.

A1.5 Mitochondrial Dynamics and Mitophagy

A1.5a The PINK1/Parkin Pathway in Mitophagy and Mitochondrial Dynamics

Recently, a large effort has been dedicated to understanding how the PINK1/parkin pathway contributes to the maintenance of cellular and mitochondrial homeostasis. There is evidence showing that this pathway is involved with the regulation of selective mitophagy of damaged mitochondria, as well as mitochondrial function and dynamics. Moreover, improper regulation of the PINK1/parkin pathway, mitophagy, and

mitochondrial fusion and fission have been implicated in disease pathology, specifically in Parkinson's disease (PD).

PTEN-induced kinase 1 (PINK1) is a Ser/Thr protein kinase with an N-terminal mitochondrial targeting signal, a putative transmembrane domain, and a C-terminal regulatory domain that governs kinase activity and substrate selectivity (Mills *et al.*, 2008;Chu, 2010). More than 50 mutations have been mapped throughout the kinase and C-terminal domain of PINK1, which have differing effects on the activity and stability of the protein (Dagda and Chu, 2009). Parkin is a cytosolic E3 ubiquitin ligase. Mutations in parkin have been identified with disease causing mutations often disrupting parkin ligase activity (Lee *et al.*, 2010). Loss-of-function mutations in PINK1 and parkin are the main cause of early-onset autosomal recessive forms of PD (Gasser, 2009), which supports a role for these proteins in neuroprotection and cellular quality control. Interestingly, mice that have PINK1 and parkin knocked out display a mild phenotype and do not have the dopaminergic (DA) neuron loss in the substantia nigra observed in humans (Whitworth and Pallanck, 2009). These single gene knockout mice display similar functional defects in the dopaminergic system, yet the morphology and numbers of DA neurons are normal (Goldberg *et al.*, 2003;Kitada *et al.*, 2007). PINK1 deficient mice display mitochondrial dysfunction prior to the onset of any neurodegeneration (Gispert *et al.*, 2009). A triple knockout of PINK1, parkin, and DJ-1 also display normal morphology and cell number in the substantia nigra and is insufficient to cause significant nigral degeneration in the mice (Kitada *et al.*, 2009). Again, as yet unknown, compensatory mechanisms may be held responsible.

Both PINK1 and parkin play a role in mitophagy, although the mechanism is still not fully understood. It is known that upon selective recruitment of cytosolic parkin to depolarized mitochondria, the dysfunctional units are eliminated via the autophagic machinery (Narendra *et al.*, 2010). PINK1 expression and function is required for this process (Geisler *et al.*, 2010;Vives-Bauza and Przedborski, 2010a;Vives-Bauza *et al.*, 2010b). Overexpression of wild-type PINK1 is sufficient to induce recruitment of parkin to mitochondria, even if mitochondrial membrane potential remains intact. In addition, mutations in either PINK1 or parkin inhibit parkin recruitment to mitochondria and subsequent mitophagy (Vives-Bauza *et al.*, 2010a). PINK1 or parkin mutations alone or PINK1/parkin double mutants display a similar phenotype, indicating that they operate in the same pathway. Interestingly, overexpression of parkin can compensate for loss of PINK1, while the reverse does not occur, suggesting that parkin acts downstream of PINK1 (Clark *et al.*, 2006;Whitworth *et al.*, 2009).

Loss of PINK1 leads to alterations in mitochondrial function and morphology in a number of mammalian systems. There seems to be a universal decrease in mitochondrial membrane potential and ATP synthesis in the systems where this has been studied (Exner *et al.*, 2007;Liu *et al.*, 2009a;Chu, 2010). The same phenotype is observed with expression of mutated forms of PINK1 (Grunewald *et al.*, 2009;Marongiu *et al.*, 2009). Loss of PINK1 also seems to increase ROS in mammalian cells. An increase in superoxide has been demonstrated in mouse cortical neurons, human dopaminergic neurons (Wood-Kaczmar *et al.*, 2008;Gandhi *et al.*, 2009), and human SH-SY5Y neuroblastoma cells (Dagda *et al.*, 2009), as well as a decrease in glutathione levels in some of these cell lines. There is also evidence for induction of mitophagy or

mitochondrial association with lysosomes in a number of these studies. Interestingly, there are also changes in mitochondrial morphology with loss of PINK1, in mammalian systems this generally correlates with an increase in fragmentation (Sandebring *et al.*, 2009). Unraveling the connection between autophagy, the PINK1/parkin pathway, and mitochondrial morphology is critical to further understanding the role mitochondrial quality control. Although, the mitochondrial morphology phenotype of PINK1/parkin deficiency remains controversial between studies in *Drosophila* and higher eukaryotes, one thing is clear: loss of PINK1/parkin does lead to alterations in mitochondrial morphology.

The PINK1/parkin pathway interacts with components of the mitochondrial dynamics machinery. Much of the work dissecting the connection between PINK1/parkin and mitochondrial fusion and fission machinery has been done in *Drosophila*. The expression of mitofusin is inversely correlated with the activity of PINK1 and parkin in *Drosophila*. On the other hand, loss of PINK1 or parkin does not change the steady-state expression of Drp1 or Opa1, or the subcellular distribution of Drp1 (Poole *et al.*, 2010). Ziviani et al. demonstrated that Mfn is ubiquitinated by Parkin when it is recruited to dysfunctional mitochondria (Ziviani *et al.*, 2010). They also show that loss of PINK1 or parkin leads to an increase in the expression of Mfn and an elongated mitochondrial morphology. Additionally, knockdown of Mfn or OPA1 or overexpression of Drp1, rescues the mitochondrial abnormalities in PINK1 or parkin mutants (Poole *et al.*, 2008;Park *et al.*, 2009). There is also evidence that the PINK1/parkin pathway negatively regulates Mfn and OPA1 function and positively regulates Drp1 (Deng *et al.*, 2008). Yang *et al.* propose that Fis1 acts between PINK1 and Drp1 promoting

mitochondrial fission (Yang *et al.*, 2008). All of this experimental evidence suggests that the Pink1/Parkin pathway regulates mitochondrial morphology by either promoting mitochondrial fission or inhibiting fusion in *Drosophila*. This fits with the hypothesized model that the higher the frequency of mitochondrial fission, the higher the probability that dysfunctional units will be segregated and eliminated, as will be discussed in the following sections. These data suggest a scheme where PINK1/parkin promote mitochondrial fission and elimination via mitophagy, therefore providing a connection between this pathway and both mitochondrial dynamics and autophagy.

Ubiquitination of Mfn2 by parkin is hypothesized to promote autophagy of damaged mitochondria. It is thought that the mechanism by which this occurs is that ubiquitination of the outer mitochondrial membrane acts as a recruitment signal for p62/SQSTM1, which is required for PINK1/Parkin-mediated mitophagy (Geisler *et al.*, 2010). Although, this could also be mediated by parkin-mediated poly-ubiquitination of the voltage-dependent anion channel 1 (VDAC1), which has been shown to be necessary for PINK1/parkin-directed mitophagy. Ziviani and Whitworth provide additional potential mechanisms for the role of Mfn2 ubiquitination in mitophagy that focus on the function of Mfn2 in mitochondrial fusion. For instance, poly-ubiquitinated Mfn may be degraded consequently inhibiting fusion, with the possibility that this mechanism is specific to damaged mitochondria. If Mfn is mono-ubiquitinated, it is unlikely that it will be degraded, but it could still provide a useful regulatory mechanism. An example of this is that ubiquitination may prevent dimerization and therefore tethering of Mfn and in this manner prevents mitochondrial fusion (Ziviani and Whitworth, 2010).

Interestingly, contradictory mitochondrial morphology findings have been reported in human SH-SY5Y neuroblastoma cells and other mammalian systems. Dagda *et al.* demonstrate that stable PINK1 knockdown in SH-SY5Y cells results in a fragmented mitochondrial morphology, increased oxidative stress, and an increase in mitophagy, which correlates with a 50% reduction in mitochondrial mass, which was assessed by western blotting for mitochondrial proteins (Dagda *et al.*, 2009). Conversely, overexpression of PINK1 lead to an increase in mitochondrial connectivity and an elongated morphology with some abnormally enlarged mitochondria, yet there was no autophagic response to these irregular mitochondria; in fact PINK1 overexpression inhibited 6-hydroxydopamine (6-ODHA)-induced mitophagy. Interestingly, dominant negative Drp1 expression rescued the morphology and autophagy effect in the PINK1 knockdown; leading to more elongated mitochondria and decreased mitophagy (Dagda *et al.*, 2009). This study also shows that autophagy machinery is necessary for mitochondrial fragmentation, which was demonstrated by utilizing siRNA targeting Atg7 and Atg8/LC3B. Knockdown of these proteins inhibited autophagy and reversed the mitochondrial fragmentation observed in PINK1 knockdown cells to levels similar to that in control cells.

Decreased PINK1 expression in SH-SY5Y cells causes reduced autophagic flux that corresponds with decreased ATP synthesis (Gegg *et al.*, 2010),which can be rescued by overexpression of parkin. Inducing mitochondrial dysfunction using the electron transport chain uncoupler, CCCP, demonstrated that PINK1 and parkin are required for mitophagy. Gegg *et al.* show that ubiquitination of Mfn1 and Mfn2 occurs within 3 hours of CCCP treatment and that this process may identify mitochondria for degradation via mitophagy.

The ubiquitination of these mitochondrial dynamics proteins is inhibited with knockdown of PINK1 or parkin expression, implicating that PINK1 and parkin are essential for mitophagy, specifically for removal of damaged mitochondria. These data point to interdependency between mitochondrial dynamics and autophagy, demonstrating that mitochondrial fusion/fission machinery is required for PINK1 mediated mitochondrial degradation and suggests that autophagy participates in mitochondrial remodeling. Loss of PINK1 or parkin in SH-SY5Y cells causes a fragmented mitochondrial morphology (Lutz *et al.*, 2009). Overexpression of Mfn2 and OPA1 or a dominant negative mutation of Drp1 (Drp1-DN) were able to rescue the effects loss of PINK1 or parkin had on mitochondrial morphology and function. Conversely, expression of parkin or PINK1 was able to suppress mitochondrial fragmentation induced by Drp1 expression. Furthermore, Drp1-DN expressing cells that were also knockdown for PINK1 or parkin did not display the expected fragmented mitochondrial morphology phenotype or a decrease in ATP. This implies that mitochondrial alterations in parkin- or PINK1-deficient cells are associated with an increase in mitochondrial fission and relies on mitochondrial dynamics proteins and machinery. In agreement with this research, expression of human mutant PINK1 in a rat dopaminergic cell line leads to fragmented mitochondria via an increased ratio of fission to fusion proteins thereby promoting mitochondrial fission. Mitochondrial division inhibitor (mdivi-1), a small molecule inhibitor of Drp1, rescued both the morphological and functional mitochondrial defects caused by the expression of mutant PINK1 (Cui *et al.*, 2010).

Lutz *et al.* suggest that possible explanations for the difference observed in *Drosophila* and mammalian cells could be the time points that analysis of PINK1/parkin deficiency occurred and/or that there could be fundamental differences in the regulation of mitochondrial fusion and fission and mitophagy in mammalian systems (Lutz *et al.*, 2009). Mitochondrial dynamics and mitophagy could also be regulated in a tissue-specific manner. Regardless of the controversial conclusions obtained when examining PINK1/parkin, it is clear that this pathway provides an interesting mechanism that may connect mitochondrial dynamics with mitophagy. The mechanism behind how loss of mitochondrial membrane potential triggers PINK1 signaling, PINK1 triggers parkin recruitment, and parkin is localized to mitochondria remain unknown at this time. Yet, what is known is that PINK1 and parkin affect mitochondrial morphology. It has also been demonstrated that mitochondrial depolarization is critical to the PINK1/parkin pathway and is necessary for mitophagy. The connection between mitochondrial fusion and fission, membrane potential, and mitophagy has been studied extensively in mammalian cells in the context of the lifecycle of a mitochondrion. Currently, interdependence between mitochondrial dynamics, function, and depolarization has been shown to influence selective degradation of damaged mitochondria through autophagy.

A1.5b The Lifecycle of a Mitochondrion

As previously discussed, mitochondria go through continuous cycles of fusion and fission, which is thought to play a role in mitochondrial complementation, allowing for mixing of matrix solutes and metabolites, mtDNA, and mitochondrial membrane components (these occur at different rates with membrane components having the slowest rate). This sharing of proteins and solutes between mitochondria through fusion

occurs as a first line of defense in an attempt to recover function in damaged mitochondria. This complementary rescue ensures that dysfunctional mitochondria do not become an energetic strain on the rest of the mitochondrial population. Mitochondrial turnover, which is a balance between mitochondrial degradation and biogenesis, is also required for a healthy mitochondrial network. This allows dysfunctional mitochondrial to be removed by mitophagy while maintaining the population and allowing propagation of the most apt mitochondria. The interplay between mitochondrial dynamics and mitophagy is a key determinant of mitochondrial homeostasis, which can be exemplified by the mitochondrial life cycle.

The life cycle of a mitochondrion has been studied by Twig et al. in INS-1 cells, a rat insulinoma cell line, where mitochondrial fission, selective fusion, and autophagy are thought to contribute to mitochondrial quality control, as shown schematically in Figure 3 (Twig *et al.*, 2008a;Mouli *et al.*, 2009). It involves cycles of fusion periods, each followed by fission. Following the fission event, mitochondria enter a solitary state and are available for subsequent fusion events. This solitary state is ~20-fold longer than the fused period and if a mitochondrion maintains a polarized membrane potential during this period, it can re-enter the mitochondrial web by means of a subsequent fusion event with another mitochondrion. On the other hand, if the daughter mitochondrion loses membrane potential and becomes depolarized, it will remain segregated and it can either be targeted for autophagy or it may repolarize and be recovered by the network. This suggests that mitochondrial fusion is selective for functional mitochondrial units.
It is reasonable to consider that fission may merely decrease mitochondrial size making it more accessible for degradation. Although upon further reflection the creation of two

dissimilar daughter units argues against this availability theory, given that size will be similar but it is function that becomes divergent. In addition, it has been shown that mitochondrial fusion depends on mitochondrial membrane potential and cannot occur in depolarized mitochondria regardless of size or the close proximity of other polarized, fusion-ready mitochondria (Twig and Shirihai, 2010). These metabolically dysfunctional, depolarized mitochondria cannot fuse with other mitochondria and are preferentially targeted for degradation by the autophagosome, although the exact mechanism behind this remains unclear. However, it suggests that fusion itself may be partially responsible by unevenly redistributing components between mitochondria, which with the successive fission event results in two functionally divergent mitochondria. This ability to reorganize mitochondrial components may allow the mitochondrial population to separate and remove damaged units at a faster rate making them less energetically wasteful.

The role of depolarization and how it prevents further fusion is in question when examining the life cycle of a mitochondrion. While all of the mitochondria that are targeted for autophagy are depolarized, the timeline of depolarization to engulfment provides further information regarding how autophagy is induced in these cells and whether depolarization is a cause or effect of autophagy. Twig *et al.* found that mitochondrial depolarization occurs at least one hour before engulfment, indicating that removal by autophagy is not the explanation for why depolarized mitochondria cannot re-fuse with the network. This time gap between depolarization and mitophagy demonstrates that mitochondrial fission is a principal route by which depolarized mitochondria are generated and fusion is selective for polarized units. It is important to

note that while mitochondrial depolarization is a necessary prerequisite for mitophagy, depolarization alone is not sufficient to cause mitochondrial autophagy.

With the knowledge that a mitochondrion spends a substantial amount of time as a non-fusing, segregated mitochondrion before it is degraded, the question is raised as to what the mechanistic explanation is for the observation that a depolarized mitochondrion cannot go through a subsequent fusion event. It was shown that the underlying mechanism for the membrane potential dependency of fusion is actually an impaired fusion capacity within these mitochondria. Indeed, co-staining mitochondria with mitochondrial matrix targeted photo-activatable green fluorescent protein (mtPA-GFP), to identify non-fusing mitochondria, and TMRE, a mitochondrial membrane potential dependent dye, or an anti-OPA1 antibody provided some mechanistic insight into the membrane potential and fusion state of these mitochondria. Twig *et al.* show that non-fusing mitochondria are depolarized and display an increase in proteolytic cleavage, or degradation, of the fusion protein, OPA1, with approximately 50% less OPA1 than in wild-type fusing mitochondria (Twig *et al.*, 2008a). Cleavage of OPA1 has been shown to be triggered by reduction in mitochondrial ATP and by mitochondrial depolarization (Griparic *et al.*, 2004;Duvezin-Caubet *et al.*, 2006;Song *et al.*, 2007). This implicates a targeted fusion deficiency as the explanation for a lack of mitochondrial fusion in depolarized mitochondria.

The interdependence of mitochondrial dynamics and mitophagy are also revealed by utilizing tools to either knockdown or overexpress mitochondrial dynamics proteins prior to studying autophagy (Table 1). Retinal ganglion cells (RGCs) from mice heterozygous

for a nonsense mutation in OPA1 display an increase in autophagosomes (White *et al.*, 2009). The authors suggest that this induction of autophagy is due to accumulation of abnormal mitochondria in the RGC layer. Induction of fusion by overexpression of OPA1 using adenovirus in INS1 cells resulted in a decrease in mitophagy by 64%. This was not due to increased mitochondrial size, but to an increase in fusion capacity. Mitochondrial fission is also essential for mitophagy. Stimulation of fission decreases mitochondrial mass in HeLa cells (Frieden *et al.*, 2004;Gomes and Scorrano, 2008) and INS1 cells (Park *et al.*, 2008), consistent with the concept of an increase in mitophagy. This reduction in autophagy is mitophagy specific because other forms of autophagy, such as ER autophagy (reticulophagy) remain intact, indicated by no alterations in the levels of ER mass. Overexpression of Fis1 causes cells to accumulate fragmented mitochondria and autophagosomes, with the observation that there is selective autophagy of damaged mitochondria. Using Fis1 mutants, it was demonstrated that induction of punctate mitochondria and autophagic vesicles correlated with mitochondrial dysfunction not fragmentation, indicating that it is function not morphology that determines whether a cell will trigger mitophagy (Gomes *et al.*, 2008). Promoting fission by overexpression of Drp1 stimulates mitochondrial elimination under pro-apoptotic stimuli (Arnoult *et al.*, 2005b). Furthermore, inhibiting fission using either Fis1 RNAi or Drp1-DN results in a reduction in mitochondrial-specific autophagy (Barsoum *et al.*, 2006;Twig *et al.*, 2008a;Gottlieb *et al.*, 2010). Moreover, pharmacological inhibition of autophagy affects mitochondrial dynamics and metabolic function. Treatment of rat myoblasts with 3MA to inhibit autophagy leads to a decrease in mitochondrial membrane potential, inhibition of mitochondrial fusion (attributed to by a decrease in OPA1), and

accumulation of 'giant' mitochondria (Navratil *et al.*, 2008). These works imply that both fusion and fission play a critical role in mitochondrial turnover and quality control by influencing mitophagy.

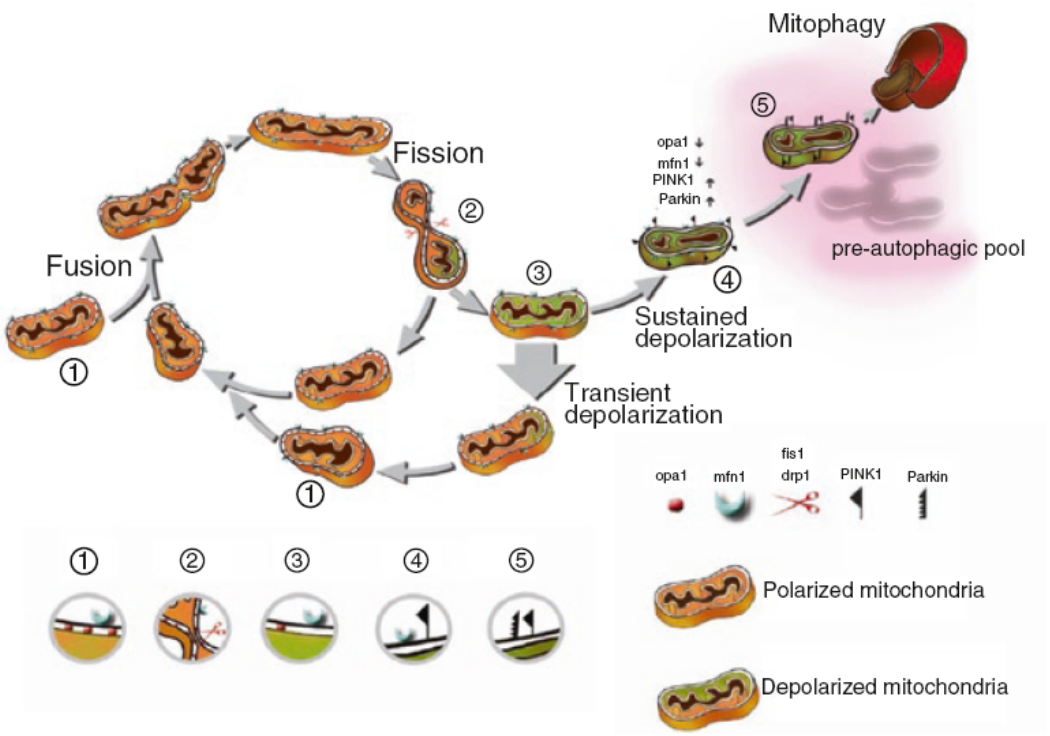

Figure 3: The lifecycle of a mitochondrion; the role of fission, fusion, and autophagy in the segregation of dysfunction mitochondria. The mitochondrion shifts between a networked postfusion state (*1*) and a solitary post-fission state (*2*). Following a fission event, the daughter mitochondrion may either maintain membrane potential (*red mitochondrion*), or depolarize (*green mitochondrion*). If depolarization occurs, the mitochondrion is unlikely to undergo further fusion events for the entire depolarization interval (*3*). If mitochondrial depolarization is transient and membrane potential is restored, fusion capacity is also restored. However, if mitochondrial membrane potential depolarization is sustained (*4*), reduction in OPA1 levels and increases in PINK1 activity and parkin translocation follows and elimination by autophagy occurs (*5*) (Figure courtesy of (Twig *et al.*, 2010)). (Originally published in **Linsey Stiles**, Andrew Ferree, Orian Shirihai. (2011) Mitochondrial Dyanmics and Autophagy. Bingwei Lu (editor), Mitochondrial Dynamics and Neurodegeneration. Springer.)

Table 1: The Effect of Manipulations in Mitochondrial Protein Expression on Mitochondrial Morphology and Mitophagy

Manipulation	Cell type	Effect on Morphology	Effect on mitophagy	Reference
Fis1 RNAi	INS1 β-cells	Elongation	Reduction in autophagosomes containing mitochondria by 70%	(Twig *et al.*, 2008a)
Fis1 Overexpression	HeLa cells INS1 β -cells	Fragmentation	Enhanced autophagosome formation by 50% Reduce total mitochondrial volume by 50%	(Frieden *et al.*, 2004;Gomes *et al.*, 2008;Park *et al.*, 2008)
Drp1K38A (dominant negative Drp1)	INS1 β -cells	Fragmented, swollen mitochondria	Reduction in autophagosomes containing mitochondria by 75%	(Twig *et al.*, 2008a)
Drp1 RNAi	HeLa cells	Tubular, elongated mitochondria	Decrease in mitophagy (qualitative)	(Parone *et al.*, 2008)
Drp1 Overexpression	HeLa cells	Fragmenation	Decrease in mitochondrial mass by 70%	(Arnoult *et al.*, 2005b)
Opa1 Overexpression	INS1 β -cells	Reduction in mitochondrial size with intact fusion ability	Reduction in autophagosomes containing mitochondria by 63%	(Twig *et al.*, 2008a)
Opa1 heterozygous mutated mice	Retinal Ganglion cells	Increased percentage of opaque mitochondria	An increase in general autophagy	(White *et al.*, 2009)
Mfn1 Overexpression	INS1 β -cells	Mitochondrial aggregation	Decrease in mitochondrial volume by 40%	(Park *et al.*, 2008)
Mfn1 Loss-of function (Overexpression of Mfn1 DN)	INS1 β -cells	Fragmentation	Unchanged mitochondrial mass	(Park *et al.*, 2008)
Mfn2 Knockout	MEFs	Fragmentation and perinuclear	Inhibition of autophagy	(Hailey *et al.*, 2010)

		clustering		
PINK1 Knockdown	Human neuronal SH-SY5Y cells	Fragmentation	Increased autophagic sequestration of depolarized mitochondria Decreased in mitochondrial volume by 50%	(Dagda *et al.*, 2009)
PINK1 Overexpression	Human neuronal SH-SY5Y cells	Increased interconnectivity and elongation Abnormally enlarged mitochondria	Autophagic vacuole number remained low	(Dagda *et al.*, 2009)
DJ-1 Knockdown	M17 human dopaminergic cell line	Fragmentation	Increased general autophagy	(Thomas *et al.*, 2010)

A1.5c Lessons from Simulation Experiments

Further support for the potential role of mitochondrial dynamics in mitochondrial quality control comes from simulation experiments from Mouli *et al.* They measured parameters of fusion and fission that may influence maintenance of mitochondrial function. By using a programmed simulation based on experimental findings they were able to investigate the effects of fusion, fission and autophagy over an extended time period in a large population of mitochondria (Mouli *et al.*, 2009). A model was developed where there is an optimal frequency of fusion and fission events that maintains mitochondrial function, such as respiration, even with a persistent damaging algorithm that should compromise mitochondrial function by inactivating mitochondrial components. In this model, where the extent of fusion and fission contribute to mitochondrial activity, it was determined that autophagy alone was the process by which damaged, "low-activity"

mitochondria were removed, working to preserve function, even when this process is nonselective. Indeed, even in the absence of repair mechanisms, mitochondrial dynamics and autophagy may be adequate to restore mitochondrial function, given that fusion allows for redistribution of damaged components that can be removed quickly and preferentially by mitophagy.

When mitochondrial activity under selective fusion is considered, especially with high levels of damage, there is a considerable affect on mitochondrial function. Selectivity allows for removal of damaged units by promoting increased fusion frequency of functional mitochondrial. This is accomplished without compromising autophagy of damaged mitochondria. This gives selective fusion a two-fold purpose in maintaining mitochondrial function, first as a means of intramitochondrial complementation and second as a way to segregate damaged mitochondria prior to autophagy (Nakada *et al.*, 2001;Mouli *et al.*, 2009). It also suggests that along with the key element of selective fusion, it is the rate of fission (not just the balance between fusion and fission) that determines the efficacy of quality control mechanisms (fusion, fission, and autophagy). A higher frequency of fission results in an increased probability of dysfunctional mitochondria being isolated and eliminated by mitophagy. This work further explores the interconnected nature of fusion, fission, and autophagy and how the occurrence and frequency of these processes maintains mitochondrial function.

A1.5d Mitochondrial Motility and Dynamics

Mitochondrial movement regulates mitochondrial morphology by controlling the spatial distribution of mitochondria. Mitochondrial fusion requires and in some cases can

promote (i.e. transient fusion) mitochondrial motility. Approximately 90% of all fusion events involve moving mitochondria, yet the number of moving and stationary mitochondria in the whole mitochondrial population is similar in rat heart-derived H9c2 cells, demonstrating that mitochondrial motility facilitates fusion (Twig *et al.*, 2010). The extent of mitochondrial fusion depends on the location of mitochondria along microtubules, whether they are located on the same or separate microtubules, and the direction in which they are moving (Liu *et al.*, 2009c). Mitochondria move along microtubules via kinesin motors with the assistance of the Miro/Milton complex. Miro1 and Miro2 are atypical RhoGTPases located on the outer mitochondrial membrane that allow for the kinesin-1 motor to interact with mitochondria. Milton is an adaptor protein, which connects Miro and kinesin to facilitate mitochondrial motility and trafficking. Miro has two Ca^{2+}–binding EF-hands, which controls calcium-sensitivity (Chen and Chan, 2009). Mitochondria are immobilized by high calcium concentrations, which is thought to assist in calcium buffering by mitochondria and localized ATP production, specifically in neurons, which have high energy demands for neurotransmitter release (Liu and Hajnoczky, 2009b;Stephenson, 2010).

The connection between mitochondrial motility and mitophagy has not yet been determined, although it has been demonstrated that PINK1 interacts with the Miro/Milton complex (Weihofen *et al.*, 2009). The interdependence of mitochondrial motility and morphology is beginning to be elucidated. Mfn1 and Mfn2 have been shown to interact with the Miro/Milton complex (Misko *et al.*, 2010). In addition, Mfn2 is necessary for axonal transport of mitochondria in dorsal root ganglia neuronal cultures, which is independent of its role in mitochondrial fusion. Loss of OPA1 has no effect on motility

indicating that loss of inner membrane fusion is not required for mitochondrial axonal transport along the microtubule. Overexpression of Miro and Milton causes mitochondrial elongation, clustering and aggregation and inhibits the mitochondrial fragmentation caused by loss of PINK1 (Glater *et al.*, 2006;Saotome *et al.*, 2008;Weihofen *et al.*, 2009). Loss of Miro function leads to suppression of mitochondrial motility and Drp1 mediated mitochondrial fragmentation (Fransson *et al.*, 2006;Saotome *et al.*, 2008;Liu *et al.*, 2009b). These data provide evidence that mitochondrial motility and dynamics occur in a common pathway and suggest that motility may also influence mitophagy. Figure 4 overviews the role of PINK1 in mitochondrial motility, morphology, and autophagy, presenting the possibility that PINK1 may play a role in mitochondrial quality control (Whitworth *et al.*, 2009).

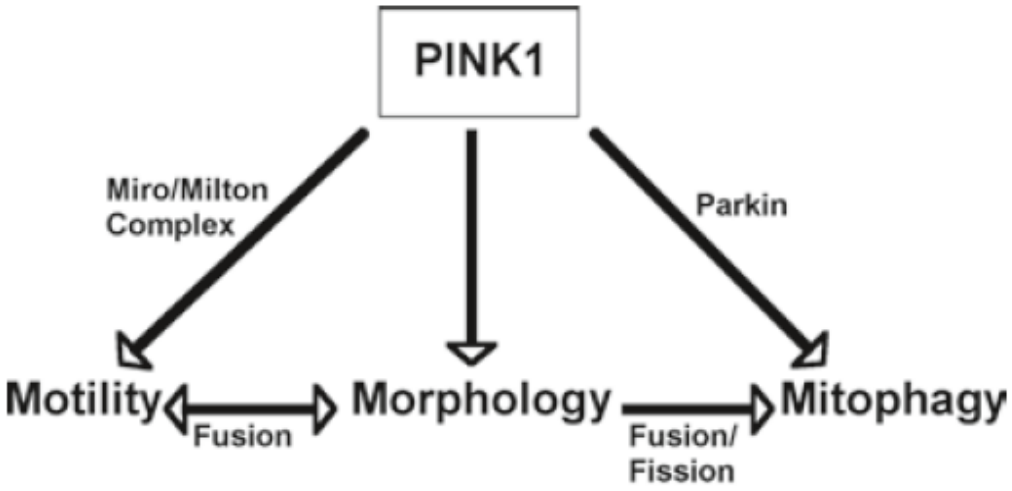

Figure 4: The role of PINK1 in mitochondrial motility, morphology, and mitophagy. PINK1 has been shown to interact with the mitochondrial motility complex Miro/Milton, yet the exact role PINK1 plays in this complex has yet to be determined. However, it is hypothesized that PINK1 may pay a role in mitochondrial trafficking. A connection between mitochondrial motility and morphology exists, where fusion requires and can promote motility. It has been well established that changes in PINK1 expression affects mitochondrial morphology; in mammalian cells PINK1 promotes fusion and an elongated mitochondrial morphology. PINK1 also promotes mitophagy upon parkin recruitment to

the mitochondria. A relationship between mitochondrial dynamics and mitophagy exists where fission followed by selective fusion allows for segregation of dysfunctional mitochondria that can be targeted for mitophagy. Mitochondrial motility, morphology, and autophagy are thought to exert mitochondrial quality control, which determines mitochondrial function. Thus, as PINK1 has been shown to regulate all these processes, it is a solid candidate as a master regulator of mitochondrial quality control. (Originally published in **Linsey Stiles**, Andrew Ferree, Orian Shirihai. (2011) Mitochondrial Dyanmics and Autophagy. Bingwei Lu (editor), Mitochondrial Dynamics and Neurodegeneration. Springer.)

A1.5e Mitochondrial Motility, Dynamics, and Mitophagy as a Quality Control Axis

Mitochondrial motility along microtubules is required for mitochondrial fusion (Liu *et al.*, 2009c). The observation that mitochondrial fusion is a membrane potential-dependent process guarantees that dysfunctional organelles will avoid fusion, while intact mitochondria will benefit from complementation. Segregation of dysfunctional mitochondria from the fusing population results in the generation of small, depolarized mitochondria that can be targeted for degradation by mitophagy. This sets up a possible hierarchy of mitochondrial quality control mechanisms with mitochondrial movement at the top, followed by fusion, which utilizes a complementary "rescue" mechanism, followed by fission which provides dissimilar daughter cells and ending with mitophagy as the recipient of the depolarized units. Importantly, the idea of this quality control axis advocates that it is not just the balance between fusion and fission that can contribute to maintenance of the mitochondrial population, but also the absolute rate of events. Specifically, it is thought that the higher the fission frequency, the higher the probability that dysfunctional units will be segregated and eliminated (Twig *et al.*, 2008b).

A1.6 When Quality Control Breaks Down: Implications in Aging and Neurodegeneration

Mitochondrial quality control is critical for maintenance of a healthy mitochondrial population. Both mitochondrial dynamics and selective mitochondrial autophagy are thought to play a key role in maintaining mitochondrial function and promoting turnover. Therefore, it is not surprising that these processes have been implicated in a number of diseases.

A1.6a Role of Mitochondrial Dynamics and Mitophagy in Aging

Mitochondria have been proposed to play a prominent role in the aging process, namely dysfunctional mitochondrial quality control leads to an accumulation of damaged mitochondria, which could lead to further cellular impairment. 'Giant' or swollen mitochondria are often observed in aged cells. These mitochondria are enlarged with accumulated mtDNA and oxidized proteins, which are indicative of a lack of mitochondrial turnover (Yen and Klionsky, 2008). This implicates mitochondrial fusion and fission, as well as mitophagy, as mechanisms of aging. Indeed, mitochondrial dynamics, selective mitochondrial autophagy, ROS, and mtDNA maintenance are all hypothesized to play a role in the aging process (Weber and Reichert, 2010). There are a number of other aging theories that have been proposed and even additional mitochondrial-related pathways that are thought to be involved with this process, such as caloric restriction, the insulin signaling pathway/insulin sensitivity, and sirtuins, but these do not strictly fit into the scope of mitochondrial dynamics and autophagy and are beyond the scope of this chapter.

Oxidative stress is an interesting starting point when examining the role mitochondria play in the aging process. Mitochondria are both the main source and, due to their close proximity and less efficient DNA proofreading enzymes, target of ROS. The 'free radical theory of aging' proposed by Harman in the 1950's is based on the fact that ROS induce mitochondrial dysfunction and mitochondrial dysfunction generates more ROS, leading to a vicious cycle of mitochondrial damage (HARMAN, 1956). It is important to note that not all ROS is deleterious, it also acts as a physiological cellular signal. For instance, at low levels ROS can be a signal to stimulate ROS scavenging pathways, mitochondrial biogenesis, and MPTP, which may lead to mitophagy. As ROS levels and oxidative damage increase, instead of promoting survival of mitochondria may instead trigger release of factors that initiate apoptosis.

Increased ROS levels may also elevate mitochondrial DNA mutations. Mitochondria have increased incidences for DNA mutation compared to genomic DNA due to a number of reasons including being in close proximity to higher levels of ROS and decreased repair mechanisms. Increased accumulation of mtDNA mutations has also been proposed as an aging mechanism and is a cause for heterogeneity in the mitochondrial population. Accumulation of mutated mtDNA is an indication that mitochondrial quality control mechanisms are dysfunctional. It has been hypothesized that certain mtDNA mutations that decrease mitochondrial respiration and therefore ROS production (a seemingly beneficial result in circumstances of mitochondrial damage and high ROS production) may also decrease mitophagy (Lemasters, 2005). This provides another mechanism by which impaired mitochondrial dynamics and mitophagy is implicated in the aging process.

Mitophagy is known to be upregulated in response to dysfunctional mitochondria and has been proposed to slow the aging process. Specifically, it has been shown that there is an age-related decline in lysosomal systems. Accumulation of damaged mitochondria due to impaired removal/degradation of these organelles is thought to result in decreased cell viability. Therefore, functional selective autophagy of damaged mitochondria is crucial for the preservation of a healthy mitochondrial population and maintenance of cellular integrity. All of the aging pathways described thus far have a common feature in that they converge together to lead to mitochondrial damage and impaired quality control. Mitochondrial dynamics may also play a role in the aging process. Yeast deficient in Dmn1 (homolog of Drp1) have an increased lifespan. It has been demonstrated in *P. anserine* that mitochondrial fragmentation occurs progressively with age, which was reversed by Dnm1 knockout (Scheckhuber *et al.*, 2007), although this does not occur in mammalian systems where Drp1 knockout is embryonically lethal. Although, this does not rule out the possibility that a small shift in the balance of mitochondrial dynamics could be beneficial to the cellular environment. Additionally, changes in mitochondrial morphology are observed in disease states that are concurrent with aging. It is often difficult to determine whether changes to mitochondrial dynamics are the cause or an effect of pathology, likely it is probably not that simple with a more cyclical mechanism expected. We do know, however, that effective mitochondrial dynamics, including complementation and selective fusion, influence mitophagy and are key determinants of quality control, which helps to maintain a healthy mitochondrial and therefore cellular population.

A1.6b Mitochondrial-Lysosomal Axis Theory of Aging

While essential, the task of degrading mitochondria via autophagy is no easy task. With lipid-rich membranes and several iron containing enzyme complexes, mitochondria represent a challenging substrate for the lysosome. Moreover damaged mitochondria are a serious hazard through their capacity to produce large quantities of ROS. This delicate and dangerous dynamic is especially relevant for neurons and has been elegantly described in the mitochondrial-lysosomal axis theory of aging proposed by Terman and Brunk. In their theory, high levels of intralysosomal iron combined with hydrogen peroxide leads to peroxidation of cargo in autophagosomes and lysosomes. This oxidative modification renders the cargo resistant to degradation by lysosomal hydrolytic enzymes. A non-degradable polymer of cross-linked protein and lipid residues, known as lipofuscin or ceroid, accumulates in the lysosomes and decreases autophagic clearance. Impaired mitophagy, in turn exacerbates the situation by allowing more time for reactive oxidative species to escape from damaged mitochondria. Under extreme oxidative stress, damage to the membrane of the lysosome leads to subsequent permeabilization and the pro-apoptotic leakage of lysosomal enzymes into the cytoplasm.

Mechanisms of aging and neurodegeneration in humans are inherently difficult to prove yet there is a rapidly growing body of evidence in support of the mitochondrial-lysosomal axis theory. Examples specific to neurodegeneration come from studies of autopsied brains of patients with Alzheimer's disease and Parkinson's disease. Several researchers have documented evidence of aberrant mitophagy in AD (Moreira *et al.*, 2007b;Chen *et al.*, 2009;Santos *et al.*, 2010) including increased quantities of mitochondrial lipoic acid associated with lipofuscin (Moreira *et al.*, 2007a;Moreira *et al.*, 2007b). Nixon and

collaborators have documented numerous lysosomal-related abnormalities in sporadic AD suggestive of impaired clearance, including a striking accumulation of autophagosomes and autophagolysosomes within degenerating neurites. Further mechanistic support for their interpretations come from studies of presenilin-1, the most common cause of early-onset familial Alzhemiers disease. Tissues from patients and transgenic animals with presenilin-1 mutations display several lines of evidence indicating impaired autophagic clearance. In relation to PD, Dehay *et al.* report lysosomal depletion following administration of the neurotoxin MPTP which targets mitochondrial complex I (Dehay *et al.*, 2010;Vila *et al.*, 2010). The loss of lysosomes was preceded by a permeabilization of lysosomal membranes due to oxidative damage resulting from increased mitophagy. Supporting their data in toxin models, Dehay *et al.*, also found evidence of lysosomal breakdown and autophagosome accumulation in brain tissue from PD patients. Enhancement of autophagic-lysosomal function through genetic and pharmacologic modifications was protective against the toxicity of MPTP and, most importantly, attenuated the PD-related dopaminergic neurodegeneration. These studies illustrate the lysosomal hazards of mitophagy and point to the great potential for treatments of neurodegenerative conditions through modulation of the mitochondrial-lysosomal axis.

A1.6c Mitochondrial dynamics, Mitophagy, and Neurodegeneration

All of the factors that have been implicated in aging also play a role in neurodegeneration. It is, therefore, not surprising that neurodegeneration is often a late-onset, age-associated disease. It has even been suggested that aging is a 'benign' form of neurodegeneration. Excessive and unbalanced mitochondrial dynamics have been shown

to have deleterious effects in a variety of tissues and cell types including, but not limited to, pancreatic β-cells, skeletal and cardiac myocytes, and neurons. Mitochondrial dynamics and mitophagy are required for quality control in neurons, and it has been shown that both are essential for normal neuronal function and disruptions in these processes can lead to disease states. In particular, dysfunctional mitophagy has been implicated and extensively studied in the pathogenesis of Parkinson's disease, although it has also been associated with Alzheimer's disease, amyotrophic lateral sclerosis (ALS), and Huntington's disease.

Parkinson's disease is the most common neurodegenerative movement disorder and mutations in PINK1 and PARKIN genes are the most frequent cause of familial Parkinson's disease. PD is characterized by degeneration of dopaminergic neurons in the substantia nigra and often by the formation of protein aggregates called Lewy bodies. The primary symptom of PD is a progressive dysfunction in movement, including impairment in motor skills and speech. Interestingly, chemical compounds that inhibit complex I of the electron transport chain (ETC), such as rotenone or MPTP (1-methyl-4-phenyl-1,2,3,6-tetrahydropyridine), also cause PD-like symptoms in humans and rodents. Mitochondrial dysfunction has been observed in both human PD and murine animal models of the disease. Deletions and mutations in mtDNA have been found in these models as well as increased oxidative stress. A decrease in mitochondrial respiratory complexes is present in PD models and patients (including sporadic PD patients), specifically a deficiency in complex I expression and activity has been observed. An accumulation of α-synuclein, the major component of Lewy bodies, in mitochondria of dopaminergic neurons may be responsible, at least in part, for the ETC complex

deficiency and also increased ROS production. PINK1 deficient mice and *Drosophila* display age-related decreases in complex I activity and mitochondrial depolarization. Of the thirteen ETC subunits encoded for by mtDNA, eight encode for complex I, again implying that mutations or deletions in mtDNA in PD may be responsible for the loss of complex I activity.

There is experimental evidence that mitochondrial fusion and fission are altered in animal models of PD. Neurotoxin exposure (such as MPTP) leads to mitochondrial fragmentation and swelling along with increased levels of ROS, mitochondrial dysfunction, and mitophagy. There is also data showing morphological changes in various tissues from PD patients. In brain biopsies from PD patients, heterogeneity in mitochondrial size was observed, as well as mitochondrial swelling. Increased ERK1/2 phosphorylation localized to mitochondria in autophagomes has also been observed in brains of PD patients, which is indicative of an induction of mitophagy and/or impaired clearance of autophagosomes (Zhu *et al.*, 2003;Dagda *et al.*, 2008). Studies of cytoplasmic hybrid (cybrid) cell lines, which contain mtDNA from PD subjects, have shown alterations in mitochondrial respiration and dramatic restructuring of mitochondrial architecture (Esteves *et al.*, 2010), including mitochondrial swelling, changes to cristae structure and the outer mitochondrial membrane.

Autophagy and mitophagy dysfunction in PD have been a focus of research in this field. It has been reported that in human PD both increased autophagy and mitophagy are present (Zhu and Chu, 2010). Activation of the autophagic response is observed in peripheral blood mononuclear cells (PBMCs) from PD patients, which is hypothesized to

be a protective mechanism against abnormal protein accumulation and help prevent or slow α-synuclein aggregation (Prigione *et al.*, 2010). This finding from peripheral tissue may also represent an impairment of flux, with increased signaling for activation of autophagy concurrent with decreased clearance of autophagosomes. Dementia with Lewy Bodies (DLB) patients display elevated levels of neuronal mTor and reduced Atg7 expression, although this was not observed in brains of PD patients (Crews *et al.*, 2010). The DLB patients also showed increased expression of lysosomal markers in neurons, with the presence of enlarged lysosomes and abundant, abnormal autophagosomes. In addition, alterations in autophagy and/or mitophagy have been reported in other models of PD, such as MPTP and PINK1 or parkin deficiency. A loss in the ability of neurons to clear damaged mitochondria or proteins may be a main mechanism in the pathogenesis of PD.

It is evident that PD is associated with impairment in the ability of mitochondria to regulate repair, recovery, and/or recycling of damaged units. Yet these changes to mitochondrial function do not reveal whether the alterations in mitochondrial function and the quality control axis are a cause or consequence of PD. Although, familial PD caused by mutations in PINK1 and parkin suggests that mitochondrial quality control plays a mechanistic role in the early pathogenesis of PD. Additionally, alterations in mitochondrial fusion and fission proteins are known to be associated with human neurodegenerative disorders. Mitochondrial dysfunction has been implicated in a number of diseases and determining the mechanisms by which these pathways impact disease progression may provide pharmaceutical targets for treatment.

A1.6d The A9-Dopaminergic Neuron: A Mitochondrial Perfect Storm

Selective vulnerability is a common characteristic of many neurodegenerative diseases such as Parkinson's disease, Alzheimer's disease, Huntington's disease and amyotrophic lateral sclerosis. These diseases are marked by a patterned pathology in specific neuronal sub-populations that likely provides a clue to the disease mechanism. Of all the cells in the body, neurons are among the most sensitive to interruptions in mitochondria dynamics, motility, and autophagy. This vulnerability results from extreme energy demands and complex, polarized cell structures, exemplified by neurons that degenerate in forms of parkinsonism, the A9-subtype dopaminergic neurons of the substantia nigra pars compacta (A9-DA). The A9-DA neurons have multiple physical and physiological characteristics that likely render them highly susceptible to loss of function in the mitochondrial network (Figure 5).

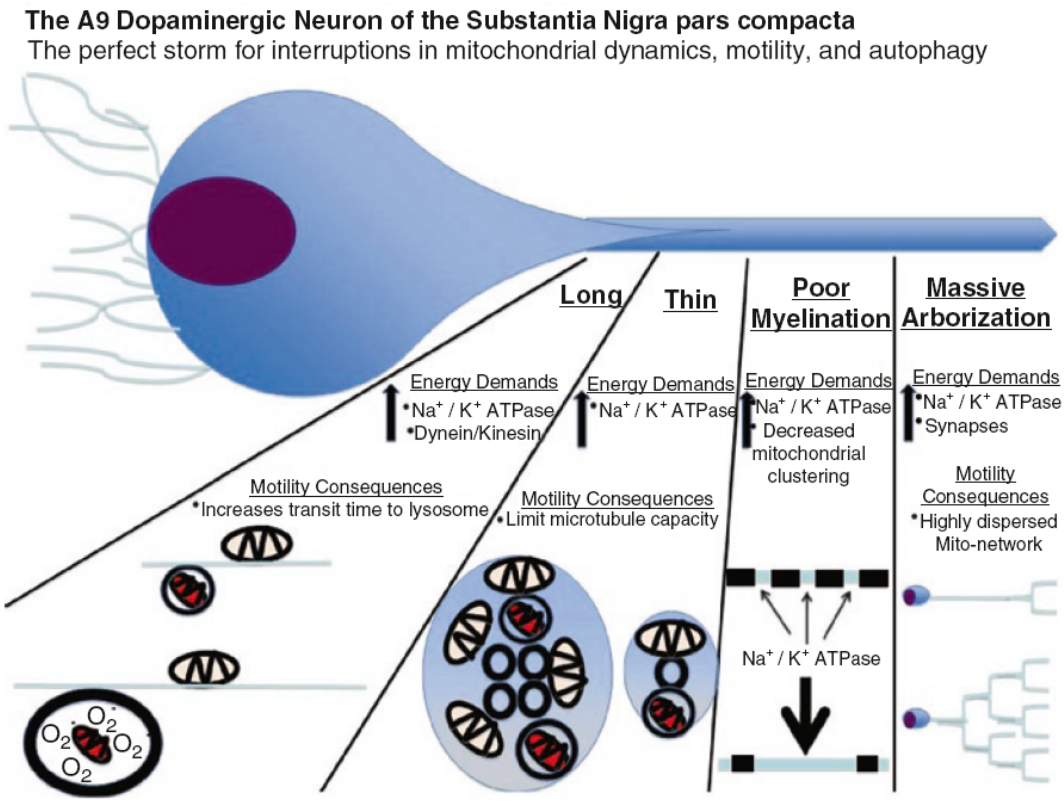

Figure 5: The A9-dopaminergic neuron has axonal characteristics that simultaneously increase metabolic demand while impeding mitochondrial dynamics, transport, and mitophagy. Long axons have higher energy demands to accommodate transport machinery and longer autophagosomal transit times from synapse to soma. Thin caliber axons have higher metabolic demands from increased Na+ / K + ATPase activity and reduced transport capacity. Lack of nodes of Ranvier also elevates Na+ / K + ATPase activity and necessitates a more distributed source of energy, thus denying the benefits of nodal mitochondrial clustering seen in well-myelinated axons. Massive axonal branching requires a highly dispersed mitochondrial network and increases metabolic demands at energy-intensive synapses. (Originally published in **Linsey Stiles**, Andrew Ferree, Orian Shirihai. (2011) Mitochondrial Dyanmics and Autophagy. Bingwei Lu (editor), Mitochondrial Dynamics and Neurodegeneration. Springer.)

Nigral A9-DA neurons are examples of extreme physical polarization with somata accounting for less than 1% of cell volume due to massive axonal and dendritic branching (Sulzer, 2007). These projection neurons have long, thin, poorly-myelinated axons that terminate in the striatum (Braak *et al.*, 2004;Matsuda *et al.*, 2009). Each of these morphological aspects increases metabolic requirements and risk of oxidative stress. Long axons raises ATP demand and travel time needed for transporting cargo back and forth from soma to synapse. Longer transport times for damaged mitochondria autophagocytosed at synapses increases risk and extent of oxidative damage *en route* to lysosomes located in the soma (Yue, 2007;Terman *et al.*, 2010). Like lanes on a highway, thin axons have reduced transport capacity. This spatial limitation impairs motility for both mitochondria and autophagosomes, and also has the potential to lengthen transport time for mitophagic vesicles. Increased surface to volume ratios cause thin caliber axons to have elevated Na^+/K^+ ATPase activity, this in turn increases energy demands and has been shown to directly impair mitochondrial motility by inhibiting transport by miro (Zhang *et al.*, 2010). Myelination has a more obvious impact on energy demands, as unmyelinated axons have a less efficient action potential conduction mechanism. Moreover, well-myelinated axons benefit by concentrating their

mitochondria at nodes of Ranvier the unmyelinated gaps at the sites of highest Na^+/K^+ ATPase activity. The thin, poorly-myelinated axons of A9-DA neurons require high Na^+/K^+ ATPase activity throughout the length of the axon and thus are likely denied the benefits of mitochondrial clustering. Each A9-DA neuron is estimated to have as many as ~370,000 synapses in their axonal field (Arbuthnott and Wickens, 2007;Surmeier *et al.*, 2010). Synapses are inherently energy demanding and sites of voltage-gated calcium influx and thus are packed with mitochondria. The tremendous axonal branching of the A9-DA neuron establishes a logistical challenge for its mitochondrial network in terms of dynamics and transport. Synapses are also points of vulnerability and considered the earliest sites of pathology in many forms of neurodegeneration, underscoring the need for effective autophagic clearance.

In addition to the extreme energy demands resulting from physical characteristics, unique physiological characteristics of A9-DA neurons places strain on the mitochondrial and lysosomal networks. Surmeier and colleagues have convincingly implicated L-type calcium channels that drive spontaneous activity in A9-DA neurons as key components of their selective vulnerability (Surmeier *et al.*, 2010). Without protective binding proteins such as calbindin, A9-DA neurons rely heavily on mitochondria to constantly supply energy for calcium pumps and to buffer high levels of cytosolic calcium directly. In addition to stress on the mitochondrial network by calcium overloading, high cytosolic calcium limits mitochondrial transport by binding to Miro and causing detachment from microtubules (Saotome *et al.*, 2008;Macaskill *et al.*, 2009;Wang and Schwarz, 2009). Another crucial protective role for mitochondria in A9-DA neurons results from the oxidizing properties of dopamine. The outer mitochondrial membrane contains

monoamine oxidase (MAO), which is an enzyme essential for defending the A9-DA neurons from toxicity associated with non-vesicular cytosolic dopamine. This protection comes with a tradeoff as increased MAO activity inhibits mitochondrial respiration (Gluck and Zeevalk, 2004). Finally, as a consequence of high levels of ROS from mitochondria and dopamine itself, the cell bodies of A9-DA neurons contain lysosomes with high levels of lipofuscin and neuromelanin that likely reduce degradation capacity (Figure 6). Collectively, the morphological and physiological characteristics of the A9-DA neuron represent a perfect storm for heightened sensitivity to disruptions in mitochondrial dynamics, motility, and mitophagy.

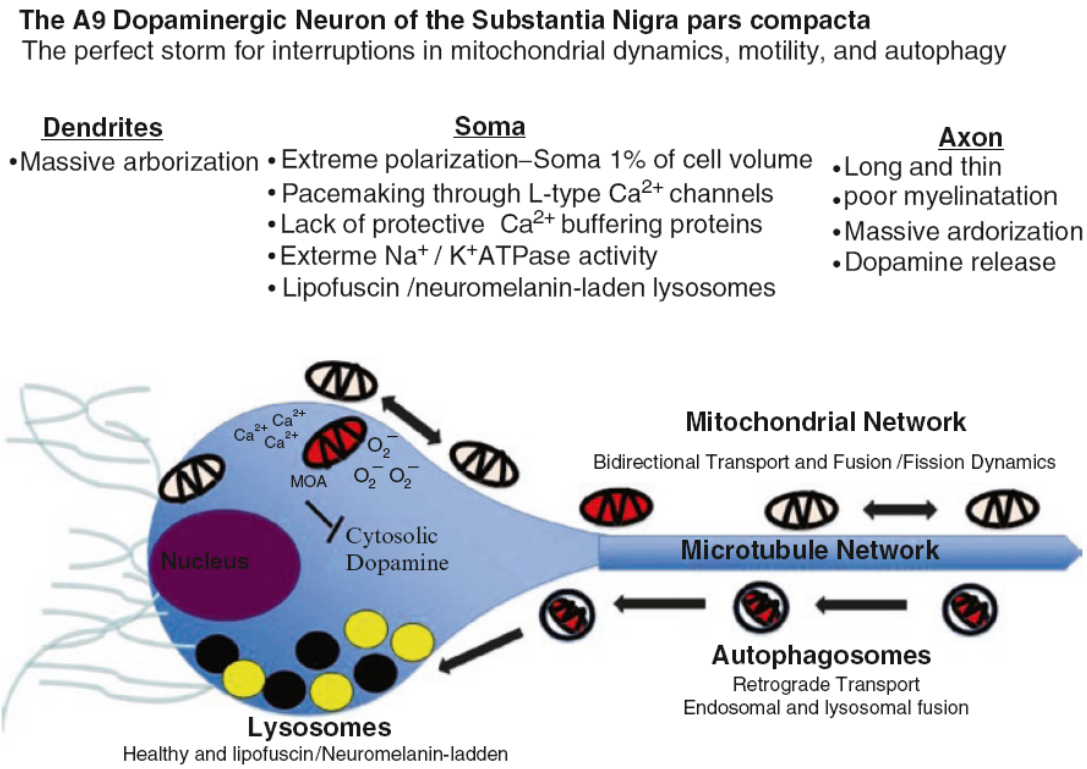

Figure 6: Morphological and physiological characteristics of the dentrites, soma, and axon of the A9-dopaminergic neuron increase susceptibility to dysfunction in mitochondrial dynamics, motility, and mitophagy. The mitochondrial network is highly dispersed over an exceptionally polarized cell structure yet must accommodate extremely high Na+ / K + ATPase activity. Mitochondria also serve as a protective barrier against toxicities associated with cytosolic dopamine and calcium. Finally,

lysosomes laden with lipofuscin and neuromelanin indicate compromised lysosomal capacity for autophagosome clearance. (Originally published in **Linsey Stiles**, Andrew Ferree, Orian Shirihai. (2011) Mitochondrial Dyanmics and Autophagy. Bingwei Lu (editor), Mitochondrial Dynamics and Neurodegeneration. Springer.)

Appendix 2: Mitochondrial Fusion and Fusion Proteins Represent Important Points of Regulation for Mitophagy

Authors: Linsey Stiles, Anthony Molina, and Orian Shirihai

A2.1 Mitochondrial Dynamics and Autophagy

Mitochondria play a critical role in a number of cellular functions including oxidative phosphorylation, Ca^{2+} buffering and signaling, and apoptosis. Mitochondria are also a main source and target of reactive oxygen species (ROS). This is driven by the generation of ROS by the electron transport chain (ETC), which is in close proximity to mtDNA and can consequently cause damage to mtDNA and proteins. Since mtDNA encodes for subunits of ETC complexes, mutations or deletions in mtDNA can hinder ETC function and as a result cause additional ROS production, generating a vicious cycle of ROS production and damage (Thompson, 2006). Therefore, the mitochondrial population must remain healthy and functional in order to maintain proper function. Mitochondrial quality control involves both mitochondrial biogenesis and turnover (Gottlieb *et al.*, 2010). It is required to remove damaged mitochondria from the network and hence maintains the mitochondrial population.

Macroautophagy, herein referred to as autophagy, is a process by which proteins, marcomolecules, and organelles, such as mitochondria, are degraded and recycled. Autophagy is a multi-step process that is initiated by the formation of the phagophore. Elongation and closure of the phagophore forms the autophagosome (AP). These double membrane structures engulf the cargo that will be degraded. Maturation of the autophagosome occurs upon fusion with a lysosome, generating the autophagolysosome. Acidic hydrolases degrade the cargo, the products of which can be transported out of the

autophagolysosome through permeases for recycling (Yang *et al.*, 2010b). Autophagy can be induced under conditions such as starvation and oxidative stress originating from the mitochondria.

Selective degradation of mitochondria through autophagy, termed mitophagy, is a critical component of mitochondrial quality control (Gottlieb *et al.*, 2010). It has been known since 1957 that mitochondria are degraded by autophagy (CLARK, Jr., 1957). Originally, it was thought that this was a nonselective process, but recently evidence has emerged indicating that it is, in fact, dysfunctional mitochondria that are targeted for degradation. Specific proteins that are involved with targeting mitochondria for sequestration into APs have been discovered in yeast. This process remains largely undetermined in mammalian cells; nonetheless, characteristics that target mitochondria for mitophagy have been identified, including mitochondrial depolarization (Twig *et al.*, 2008a;Youle and Narendra, 2011)

Twig *et al.* demonstrated that mitochondrial dynamics is playing a key role in producing mitochondria that are then targeted to autophagy. Mitochondria undergo continuous cycles of fusion and fission, which have been termed mitochondrial dynamics. A number of proteins have been identified that contribute to the control of mitochondrial fusion and fission. Fusion is regulated by mitofusin 1 and 2 (Mfn1/Mfn2) on the outer mitochondrial membrane and OPA1 on the inner mitochondrial membrane. On the other hand, Fis1, Mff and Drp1 regulate mitochondrial fission. Prior to a fission event, Drp1 is recruited from the cytosol to Fis1 and Mff sites on the outer mitochondrial membrane; scission of the mitochondrial membrane occurs at the sites where Drp1 is localized. The

aim of this review is to examine the interdependence of mitochondrial dynamics and mitophagy with a particular focus on how mitochondrial fusion and fusion protein contribute to mitochondrial quality control.

A2.2 Mitochondrial Quality Control

We demonstrated that mitochondrial fusion and fission are paired events and generally occur as a fusion event quickly followed by a fission event (Figure1). Statistical analysis of the timing of the events concluded that mitochondrial fusion triggers fission events, while fission events have no influence on the timing of subsequent fusion. A fission event generates two daughter mitochondria, one that is hyperpolarized and one that is depolarized in respect to the mother mitochondria. Ensuing fusion events are selective based on mitochondrial membrane potential, with a decreased probability that depolarized mitochondria will re-fuse with the network. The depolarized mitochondrion then has two options: it can either repolarize and subsequently fuse back with the network or it can be target for degradation. This demonstrated that mitochondrial fusion is selective for functional mitochondria (Twig *et al.*, 2008a).

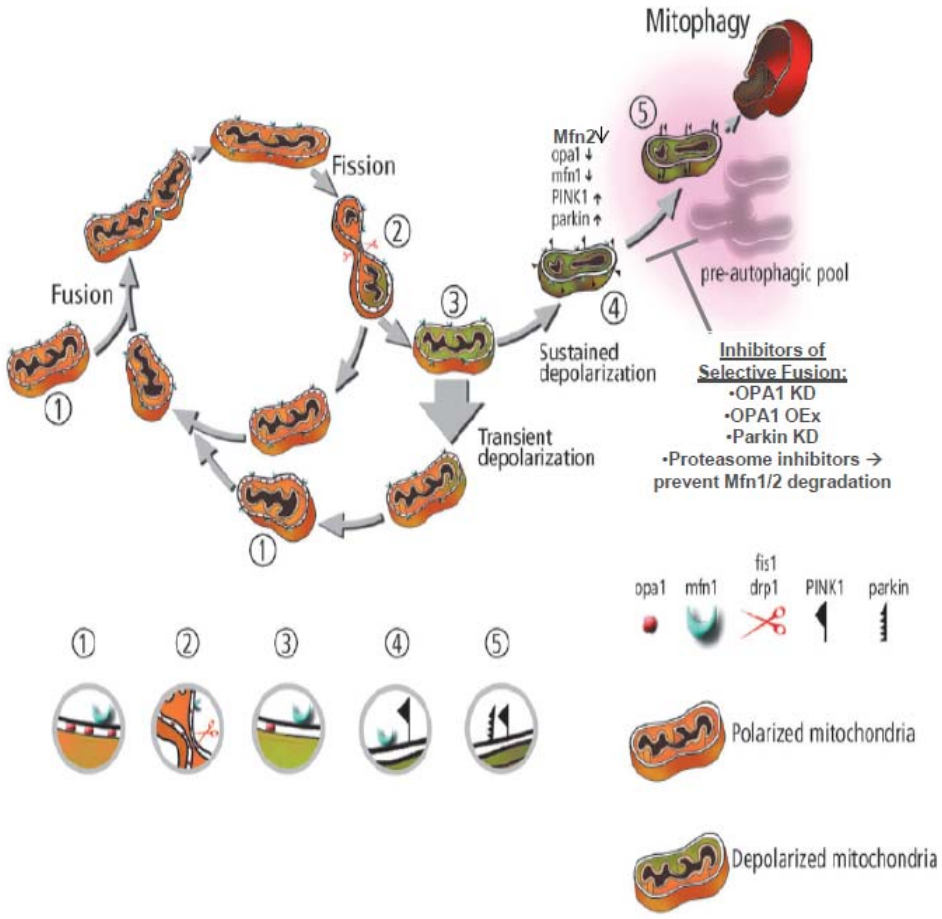

Figure A.1 Mitochondrial quality control with points of regulation by selective inhibitors of mitochondrial fusion.

Mitochondria that are targeted for degradation have to be segregated from the functional mitochondrial network. This occurs through fission and selective fusion, both of which are required to maintain a healthy population. Selectivity goes well beyond membrane potential as demonstrated by the finding that close proximity of two mitochondria do not increase the likelihood of a fusion event, suggesting that individual, intrinsic properties of mitochondria dictate whether they will fuse (Twig *et al.*, 2010). Indeed, both occurrence of prior fusion history and mitochondrial motility facilitate fusion events, while mitochondrial length is does not. The molecular mechanism behind the selectivity has

been studied to some extent and includes the degradation of the fusion proteins OPA1, Mfn1 and Mfn2 (Twig *et al.*, 2008a).

The importance of mitochondrial fusion and fission in mitophagy is highlighted by the fact that alterations in mitochondrial dynamics proteins have been shown to lead to changes in mitophagy, as overviewed in table 1 (Twig and Shirihai, 2011). Mitochondrial fission produces the fusion-deficient, depolarized mitochondria that are targeted for autophagy. Preventing mitochondrial fragmentation by either inhibiting fission directly or indirectly, by increasing fusion, results in decreased mitophagy. This was done by employing Fis1 RNAi or Drp1 dominant negative (Drp1-DN) to inhibit fission or OPA1 overexpression to promote mitochondrial fusion. Increased mitochondrial fission achieved by overexpressing Fis1 in HeLa cells or MEFs leads to mitochondrial fragmentation and increased LC3 puncta indicative of autophagy. Gomes *et al* used different mutations in Fis1 to investigate whether fragmentation or dysfunction leads to the increase in mitophagy found in these cells (Gomes *et al.*, 2008). They found that the induction of autophagy by overexpression of Fis1 correlated with mitochondrial dysfunction, characterized by swollen mitochondria, and was not due to mitochondrial fragmentation (Yu *et al.*, 2005;Alirol *et al.*, 2006). This data provides further evidence that mitophagy is a selective process targeting damaged mitochondria and that it is the dysfunction not necessarily the fragmentation that is critical for this process.

A2.3 Selectivity of Mitochondrial Fusion is Necessary for Mitophagy

The conclusion that mitochondrial fission serves as a generator of segregated dysfunctional mitochondria generated much attention has left selective mitochondrial fusion regarded as a mere byproduct of this event. The notion that mitochondrial fission directly contributes to mitophagy is beginning to change with studies showing that fission alone is not sufficient to induce mitophagy, mitochondrial dysfunction must also be present. Interestingly, we find that knockdown of OPA1 result in an increase in basal mitochondrial subcellular heterogeneity as shown in Figure 2.

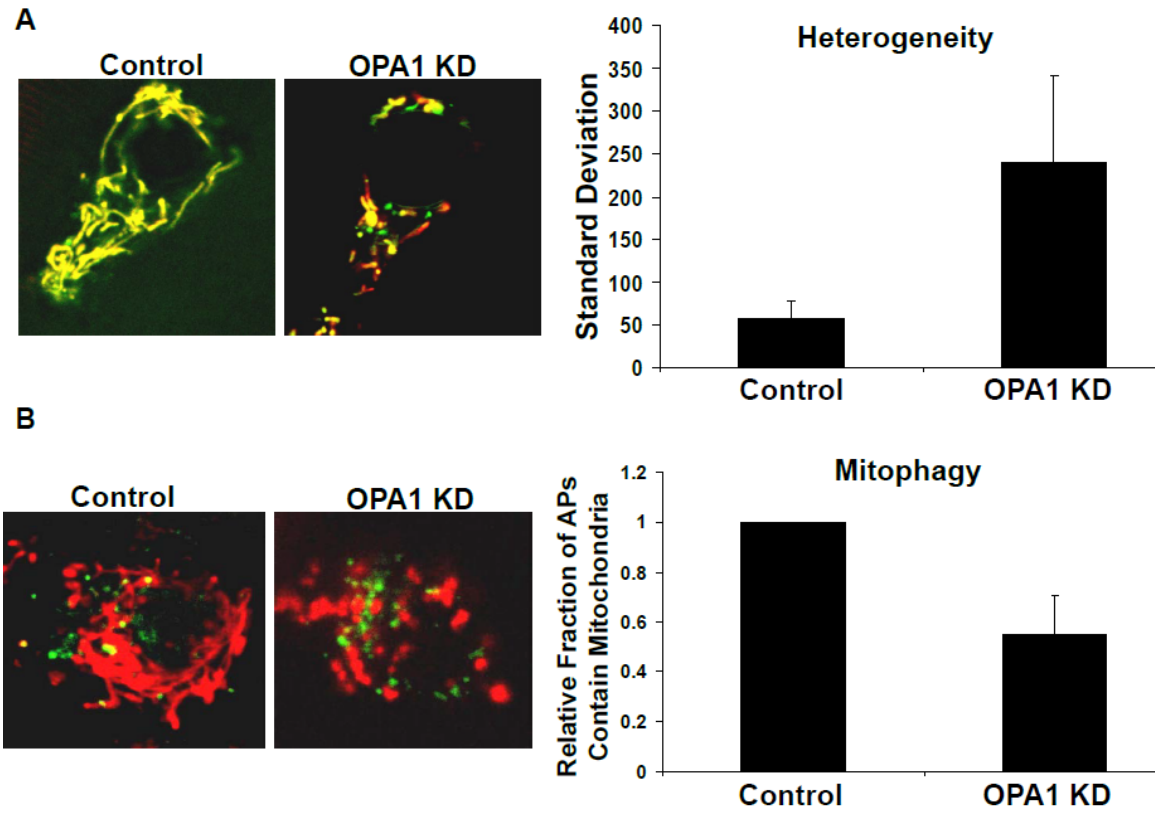

Figure A.2 OPA1 knockdown in INS1 cells results in increased heterogeneity and decreased mitophagy. A. Mitochondrial heterogeneity was measure in OPA1KD and control INS1 stained with TMRE and MTG. There is a significant increase in heterogeneity in OPA1KD cells. B. Mitophagy measued in OPA1KD and control INS1 cells. OPA1KD cells were found to have decreased mitophagy compared with control cells.

INS1 cells knockdown for OPA1 display increased subcellular heterogeneity of mitochondrial membrane potential (Figure2a). INS1 cells were stained with TMRE, a $\Delta\psi_m$–dependent dye, and mitotracker green (MTG), a $\Delta\psi_m$–independent dye. Control cells infected with PA-GFP that was not photo-converted display mainly yellow mitochondria (indicative of colocalization of TMRE and MTG), indicating that the majority of the mitochondrial population is able to maintain membrane potential. On the other hand, the OPA1 KD cells have a large increase in heterogeneity, with many completely depolarized mitochondria present that are not degraded, and these cells also display a fragmented mitochondrial morphology in comparison to the control INS1 cells. This is surprising as one would expect that autophagy will be recruited to remove dysfunctional mitochondria. Moreover, in the absence of OPA1 mitochondria are fragmented and thus expected to be more available for removal by autophagy. In addition, we have shown that over expression of OPA1 inhibits mitophagy, suggesting that degradation of OPA1 in depolarized mitochondria facilitate their targeting for autophagy.

This demonstrates that while depolarized mitochondria with decreased OPA1 expression seem to be necessary for removal of damaged mitochondria, it is not sufficient for this process to occur, at least not in INS1 cells. In support of this, we find that OPA1 KD INS1 cells also have decreased mitochondrial autophagy assessed by the AP marker, LC3-GFP puncta, co-localized with mitochondrial-targeted DsRed. We find that there is a decrease in the fraction of APs containing mitochondria (figure 2b). Therefore, knockdown of OPA1 paradoxically leads to an increase in the preautophagic

mitochondrial pool and a decrease in mitophagy; the question then is what is causing this to occur?

Two situations seem plausible: one, that there is a problem with the ability of dysfunctional mitochondria to be recognized and become targeted for autophagy and two, the autophagic machinery itself could be compromised. Analysis of the total APs, measured as LC3-GFP puncta, that do not contain mitochondria indicated that there was no difference in total autophagy only in mitophagy. While more research needs to be completed to confirm this, it suggests that it is not a problem with the autophagic machinery that inhibits mitophagy in OPA1 KD cells, but instead a defect in the targeting of dysfunctional mitochondria to APs.

Decreased mitophagy in OPA1 KD INS1 cells yet again demonstrates the important of selective mitochondrial fusion during the lifecycle of a mitochondrion and for proper quality control over the entire network. Mitochondrial fusion may be required due to its role as an inter-complementation mechanism that allows for mixing of mtDNA, metabolites, and solutes. Interestingly, even though fusion allows for mixing between mitochondria, membranous components and mtDNA do not necessarily equilibrate (Arimura *et al.*, 2004;Barsoum *et al.*, 2006). Provided that fusion and fission events are paired, complementation through fusion followed by a fission event that leads to the segregation of dysfunction, depolarized mitochondrial units could explain why fusion is such a critical component of the mitophagy process (Twig *et al.*, 2008b). This could be especially important in OPA1 knockdown cells since OPA1 is the only identified inner-membrane mitochondrial fusion protein in mammalian cells. Without the ability of

OPA1 to allow for inner membrane fusion and therefore complementation, there may also be a decrease in the ability to remove purely dysfunctional units that possess the proper signals for mitophagy from the rest of the population. This would lead to increased subcellular heterogeneity and decreased mitophagy.

One has to consider the possibility that OPA1 degradation in a selected area of the mitochondrion occurs prior to fission and marks the generation of a section which will develop into the dysfunctional daughter destined for autophagy.. If dysfunction components are separated from the rest of the population, this could explain mitochondria with decreased membrane potential or increased protein oxidation being targeted for degradation. It has been shown by Guillery et al. that OPA1 processing is mediated by membrane potential and that depolarization induced rapid processing of the long forms of OPA1 (L-OPA1) to the short isoform (S-OPA) and that these modifications are irreversible (Guillery *et al.*, 2008). However, Twig et al. have shown that depolarization does not seem to occur until after the fission event, making this second possibility less likely (Twig *et al.*, 2008a). This suggests that OPA1 degradation occurs after fission and depolarization.

A2.4 Possible Roles for OPA1 in the Signaling for Mitophagy

Mitochondrial fusion plays an essential role in the early stages of starvation-induced autophagy, contributing to the maintenance of mitochondrial and cellular viability. Gomes et al. demonstrated that mitochondria elongate when autophagy is induced by knockdown of mTOR or by starvation, with highly interconnected mitochondria observed as early as 1 hour after nutrient deprivation (Gomes and Scorrano, 2011;Gomes *et al.*,

2011). This elongation was shown to be dependent on DRP1 phosphorylation, therefore shifting the dynamic balance towards fusion, and had beneficial bioenergetics and survival effects. Elongated mitochondria maintain ATP levels and increase cristae surface area during starvation and they are not degraded. It was shown that cells that were depleted of Mfn2 could still elongate while OPA1 knockout cells could not form interconnected networks in response to starvation. Cells that do not undergo elongation in response to starvation, such as OPA -/- MEFs, did not show an increase in cristae formation and displayed decreased oligomerization of the ATPase (Gomes *et al.*, 2011).

There are 8 different isoforms of OPA1 and it has been shown that the long form of OPA1 L-OPA1) can undergo proteolytic cleavage by mitochondrial proteases (such as PARL, paraplegin, mAAA, and OMA1) under a number of conditions including cristae remodeling and apoptosis (Cipolat *et al.*, 2006;Duvezin-Caubet *et al.*, 2007;Ehses *et al.*, 2009). Proteolytic cleavage of OPA1 has also been shown to be relevant for mitophagy. Two hours of treatment with the chemical uncoupler CCCP to induce mitochondrial depolarization, leads to proteolytic cleavage of OPA1, as well as downregulation of Mfn2, and induction of mitophagy (Tanaka *et al.*, 2010). This OPA1 cleavage occurs more rapidly than Mfn2 degradation, suggesting that changes in OPA1 occur upstream of downregulation of Mfn2. How proteolytic processing and the different isoforms of OPA1 contribute to mitochondrial function, in particular mitophagy, should be further investigated. Given that OPA1 cleavage participates in cristae and matrix remodeling, it should also influence mitochondrial bioenergetics and function, which are known to be regulated by ultrastructure of the mitochondrion (Benard *et al.*, 2008;Zick *et al.*, 2009), making it plausible that it would indeed contribute to the ability to segregate

dysfunctional units and potentially the recognition of mitochondrial that need to be degraded by APs.

There is evidence that OPA1 can be released to the cytosol together with cytochrome c prior to the onset of apoptosis (Arnoult *et al.*, 2005a;Arnoult *et al.*, 2005b). Arnoult et al. suggest that this initial leak of OPA1 from the mitochondria leads to structural changes in the cristae and therefore release of the proteins that are sequestered within the cristae folds. If this was to occur on a smaller scale incapable of signaling for apoptosis, it could be possible that OPA1 release into the cytosol is a signaling mechanism for mitochondrial autophagy. Proteolytic cleavage of OPA1 could lead to soluble forms of OPA1 to be released and act as either a direct initiation signal for mitophagy or act as a way for autophagosomes to recognize mitochondria for degradation.

Gomes *et al.* found increased mitophagy in OPA1-/- MEF cells under starvation, while we show here decreased mitophagy in OPA1 knockdown INS1 cells under basal conditions. This opens up a couple of possibilities: first, OPA1 and mitochondrial fusion could be playing a different role depending on the cell type. Another possibility is that OPA1 is playing different roles at basal conditions compared to autophagy induced conditions. The induction of autophagy could be differentially regulated under varying stimuli and conditions (Kim *et al.*, 2007), for instance an environment where there is an overabundance of nutrients compared with starvation. For example, INS1 cells exposed to glucolipotoxicity (GLT) display mitochondrial fragmentation through decreased fusion capacity, mitochondrial dysfunction, and increases subscellular heterogeneity (Molina *et al.*, 2009;Wikstrom *et al.*, 2009). In this situation one would expect an increase in

mitophagy, but it was found that there is a decrease in mitophagy (Guy Las, in review of re-submission). This suggests that mitochondrial fusion capacity is a requirement for proper mitochondrial quality control.

Thus, it is possible that OPA1 may have a unique role in houskeeping mitophagy but not in starvation induced mitophagy. The targeting of mitochondria to autophagy in the absence of starvation was further studied in yeast where Atg32 identified as mitochondrial protein that recruits Atg11, an adaptor protein for autophagy, nevertheless no mammalian homolog of Atg32 has yet to be identified (Kanki *et al.*, 2009b;Okamoto *et al.*, 2009b). OPA1 processing alone or in conjunction with other proteins could present an interesting candidate. It has already been shown to change in response to mitochondrial dysfunction prior to mitophagy and additionally it is known to move from being shielded inside the mitochondria to being released into the cytosol under comparable conditions to those that are known to trigger mitophagy (Duvezin-Caubet *et al.*, 2006).

A2.5 A Role for Mfn2 and the PINK1/parkin Pathway in Mitophagy

It has been proposed that the outer mitochondrial membrane fusion protein, Mfn2, may also be involved in mitophagy through degradation and interaction with the PINK1/parkin pathway (Matsuda and Tanaka, 2010). Tanaka et al have shown that depolarization induced by CCCP first causes OPA1 processing to a fusion-inactive form, followed by parkin translocation to the mitochondrion, and finally Mfn1 and Mfn2 degradation mediated by the proteasome and p97. This demonstrates that alterations in both inner and outer membrane fusion proteins occur prior to mitophagy leading to a

complete disruption in fusion capacity in these depolarized mitochondria and inability to rejoin the mitochondrial network (Tanaka *et al.*, 2010). PINK1 and parkin have been shown to be critical to the induction of autophagy in a number of different systems and there is growing evidence that these proteins also influence mitochondrial dynamics.

PTEN-induced putative kinase 1 (PINK1) is a mitochondrial serine/threonine kinase that recruits the E3 ubiquitin ligase parkin to dysfunctional mitochondria, for example depolarized mitochondria (Narendra *et al.*, 2008;Matsuda *et al.*, 2010). This pathway has been proposed to act as a quality control mechanism to regulate mitophagy of only damaged mitochondria (Whitworth *et al.*, 2009;Narendra and Youle, 2011). PINK1 and parkin also effect mitochondrial morphology with knockdown of PINK1 or parkin leading to mitochondrial fragmentation in human SH-SY5Y cell (Lutz *et al.*, 2009), implicating them as either a direct or indirect regulator of mitochondrial dynamics. The fragmentation observed in PINK1 or parkin deficient cells could be rescued with expression of Mfn2, OPA1, or DN-Drp1. They determined that PINK1 or parkin deficiency promotes increased fission, suggesting that normal PINK1 and parkin expression may play a role in the regulation of mitochondrial fusion (Lutz *et al.*, 2009). However, Tanaka et al demonstrate that parkin recruitment to a mitochondrion prevents or postpones re-fusion with the network. Although, this role for parkin mediated inhibition of re-fusion with the netowrk is probably occurring indirectly through the degradation of mitofusins (Tanaka *et al.*, 2010).

Interestingly, it has been shown that the localization and stability of PINK1 depends on the mitochondrial protease PARL. In addition, PARL deficiencies were shown to disrupt

parkin recruitment to mitochondria (Shi *et al.*, 2011). Cleavage of PINK1 is dependent on mitochondrial membrane potential. MEFs treated with CCCP generated a stabilized form of PINK1that localized to the outer mitochondrial membrane, where it can recruit parkin (Jin *et al.*, 2010). PARL is also known to be involved with OPA1 proteolytic processing, suggesting that specific isoforms of OPA1 could also be involved in regulating mitophagy by inducing the PINK1/parkin pathway (Cipolat *et al.*, 2006). Lutz et al. demonstrated that there is no change in OPA1 processing in either PINK1 or parkin deficient cells, even though they do have a shift toward fragmented morphology(Lutz *et al.*, 2009). This could imply that OPA1 processing is not involved with regulating mitophagy through the PINK1/parkin pathway. However, it has been shown that OPA1 degradation in responses to depolarization occurs before the recruitment of parkin to mitochondria (Guillery *et al.*, 2008); therefore, if OPA1 processing is upstream of PINK1/parkin activation it is not unexpected that knockdown of PINK1 or parkin does not lead to changes in the expression of OPA1 isoforms. Whether OPA1 processing is indeed able to regulate the PINK1/parkin pathway needs to be studied further.

The PINK1/parkin pathway represents an important addition to the regulation of mitochondrial quality control. It provides a pathway that connects mitochondrial dysfunction to mitophagy through regulation of mitochondrial morphology and as a mechanism for dysfunctional mitochondria to be monitored (Tanaka, 2010;Springer and Kahle, 2011). Pharmacological induction of mitochondrial depolarization, a known trigger of mitophagy, has been shown to be regulated by PINK1 and parkin. When either PINK1 or parkin is depleted, CCCP fails to cause proteosomal degradation of the mitofusins or to induce mitophagy. Furthermore, it was shown that the ability of parkin

to translocate to mitochondria is critical for depolarization-induced mitophagy (Tanaka *et al.*, 2010). Parkin has also been shown to be recruited to mitochondria in cells treated with paraquat to induce oxidative stress (Narendra *et al.*, 2008;Narendra *et al.*, 2011). Therefore, parkin provides many points of regulation for mitochondrial quality control: it can identify, by means of PINK1, and label dysfunctional mitochondria, prevent fusion of damaged units to back to the network by degrading fusion proteins such as Mfn2, and it is necessary for depolarization-induced mitophagy.

The contribution of parkin, an ubiquitin ligase, to mitophagy also demonstrates the important role the proteasome plays in mitochondrial degradation (Chan and Chan, 2011;Karbowski and Youle, 2011). As was already discussed, parkin can activate the ubiquitin-proteasome system to induce degradation of the fusion proteins Mfn1 and Mfn2 on depolarized mitochondria (Tanaka *et al.*, 2010;Gegg *et al.*, 2010). While important in preventing re-fusion of damaged mitochondria with the network, these are not the only outer mitochondrial membrane proteins degraded by the proteasome in a parkin-induced fashion that are also essential for the progression of mitophagy. The degradation of other outer membrane proteins occurs with slower kinetics than with Mfn1/2, yet undeniably represent areas of regulation that are essential for mitochondrial function. Outer membrane proteins involved with solute transport, apoptosis, mitochondrial fission (Fis1), and protein import are all degraded upon CCCP treatment (Chan *et al.*, 2011). Interestingly, Chan et al. show that degradation of these proteins is independent of autophagy, as this still occurs in autophagy-deficient Atg3-null MEFs. When the proteasome is inhibited, parkin-mediated mitophagy is abolished (Chan *et al.*, 2011). This demonstrates that the ubiquitin-proteasome system may have an important role in

mitochondrial quality control and the degradation of dysfunctional mitochondria that is unique and independent of autophagy.

One question that remains to be answered is what is inducing mitophagy in cells that express little to no endogenous parkin? A number of studies on parkin-induced mitophagy have been done in the presence of parkin overexpression because those cells do not express endogenous parkin. While it provides an efficient approach to the study of the role of parkin in a system that does not have any confounding endogenous protein to influence the results of an experiment, it does not provide evidence for what is mediating mitochondrial turnover in these systems. Determining where parkin-induced mitophagy occurs and what other pathways could be inducing mitophagy or mitochondrial turnover when parkin is not expressed will be crucial in understanding the differential regulation of mitophagy.

It has also been proposed that mitochondria may provide membrane components for APs and that Mfn2 is critical to this process. Hailey et al. show that when autophagy is induced by starvation, a mitochondrial outer membrane marker overlapped with APs 2 hours after treatment, and this colocalization was not attributable to mitophagy. Althought, the contribution of mitochondrial membranes to APs seems to be a starvation-specific process in that it was not observed under any other autophagy inducing conditions. When Mfn2-/- cells were starved for 2 hours there was no induction of autophagy (Hailey *et al.*, 2010). This represents another scenario where mitochondrial fusion plays an important role in the progression of autophagy.

A2.6 Conclusions

While our knowledge of mitochondrial quality control and mitophagy has been expanding rapidly in the last few years, a number of important questions remain unanswered. For instance how mitochondria are targeted to the AP remains to be fully understood. We hypotesize that both mitochondrial fusion itself and mitochondrial fusion proteins act as key regulators of mitochondrial autophagy. For the most comprehensive quality control to take place, complete cycles of fusion and fission may be a requirement. Selective fusion is important because it functions to generate a preautophagic pool of dysfunctional mitochondria. We speculate that OPA1 processing alone or in combination with other proteins could be involved in signaling for mitophagy or recruiting APs to dysfunctional mitochondria. Additionally, the PINK1/parkin pathway plays an important role in mitochondrial quality control and regulates both mitochondrial morphology through downregulation of fusion proteins and the induction of mitophagy. Disruptions in both mitochondrial fusion and turnover have been implicated in the pathology of a number of diseases and aging, therefore it is critical to determine their full contribute to mitochondrial quality control (reviewed in: (Batlevi and La Spada, 2011;Barnett and Brewer, 2011;Taylor and Goldman, 2011).

Table A.1: Relationship between Mitochondrial Fusion and Fission and Mitophagy.

Manipulation	Cell type	Effect on Morphology	Effect on mitophagy	Reference
Fis1 RNAi	INS1 β-cells	Elongation	Reduction in APs containing mitochondria by 70%	(Twig *et al.*, 2008a)

Fis1 Overexpression	HeLa cells INS1 β -cells	Fragmentation	Enhanced AP formation by 50% Reduce total mitochondrial volume by 50%	(Frieden *et al.*, 2004;Gomes *et al.*, 2008;Park *et al.*, 2008)
Drp1K38A (dominant negative Drp1)	INS1 β -cells	Fragmented, swollen mitochondria	Reduction in APs containing mitochondria by 75%	(Twig *et al.*, 2008a)
Drp1 RNAi	HeLa cells	Tubular, elongated mitochondria	Decrease in mitophagy (qualitative)	(Parone *et al.*, 2008)
DRP1 Knockout	MEF	Excessively fused mitochondria	Decreased parkin-induced mitophagy	(Tanaka et al., 2010)
Drp1 Overexpression	HeLa cells	Fragmentation	Decrease in mitochondrial mass by 70%	(Arnoult *et al.*, 2005b)
OPA1 Overexpression	INS1 β -cells	Reduction in mitochondrial size with intact fusion ability	Reduction in APs containing mitochondria by 63%	(Twig *et al.*, 2008a)
OPA1 heterozygous mutated mice	Retinal Ganglion cells	Increased percentage of opaque mitochondria	An increase in autophagy; Mitophagy not measured	(White *et al.*, 2009)
OPA1 shRNA	INS1 β -cells	Fragmentation	Reduction in APs containing mitochondria by 45%	unpublished
OPA1 Knockout	MEFs	Fragmentation	Increased APs containing mitochondria after 24 hours starvation.	(Gomes et al., 2011)
Mfn1 Overexpression	INS1 β -cells	Mitochondrial aggregation	Decrease in mitochondrial volume by 40%	(Park *et al.*, 2008)
Mfn1 Loss-of function (Overexpression of Mfn1 DN)	INS1 β -cells	Fragmentation	Unchanged mitochondrial mass	(Park *et al.*, 2008)
Mfn2 Knockout	MEFs	Fragmentation and perinuclear clustering	Inhibition of autophagy	(Hailey *et al.*, 2010)

PINK1 Knockdown	Human neuronal SH-SY5Y cells	Fragmentation	Increased autophagic sequestration of depolarized mitochondria Decreased in mitochondrial volume by 50%	(Dagda *et al.*, 2009)
PINK1 Overexpression	Human neuronal SH-SY5Y cells	Increased interconnectivity and elongation Abnormally enlarged mitochondria	Autophagic vacuole number remained low	(Dagda *et al.*, 2009)
Parkin null	HeLa cells (express little to no endogenous parkin)	Mfn1/2 degradation is inhibited; ability to re-fuse accelerated after CCCP treatment	Inhibition of CCCP-induced mitophagy	(Narendra et al., 2008; Tanaka et al., 2010)

Chapter 6: Bibliography

REFERENCES

1. Adhami F, Liao G, Morozov YM, Schloemer A, Schmithorst VJ, Lorenz JN, Dunn RS, Vorhees CV, Wills-Karp M, Degen JL, Davis RJ, Mizushima N, Rakic P, Dardzinski BJ, Holland SK, Sharp FR, and Kuan CY (2006) Cerebral ischemia-hypoxia induces intravascular coagulation and autophagy. *Am J Pathol,* **169,** 566-583.

2. Affourtit C and Brand MD (2008a) On the role of uncoupling protein-2 in pancreatic beta cells. *Biochim Biophys Acta,* **1777,** 973-979.

3. Affourtit C and Brand MD (2008b) Uncoupling protein-2 contributes significantly to high mitochondrial proton leak in INS-1E insulinoma cells and attenuates glucose-stimulated insulin secretion. *Biochem J,* **409,** 199-204.

4. Akepati VR, Muller EC, Otto A, Strauss HM, Portwich M, and Alexander C (2008) Characterization of OPA1 isoforms isolated from mouse tissues. *J Neurochem,* **106,** 372-383.

5. Alexander C, Votruba M, Pesch UE, Thiselton DL, Mayer S, Moore A, Rodriguez M, Kellner U, Leo-Kottler B, Auburger G, Bhattacharya SS, and Wissinger B (2000) OPA1, encoding a dynamin-related GTPase, is mutated in autosomal dominant optic atrophy linked to chromosome 3q28. *Nat Genet,* **26,** 211-215.

6. Alirol E, James D, Huber D, Marchetto A, Vergani L, Martinou JC, and Scorrano L (2006) The mitochondrial fission protein hFis1 requires the endoplasmic reticulum gateway to induce apoptosis. *Mol Biol Cell,* **17,** 4593-4605.

7. Amchenkova AA, Bakeeva LE, Chentsov YS, Skulachev VP, and Zorov DB (1988) Coupling membranes as energy-transmitting cables. I. Filamentous mitochondria in fibroblasts and mitochondrial clusters in cardiomyocytes. *J Cell Biol,* **107,** 481-495.

8. Anello M, Lupi R, Spampinato D, Piro S, Masini M, Boggi U, Del PS, Rabuazzo AM, Purrello F, and Marchetti P (2005) Functional and morphological alterations of mitochondria in pancreatic beta cells from type 2 diabetic patients. *Diabetologia,* **48,** 282-289.

9. Anglade P, Vyas S, Javoy-Agid F, Herrero MT, Michel PP, Marquez J, Mouatt-Prigent A, Ruberg M, Hirsch EC, and Agid Y (1997) Apoptosis and autophagy in nigral neurons of patients with Parkinson's disease. *Histol Histopathol,* **12,** 25-31.

10. Aquilante CL (2010) Sulfonylurea pharmacogenomics in Type 2 diabetes: the influence of drug target and diabetes risk polymorphisms. *Expert Rev Cardiovasc Ther,* **8,** 359-372.

11. Arai R, Ito K, Wakiyama M, Matsumoto E, Sakamoto A, Etou Y, Otsuki M, Inoue M, Hayashizaki Y, Miyagishi M, Taira K, Shirouzu M, and Yokoyama S (2004) Establishment of stable hFis1 knockdown cells with an siRNA expression vector. *J Biochem,* **136,** 421-425.

12. Arbuthnott GW and Wickens J (2007) Space, time and dopamine. *Trends Neurosci,* **30,** 62-69.

13. Arimura S, Yamamoto J, Aida GP, Nakazono M, and Tsutsumi N (2004) Frequent fusion and fission of plant mitochondria with unequal nucleoid distribution. *Proc Natl Acad Sci U S A,* **101,** 7805-7808.

14. Arnoult D, Grodet A, Lee YJ, Estaquier J, and Blackstone C (2005a) Release of OPA1 during apoptosis participates in the rapid and complete release of cytochrome c and subsequent mitochondrial fragmentation. *J Biol Chem,* **280,** 35742-35750.

15. Arnoult D, Rismanchi N, Grodet A, Roberts RG, Seeburg DP, Estaquier J, Sheng M, and Blackstone C (2005b) Bax/Bak-dependent release of DDP/TIMM8a promotes Drp1-mediated mitochondrial fission and mitoptosis during programmed cell death. *Curr Biol,* **15,** 2112-2118.

16. Attali V, Parnes M, Ariav Y, Cerasi E, Kaiser N, and Leibowitz G (2006) Regulation of insulin secretion and proinsulin biosynthesis by succinate. *Endocrinology,* **147,** 5110-5118.

17. Azzu V, Parker N, and Brand MD (2008) High membrane potential promotes alkenal-induced mitochondrial uncoupling and influences adenine nucleotide translocase conformation. *Biochem J,* **413,** 323-332.

18. Bach D, Naon D, Pich S, Soriano FX, Vega N, Rieusset J, Laville M, Guillet C, Boirie Y, Wallberg-Henriksson H, Manco M, Calvani M, Castagneto M, Palacin M, Mingrone G, Zierath JR, Vidal H, and Zorzano A (2005) Expression of Mfn2, the Charcot-Marie-Tooth neuropathy type 2A gene, in human skeletal muscle: effects of type 2 diabetes, obesity, weight loss, and the regulatory role of tumor necrosis factor alpha and interleukin-6. *Diabetes,* **54,** 2685-2693.

19. Bach D, Pich S, Soriano FX, Vega N, Baumgartner B, Oriola J, Daugaard JR, Lloberas J, Camps M, Zierath JR, Rabasa-Lhoret R, Wallberg-Henriksson H, Laville M, Palacin M, Vidal H, Rivera F, Brand M, and Zorzano A (2003) Mitofusin-2 determines mitochondrial network architecture and mitochondrial metabolism. A novel regulatory mechanism altered in obesity. *J Biol Chem,* **278,** 17190-17197.

20. Banas SM, Rouch C, Kassis N, Markaki EM, and Gerozissis K (2009) A dietary fat excess alters metabolic and neuroendocrine responses before the onset of metabolic diseases. *Cell Mol Neurobiol,* **29,** 157-168.

21. Banks WA and Kastin AJ (1998) Differential permeability of the blood-brain barrier to two pancreatic peptides: insulin and amylin. *Peptides,* **19,** 883-889.

22. Barnett A and Brewer GJ (2011) Autophagy in aging and Alzheimer's disease: pathologic or protective? *J Alzheimers Dis,* **25,** 385-394.

23. Barsoum MJ, Yuan H, Gerencser AA, Liot G, Kushnareva Y, Graber S, Kovacs I, Lee WD, Waggoner J, Cui J, White AD, Bossy B, Martinou JC, Youle RJ, Lipton SA, Ellisman MH, Perkins GA, and Bossy-Wetzel E (2006) Nitric oxide-induced mitochondrial fission is regulated by dynamin-related GTPases in neurons. *EMBO J,* **25,** 3900-3911.

24. Batlevi Y and La Spada AR (2011) Mitochondrial autophagy in neural function, neurodegenerative disease, neuron cell death, and aging. *Neurobiol Dis,* **43,** 46-51.

25. Benard G, Bellance N, James D, Parrone P, Fernandez H, Letellier T, and Rossignol R (2007) Mitochondrial bioenergetics and structural network organization. *J Cell Sci,* **120,** 838-848.

26. Benard G and Rossignol R (2008) Ultrastructure of the mitochondrion and its bearing on function and bioenergetics. *Antioxid Redox Signal,* **10,** 1313-1342.

27. Bereiter-Hahn J and Voth M (1994) Dynamics of mitochondria in living cells: shape changes, dislocations, fusion, and fission of mitochondria. *Microsc Res Tech,* **27,** 198-219.

28. Bindokas VP, Kuznetsov A, Sreenan S, Polonsky KS, Roe MW, and Philipson LH (2003) Visualizing superoxide production in normal and diabetic rat islets of Langerhans. *J Biol Chem,* **278,** 9796-9801.

29. Bolzan AD and Bianchi MS (2002) Genotoxicity of streptozotocin. *Mutat Res,* **512,** 121-134.

30. Bossy-Wetzel E, Barsoum MJ, Godzik A, Schwarzenbacher R, and Lipton SA (2003) Mitochondrial fission in apoptosis, neurodegeneration and aging. *Curr Opin Cell Biol,* **15,** 706-716.

31. Braak H, Ghebremedhin E, Rub U, Bratzke H, and Del TK (2004) Stages in the development of Parkinson's disease-related pathology. *Cell Tissue Res,* **318,** 121-134.

32. Brand MD, Brindle KM, Buckingham JA, Harper JA, Rolfe DF, and Stuart JA (1999) The significance and mechanism of mitochondrial proton conductance. *Int J Obes Relat Metab Disord,* **23 Suppl 6,** S4-11.

33. Brand MD and Nicholls DG (2011) Assessing mitochondrial dysfunction in cells. *Biochem J,* **435,** 297-312.

34. Brand MD, Pakay JL, Ocloo A, Kokoszka J, Wallace DC, Brookes PS, and Cornwall EJ (2005) The basal proton conductance of mitochondria depends on adenine nucleotide translocase content. *Biochem J,* **392,** 353-362.

35. Brief DJ and Davis JD (1984) Reduction of food intake and body weight by chronic intraventricular insulin infusion. *Brain Res Bull,* **12,** 571-575.

36. Brookes PS (2005) Mitochondrial H(+) leak and ROS generation: an odd couple. *Free Radic Biol Med,* **38,** 12-23.

37. Brooks C, Wei Q, Feng L, Dong G, Tao Y, Mei L, Xie ZJ, and Dong Z (2007) Bak regulates mitochondrial morphology and pathology during apoptosis by interacting with mitofusins. *Proc Natl Acad Sci U S A,* **104,** 11649-11654.

38. Brownlee M (2003) A radical explanation for glucose-induced beta cell dysfunction. *J Clin Invest,* **112,** 1788-1790.

39. Bruning JC, Gautam D, Burks DJ, Gillette J, Schubert M, Orban PC, Klein R, Krone W, Muller-Wieland D, and Kahn CR (2000) Role of brain insulin receptor in control of body weight and reproduction. *Science,* **289,** 2122-2125.

40. Campbell CL and Thorsness PE (1998) Escape of mitochondrial DNA to the nucleus in yme1 yeast is mediated by vacuolar-dependent turnover of abnormal mitochondrial compartments. *J Cell Sci,* **111 (Pt 16),** 2455-2464.

41. Carlsson C, Borg LA, and Welsh N (1999) Sodium palmitate induces partial mitochondrial uncoupling and reactive oxygen species in rat pancreatic islets in vitro. *Endocrinology,* **140,** 3422-3428.

42. Cartoni R, Leger B, Hock MB, Praz M, Crettenand A, Pich S, Ziltener JL, Luthi F, Deriaz O, Zorzano A, Gobelet C, Kralli A, and Russell AP (2005) Mitofusins 1/2 and ERRalpha expression are increased in human skeletal muscle after physical exercise. *J Physiol,* **567,** 349-358.

43. Castro FA, Mariani D, Panek AD, Eleutherio EC, and Pereira MD (2008) Cytotoxicity mechanism of two naphthoquinones (menadione and plumbagin) in Saccharomyces cerevisiae. *PLoS One,* **3,** e3999.

44. Cereghetti GM, Stangherlin A, Martins de BO, Chang CR, Blackstone C, Bernardi P, and Scorrano L (2008) Dephosphorylation by calcineurin regulates

translocation of Drp1 to mitochondria. *Proc Natl Acad Sci U S A,* **105,** 15803-15808.

45. Chan NC and Chan DC (2011) Parkin uses the UPS to ship off dysfunctional mitochondria. *Autophagy,* **7,** 771-772.

46. Chan NC, Salazar AM, Pham AH, Sweredoski MJ, Kolawa NJ, Graham RL, Hess S, and Chan DC (2011) Broad activation of the ubiquitin-proteasome system by Parkin is critical for mitophagy. *Hum Mol Genet,* **20,** 1726-1737.

47. Chaput JP, Tremblay A, Rimm EB, Bouchard C, and Ludwig DS (2008) A novel interaction between dietary composition and insulin secretion: effects on weight gain in the Quebec Family Study. *Am J Clin Nutr,* **87,** 303-309.

48. Chen H and Chan DC (2005a) Emerging functions of mammalian mitochondrial fusion and fission. *Hum Mol Genet,* **14 Spec No. 2,** R283-R289.

49. Chen H and Chan DC (2009) Mitochondrial dynamics--fusion, fission, movement, and mitophagy--in neurodegenerative diseases. *Hum Mol Genet,* **18,** R169-R176.

50. Chen H and Chan DC (2010) Physiological functions of mitochondrial fusion. *Ann N Y Acad Sci,* **1201,** 21-25.

51. Chen H, Chomyn A, and Chan DC (2005b) Disruption of fusion results in mitochondrial heterogeneity and dysfunction. *J Biol Chem,* **280,** 26185-26192.

52. Chen H, Detmer SA, Ewald AJ, Griffin EE, Fraser SE, and Chan DC (2003) Mitofusins Mfn1 and Mfn2 coordinately regulate mitochondrial fusion and are essential for embryonic development. *J Cell Biol,* **160,** 189-200.

53. Chen KH, Guo X, Ma D, Guo Y, Li Q, Yang D, Li P, Qiu X, Wen S, Xiao RP, and Tang J (2004) Dysregulation of HSG triggers vascular proliferative disorders. *Nat Cell Biol,* **6,** 872-883.

54. Choi SE, Kim HE, Shin HC, Jang HJ, Lee KW, Kim Y, Kang SS, Chun J, and Kang Y (2007) Involvement of Ca2+-mediated apoptotic signals in palmitate-induced MIN6N8a beta cell death. *Mol Cell Endocrinol,* **272,** 50-62.

55. Choudhury AI, Heffron H, Smith MA, Al-Qassab H, Xu AW, Selman C, Simmgen M, Clements M, Claret M, Maccoll G, Bedford DC, Hisadome K, Diakonov I, Moosajee V, Bell JD, Speakman JR, Batterham RL, Barsh GS, Ashford ML, and Withers DJ (2005) The role of insulin receptor substrate 2 in hypothalamic and beta cell function. *J Clin Invest,* **115,** 940-950.

56. Chu CT (2010) Tickled PINK1: mitochondrial homeostasis and autophagy in recessive Parkinsonism. *Biochim Biophys Acta,* **1802,** 20-28.

57. Cipolat S, Martins de BO, Dal ZB, and Scorrano L (2004) OPA1 requires mitofusin 1 to promote mitochondrial fusion. *Proc Natl Acad Sci U S A,* **101,** 15927-15932.

58. Cipolat S, Rudka T, Hartmann D, Costa V, Serneels L, Craessaerts K, Metzger K, Frezza C, Annaert W, D'Adamio L, Derks C, Dejaegere T, Pellegrini L, D'Hooge R, Scorrano L, and De SB (2006) Mitochondrial rhomboid PARL regulates cytochrome c release during apoptosis via OPA1-dependent cristae remodeling. *Cell,* **126,** 163-175.

59. Clark IE, Dodson MW, Jiang C, Cao JH, Huh JR, Seol JH, Yoo SJ, Hay BA, and Guo M (2006) Drosophila pink1 is required for mitochondrial function and interacts genetically with parkin. *Nature,* **441,** 1162-1166.

60. CLARK SL, Jr. (1957) Cellular differentiation in the kidneys of newborn mice studies with the electron microscope. *J Biophys Biochem Cytol,* **3,** 349-362.

61. Clarke DW, Mudd L, Boyd FT, Jr., Fields M, and Raizada MK (1986) Insulin is released from rat brain neuronal cells in culture. *J Neurochem,* **47,** 831-836.

62. Clayton DA, Doda JN, and Friedberg EC (1974) The absence of a pyrimidine dimer repair mechanism in mammalian mitochondria. *Proc Natl Acad Sci U S A,* **71,** 2777-2781.

63. Coleman DL (1978) Obese and diabetes: two mutant genes causing diabetes-obesity syndromes in mice. *Diabetologia,* **14,** 141-148.

64. Collins TJ, Berridge MJ, Lipp P, and Bootman MD (2002) Mitochondria are morphologically and functionally heterogeneous within cells. *EMBO J,* **21,** 1616-1627.

65. Costa RA, Romagna CD, Pereira JL, and Souza-Pinto NC (2011) The role of mitochondrial DNA damage in the citotoxicity of reactive oxygen species. *J Bioenerg Biomembr,* **43,** 25-29.

66. Covey SD, Wideman RD, McDonald C, Unniappan S, Huynh F, Asadi A, Speck M, Webber T, Chua SC, and Kieffer TJ (2006) The pancreatic beta cell is a key site for mediating the effects of leptin on glucose homeostasis. *Cell Metab,* **4,** 291-302.

67. Crews L, Spencer B, Desplats P, Patrick C, Paulino A, Rockenstein E, Hansen L, Adame A, Galasko D, and Masliah E (2010) Selective molecular alterations in the autophagy pathway in patients with Lewy body disease and in models of alpha-synucleinopathy. *PLoS One,* **5,** e9313.

68. Cribbs JT and Strack S (2007) Reversible phosphorylation of Drp1 by cyclic AMP-dependent protein kinase and calcineurin regulates mitochondrial fission and cell death. *EMBO Rep,* **8,** 939-944.

69. Cuervo AM (2006) Autophagy in neurons: it is not all about food. *Trends Mol Med,* **12,** 461-464.

70. Cui M, Tang X, Christian WV, Yoon Y, and Tieu K (2010) Perturbations in mitochondrial dynamics induced by human mutant PINK1 can be rescued by the mitochondrial division inhibitor mdivi-1. *J Biol Chem,* **285,** 11740-11752.

71. Cui Y, Huang L, Elefteriou F, Yang G, Shelton JM, Giles JE, Oz OK, Pourbahrami T, Lu CY, Richardson JA, Karsenty G, and Li C (2004) Essential role of STAT3 in body weight and glucose homeostasis. *Mol Cell Biol,* **24,** 258-269.

72. Dagda RK, Cherra SJ, III, Kulich SM, Tandon A, Park D, and Chu CT (2009) Loss of PINK1 function promotes mitophagy through effects on oxidative stress and mitochondrial fission. *J Biol Chem,* **284,** 13843-13855.

73. Dagda RK and Chu CT (2009) Mitochondrial quality control: insights on how Parkinson's disease related genes PINK1, parkin, and Omi/HtrA2 interact to maintain mitochondrial homeostasis. *J Bioenerg Biomembr,* **41,** 473-479.

74. Dagda RK, Zhu J, Kulich SM, and Chu CT (2008) Mitochondrially localized ERK2 regulates mitophagy and autophagic cell stress: implications for Parkinson's disease. *Autophagy,* **4,** 770-782.

75. Danaei G, Finucane MM, Lu Y, Singh GM, Cowan MJ, Paciorek CJ, Lin JK, Farzadfar F, Khang YH, Stevens GA, Rao M, Ali MK, Riley LM, Robinson CA, and Ezzati M (2011) National, regional, and global trends in fasting plasma glucose and diabetes prevalence since 1980: systematic analysis of health examination surveys and epidemiological studies with 370 country-years and 2.7 million participants. *Lancet,* **378,** 31-40.

76. Danial NN and Korsmeyer SJ (2004) Cell death: critical control points. *Cell,* **116,** 205-219.

77. Davalli AM, Ogawa Y, Scaglia L, Wu YJ, Hollister J, Bonner-Weir S, and Weir GC (1995) Function, mass, and replication of porcine and rat islets transplanted into diabetic nude mice. *Diabetes,* **44,** 104-111.

78. de Brito OM and Scorrano L (2008) Mitofusin 2 tethers endoplasmic reticulum to mitochondria. *Nature,* **456,** 605-610.

79. Deeney JT, Gromada J, Hoy M, Olsen HL, Rhodes CJ, Prentki M, Berggren PO, and Corkey BE (2000a) Acute stimulation with long chain acyl-CoA enhances exocytosis in insulin-secreting cells (HIT T-15 and NMRI beta-cells). *J Biol Chem,* **275,** 9363-9368.

80. Deeney JT, Prentki M, and Corkey BE (2000b) Metabolic control of beta-cell function. *Semin Cell Dev Biol,* **11,** 267-275.

81. Dehay B, Bove J, Rodriguez-Muela N, Perier C, Recasens A, Boya P, and Vila M (2010) Pathogenic lysosomal depletion in Parkinson's disease. *J Neurosci,* **30,** 12535-12544.

82. Deng H, Dodson MW, Huang H, and Guo M (2008) The Parkinson's disease genes pink1 and parkin promote mitochondrial fission and/or inhibit fusion in Drosophila. *Proc Natl Acad Sci U S A,* **105,** 14503-14508.

83. Deter RL, Baudhuin P, and De DC (1967) Participation of lysosomes in cellular autophagy induced in rat liver by glucagon. *J Cell Biol,* **35,** C11-C16.

84. Deter RL and De DC (1967) Influence of glucagon, an inducer of cellular autophagy, on some physical properties of rat liver lysosomes. *J Cell Biol,* **33,** 437-449.

85. Ding WX, Ni HM, Li M, Liao Y, Chen X, Stolz DB, Dorn Ii GW, and Yin XM (2010) Nix is critical to two distinct phases of mitophagy: reactive oxygen species (ROS)-mediated autophagy induction and Parkin-ubiqutin-p62-mediated mitochondria priming. *J Biol Chem*.

86. Downward J (2004) PI 3-kinase, Akt and cell survival. *Semin Cell Dev Biol,* **15,** 177-182.

87. Dudkina NV, Kouril R, Peters K, Braun HP, and Boekema EJ (2010) Structure and function of mitochondrial supercomplexes. *Biochim Biophys Acta,* **1797,** 664-670.

88. Duvezin-Caubet S, Jagasia R, Wagener J, Hofmann S, Trifunovic A, Hansson A, Chomyn A, Bauer MF, Attardi G, Larsson NG, Neupert W, and Reichert AS (2006) Proteolytic processing of OPA1 links mitochondrial dysfunction to alterations in mitochondrial morphology. *J Biol Chem,* **281,** 37972-37979.

89. Duvezin-Caubet S, Koppen M, Wagener J, Zick M, Israel L, Bernacchia A, Jagasia R, Rugarli EI, Imhof A, Neupert W, Langer T, and Reichert AS (2007) OPA1 processing reconstituted in yeast depends on the subunit composition of the m-AAA protease in mitochondria. *Mol Biol Cell,* **18,** 3582-3590.

90. Echtay KS and Brand MD (2007) 4-hydroxy-2-nonenal and uncoupling proteins: an approach for regulation of mitochondrial ROS production. *Redox Rep,* **12,** 26-29.

91. Echtay KS, Roussel D, St-Pierre J, Jekabsons MB, Cadenas S, Stuart JA, Harper JA, Roebuck SJ, Morrison A, Pickering S, Clapham JC, and Brand MD (2002) Superoxide activates mitochondrial uncoupling proteins. *Nature,* **415,** 96-99.

92. Ehses S, Raschke I, Mancuso G, Bernacchia A, Geimer S, Tondera D, Martinou JC, Westermann B, Rugarli EI, and Langer T (2009) Regulation of OPA1

processing and mitochondrial fusion by m-AAA protease isoenzymes and OMA1. *J Cell Biol,* **187,** 1023-1036.

93. El-Assaad W, Buteau J, Peyot ML, Nolan C, Roduit R, Hardy S, Joly E, Dbaibo G, Rosenberg L, and Prentki M (2003) Saturated fatty acids synergize with elevated glucose to cause pancreatic beta-cell death. *Endocrinology,* **144,** 4154-4163.

94. Elmore SP, Qian T, Grissom SF, and Lemasters JJ (2001) The mitochondrial permeability transition initiates autophagy in rat hepatocytes. *FASEB J,* **15,** 2286-2287.

95. Eskelinen EL (2008) New insights into the mechanisms of macroautophagy in mammalian cells. *Int Rev Cell Mol Biol,* **266,** 207-247.

96. Essick EE and Sam F (2010) Oxidative stress and autophagy in cardiac disease, neurological disorders, aging and cancer. *Oxid Med Cell Longev,* **3,** 168-177.

97. Esteves AR, Lu J, Rodova M, Onyango I, Lezi E, Dubinsky R, Lyons KE, Pahwa R, Burns JM, Cardoso SM, and Swerdlow RH (2010) Mitochondrial respiration and respiration-associated proteins in cell lines created through Parkinson's subject mitochondrial transfer. *J Neurochem,* **113,** 674-682.

98. Esteves TC, Parker N, and Brand MD (2006) Synergy of fatty acid and reactive alkenal activation of proton conductance through uncoupling protein 1 in mitochondria. *Biochem J,* **395,** 619-628.

99. Exner N, Treske B, Paquet D, Holmstrom K, Schiesling C, Gispert S, Carballo-Carbajal I, Berg D, Hoepken HH, Gasser T, Kruger R, Winklhofer KF, Vogel F, Reichert AS, Auburger G, Kahle PJ, Schmid B, and Haass C (2007) Loss-of-function of human PINK1 results in mitochondrial pathology and can be rescued by parkin. *J Neurosci,* **27,** 12413-12418.

100. Ferre M, mati-Bonneau P, Tourmen Y, Malthiery Y, and Reynier P (2005) eOPA1: an online database for OPA1 mutations. *Hum Mutat,* **25,** 423-428.

101. Ferrick DA, Neilson A, and Beeson C (2008) Advances in measuring cellular bioenergetics using extracellular flux. *Drug Discov Today,* **13,** 268-274.

102. Fex M, Nitert MD, Wierup N, Sundler F, Ling C, and Mulder H (2007) Enhanced mitochondrial metabolism may account for the adaptation to insulin resistance in islets from C57BL/6J mice fed a high-fat diet. *Diabetologia,* **50,** 74-83.

103. Frank S, Gaume B, Bergmann-Leitner ES, Leitner WW, Robert EG, Catez F, Smith CL, and Youle RJ (2001) The role of dynamin-related protein 1, a mediator of mitochondrial fission, in apoptosis. *Dev Cell,* **1,** 515-525.

104. Fransson S, Ruusala A, and Aspenstrom P (2006) The atypical Rho GTPases Miro-1 and Miro-2 have essential roles in mitochondrial trafficking. *Biochem Biophys Res Commun,* **344,** 500-510.

105. Frezza C, Cipolat S, Martins de BO, Micaroni M, Beznoussenko GV, Rudka T, Bartoli D, Polishuck RS, Danial NN, De SB, and Scorrano L (2006) OPA1 controls apoptotic cristae remodeling independently from mitochondrial fusion. *Cell,* **126,** 177-189.

106. Frieden M, James D, Castelbou C, Danckaert A, Martinou JC, and Demaurex N (2004) Ca(2+) homeostasis during mitochondrial fragmentation and perinuclear clustering induced by hFis1. *J Biol Chem,* **279,** 22704-22714.

107. Fujita N, Hayashi-Nishino M, Fukumoto H, Omori H, Yamamoto A, Noda T, and Yoshimori T (2008) An Atg4B mutant hampers the lipidation of LC3 paralogues and causes defects in autophagosome closure. *Mol Biol Cell,* **19,** 4651-4659.

108. Fujitani Y, Ueno T, and Watada H (2010) Autophagy in health and disease. 4. The role of pancreatic beta-cell autophagy in health and diabetes. *Am J Physiol Cell Physiol,* **299,** C1-C6.

109. Gandhi S, Wood-Kaczmar A, Yao Z, Plun-Favreau H, Deas E, Klupsch K, Downward J, Latchman DS, Tabrizi SJ, Wood NW, Duchen MR, and Abramov AY (2009) PINK1-associated Parkinson's disease is caused by neuronal vulnerability to calcium-induced cell death. *Mol Cell,* **33,** 627-638.

110. Gandre-Babbe S and van der Bliek AM (2008) The novel tail-anchored membrane protein Mff controls mitochondrial and peroxisomal fission in mammalian cells. *Mol Biol Cell,* **19,** 2402-2412.

111. Gasser T (2009) Molecular pathogenesis of Parkinson disease: insights from genetic studies. *Expert Rev Mol Med,* **11,** e22.

112. Gastaldi G, Russell A, Golay A, Giacobino JP, Habicht F, Barthassat V, Muzzin P, and Bobbioni-Harsch E (2007) Upregulation of peroxisome proliferator-activated receptor gamma coactivator gene (PGC1A) during weight loss is related to insulin sensitivity but not to energy expenditure. *Diabetologia,* **50,** 2348-2355.

113. Gegg ME, Cooper JM, Chau KY, Rojo M, Schapira AH, and Taanman JW (2010) Mitofusin 1 and mitofusin 2 are ubiquitinated in a PINK1/parkin-dependent manner upon induction of mitophagy. *Hum Mol Genet,* **19,** 4861-4870.

114. Geisler S, Holmstrom KM, Skujat D, Fiesel FC, Rothfuss OC, Kahle PJ, and Springer W (2010) PINK1/Parkin-mediated mitophagy is dependent on VDAC1 and p62/SQSTM1. *Nat Cell Biol,* **12,** 119-131.

115. Gerozissis K (2008) Brain insulin, energy and glucose homeostasis; genes, environment and metabolic pathologies. *Eur J Pharmacol,* **585,** 38-49.

116. Getty-Kaushik L, Richard AM, Deeney JT, Krawczyk S, Shirihai O, and Corkey BE (2009) The CB1 antagonist rimonabant decreases insulin hypersecretion in rat pancreatic islets. *Obesity (Silver Spring),* **17,** 1856-1860.

117. Giam M, Huang DC, and Bouillet P (2008) BH3-only proteins and their roles in programmed cell death. *Oncogene,* **27 Suppl 1,** S128-S136.

118. Gispert S, Ricciardi F, Kurz A, Azizov M, Hoepken HH, Becker D, Voos W, Leuner K, Muller WE, Kudin AP, Kunz WS, Zimmermann A, Roeper J, Wenzel D, Jendrach M, Garcia-Arencibia M, Fernandez-Ruiz J, Huber L, Rohrer H, Barrera M, Reichert AS, Rub U, Chen A, Nussbaum RL, and Auburger G (2009) Parkinson phenotype in aged PINK1-deficient mice is accompanied by progressive mitochondrial dysfunction in absence of neurodegeneration. *PLoS One,* **4,** e5777.

119. Glater EE, Megeath LJ, Stowers RS, and Schwarz TL (2006) Axonal transport of mitochondria requires milton to recruit kinesin heavy chain and is light chain independent. *J Cell Biol,* **173,** 545-557.

120. Glick D, Barth S, and Macleod KF (2010) Autophagy: cellular and molecular mechanisms. *J Pathol,* **221,** 3-12.

121. Gluck MR and Zeevalk GD (2004) Inhibition of brain mitochondrial respiration by dopamine and its metabolites: implications for Parkinson's disease and catecholamine-associated diseases. *J Neurochem,* **91,** 788-795.

122. Goldberg MS, Fleming SM, Palacino JJ, Cepeda C, Lam HA, Bhatnagar A, Meloni EG, Wu N, Ackerson LC, Klapstein GJ, Gajendiran M, Roth BL, Chesselet MF, Maidment NT, Levine MS, and Shen J (2003) Parkin-deficient mice exhibit nigrostriatal deficits but not loss of dopaminergic neurons. *J Biol Chem,* **278,** 43628-43635.

123. Goldman SJ, Taylor R, Zhang Y, and Jin S (2010) Autophagy and the degradation of mitochondria. *Mitochondrion,* **10,** 309-315.

124. Gomes LC, Di BG, and Scorrano L (2011) During autophagy mitochondria elongate, are spared from degradation and sustain cell viability. *Nat Cell Biol,* **13,** 589-598.

125. Gomes LC and Scorrano L (2008) High levels of Fis1, a pro-fission mitochondrial protein, trigger autophagy. *Biochim Biophys Acta,* **1777,** 860-866.

126. Gomes LC and Scorrano L (2011) Mitochondrial elongation during autophagy: A stereotypical response to survive in difficult times. *Autophagy,* **7**.

127. Gottlieb RA and Carreira RS (2010) Autophagy in health and disease. 5. Mitophagy as a way of life. *Am J Physiol Cell Physiol,* **299,** C203-C210.

128. Griparic L, van der Wel NN, Orozco IJ, Peters PJ, and van der Bliek AM (2004) Loss of the intermembrane space protein Mgm1/OPA1 induces swelling and localized constrictions along the lengths of mitochondria. *J Biol Chem,* **279,** 18792-18798.

129. Grunblatt E, Salkovic-Petrisic M, Osmanovic J, Riederer P, and Hoyer S (2007) Brain insulin system dysfunction in streptozotocin intracerebroventricularly treated rats generates hyperphosphorylated tau protein. *J Neurochem,* **101,** 757-770.

130. Grunewald A, Gegg ME, Taanman JW, King RH, Kock N, Klein C, and Schapira AH (2009) Differential effects of PINK1 nonsense and missense mutations on mitochondrial function and morphology. *Exp Neurol,* **219,** 266-273.

131. Guillery O, Malka F, Landes T, Guillou E, Blackstone C, Lombes A, Belenguer P, Arnoult D, and Rojo M (2008) Metalloprotease-mediated OPA1 processing is modulated by the mitochondrial membrane potential. *Biol Cell,* **100,** 315-325.

132. Guo YH, Chen K, Gao W, Li Q, Chen L, Wang GS, and Tang J (2007) Overexpression of Mitofusin 2 inhibited oxidized low-density lipoprotein induced vascular smooth muscle cell proliferation and reduced atherosclerotic lesion formation in rabbit. *Biochem Biophys Res Commun,* **363,** 411-417.

133. Hagman DK, Latour MG, Chakrabarti SK, Fontes G, Amyot J, Tremblay C, Semache M, Lausier JA, Roskens V, Mirmira RG, Jetton TL, and Poitout V (2008) Cyclical and alternating infusions of glucose and intralipid in rats inhibit insulin gene expression and Pdx-1 binding in islets. *Diabetes,* **57,** 424-431.

134. Hailey DW, Rambold AS, Satpute-Krishnan P, Mitra K, Sougrat R, Kim PK, and Lippincott-Schwartz J (2010) Mitochondria supply membranes for autophagosome biogenesis during starvation. *Cell,* **141,** 656-667.

135. Han XJ, Tomizawa K, Fujimura A, Ohmori I, Nishiki T, Matsushita M, and Matsui H (2011) Regulation of mitochondrial dynamics and neurodegenerative diseases. *Acta Med Okayama,* **65,** 1-10.

136. Hara T, Nakamura K, Matsui M, Yamamoto A, Nakahara Y, Suzuki-Migishima R, Yokoyama M, Mishima K, Saito I, Okano H, and Mizushima N (2006) Suppression of basal autophagy in neural cells causes neurodegenerative disease in mice. *Nature,* **441,** 885-889.

137. HARMAN D (1956) Aging: a theory based on free radical and radiation chemistry. *J Gerontol,* **11,** 298-300.

138. Havrankova J, Roth J, and Brownstein M (1978a) Insulin receptors are widely distributed in the central nervous system of the rat. *Nature,* **272,** 827-829.

139. Havrankova J, Schmechel D, Roth J, and Brownstein M (1978b) Identification of insulin in rat brain. *Proc Natl Acad Sci U S A,* **75,** 5737-5741.

140. Heart E, Corkey RF, Wikstrom JD, Shirihai OS, and Corkey BE (2006) Glucose-dependent increase in mitochondrial membrane potential, but not cytoplasmic calcium, correlates with insulin secretion in single islet cells. *Am J Physiol Endocrinol Metab,* **290,** E143-E148.

141. Heath-Engel HM and Shore GC (2006) Mitochondrial membrane dynamics, cristae remodelling and apoptosis. *Biochim Biophys Acta,* **1763,** 549-560.

142. Henquin JC (2000) Triggering and amplifying pathways of regulation of insulin secretion by glucose. *Diabetes,* **49,** 1751-1760.

143. Henquin JC (2011) The dual control of insulin secretion by glucose involves triggering and amplifying pathways in beta-cells. *Diabetes Res Clin Pract,* **93 Suppl 1,** S27-S31.

144. Heuett WJ and Periwal V (2010) Autoregulation of free radicals via uncoupling protein control in pancreatic beta-cell mitochondria. *Biophys J,* **98,** 207-217.

145. Higa M, Zhou YT, Ravazzola M, Baetens D, Orci L, and Unger RH (1999) Troglitazone prevents mitochondrial alterations, beta cell destruction, and diabetes in obese prediabetic rats. *Proc Natl Acad Sci U S A,* **96,** 11513-11518.

146. Hrytsenko O, Wright JR, Jr., Morrison CM, and Pohajdak B (2007) Insulin expression in the brain and pituitary cells of tilapia (Oreochromis niloticus). *Brain Res,* **1135,** 31-40.

147. Huang P, Yu T, and Yoon Y (2007) Mitochondrial clustering induced by overexpression of the mitochondrial fusion protein Mfn2 causes mitochondrial dysfunction and cell death. *Eur J Cell Biol,* **86,** 289-302.

148. Hyde BB, Twig G, and Shirihai OS (2010) Organellar vs cellular control of mitochondrial dynamics. *Semin Cell Dev Biol,* **21,** 575-581.

149. Inberg A and Linial M (2010) Protection of pancreatic beta-cells from various stress conditions is mediated by DJ-1. *J Biol Chem,* **285,** 25686-25698.

150. James DI, Parone PA, Mattenberger Y, and Martinou JC (2003) hFis1, a novel component of the mammalian mitochondrial fission machinery. *J Biol Chem,* **278,** 36373-36379.

151. Jensen MV, Joseph JW, Ronnebaum SM, Burgess SC, Sherry AD, and Newgard CB (2008) Metabolic cycling in control of glucose-stimulated insulin secretion. *Am J Physiol Endocrinol Metab,* **295,** E1287-E1297.

152. Jetton TL, Lausier J, LaRock K, Trotman WE, Larmie B, Habibovic A, Peshavaria M, and Leahy JL (2005) Mechanisms of compensatory beta-cell growth in insulin-resistant rats: roles of Akt kinase. *Diabetes,* **54,** 2294-2304.

153. Jin SM, Lazarou M, Wang C, Kane LA, Narendra DP, and Youle RJ (2010) Mitochondrial membrane potential regulates PINK1 import and proteolytic destabilization by PARL. *J Cell Biol,* **191,** 933-942.

154. Jitrapakdee S, Wutthisathapornchai A, Wallace JC, and MacDonald MJ (2010) Regulation of insulin secretion: role of mitochondrial signalling. *Diabetologia,* **53,** 1019-1032.

155. Ju JS and Weihl CC (2010) Inclusion body myopathy, Paget's disease of the bone and fronto-temporal dementia: a disorder of autophagy. *Hum Mol Genet,* **19,** R38-R45.

156. Kadenbach B (2003) Intrinsic and extrinsic uncoupling of oxidative phosphorylation. *Biochim Biophys Acta,* **1604,** 77-94.

157. Kaneto H, Xu G, Fujii N, Kim S, Bonner-Weir S, and Weir GC (2002) Involvement of c-Jun N-terminal kinase in oxidative stress-mediated suppression of insulin gene expression. *J Biol Chem,* **277,** 30010-30018.

158. Kanki T and Klionsky DJ (2010) The molecular mechanism of mitochondria autophagy in yeast. *Mol Microbiol,* **75,** 795-800.

159. Kanki T, Wang K, Baba M, Bartholomew CR, Lynch-Day MA, Du Z, Geng J, Mao K, Yang Z, Yen WL, and Klionsky DJ (2009a) A genomic screen for yeast mutants defective in selective mitochondria autophagy. *Mol Biol Cell,* **20,** 4730-4738.

160. Kanki T, Wang K, Cao Y, Baba M, and Klionsky DJ (2009b) Atg32 is a mitochondrial protein that confers selectivity during mitophagy. *Dev Cell,* **17,** 98-109.

161. Karbowski M (2010) Mitochondria on guard: role of mitochondrial fusion and fission in the regulation of apoptosis. *Adv Exp Med Biol,* **687,** 131-142.

162. Karbowski M, Arnoult D, Chen H, Chan DC, Smith CL, and Youle RJ (2004) Quantitation of mitochondrial dynamics by photolabeling of individual organelles shows that mitochondrial fusion is blocked during the Bax activation phase of apoptosis. *J Cell Biol,* **164,** 493-499.

163. Karbowski M and Youle RJ (2011) Regulating mitochondrial outer membrane proteins by ubiquitination and proteasomal degradation. *Curr Opin Cell Biol,* **23,** 476-482.

164. Katzman SM, Messerli MA, Barry DT, Grossman A, Harel T, Wikstrom JD, Corkey BE, Smith PJ, and Shirihai OS (2004) Mitochondrial metabolism reveals a functional architecture in intact islets of Langerhans from normal and diabetic Psammomys obesus. *Am J Physiol Endocrinol Metab,* **287,** E1090-E1099.

165. Kelley DE, He J, Menshikova EV, and Ritov VB (2002) Dysfunction of mitochondria in human skeletal muscle in type 2 diabetes. *Diabetes,* **51,** 2944-2950.

166. Kibbey RG, Pongratz RL, Romanelli AJ, Wollheim CB, Cline GW, and Shulman GI (2007) Mitochondrial GTP regulates glucose-stimulated insulin secretion. *Cell Metab,* **5,** 253-264.

167. Kim H, Rafiuddin-Shah M, Tu HC, Jeffers JR, Zambetti GP, Hsieh JJ, and Cheng EH (2006) Hierarchical regulation of mitochondrion-dependent apoptosis by BCL-2 subfamilies. *Nat Cell Biol,* **8,** 1348-1358.

168. Kim I, Rodriguez-Enriquez S, and Lemasters JJ (2007) Selective degradation of mitochondria by mitophagy. *Arch Biochem Biophys,* **462,** 245-253.

169. Kim SP, Ellmerer M, Van Citters GW, and Bergman RN (2003) Primacy of hepatic insulin resistance in the development of the metabolic syndrome induced by an isocaloric moderate-fat diet in the dog. *Diabetes,* **52,** 2453-2460.

170. Kinnally KW and Antonsson B (2007) A tale of two mitochondrial channels, MAC and PTP, in apoptosis. *Apoptosis,* **12,** 857-868.

171. Kissova I, Deffieu M, Manon S, and Camougrand N (2004) Uth1p is involved in the autophagic degradation of mitochondria. *J Biol Chem,* **279,** 39068-39074.

172. Kitada T, Pisani A, Porter DR, Yamaguchi H, Tscherter A, Martella G, Bonsi P, Zhang C, Pothos EN, and Shen J (2007) Impaired dopamine release and synaptic plasticity in the striatum of PINK1-deficient mice. *Proc Natl Acad Sci U S A,* **104,** 11441-11446.

173. Kitada T, Tong Y, Gautier CA, and Shen J (2009) Absence of nigral degeneration in aged parkin/DJ-1/PINK1 triple knockout mice. *J Neurochem,* **111,** 696-702.

174. Klingenberg M and Buchholz M (1973) On the mechanism of bongkrekate effect on the mitochondrial adenine-nucleotide carrier as studied through the binding of ADP. *Eur J Biochem,* **38,** 346-358.

175. Klionsky DJ (2007) Autophagy: from phenomenology to molecular understanding in less than a decade. *Nat Rev Mol Cell Biol,* **8,** 931-937.

176. Knight JA (2011) Diseases and disorders associated with excess body weight. *Ann Clin Lab Sci,* **41,** 107-121.

177. Koch A, Thiemann M, Grabenbauer M, Yoon Y, McNiven MA, and Schrader M (2003) Dynamin-like protein 1 is involved in peroxisomal fission. *J Biol Chem,* **278,** 8597-8605.

178. Koch A, Yoon Y, Bonekamp NA, McNiven MA, and Schrader M (2005) A role for Fis1 in both mitochondrial and peroxisomal fission in mammalian cells. *Mol Biol Cell,* **16,** 5077-5086.

179. Koch L, Wunderlich FT, Seibler J, Konner AC, Hampel B, Irlenbusch S, Brabant G, Kahn CR, Schwenk F, and Bruning JC (2008) Central insulin action regulates peripheral glucose and fat metabolism in mice. *J Clin Invest,* **118,** 2132-2147.

180. Komatsu M, Waguri S, Chiba T, Murata S, Iwata J, Tanida I, Ueno T, Koike M, Uchiyama Y, Kominami E, and Tanaka K (2006) Loss of autophagy in the central nervous system causes neurodegeneration in mice. *Nature,* **441,** 880-884.

181. Komatsu M, Wang QJ, Holstein GR, Friedrich VL, Jr., Iwata J, Kominami E, Chait BT, Tanaka K, and Yue Z (2007) Essential role for autophagy protein Atg7 in the maintenance of axonal homeostasis and the prevention of axonal degeneration. *Proc Natl Acad Sci U S A,* **104,** 14489-14494.

182. Kundu M, Lindsten T, Yang CY, Wu J, Zhao F, Zhang J, Selak MA, Ney PA, and Thompson CB (2008) Ulk1 plays a critical role in the autophagic clearance of mitochondria and ribosomes during reticulocyte maturation. *Blood,* **112,** 1493-1502.

183. Lacy PE and Kostianovsky M (1967) Method for the isolation of intact islets of Langerhans from the rat pancreas. *Diabetes,* **16,** 35-39.

184. Le SC and Bougneres P (1994) Early changes in postprandial insulin secretion, not in insulin sensitivity, characterize juvenile obesity. *Diabetes,* **43,** 696-702.

185. Le SC, Fallin D, Schork NJ, and Bougneres P (2000) The insulin gene VNTR is associated with fasting insulin levels and development of juvenile obesity. *Nat Genet,* **26,** 444-446.

186. Lee J, Schriner SE, and Wallace DC (2009a) Adenine nucleotide translocator 1 deficiency increases resistance of mouse brain and neurons to excitotoxic insults. *Biochim Biophys Acta,* **1787,** 364-370.

187. Lee J, Schriner SE, and Wallace DC (2009b) Adenine nucleotide translocator 1 deficiency increases resistance of mouse brain and neurons to excitotoxic insults. *Biochim Biophys Acta,* **1787,** 364-370.

188. Lee JA and Gao FB (2008) ESCRT, autophagy, and frontotemporal dementia. *BMB Rep,* **41,** 827-832.

189. Lee JY, Nagano Y, Taylor JP, Lim KL, and Yao TP (2010) Disease-causing mutations in parkin impair mitochondrial ubiquitination, aggregation, and HDAC6-dependent mitophagy. *J Cell Biol,* **189,** 671-679.

190. Lee JY, Ristow M, Lin X, White MF, Magnuson MA, and Hennighausen L (2006) RIP-Cre revisited, evidence for impairments of pancreatic beta-cell function. *J Biol Chem,* **281,** 2649-2653.

191. Lee YJ, Jeong SY, Karbowski M, Smith CL, and Youle RJ (2004) Roles of the mammalian mitochondrial fission and fusion mediators Fis1, Drp1, and Opa1 in apoptosis. *Mol Biol Cell,* **15,** 5001-5011.

192. Lemasters JJ (2005) Selective mitochondrial autophagy, or mitophagy, as a targeted defense against oxidative stress, mitochondrial dysfunction, and aging. *Rejuvenation Res,* **8,** 3-5.

193. Lemasters JJ, Nieminen AL, Qian T, Trost LC, Elmore SP, Nishimura Y, Crowe RA, Cascio WE, Bradham CA, Brenner DA, and Herman B (1998) The mitochondrial permeability transition in cell death: a common mechanism in necrosis, apoptosis and autophagy. *Biochim Biophys Acta,* **1366,** 177-196.

194. Letai A, Bassik MC, Walensky LD, Sorcinelli MD, Weiler S, and Korsmeyer SJ (2002) Distinct BH3 domains either sensitize or activate mitochondrial apoptosis, serving as prototype cancer therapeutics. *Cancer Cell,* **2,** 183-192.

195. Lev N, Ickowicz D, Melamed E, and Offen D (2008) Oxidative insults induce DJ-1 upregulation and redistribution: implications for neuroprotection. *Neurotoxicology,* **29,** 397-405.

196. Liesa M, Palacin M, and Zorzano A (2009) Mitochondrial dynamics in mammalian health and disease. *Physiol Rev,* **89,** 799-845.

197. Lin X, Taguchi A, Park S, Kushner JA, Li F, Li Y, and White MF (2004) Dysregulation of insulin receptor substrate 2 in beta cells and brain causes obesity and diabetes. *J Clin Invest,* **114,** 908-916.

198. Liu W, Vives-Bauza C, Acin P, Yamamoto A, Tan Y, Li Y, Magrane J, Stavarache MA, Shaffer S, Chang S, Kaplitt MG, Huang XY, Beal MF, Manfredi G, and Li C (2009a) PINK1 defect causes mitochondrial dysfunction, proteasomal deficit and alpha-synuclein aggregation in cell culture models of Parkinson's disease. *PLoS One,* **4,** e4597.

199. Liu X and Hajnoczky G (2009b) Ca2+-dependent regulation of mitochondrial dynamics by the Miro-Milton complex. *Int J Biochem Cell Biol,* **41,** 1972-1976.

200. Liu X, Weaver D, Shirihai O, and Hajnoczky G (2009c) Mitochondrial 'kiss-and-run': interplay between mitochondrial motility and fusion-fission dynamics. *EMBO J,* **28,** 3074-3089.

201. Loiseau D, Chevrollier A, Verny C, Guillet V, Gueguen N, Pou de Crescenzo MA, Ferre M, Malinge MC, Guichet A, Nicolas G, mati-Bonneau P, Malthiery Y, Bonneau D, and Reynier P (2007) Mitochondrial coupling defect in Charcot-Marie-Tooth type 2A disease. *Ann Neurol,* **61,** 315-323.

202. Lowell BB and Shulman GI (2005) Mitochondrial dysfunction and type 2 diabetes. *Science,* **307,** 384-387.

203. Lund A, Knop FK, and Vilsboll T (2011) Emerging GLP-1 receptor agonists. *Expert Opin Emerg Drugs*.

204. Lutz AK, Exner N, Fett ME, Schlehe JS, Kloos K, Lammermann K, Brunner B, Kurz-Drexler A, Vogel F, Reichert AS, Bouman L, Vogt-Weisenhorn D, Wurst W, Tatzelt J, Haass C, and Winklhofer KF (2009) Loss of parkin or PINK1 function increases Drp1-dependent mitochondrial fragmentation. *J Biol Chem,* **284,** 22938-22951.

205. Macaskill AF, Rinholm JE, Twelvetrees AE, rancibia-Carcamo IL, Muir J, Fransson A, Aspenstrom P, Attwell D, and Kittler JT (2009) Miro1 is a calcium sensor for glutamate receptor-dependent localization of mitochondria at synapses. *Neuron,* **61,** 541-555.

206. Madadi G, Dalvi PS, and Belsham DD (2008) Regulation of brain insulin mRNA by glucose and glucagon-like peptide 1. *Biochem Biophys Res Commun,* **376,** 694-699.

207. Maechler P (2002) Mitochondria as the conductor of metabolic signals for insulin exocytosis in pancreatic beta-cells. *Cell Mol Life Sci,* **59,** 1803-1818.

208. Maechler P, Carobbio S, and Rubi B (2006) In beta-cells, mitochondria integrate and generate metabolic signals controlling insulin secretion. *Int J Biochem Cell Biol,* **38,** 696-709.

209. Maechler P, Jornot L, and Wollheim CB (1999) Hydrogen peroxide alters mitochondrial activation and insulin secretion in pancreatic beta cells. *J Biol Chem,* **274,** 27905-27913.

210. Maechler P and Wollheim CB (2001) Mitochondrial function in normal and diabetic beta-cells. *Nature,* **414,** 807-812.

211. Marongiu R, Spencer B, Crews L, Adame A, Patrick C, Trejo M, Dallapiccola B, Valente EM, and Masliah E (2009) Mutant Pink1 induces mitochondrial dysfunction in a neuronal cell model of Parkinson's disease by disturbing calcium flux. *J Neurochem,* **108,** 1561-1574.

212. Matsuda N, Sato S, Shiba K, Okatsu K, Saisho K, Gautier CA, Sou YS, Saiki S, Kawajiri S, Sato F, Kimura M, Komatsu M, Hattori N, and Tanaka K (2010)

PINK1 stabilized by mitochondrial depolarization recruits Parkin to damaged mitochondria and activates latent Parkin for mitophagy. *J Cell Biol,* **189,** 211-221.

213. Matsuda N and Tanaka K (2010) Uncovering the roles of PINK1 and parkin in mitophagy. *Autophagy,* **6,** 952-954.

214. Matsuda W, Furuta T, Nakamura KC, Hioki H, Fujiyama F, Arai R, and Kaneko T (2009) Single nigrostriatal dopaminergic neurons form widely spread and highly dense axonal arborizations in the neostriatum. *J Neurosci,* **29,** 444-453.

215. Maynard S, Schurman SH, Harboe C, de Souza-Pinto NC, and Bohr VA (2009) Base excision repair of oxidative DNA damage and association with cancer and aging. *Carcinogenesis,* **30,** 2-10.

216. Mazure NM and Pouyssegur J (2009) Atypical BH3-domains of BNIP3 and BNIP3L lead to autophagy in hypoxia. *Autophagy,* **5,** 868-869.

217. Meeusen SL and Nunnari J (2007) Mitochondrial fusion in vitro. *Methods Mol Biol,* **372,** 461-466.

218. Men X, Wang H, Li M, Cai H, Xu S, Zhang W, Xu Y, Ye L, Yang W, Wollheim CB, and Lou J (2009) Dynamin-related protein 1 mediates high glucose induced pancreatic beta cell apoptosis. *Int J Biochem Cell Biol,* **41,** 879-890.

219. Merz S, Hammermeister M, Altmann K, Durr M, and Westermann B (2007) Molecular machinery of mitochondrial dynamics in yeast. *Biol Chem,* **388,** 917-926.

220. Mills RD, Sim CH, Mok SS, Mulhern TD, Culvenor JG, and Cheng HC (2008) Biochemical aspects of the neuroprotective mechanism of PTEN-induced kinase-1 (PINK1). *J Neurochem,* **105,** 18-33.

221. Mingrone G, Manco M, Calvani M, Castagneto M, Naon D, and Zorzano A (2005) Could the low level of expression of the gene encoding skeletal muscle mitofusin-2 account for the metabolic inflexibility of obesity? *Diabetologia,* **48,** 2108-2114.

222. Misaka T, Miyashita T, and Kubo Y (2002) Primary structure of a dynamin-related mouse mitochondrial GTPase and its distribution in brain, subcellular localization, and effect on mitochondrial morphology. *J Biol Chem,* **277,** 15834-15842.

223. Misko A, Jiang S, Wegorzewska I, Milbrandt J, and Baloh RH (2010) Mitofusin 2 is necessary for transport of axonal mitochondria and interacts with the Miro/Milton complex. *J Neurosci,* **30,** 4232-4240.

224. Molina AJ and Shirihai OS (2009) Monitoring mitochondrial dynamics with photoactivatable [corrected] green fluorescent protein. *Methods Enzymol,* **457,** 289-304.

225. Molina AJ, Wikstrom JD, Stiles L, Las G, Mohamed H, Elorza A, Walzer G, Twig G, Katz S, Corkey BE, and Shirihai OS (2009) Mitochondrial networking protects beta-cells from nutrient-induced apoptosis. *Diabetes,* **58,** 2303-2315.

226. Moore DJ, Zhang L, Troncoso J, Lee MK, Hattori N, Mizuno Y, Dawson TM, and Dawson VL (2005) Association of DJ-1 and parkin mediated by pathogenic DJ-1 mutations and oxidative stress. *Hum Mol Genet,* **14,** 71-84.

227. Moreira PI, Siedlak SL, Wang X, Santos MS, Oliveira CR, Tabaton M, Nunomura A, Szweda LI, Aliev G, Smith MA, Zhu X, and Perry G (2007a) Autophagocytosis of mitochondria is prominent in Alzheimer disease. *J Neuropathol Exp Neurol,* **66,** 525-532.

228. Moreira PI, Siedlak SL, Wang X, Santos MS, Oliveira CR, Tabaton M, Nunomura A, Szweda LI, Aliev G, Smith MA, Zhu X, and Perry G (2007b) Increased autophagic degradation of mitochondria in Alzheimer disease. *Autophagy,* **3,** 614-615.

229. Mori H, Inoki K, Munzberg H, Opland D, Faouzi M, Villanueva EC, Ikenoue T, Kwiatkowski D, MacDougald OA, Myers MG, Jr., and Guan KL (2009) Critical role for hypothalamic mTOR activity in energy balance. *Cell Metab,* **9,** 362-374.

230. Mouli PK, Twig G, and Shirihai OS (2009) Frequency and selectivity of mitochondrial fusion are key to its quality maintenance function. *Biophys J,* **96,** 3509-3518.

231. Nagakubo D, Taira T, Kitaura H, Ikeda M, Tamai K, Iguchi-Ariga SM, and Ariga H (1997) DJ-1, a novel oncogene which transforms mouse NIH3T3 cells in cooperation with ras. *Biochem Biophys Res Commun,* **231,** 509-513.

232. Nakada K, Inoue K, Ono T, Isobe K, Ogura A, Goto YI, Nonaka I, and Hayashi JI (2001) Inter-mitochondrial complementation: Mitochondria-specific system preventing mice from expression of disease phenotypes by mutant mtDNA. *Nat Med,* **7,** 934-940.

233. Narendra D, Tanaka A, Suen DF, and Youle RJ (2008) Parkin is recruited selectively to impaired mitochondria and promotes their autophagy. *J Cell Biol,* **183,** 795-803.

234. Narendra DP, Jin SM, Tanaka A, Suen DF, Gautier CA, Shen J, Cookson MR, and Youle RJ (2010) PINK1 is selectively stabilized on impaired mitochondria to activate Parkin. *PLoS Biol,* **8,** e1000298.

235. Narendra DP and Youle RJ (2011) Targeting mitochondrial dysfunction: role for PINK1 and Parkin in mitochondrial quality control. *Antioxid Redox Signal,* **14,** 1929-1938.

236. Navratil M, Terman A, and Arriaga EA (2008) Giant mitochondria do not fuse and exchange their contents with normal mitochondria. *Exp Cell Res,* **314,** 164-172.

237. Nice DC, Sato TK, Stromhaug PE, Emr SD, and Klionsky DJ (2002) Cooperative binding of the cytoplasm to vacuole targeting pathway proteins, Cvt13 and Cvt20, to phosphatidylinositol 3-phosphate at the pre-autophagosomal structure is required for selective autophagy. *J Biol Chem,* **277,** 30198-30207.

238. Nishida Y, Arakawa S, Fujitani K, Yamaguchi H, Mizuta T, Kanaseki T, Komatsu M, Otsu K, Tsujimoto Y, and Shimizu S (2009) Discovery of Atg5/Atg7-independent alternative macroautophagy. *Nature,* **461,** 654-658.

239. Nixon RA (2006) Autophagy in neurodegenerative disease: friend, foe or turncoat? *Trends Neurosci,* **29,** 528-535.

240. Nixon RA, Wegiel J, Kumar A, Yu WH, Peterhoff C, Cataldo A, and Cuervo AM (2005) Extensive involvement of autophagy in Alzheimer disease: an immuno-electron microscopy study. *J Neuropathol Exp Neurol,* **64,** 113-122.

241. Nobes CD, Hay WW, Jr., and Brand MD (1990) The mechanism of stimulation of respiration by fatty acids in isolated hepatocytes. *J Biol Chem,* **265,** 12910-12915.

242. Noske AB, Costin AJ, Morgan GP, and Marsh BJ (2008) Expedited approaches to whole cell electron tomography and organelle mark-up in situ in high-pressure frozen pancreatic islets. *J Struct Biol,* **161,** 298-313.

243. Nowikovsky K, Reipert S, Devenish RJ, and Schweyen RJ (2007) Mdm38 protein depletion causes loss of mitochondrial K+/H+ exchange activity, osmotic swelling and mitophagy. *Cell Death Differ,* **14,** 1647-1656.

244. Okamoto K, Kondo-Okamoto N, and Ohsumi Y (2009a) A landmark protein essential for mitophagy: Atg32 recruits the autophagic machinery to mitochondria. *Autophagy,* **5,** 1203-1205.

245. Okamoto K, Kondo-Okamoto N, and Ohsumi Y (2009b) Mitochondria-anchored receptor Atg32 mediates degradation of mitochondria via selective autophagy. *Dev Cell,* **17,** 87-97.

246. Olichon A, Baricault L, Gas N, Guillou E, Valette A, Belenguer P, and Lenaers G (2003) Loss of OPA1 perturbates the mitochondrial inner membrane structure and integrity, leading to cytochrome c release and apoptosis. *J Biol Chem,* **278,** 7743-7746.

247. Orenstein SJ and Cuervo AM (2010) Chaperone-mediated autophagy: Molecular mechanisms and physiological relevance. *Semin Cell Dev Biol*.

248. Orrenius S (1985) Oxidative stress studied in intact mammalian cells. *Philos Trans R Soc Lond B Biol Sci,* **311,** 673-677.

249. Otera H and Mihara K (2011) Molecular mechanisms and physiologic functions of mitochondrial dynamics. *J Biochem,* **149,** 241-251.

250. Otera H, Wang C, Cleland MM, Setoguchi K, Yokota S, Youle RJ, and Mihara K (2010) Mff is an essential factor for mitochondrial recruitment of Drp1 during mitochondrial fission in mammalian cells. *J Cell Biol,* **191,** 1141-1158.

251. Papanicolaou KN, Khairallah RJ, Ngoh GA, Chikando A, Luptak I, O'Shea KM, Riley DD, Lugus JJ, Colucci WS, Lederer WJ, Stanley WC, and Walsh K (2011) Mitofusin-2 maintains mitochondrial structure and contributes to stress-induced permeability transition in cardiac myocytes. *Mol Cell Biol,* **31,** 1309-1328.

252. Park J, Lee G, and Chung J (2009) The PINK1-Parkin pathway is involved in the regulation of mitochondrial remodeling process. *Biochem Biophys Res Commun,* **378,** 518-523.

253. Park KS, Wiederkehr A, Kirkpatrick C, Mattenberger Y, Martinou JC, Marchetti P, Demaurex N, and Wollheim CB (2008) Selective actions of mitochondrial fission/fusion genes on metabolism-secretion coupling in insulin-releasing cells. *J Biol Chem,* **283,** 33347-33356.

254. Parone PA, Da CS, Tondera D, Mattenberger Y, James DI, Maechler P, Barja F, and Martinou JC (2008) Preventing mitochondrial fission impairs mitochondrial function and leads to loss of mitochondrial DNA. *PLoS One,* **3,** e3257.

255. Parone PA, James DI, Da CS, Mattenberger Y, Donze O, Barja F, and Martinou JC (2006) Inhibiting the mitochondrial fission machinery does not prevent Bax/Bak-dependent apoptosis. *Mol Cell Biol,* **26,** 7397-7408.

256. Patel M and Day BJ (1999) Metalloporphyrin class of therapeutic catalytic antioxidants. *Trends Pharmacol Sci,* **20,** 359-364.

257. Perez-Campo R, Lopez-Torres M, Cadenas S, Rojas C, and Barja G (1998) The rate of free radical production as a determinant of the rate of aging: evidence from the comparative approach. *J Comp Physiol B,* **168,** 149-158.

258. Pi J, Bai Y, Zhang Q, Wong V, Floering LM, Daniel K, Reece JM, Deeney JT, Andersen ME, Corkey BE, and Collins S (2007) Reactive oxygen species as a signal in glucose-stimulated insulin secretion. *Diabetes,* **56,** 1783-1791.

259. Pich S, Bach D, Briones P, Liesa M, Camps M, Testar X, Palacin M, and Zorzano A (2005) The Charcot-Marie-Tooth type 2A gene product, Mfn2, up-regulates

fuel oxidation through expression of OXPHOS system. *Hum Mol Genet,* **14,** 1405-1415.

260. Poitout V (2008) Glucolipotoxicity of the pancreatic beta-cell: myth or reality? *Biochem Soc Trans,* **36,** 901-904.

261. Poitout V and Robertson RP (2002) Minireview: Secondary beta-cell failure in type 2 diabetes--a convergence of glucotoxicity and lipotoxicity. *Endocrinology,* **143,** 339-342.

262. Poitout V and Robertson RP (2008) Glucolipotoxicity: fuel excess and beta-cell dysfunction. *Endocr Rev,* **29,** 351-366.

263. Poole AC, Thomas RE, Andrews LA, McBride HM, Whitworth AJ, and Pallanck LJ (2008) The PINK1/Parkin pathway regulates mitochondrial morphology. *Proc Natl Acad Sci U S A,* **105,** 1638-1643.

264. Poole AC, Thomas RE, Yu S, Vincow ES, and Pallanck L (2010) The mitochondrial fusion-promoting factor mitofusin is a substrate of the PINK1/parkin pathway. *PLoS One,* **5,** e10054.

265. Pories WJ, Swanson MS, MacDonald KG, Long SB, Morris PG, Brown BM, Barakat HA, deRamon RA, Israel G, Dolezal JM, and . (1995) Who would have thought it? An operation proves to be the most effective therapy for adult-onset diabetes mellitus. *Ann Surg,* **222,** 339-350.

266. Praefcke GJ and McMahon HT (2004) The dynamin superfamily: universal membrane tubulation and fission molecules? *Nat Rev Mol Cell Biol,* **5,** 133-147.

267. Prigione A, Piazza F, Brighina L, Begni B, Galbussera A, Difrancesco JC, Andreoni S, Piolti R, and Ferrarese C (2010) Alpha-synuclein nitration and autophagy response are induced in peripheral blood cells from patients with Parkinson disease. *Neurosci Lett,* **477,** 6-10.

268. Rasola A and Bernardi P (2007) The mitochondrial permeability transition pore and its involvement in cell death and in disease pathogenesis. *Apoptosis,* **12,** 815-833.

269. Reggiori F, Tucker KA, Stromhaug PE, and Klionsky DJ (2004) The Atg1-Atg13 complex regulates Atg9 and Atg23 retrieval transport from the pre-autophagosomal structure. *Dev Cell,* **6,** 79-90.

270. Rich PR (2003) The molecular machinery of Keilin's respiratory chain. *Biochem Soc Trans,* **31,** 1095-1105.

271. Richard D and Picard F (2011) Brown fat biology and thermogenesis. *Front Biosci,* **16,** 1233-1260.

272. Robertson R, Zhou H, Zhang T, and Harmon JS (2007) Chronic oxidative stress as a mechanism for glucose toxicity of the beta cell in type 2 diabetes. *Cell Biochem Biophys,* **48,** 139-146.

273. Robertson RP (2006) Oxidative stress and impaired insulin secretion in type 2 diabetes. *Curr Opin Pharmacol,* **6,** 615-619.

274. Roduit R, Morin J, Masse F, Segall L, Roche E, Newgard CB, ssimacopoulos-Jeannet F, and Prentki M (2000) Glucose down-regulates the expression of the peroxisome proliferator-activated receptor-alpha gene in the pancreatic beta -cell. *J Biol Chem,* **275,** 35799-35806.

275. Rolfe DF and Brand MD (1996) Contribution of mitochondrial proton leak to skeletal muscle respiration and to standard metabolic rate. *Am J Physiol,* **271,** C1380-C1389.

276. Rolfe DF and Brand MD (1997) The physiological significance of mitochondrial proton leak in animal cells and tissues. *Biosci Rep,* **17,** 9-16.

277. Rubinson DA, Dillon CP, Kwiatkowski AV, Sievers C, Yang L, Kopinja J, Rooney DL, Zhang M, Ihrig MM, McManus MT, Gertler FB, Scott ML, and Van PL (2003) A lentivirus-based system to functionally silence genes in primary mammalian cells, stem cells and transgenic mice by RNA interference. *Nat Genet,* **33,** 401-406.

278. Rujiviphat J, Meglei G, Rubinstein JL, and McQuibban GA (2009) Phospholipid association is essential for dynamin-related protein Mgm1 to function in mitochondrial membrane fusion. *J Biol Chem,* **284,** 28682-28686.

279. Sandebring A, Thomas KJ, Beilina A, van der BM, Cleland MM, Ahmad R, Miller DW, Zambrano I, Cowburn RF, Behbahani H, Cedazo-Minguez A, and Cookson MR (2009) Mitochondrial alterations in PINK1 deficient cells are influenced by calcineurin-dependent dephosphorylation of dynamin-related protein 1. *PLoS One,* **4,** e5701.

280. Santel A and Fuller MT (2001) Control of mitochondrial morphology by a human mitofusin. *J Cell Sci,* **114,** 867-874.

281. Santos JH, Meyer JN, Mandavilli BS, and Van HB (2006) Quantitative PCR-based measurement of nuclear and mitochondrial DNA damage and repair in mammalian cells. *Methods Mol Biol,* **314,** 183-199.

282. Santos RX, Correia SC, Wang X, Perry G, Smith MA, Moreira PI, and Zhu X (2010) A synergistic dysfunction of mitochondrial fission/fusion dynamics and mitophagy in Alzheimer's disease. *J Alzheimers Dis,* **20 Suppl 2,** S401-S412.

283. Saotome M, Safiulina D, Szabadkai G, Das S, Fransson A, Aspenstrom P, Rizzuto R, and Hajnoczky G (2008) Bidirectional Ca2+-dependent control of

mitochondrial dynamics by the Miro GTPase. *Proc Natl Acad Sci U S A,* **105,** 20728-20733.

284. Schafer A and Reichert AS (2009) Emerging roles of mitochondrial membrane dynamics in health and disease. *Biol Chem,* **390,** 707-715.

285. Schechter R, Beju D, Gaffney T, Schaefer F, and Whetsell L (1996) Preproinsulin I and II mRNAs and insulin electron microscopic immunoreaction are present within the rat fetal nervous system. *Brain Res,* **736,** 16-27.

286. Scheckhuber CQ, Erjavec N, Tinazli A, Hamann A, Nystrom T, and Osiewacz HD (2007) Reducing mitochondrial fission results in increased life span and fitness of two fungal ageing models. *Nat Cell Biol,* **9,** 99-105.

287. Schwanstecher C and Schwanstecher M (2011) Targeting type 2 diabetes. *Handb Exp Pharmacol,* 1-33.

288. Scorrano L, Ashiya M, Buttle K, Weiler S, Oakes SA, Mannella CA, and Korsmeyer SJ (2002) A distinct pathway remodels mitochondrial cristae and mobilizes cytochrome c during apoptosis. *Dev Cell,* **2,** 55-67.

289. Shi G, Lee JR, Grimes DA, Racacho L, Ye D, Yang H, Ross OA, Farrer M, McQuibban GA, and Bulman DE (2011) Functional alteration of PARL contributes to mitochondrial dysregulation in Parkinson's disease. *Hum Mol Genet,* **20,** 1966-1974.

290. Skre H (1974) Genetic and clinical aspects of Charcot-Marie-Tooth's disease. *Clin Genet,* **6,** 98-118.

291. Skulachev VP (2001) Mitochondrial filaments and clusters as intracellular power-transmitting cables. *Trends Biochem Sci,* **26,** 23-29.

292. Smith PM and Lightowlers RN (2011) Altering the balance between healthy and mutated mitochondrial DNA. *J Inherit Metab Dis,* **34,** 309-313.

293. Sohal RS and Allen RG (1985) Relationship between metabolic rate, free radicals, differentiation and aging: a unified theory. *Basic Life Sci,* **35,** 75-104.

294. Song J, Xu Y, Hu X, Choi B, and Tong Q (2010) Brain expression of Cre recombinase driven by pancreas-specific promoters. *Genesis,* **48,** 628-634.

295. Song Z, Chen H, Fiket M, Alexander C, and Chan DC (2007) OPA1 processing controls mitochondrial fusion and is regulated by mRNA splicing, membrane potential, and Yme1L. *J Cell Biol,* **178,** 749-755.

296. Sou YS, Waguri S, Iwata J, Ueno T, Fujimura T, Hara T, Sawada N, Yamada A, Mizushima N, Uchiyama Y, Kominami E, Tanaka K, and Komatsu M (2008) The

Atg8 conjugation system is indispensable for proper development of autophagic isolation membranes in mice. *Mol Biol Cell,* **19,** 4762-4775.

297. Springer W and Kahle PJ (2011) Regulation of PINK1-Parkin-mediated mitophagy. *Autophagy,* **7,** 266-278.

298. Srinivasan S, Bernal-Mizrachi E, Ohsugi M, and Permutt MA (2002) Glucose promotes pancreatic islet beta-cell survival through a PI 3-kinase/Akt-signaling pathway. *Am J Physiol Endocrinol Metab,* **283,** E784-E793.

299. Stack JH, DeWald DB, Takegawa K, and Emr SD (1995) Vesicle-mediated protein transport: regulatory interactions between the Vps15 protein kinase and the Vps34 PtdIns 3-kinase essential for protein sorting to the vacuole in yeast. *J Cell Biol,* **129,** 321-334.

300. Stephenson FA (2010) Activity-dependent immobilization of mitochondria: the role of miro. *Front Mol Neurosci,* **3,** 9.

301. Stojanovski D, Koutsopoulos OS, Okamoto K, and Ryan MT (2004) Levels of human Fis1 at the mitochondrial outer membrane regulate mitochondrial morphology. *J Cell Sci,* **117,** 1201-1210.

302. Suen DF, Norris KL, and Youle RJ (2008) Mitochondrial dynamics and apoptosis. *Genes Dev,* **22,** 1577-1590.

303. Sulzer D (2007) Multiple hit hypotheses for dopamine neuron loss in Parkinson's disease. *Trends Neurosci,* **30,** 244-250.

304. Surmeier DJ, Guzman JN, Sanchez-Padilla J, and Goldberg JA (2010) What causes the death of dopaminergic neurons in Parkinson's disease? *Prog Brain Res,* **183,** 59-77.

305. Surwit RS, Kuhn CM, Cochrane C, McCubbin JA, and Feinglos MN (1988) Diet-induced type II diabetes in C57BL/6J mice. *Diabetes,* **37,** 1163-1167.

306. Szabadkai G, Simoni AM, Chami M, Wieckowski MR, Youle RJ, and Rizzuto R (2004) Drp-1-dependent division of the mitochondrial network blocks intraorganellar Ca2+ waves and protects against Ca2+-mediated apoptosis. *Mol Cell,* **16,** 59-68.

307. Tahrani AA, Bailey CJ, Del PS, and Barnett AH (2011) Management of type 2 diabetes: new and future developments in treatment. *Lancet,* **378,** 182-197.

308. Takeshige K, Baba M, Tsuboi S, Noda T, and Ohsumi Y (1992) Autophagy in yeast demonstrated with proteinase-deficient mutants and conditions for its induction. *J Cell Biol,* **119,** 301-311.

309. Tal R, Winter G, Ecker N, Klionsky DJ, and Abeliovich H (2007) Aup1p, a yeast mitochondrial protein phosphatase homolog, is required for efficient stationary phase mitophagy and cell survival. *J Biol Chem,* **282,** 5617-5624.

310. Tanaka A (2010) Parkin-mediated selective mitochondrial autophagy, mitophagy: Parkin purges damaged organelles from the vital mitochondrial network. *FEBS Lett,* **584,** 1386-1392.

311. Tanaka A, Cleland MM, Xu S, Narendra DP, Suen DF, Karbowski M, and Youle RJ (2010) Proteasome and p97 mediate mitophagy and degradation of mitofusins induced by Parkin. *J Cell Biol,* **191,** 1367-1380.

312. Tanida I, Sou YS, Minematsu-Ikeguchi N, Ueno T, and Kominami E (2006) Atg8L/Apg8L is the fourth mammalian modifier of mammalian Atg8 conjugation mediated by human Atg4B, Atg7 and Atg3. *FEBS J,* **273,** 2553-2562.

313. Taylor R and Goldman SJ (2011) Mitophagy and Disease: New Avenues for Pharmacological Intervention. *Curr Pharm Des*.

314. Terman A, Kurz T, Navratil M, Arriaga EA, and Brunk UT (2010) Mitochondrial turnover and aging of long-lived postmitotic cells: the mitochondrial-lysosomal axis theory of aging. *Antioxid Redox Signal,* **12,** 503-535.

315. Thomas KJ, McCoy MK, Blackinton J, Beilina A, van der BM, Sandebring A, Miller D, Maric D, Cedazo-Minguez A, and Cookson MR (2010) DJ-1 acts in parallel to the PINK1/parkin pathway to control mitochondrial function and autophagy. *Hum Mol Genet*.

316. Thompson LV (2006) Oxidative stress, mitochondria and mtDNA-mutator mice. *Exp Gerontol,* **41,** 1220-1222.

317. Tiedge M, Lortz S, Drinkgern J, and Lenzen S (1997) Relation between antioxidant enzyme gene expression and antioxidative defense status of insulin-producing cells. *Diabetes,* **46,** 1733-1742.

318. Toledo FG, Watkins S, and Kelley DE (2006) Changes induced by physical activity and weight loss in the morphology of intermyofibrillar mitochondria in obese men and women. *J Clin Endocrinol Metab,* **91,** 3224-3227.

319. Tschritter O, Preissl H, Hennige AM, Stumvoll M, Porubska K, Frost R, Marx H, Klosel B, Lutzenberger W, Birbaumer N, Haring HU, and Fritsche A (2006) The cerebrocortical response to hyperinsulinemia is reduced in overweight humans: a magnetoencephalographic study. *Proc Natl Acad Sci U S A,* **103,** 12103-12108.

320. Tuttle RL, Gill NS, Pugh W, Lee JP, Koeberlein B, Furth EE, Polonsky KS, Naji A, and Birnbaum MJ (2001) Regulation of pancreatic beta-cell growth and survival by the serine/threonine protein kinase Akt1/PKBalpha. *Nat Med,* **7,** 1133-1137.

321. Twig G, Elorza A, Molina AJ, Mohamed H, Wikstrom JD, Walzer G, Stiles L, Haigh SE, Katz S, Las G, Alroy J, Wu M, Py BF, Yuan J, Deeney JT, Corkey BE, and Shirihai OS (2008a) Fission and selective fusion govern mitochondrial segregation and elimination by autophagy. *EMBO J,* **27,** 433-446.

322. Twig G, Graf SA, Wikstrom JD, Mohamed H, Haigh SE, Elorza A, Deutsch M, Zurgil N, Reynolds N, and Shirihai OS (2006) Tagging and tracking individual networks within a complex mitochondrial web with photoactivatable GFP. *Am J Physiol Cell Physiol,* **291,** C176-C184.

323. Twig G, Hyde B, and Shirihai OS (2008b) Mitochondrial fusion, fission and autophagy as a quality control axis: the bioenergetic view. *Biochim Biophys Acta,* **1777,** 1092-1097.

324. Twig G, Liu X, Liesa M, Wikstrom JD, Molina AJ, Las G, Yaniv G, Hajnoczky G, and Shirihai OS (2010) Biophysical properties of mitochondrial fusion events in pancreatic beta-cells and cardiac cells unravel potential control mechanisms of its selectivity. *Am J Physiol Cell Physiol,* **299,** C477-C487.

325. Twig G and Shirihai OS (2010) The interplay between mitochondrial dynamics and mitophagy. *Antioxid Redox Signal*.

326. Twig G and Shirihai OS (2011) The interplay between mitochondrial dynamics and mitophagy. *Antioxid Redox Signal,* **14,** 1939-1951.

327. Unger RH (1995) Lipotoxicity in the pathogenesis of obesity-dependent NIDDM. Genetic and clinical implications. *Diabetes,* **44,** 863-870.

328. Unger RH and Grundy S (1985) Hyperglycaemia as an inducer as well as a consequence of impaired islet cell function and insulin resistance: implications for the management of diabetes. *Diabetologia,* **28,** 119-121.

329. Valko M, Leibfritz D, Moncol J, Cronin MT, Mazur M, and Telser J (2007) Free radicals and antioxidants in normal physiological functions and human disease. *Int J Biochem Cell Biol,* **39,** 44-84.

330. Vallar L, Biden TJ, and Wollheim CB (1987) Guanine nucleotides induce Ca2+-independent insulin secretion from permeabilized RINm5F cells. *J Biol Chem,* **262,** 5049-5056.

331. Valle MM, Graciano MF, Lopes de Oliveira ER, Camporez JP, Akamine EH, Carvalho CR, Curi R, and Carpinelli AR (2011) Alterations of NADPH oxidase activity in rat pancreatic islets induced by a high-fat diet. *Pancreas,* **40,** 390-395.

332. Vila M, Bove J, Dehay B, Rodriguez-Muela N, and Boya P (2010) Lysosomal membrane permeabilization in Parkinson disease. *Autophagy,* **7,** 98-100.

333. Vives-Bauza C and Przedborski S (2010a) PINK1 points Parkin to mitochondria. *Autophagy,* **6**.

334. Vives-Bauza C, Zhou C, Huang Y, Cui M, de Vries RL, Kim J, May J, Tocilescu MA, Liu W, Ko HS, Magrane J, Moore DJ, Dawson VL, Grailhe R, Dawson TM, Li C, Tieu K, and Przedborski S (2010b) PINK1-dependent recruitment of Parkin to mitochondria in mitophagy. *Proc Natl Acad Sci U S A,* **107,** 378-383.

335. Wang X and Schwarz TL (2009) The mechanism of Ca2+ -dependent regulation of kinesin-mediated mitochondrial motility. *Cell,* **136,** 163-174.

336. Weber TA and Reichert AS (2010) Impaired quality control of mitochondria: aging from a new perspective. *Exp Gerontol,* **45,** 503-511.

337. Weihofen A, Thomas KJ, Ostaszewski BL, Cookson MR, and Selkoe DJ (2009) Pink1 forms a multiprotein complex with Miro and Milton, linking Pink1 function to mitochondrial trafficking. *Biochemistry,* **48,** 2045-2052.

338. Weir GC and Bonner-Weir S (2004) Five stages of evolving beta-cell dysfunction during progression to diabetes. *Diabetes,* **53 Suppl 3,** S16-S21.

339. Weiss R and Caprio S (2006) Development of type 2 diabetes in children and adolescents. *Minerva Med,* **97,** 263-269.

340. Weyer C, Hanson RL, Tataranni PA, Bogardus C, and Pratley RE (2000) A high fasting plasma insulin concentration predicts type 2 diabetes independent of insulin resistance: evidence for a pathogenic role of relative hyperinsulinemia. *Diabetes,* **49,** 2094-2101.

341. White KE, Davies VJ, Hogan VE, Piechota MJ, Nichols PP, Turnbull DM, and Votruba M (2009) OPA1 deficiency associated with increased autophagy in retinal ganglion cells in a murine model of dominant optic atrophy. *Invest Ophthalmol Vis Sci,* **50,** 2567-2571.

342. Whitworth AJ and Pallanck LJ (2009) The PINK1/Parkin pathway: a mitochondrial quality control system? *J Bioenerg Biomembr,* **41,** 499-503.

343. Wicksteed B, Brissova M, Yan W, Opland DM, Plank JL, Reinert RB, Dickson LM, Tamarina NA, Philipson LH, Shostak A, Bernal-Mizrachi E, Elghazi L, Roe MW, Labosky PA, Myers MG, Jr., Gannon M, Powers AC, and Dempsey PJ (2010) Conditional gene targeting in mouse pancreatic ss-Cells: analysis of ectopic Cre transgene expression in the brain. *Diabetes,* **59,** 3090-3098.

344. Wiesner RJ, Ruegg JC, and Morano I (1992) Counting target molecules by exponential polymerase chain reaction: copy number of mitochondrial DNA in rat tissues. *Biochem Biophys Res Commun,* **183,** 553-559.

345. Wikstrom JD, Katzman SM, Mohamed H, Twig G, Graf SA, Heart E, Molina AJ, Corkey BE, de Vargas LM, Danial NN, Collins S, and Shirihai OS (2007) beta-Cell mitochondria exhibit membrane potential heterogeneity that can be altered by stimulatory or toxic fuel levels. *Diabetes,* **56,** 2569-2578.

346. Wikstrom JD, Twig G, and Shirihai OS (2009) What can mitochondrial heterogeneity tell us about mitochondrial dynamics and autophagy? *Int J Biochem Cell Biol,* **41,** 1914-1927.

347. Willis SN, Chen L, Dewson G, Wei A, Naik E, Fletcher JI, Adams JM, and Huang DC (2005) Proapoptotic Bak is sequestered by Mcl-1 and Bcl-xL, but not Bcl-2, until displaced by BH3-only proteins. *Genes Dev,* **19,** 1294-1305.

348. Willis SN, Fletcher JI, Kaufmann T, van Delft MF, Chen L, Czabotar PE, Ierino H, Lee EF, Fairlie WD, Bouillet P, Strasser A, Kluck RM, Adams JM, and Huang DC (2007) Apoptosis initiated when BH3 ligands engage multiple Bcl-2 homologs, not Bax or Bak. *Science,* **315,** 856-859.

349. Wood-Kaczmar A, Gandhi S, Yao Z, Abramov AY, Miljan EA, Keen G, Stanyer L, Hargreaves I, Klupsch K, Deas E, Downward J, Mansfield L, Jat P, Taylor J, Heales S, Duchen MR, Latchman D, Tabrizi SJ, and Wood NW (2008) PINK1 is necessary for long term survival and mitochondrial function in human dopaminergic neurons. *PLoS One,* **3,** e2455.

350. Wrede CE, Dickson LM, Lingohr MK, Briaud I, and Rhodes CJ (2002) Protein kinase B/Akt prevents fatty acid-induced apoptosis in pancreatic beta-cells (INS-1). *J Biol Chem,* **277,** 49676-49684.

351. Yan LJ and Sohal RS (1998) Mitochondrial adenine nucleotide translocase is modified oxidatively during aging. *Proc Natl Acad Sci U S A,* **95,** 12896-12901.

352. Yang Y, Ouyang Y, Yang L, Beal MF, McQuibban A, Vogel H, and Lu B (2008) Pink1 regulates mitochondrial dynamics through interaction with the fission/fusion machinery. *Proc Natl Acad Sci U S A,* **105,** 7070-7075.

353. Yang Z and Klionsky DJ (2010a) Eaten alive: a history of macroautophagy. *Nat Cell Biol,* **12,** 814-822.

354. Yang Z and Klionsky DJ (2010b) Mammalian autophagy: core molecular machinery and signaling regulation. *Curr Opin Cell Biol,* **22,** 124-131.

355. Yen WL and Klionsky DJ (2008) How to live long and prosper: autophagy, mitochondria, and aging. *Physiology (Bethesda),* **23,** 248-262.

356. Youle RJ and Narendra DP (2011) Mechanisms of mitophagy. *Nat Rev Mol Cell Biol,* **12,** 9-14.

357. Youle RJ and Strasser A (2008) The BCL-2 protein family: opposing activities that mediate cell death. *Nat Rev Mol Cell Biol,* **9,** 47-59.

358. Young AR, Chan EY, Hu XW, Kochl R, Crawshaw SG, High S, Hailey DW, Lippincott-Schwartz J, and Tooze SA (2006) Starvation and ULK1-dependent cycling of mammalian Atg9 between the TGN and endosomes. *J Cell Sci,* **119,** 3888-3900.

359. Young JE, Martinez RA, and La Spada AR (2009) Nutrient deprivation induces neuronal autophagy and implicates reduced insulin signaling in neuroprotective autophagy activation. *J Biol Chem,* **284,** 2363-2373.

360. Yu T, Fox RJ, Burwell LS, and Yoon Y (2005) Regulation of mitochondrial fission and apoptosis by the mitochondrial outer membrane protein hFis1. *J Cell Sci,* **118,** 4141-4151.

361. Yu T, Robotham JL, and Yoon Y (2006) Increased production of reactive oxygen species in hyperglycemic conditions requires dynamic change of mitochondrial morphology. *Proc Natl Acad Sci U S A,* **103,** 2653-2658.

362. Yuan H, Gerencser AA, Liot G, Lipton SA, Ellisman M, Perkins GA, and Bossy-Wetzel E (2007) Mitochondrial fission is an upstream and required event for bax foci formation in response to nitric oxide in cortical neurons. *Cell Death Differ,* **14,** 462-471.

363. Yue Z (2007) Regulation of neuronal autophagy in axon: implication of autophagy in axonal function and dysfunction/degeneration. *Autophagy,* **3,** 139-141.

364. Yue Z, Friedman L, Komatsu M, and Tanaka K (2009) The cellular pathways of neuronal autophagy and their implication in neurodegenerative diseases. *Biochim Biophys Acta,* **1793,** 1496-1507.

365. Zhang CL, Ho PL, Kintner DB, Sun D, and Chiu SY (2010) Activity-dependent regulation of mitochondrial motility by calcium and Na/K-ATPase at nodes of Ranvier of myelinated nerves. *J Neurosci,* **30,** 3555-3566.

366. Zhang J, Kundu M, and Ney PA (2009) Mitophagy in mammalian cells: the reticulocyte model. *Methods Enzymol,* **452,** 227-245.

367. Zhang J and Ney PA (2008) NIX induces mitochondrial autophagy in reticulocytes. *Autophagy,* **4,** 354-356.

368. Zhang J and Ney PA (2009) Role of BNIP3 and NIX in cell death, autophagy, and mitophagy. *Cell Death Differ,* **16,** 939-946.

369. Zhang Y and Chan DC (2007) New insights into mitochondrial fusion. *FEBS Lett,* **581,** 2168-2173.

370. Zhang Y, Qi H, Taylor R, Xu W, Liu LF, and Jin S (2007) The role of autophagy in mitochondria maintenance: characterization of mitochondrial functions in autophagy-deficient S. cerevisiae strains. *Autophagy,* **3,** 337-346.

371. Zhou X, Babu JR, da SS, Shu Q, Graef IA, Oliver T, Tomoda T, Tani T, Wooten MW, and Wang F (2007) Unc-51-like kinase 1/2-mediated endocytic processes regulate filopodia extension and branching of sensory axons. *Proc Natl Acad Sci U S A,* **104,** 5842-5847.

372. Zhou YP, Cockburn BN, Pugh W, and Polonsky KS (1999) Basal insulin hypersecretion in insulin-resistant Zucker diabetic and Zucker fatty rats: role of enhanced fuel metabolism. *Metabolism,* **48,** 857-864.

373. Zhu J and Chu CT (2010) Mitochondrial dysfunction in Parkinson's disease. *J Alzheimers Dis,* **20 Suppl 2,** S325-S334.

374. Zhu JH, Guo F, Shelburne J, Watkins S, and Chu CT (2003) Localization of phosphorylated ERK/MAP kinases to mitochondria and autophagosomes in Lewy body diseases. *Brain Pathol,* **13,** 473-481.

375. Zick M, Rabl R, and Reichert AS (2009) Cristae formation-linking ultrastructure and function of mitochondria. *Biochim Biophys Acta,* **1793,** 5-19.

376. Ziviani E, Tao RN, and Whitworth AJ (2010) Drosophila parkin requires PINK1 for mitochondrial translocation and ubiquitinates mitofusin. *Proc Natl Acad Sci U S A,* **107,** 5018-5023.

377. Ziviani E and Whitworth AJ (2010) How could Parkin-mediated ubiquitination of mitofusin promote mitophagy? *Autophagy,* **6**.

378. Zorzano A, Liesa M, and Palacin M (2009) Mitochondrial dynamics as a bridge between mitochondrial dysfunction and insulin resistance. *Arch Physiol Biochem,* **115,** 1-12.

379. Zorzano A, Liesa M, Sebastian D, Segales J, and Palacin M (2010) Mitochondrial fusion proteins: dual regulators of morphology and metabolism. *Semin Cell Dev Biol,* **21,** 566-574.

380. Zuchner S, Mersiyanova IV, Muglia M, Bissar-Tadmouri N, Rochelle J, Dadali EL, Zappia M, Nelis E, Patitucci A, Senderek J, Parman Y, Evgrafov O, Jonghe PD, Takahashi Y, Tsuji S, Pericak-Vance MA, Quattrone A, Battaloglu E, Polyakov AV, Timmerman V, Schroder JM, and Vance JM (2004) Mutations in the mitochondrial GTPase mitofusin 2 cause Charcot-Marie-Tooth neuropathy type 2A. *Nat Genet,* **36,** 449-451.